CARBON-CONCENTRATING MECHANISMS AND β-CARBOXYLATION: THEIR POTENTIAL CONTRIBUTION TO MARINE PHOTOSYNTHETIC CARBON ISOTOPE FRACTIONATION

A DISSERTATION SUBMITTED TO THE GRADUATE DIVISION OF THE UNIVERSITY OF HAWAI'I IN PARTIAL FULFILLMENT OF THE REQUIREMENTS FOR THE DEGREE OF

DOCTOR OF PHILOSOPHY

IN

OCEANOGRAPHY

DECEMBER 2003

By

Nicolas Cassar

Dissertation Committee:

Edward A. Laws, Chairperson
Robert R. Bidigare
David M. Karl
Fred T. Mackenzie
Brian N. Popp
Paul G. Falkowski

ACKNOWLEDGMENTS

I would first and foremost like to thank Ed Laws for his support and mentorship. It has been a great privilege to study under his guidance. Through the years, I have discovered that Ed's unlimited dedication to education and the community is only surpassed by his qualities as a scholar. His selfless scientific curiosity has been a great source of inspiration.

I would like to express my deep gratitude to the committee members for their support and assistance. This work has greatly benefited from their suggestions and from the work I have performed in their laboratories. Special thanks to Brian Popp, for allowing me to invade his laboratory for most of this work. I am indebted to Terri Rust for her patience, help and technical expertise. I wish to acknowledge David Hashimoto, Nancy Koike, Kathy Kozuma, and Rene Tada for their strong commitment to their work.

I am also extremely grateful to Claude Belisle for her tremendous patience, and understanding. Her unconditional support and shared enthusiasm for my research have been invaluable. Many thanks are also due to my parents and my brother, for their support and care over the years.

This work has been supported by the National Science Foundation and the Natural Sciences and Engineering Research Council of Canada.

ABSTRACT

The ability of the ocean to buffer the concentration of CO_2 in the atmosphere through the so-called biological pump depends on the extent to which the photosynthetic rate of marine phytoplankton is limited by the concentration of CO_2 in the water. If CO_2 becomes available to phytoplankton by passive diffusion through the boundary layer around the cell, then the growth of large cells, which are believed to contribute disproportionately to the biological pump, could be limited by CO_2 availability. However, many species appear to have the ability to circumvent diffusion control through the use of carbon-concentrating mechanisms (CCMs) such as active CO_2 uptake, bicarbonate (HCO_3^-) transport, and carbonic anhydrase activity. These mechanisms are likely adaptations to the fact that the main carbon fixing enzyme, ribulose-1,5-bisphosphate carboxylase-oxygenase (Rubisco), is less than half saturated at normal seawater CO_2 concentrations.

Using short-term $^{14}CO_2$-disequilibrium experiments, a clone of the marine diatom *Phaeodactylum tricornutum* was shown to take up little or no HCO_3^- even under conditions of severe CO_2 limitation. These results agree with predictions based on stable carbon isotopic fractionation data and demonstrate that combining isotopic disequilibrium experiments with continuous growth cultures and stable isotope fractionation experiments is a powerful tool for understanding the response of oceanic primary producers to anthropogenic CO_2 emissions as well as for interpreting paleoceanographic carbon isotope data.

Isotopic disequilibrium experiments were also performed in the field to estimate the extent of photosynthetic bicarbonate (HCO_3^-) uptake in the oceans. The experiments were conducted in the Southern Ocean during the Southern Ocean Iron Experiment (SOFeX). In contrast to the results with *P. tricornutum*, approximately half of the photosynthetic inorganic carbon uptake was direct HCO_3^- uptake, the other half being direct CO_2 uptake (passive and/or active uptake). A low-CO_2 treatment induced an increase in uptake of CO_2 through increased enzymatically mediated extracellular dehydration of HCO_3^- (carbonic anhydrase activity), which was at the expense of direct HCO_3^- transport across the plasmalemma. Because of the presence of CCMs, biological productivity in the Southern Ocean is unlikely to be directly regulated by natural or anthropogenic variations in atmospheric CO_2 concentration. These results are consistent with stable isotope fractionation models and could have important implications for the global biogeochemical cycle of carbon.

It is generally believed that most of the variations in stable isotope fractionation are associated with changes in CCM activity. A review and experimental study of the various factors that influence CCM activity and therefore photosynthetic carbon isotope fractionation revealed that, other than CCMs, several factors that have been essentially ignored in the scientific literature may also contribute to the isotopic signature of photosynthetic organic matter. In this study, photorespiration appeared to be of greater magnitude than commonly reported in marine diatoms, although its contribution to isotopic fractionation was negligible. Isotopic fractionation during photosynthesis in *P. tricornutum* was found to be well correlated to changes in Rubisco enzyme kinetics and to the molar organic carbon to nitrogen ratio (C/N). Contrary to the general scientific

belief, the C/N proved to be dependent on the CO_2 concentration, with the greatest dependency at lower growth rates, presumably because of luxury carbon uptake at lower growth rates. At higher growth rates, a tighter coupling of the organic nitrogen and carbon cycles may explain the lower responsiveness of C/N to changes in CO_2 concentration.

The contribution of carboxylases other than Rubisco to photosynthetic stable carbon isotope fractionation was also examined. Some β-carboxylation enzymes, such as phosphoenolpyruvate carboxylase (PEPC), have a carbon isotope discrimination factor different from Rubisco and may significantly contribute to carbon fixation. Changes in PEPC/Rubisco activity under various growth conditions may explain some of the variations in stable isotope fractionation. The β-carboxylase activity in *P. tricornutum* increased with decreasing growth rates and increasing CO_2 concentrations. PEPC activities larger than generally reported in the literature were observed. This difference may be attributable to variations in methodological approaches.

A multitude of factors may influence overall photosynthetic carbon isotope fractionation. Understanding these factors will be crucial to the use of isotopic analyses for paleo-CO_2 reconstruction.

TABLE OF CONTENTS

LIST OF TABLES

Table Page

LIST OF FIGURES

Figure Page

CHAPTER 1. INTRODUCTION

1.1. Carbon-concentrating mechanisms

Because of the effect of carbon dioxide on global climate, there is currently a significant amount of scientific interest in the ocean and its biota as potential sinks for anthropogenic carbon dioxide (CO_2), the second most important greenhouse gas after water vapor. Aquatic phototrophs, which represent only 1% of the total photosynthetic biomass on Earth, perform 40 % of net primary production on Earth (Falkowski and Raven 1997). The rate at which they fix the various forms of inorganic carbon will partially determine how efficiently the Earth's biological system can buffer excess anthropogenic CO_2 and therefore has implications regarding the rate of global warming. An increase in atmospheric CO_2 could potentially be buffered by enhanced rates of marine algal productivity. However, this negative feedback mechanism relies on the assumption that marine phototrophic biota are CO_2 limited and that an increase in anthropogenic CO_2 sources would intensify new production rates.

Inorganic carbon has rarely been considered a limiting factor to phytoplankton growth because of its high concentration in seawater. However, less than 1% of dissolved inorganic carbon (DIC) exists as CO_2 (Millero 1995), the molecule that is being fixed during photosynthesis. This has led to the hypothesis that under some conditions, algal growth may be CO_2 limited (Riebesell et al. 1993).

The CO_2 concentration in seawater is always insufficient to saturate the carbon fixing enzyme ribulose-1,5- bisphosphate carboxylase-oxygenase (Rubisco) which is less than half saturated at normal CO_2 concentrations (Raven and Johnston 1991; Badger et al.

1998). Rubisco is relatively inefficient at fixing carbon dioxide. Its k_{cat} is about 3 s^{-1} per site (3 reactions catalyzed per second) under normal carbon dioxide partial pressure whereas most enzymes have catalytic rates 2 to 4 orders of magnitudes greater (10^2 to 10^4 s^{-1}). This explains why plants invest a great proportion of their metabolic energy and nitrogen into Rubisco synthesis and maintenance. For instance, Rubisco may account for as much as 65% of the total soluble proteins in terrestrial leaf extracts (Ellis 1979). In addition to a low catalytic rate and a low specific turnover rate, Rubisco also has a low affinity for carbon dioxide (Hartwell et al. 1999) and its carboxylase activity is inhibited by the presence of oxygen. For all these reasons, Rubisco is probably the most abundant protein in the world (Ellis 1979).

To circumvent the catalytic inefficiency of their carbon-fixing enzyme, aquatic photoautotrophs have adapted by producing large quantities of Rubisco and by evolving ways to actively increase the CO_2 available for photosynthesis through processes called carbon-concentrating mechanisms (CCMs). The CCM's function is to elevate the CO_2 concentration in the vicinity of Rubisco, above the predicted concentration from passive diffusion (governed by Fick's law) to favor the carboxylation reaction at the expense of the oxygenase reaction and suppress photorespiration.

The evolutionary driving force of CCMs has been the low affinity of Rubisco for CO_2. Rubisco first evolved approximately 3.85 billion years ago in a carbon dioxide rich and oxygen poor (no or little oxygen inhibition of carboxylation) environment (Lasaga et al. 1985; Kasting 1987; Berner 1991; Berner 1994; Raven 1995; Rye et al. 1995; Berner and Kothavala 2001). Hence, on primitive Earth, there was little selective pressure for Rubisco to evolve a high affinity for CO_2. To compensate for the inefficient kinetics of

Rubisco, polyphyletic metabolic processes have evolved upstream (CCMs) and downstream (photorespiratory carbon oxidation cycle, PCOC) of Rubisco.

Active uptake of bicarbonate (HCO_3^-) and CO_2 through the cell membrane, active transport of inorganic carbon (Badger 1987; Johnston 1991) from the cellular membrane to the chloroplasts, and active conversion of bicarbonate to carbon dioxide (by carbonic anhydrase) are examples of CCMs. CO_2 diffusion through the plasmalemma involves dissolution through the phospholipid bilayer followed by dissolution into the aqueous cytoplasm. The net CO_2 diffusion rate is proportional to the hydrophobicity, which is measured by the partition coefficient (K), and to the concentration gradient across the plasmalemma. K is the ratio of the equilibrium concentration of CO_2 in the hydrophobic core of the phospholipid bilayer ($[CO_2]_p$) vs. in aqueous solution ($[CO_2]_{aq}$),

$$K = [CO_2]_p / [CO_2]_{aq} \qquad (1.1.1)$$

Unless CCMs are present, CO_2 diffusion through biological membranes is the rate-limiting stage of delivery of inorganic carbon to Rubisco since the hydrophobic core of phospholipid bilayers is considerably more viscous than aqueous solutions.

Because the cytosolic electrical potential is negative relative to the medium (electrochemical homeostasis at approximately –70 mV), and because biological membranes are relatively impermeable to charged molecules, any uptake of HCO_3^- must be energy dependent. Mediated (active) transport of HCO_3^- is thus expected if the HCO_3^- concentration is greater than that predicted by the Nernst electrochemical equilibrium potential. The movement of ions across selectively permeable membranes is dictated by the sum of the electrical potential force and the ion concentration gradient force. For

instance, in the hypothetical case of a membrane selectively permeable to only HCO_3^-, the total Gibbs free-energy change (ΔG_t) is

$$\Delta G_t = \Delta G_e + \Delta G_c \tag{1.1.2}$$

where the Gibbs free-energy change associated with the membrane electrical potential (ΔG_e) is

$$\Delta G_e = ZF\psi \tag{1.1.3}$$

and where the Gibbs free-energy generated by the HCO_3^- chemical gradient (ΔG_c) is

$$\Delta G_c = RT \ln\left(\frac{[HCO_3^-]_i}{[HCO_3^-]_e}\right) \tag{1.1.4}$$

where F, ψ, Z, T, and R are the Faraday constant (96000 coulombs mol^{-1} V^{-1}), the electrical potential (V), the valency (equal to -1 in the case of HCO_3^-), the absolute temperature (Kelvin), and the gas constant (8.28 joules $degree^{-1}$ mol^{-1}), respectively. $\frac{[HCO_3^-]_i}{[HCO_3^-]_e}$ is the ratio of intracellular (i) and extracellular (e) concentrations of HCO_3^- (brackets denote concentrations). Theoretically, activities should be used instead of concentrations, but an activity coefficient of 1 is assumed. The electrical potential is given by the Nernst equation

$$\psi = \frac{RT}{FZ} \ln\left(\frac{[HCO_3^-]_i}{[HCO_3^-]_e}\right) \tag{1.1.5}$$

At electrochemical equilibrium, the electrical potential will balance the chemical potential. In the case of biological membranes, Eq. (1.1.5) cannot be used since several ions contribute to the electrical potential. In that case, the latter is determined by the concentration of the various ions present and by the relative permeability of the

membranes to each individual ion. A modified version of the Nernst equation, the Goldman-Hodgkin-Katz (GHK) equation, is more appropriate. For example, the GHK equation for a biological membrane in the presence of potassium (K^+), sodium (Na^+), chloride (Cl^-) and HCO_3^- ions is

$$\psi = \frac{RT}{FZ}\ln\left(\frac{P_{K^+}[K^+]_e + P_{Na^+}[Na^+]_e + P_{Cl^-}[Cl^-]_i + P_{HCO_3^-}[HCO_3^-]_i}{P_{K^+}[K^+]_i + P_{Na^+}[Na^+]_i + P_{Cl^-}[Cl^-]_e + P_{HCO_3^-}[HCO_3^-]_e}\right) \quad (1.1.6)$$

where P is the membrane permeability coefficient of the subscripted ionic species. Assuming the HCO_3^- concentration is greater intracellularly than in the surrounding medium, an active CCM must be present since the total Gibbs free-energy for the intracellular translocation of HCO_3^- would be positive (see equations above), i.e. such an endergonic reaction would not occur spontaneously. In fact, an intracellular HCO_3^- concentration greater than predicted based on the electrochemical gradient across the plasmalemma (not necessarily greater than the extracellular concentration) requires active transport (since the cytosol has a negative electrical potential relative to the medium). HCO_3^- ion pairing in seawater (e.g., $MgHCO_3^+$ and $NaHCO_3^0$) could also potentially affect the carbon transport across the plasmalemma. In contrast to HCO_3^-, CO_2 is a non-polar molecule and can consequently diffuse more readily through phospholipid bilayers (about 1000 times faster) (Gutknecht et al. 1977). However, it is only delivered to the vicinity of the cell by passive diffusion since at the cell size level, advection and turbulent mixing are negligible relative to diffusion (Lazier and Mann 1989; Wolf-Gladrow and Riebesell 1997).

Increase in affinity of cells for external CO_2 and HCO_3^- and in carbonic anhydrase (CA) activity have been shown to be induced by low external C_i (inorganic carbon)

concentrations (Badger 1987; Coleman 1991; Nimer and Merrett 1996). The CCMs allow marine photoautotrophs to grow under a wide range of DIC concentrations, despite the low affinity of Rubisco for CO_2. Figures 1.1 and 1.2 show the pathways of external inorganic carbon to the site of fixation, and the putative CCMs of marine eukaryotic microalgae and cyanobacteria, respectively.

The process by which phytoplankton acquire DIC is a subject of considerable debate. Because HCO_3^- and CO_2 interconvert readily in seawater (see next section on carbonate system kinetics), the study of carbon transport remains a methodological challenge that has not been completely resolved. Several lines of evidence, based on a wide array of methods, have been used to confirm CCM activity:

- $C_i/ C_e > 1$: If the internal (C_i) is greater than the external (C_e) inorganic carbon concentration, a CCM must be active (Badger et al. 1980; Kaplan et al. 1980; Beer et al. 1990). As indicated by Badger et al. (1998), although a $C_i/ C_e > 1$ is sufficient to establish that a CCM is active, a lack of inorganic carbon accumulation internally ($C_i/ C_e \leq 1$) does not necessarily preclude the presence of a CCM. The most commonly employed method for the determination of C_i/ C_e is by ^{14}C silicone oil centrifugation (Badger and Andrews 1982; Patel and Merrett 1986; Burns and Beardall 1987; Smith and Bidwell 1989; Merrett 1991; Colman and Rotatore 1995; Johnston and Raven 1996). Most studies indicate that, in general, $C_i/ C_e > 1$ (see Table VIII in Raven 1997 for review), a finding that is consistent with an active CCM.

- $K_{1/2_{CO_2}}\{\text{Photosynthesis}\}$ vs. $K_{1/2_{CO_2}}\{\text{Rubisco}\}$: Comparison of the CO_2 half saturation constant *in vivo* vs. isolated Rubisco (Israel and Beer 1992). If

$K_{1/2_{CO_2}}\{\text{Rubisco}\} > K_{1/2_{CO_2}}\{\text{Photosynthesis}\}$, a CCM must be active. In other words, if the $K_{1/2_{CO_2}}$ of photosynthesis is lower than predicted based on passive diffusion, Rubisco's kinetic properties and abundance, a CCM must be present. One of the challenges associated with this piece of evidence is the difficulty in determining the $K_{1/2_{CO_2}}$ of isolated Rubisco.

- O_2/CO_2 competition: Oxygen (O_2) and CO_2 are competitive substrates for the active site of Rubisco. Rubisco catalyses 2 competing reactions, the carboxylation of ribulose 1,5-bisphosphate (RuBP),

$$\text{RuBP} + CO_2 + H_2O \rightarrow 2\times(\text{3-PGA}) \qquad (1.1.7)$$

and the oxygenation of RuBP,

$$\text{RuBP} + O_2 \rightarrow \text{3-PGA} + \text{2-PG} \qquad (1.1.8)$$

where 3-PGA and 2-PG are 3-phosphoglycerate and 2- phosphoglycolate, respectively. Assuming that the uptake of inorganic carbon is based solely on passive CO_2 diffusion, a decrease in O_2 or an increase in ambient CO_2 should theoretically decrease the importance of the oxygenase reaction. If a CCM is active, the O_2 level may not affect the photosynthetic rate (Beardall et al. 1976; Morris 1980; Badger et al. 1998). Similarly, a comparison of the predicted vs. observed CO_2-compensation concentration may also be used to detect CCM activity. By definition, the CO_2-compensation concentration is the CO_2 concentration at which there is no net evolution of oxygen. In the PCOC, the oxygenation of 2 moles of RuBP with 2 moles of O_2 forms 2 moles of 3-PGA and 2 moles of 2-PG. The two moles of 3-PGA reenter the photosynthetic carbon reduction cycle (PCRC). The 2 moles of 2-PG are converted through a chain of reactions to 2 moles

of glycine, which are decarboxylated to one mole of CO_2 (and 1 mole of NH_3) and 1 mole of serine. The serine is then recycled through a series of reactions to 3-PGA (which again returns to the PCRC) and therefore no further loss of CO_2 occurs in the PCOC. Hence, for every 2 moles of oxygen consumed in the PCOC, 3 moles of 3-PGA (two moles being the direct product of the oxygenase reaction, the other mole being the recycling product of 2-PG) and 1 mole of CO_2 are ultimately formed. The photorespiratory CO_2 production rate is therefore half the oxygenase activity. Consequently, assuming 1 mole of CO_2 is released with every 2 moles of oxygen consumed by Rubisco's oxygenase reaction, and ignoring dark respiration, the CO_2-compensation point is reached when Rubisco's carboxylase activity (v_c) is equal to the photorespiratory CO_2 production rate, or half the oxygenase rate (v_o):

$$v_c = \frac{1}{2} v_o \tag{1.1.9}$$

Eq. (1.1.9) assumes that all the photorespiratory phosphoglycolate is metabolized (i.e., recycled). This is generally not the case as 25% to 100% of the glycolate produced during photorespiration is excreted (Falkowski and Raven 1997). In other words, only 0 to 75 % of the photorespiratory glycolate is available for biosynthesis. Under these conditions, the CO_2-compensation point is reached when $v_c = 0$ to $(3/8)v_o$, which correspond to 100 and 25% glycolate excretion, respectively. Although inefficient in terms of the energy and carbon budgets, the excretion of all the photorespiratory glycolate causes the lowest CO_2-compensation point.

Rubisco's potential for displaying carboxylase vs. oxygenase activity is described by the selectivity factor for CO_2 over O_2 (τ) and is defined as

$$\tau = \frac{V_{CO_2} K_{1/2_{O_2}}}{V_{O_2} K_{1/2_{CO_2}}} \tag{1.1.10}$$

where V_{CO_2} and V_{O_2} are the maximal rates of the carboxylase and the oxygenase activities, respectively, and $K_{1/2_{CO_2}}$ and $K_{1/2_{O_2}}$ are the half-saturation constants of Rubisco for CO_2 and O_2. τ is essentially the ratio of the turnover times of the oxygenase ($\frac{K_{1/2_{O_2}}}{V_{O_2}}$) and the carboxylase ($\frac{K_{1/2_{CO_2}}}{V_{CO_2}}$) enzymatic reactions of Rubisco. The ratio of the oxygenase and carboxylase activities is therefore:

$$\frac{v_o}{v_c} = \frac{1}{\tau} \times \frac{[O_2]}{[CO_2]} = \frac{V_{O_2} K_{1/2_{CO_2}}}{V_{CO_2} K_{1/2_{O_2}}} \times \frac{[O_2]}{[CO_2]} \tag{1.1.11}$$

Again, assuming Eq. (1.1.9) holds, the predicted CO_2-compensation concentration will be

$$[CO_2]_{comp} = \frac{[O_2]}{2\tau} \tag{1.1.12}$$

where $[CO_2]_{comp}$ is the CO_2-compensation concentration. Hence, an observed $[CO_2]_{comp}$ less than the predicted value based on Eq. (1.1.12) implies CCM activity. The theoretical CO_2-compensation concentration ranges from zero to $\frac{3}{8}\frac{[O_2]}{\tau}$, depending on the magnitude of glycolate excretion. Unless more is known about the fate of the photorespiratory glycolate, such a range, which includes the hypothetical limit of a CO_2-compensation concentration of zero, makes it difficult to use this parameter to determine if a CCM is present or not, because the observed CO_2-compensation concentration must be greater than zero.

The presence of CA, pyrenoids and carboxysomes is also further evidence of CCM activity. Pyrenoids and carboxysomes are bodies that are found in the stroma of marine algae and the cytoplasm of many prokaryotic organisms, respectively. Both bodies have high concentrations of Rubisco (Badger et al. 1991; Price and Badger 1991; Morita et al. 1997). They are also believed to be associated with high CO_2 concentrations, which serves the dual purpose of activating Rubisco through carbamylation (Hartman and Harpel 1994), and increasing carboxylation efficiency (i.e. by suppressing photosynthetic O_2 inhibition) (Raven 1997).

One of the approaches that has been employed to understand more fully CCMs is the ^{14}C short-term disequilibrium experiment (Espie and Colman 1986; Espie et al. 1986; Korb et al. 1997; Elzenga et al. 2000; Cassar et al. 2002). This method, and how it can be used to quantitatively infer the relative contribution of HCO_3^- and CO_2 to photosynthetic inorganic carbon uptake, is described below. The first chapter focuses primarily on the principles behind the isotopic disequilibrium experiments. In the following chapter, the application of this method in the laboratory to a continuous growth culture (in conjunction with stable carbon isotope fractionation measurements) is described. A detailed description of the experimental protocol for the isotopic disequilibrium is also presented here. In the third chapter, the importance of CCMs in Southern Ocean phytoplankton was determined and compared with assessments based upon isotope fractionation models. Our current understanding of CCMs comes almost exclusively from laboratory studies. Although most algal species studied in the laboratory have the potential for actively concentrating inorganic carbon, such activity may not be expressed in natural waters. The degree of CCM activity in the world's oceans has important

implications for the global biogeochemical cycling of carbon. The third chapter presents an assessment of the ecological significance of CCM activity, of the potential for marine primary producers to be limited by CO_2 availability, and of the response (or lack thereof) of the biological pump to the rising atmospheric CO_2 concentration. In the fourth chapter, photosynthetic stable carbon isotope fractionation is discussed and presented as a tool to understand more fully the inorganic carbon transport algal physiology. The fifth chapter focuses on β-carboxylases and their potential contribution to photosynthetic stable carbon isotope fractionation. The response of β-carboxylase activities to certain environmental factors (phosphate vs. nitrate limitation, growth rate, and CO_2 concentration) is also presented in Chapter 5. A description of carbonate species equilibria and kinetics in seawater is presented in the next section for the purpose of illustrating the necessity of CCMs. The concepts in the next section will also be helpful for the understanding of the kinetic principles that underlie isotopic disequilibrium experiments.

1.2. Carbonate system thermodynamics and kinetics in seawater

Thermodynamic equilibrium of the carbonate system

Excluding the sedimentary organic and inorganic reservoirs, the oceans contain the largest pool of inorganic carbon. There is approximately 50 times more inorganic carbon in the oceans than in the atmosphere. The flux of CO_2 into the ocean is controlled by the partial pressure of CO_2 in the atmosphere:

$$CO_2(g) \rightleftharpoons CO_2(aq) \qquad (1.2.1)$$

and its concentration in solution follows Henry's law:

$$[CO_2] = k_h \cdot P_{CO_2} \tag{1.2.2}$$

where k_h and P_{CO_2} are the Henry's law constant and the partial pressure of CO_2, respectively. The k_h constant is dependent upon temperature and salinity (ionic strength). Theoretically, fugacity of CO_2 (f_{CO_2}) instead of P_{CO_2} should be used. However, because the partial pressure of CO_2 in the atmosphere is small, P_{CO_2} is a good approximation of the fugacity of CO_2. In other words,

$$\lim_{P_{CO_2} \to 0} f_{CO_2} = P_{CO_2} \tag{1.2.3}$$

Once in solution, CO_2 equilibrates with carbonic acid (H_2CO_3), bicarbonate (HCO_3^-), and carbonate (CO_3^{2-}) according to the following equilibria:

$$H_2O + CO_2 \rightleftharpoons H_2CO_3 \rightleftharpoons H^+ + HCO_3^- \rightleftharpoons 2H^+ + CO_3^{2-} \tag{1.2.4}$$

The ionic carbonate species do not contribute to the partial pressure of CO_2. The sum of all these carbonate species is defined as the dissolved inorganic carbon pool (DIC):

$$DIC = [CO_2] + [H_2CO_3] + [HCO_3^-] + [CO_3^{2-}] \tag{1.2.5}$$

The inorganic carbon acid-base ionization equilibria,

$$H_2CO_3 \rightleftharpoons H^+ + HCO_3^- \rightleftharpoons 2H^+ + CO_3^{2-} \tag{1.2.6}$$

are instantaneous relative to the hydration/dehydration and hydroxylation/dehydroxylation reactions.

Because H_2CO_3 concentration is small (approximately 400 times smaller than CO_2), and because it is chemically indistinguishable from CO_2, it is often included in the definition of CO_2. Hence, we will use the following nomenclature

$$[CO_2] \equiv [CO_2] + [H_2CO_3] \tag{1.2.7}$$

Note that the $[CO_2]$ on the left side of Eq. (1.2.7) is often referred to as $[CO_2^*]$ or $[H_2CO_3^*]$ in the literature. Eq. (1.2.7) simplifies Eq. (1.2.4) to

$$CO_2 + H_2O \overset{K_1^*}{\rightleftharpoons} H^+ + HCO_3^- \overset{K_2^*}{\rightleftharpoons} 2H^+ + CO_3^{2-} \tag{1.2.8}$$

and

$$DIC = [CO_2] + [HCO_3^-] + [CO_3^{2-}] \tag{1.2.9}$$

where

$$K_1^* = \frac{[HCO_3^-][H^+]}{[CO_2]} \tag{1.2.10}$$

and

$$K_2^* = \frac{[CO_3^{2-}][H^+]}{[HCO_3^-]} \tag{1.2.11}$$

The star superscript indicates that these are stoichiometric constants. K_1^* and K_2^* are the first and second stoichiometric dissociation constants of carbonic acid. They are related to the thermodynamic equilibrium constants as follow:

$$\frac{K_1^*}{K_1} = \frac{\gamma_{CO_2}}{\gamma_{H^+}\gamma_{HCO_3^-}} \tag{1.2.12}$$

$$\frac{K_2^*}{K_2} = \frac{\gamma_{HCO_3^-}}{\gamma_{H^+}\gamma_{CO_3^{2-}}} \tag{1.2.13}$$

where γ is the individual activity coefficient of the subscripted species. The stoichiometric constants are temperature, salinity, and pressure dependent.

From Eq. (1.2.10) and Eq. (1.2.11),

$$[HCO_3^-] = \frac{K_1^*[CO_2]}{[H^+]} \tag{1.2.14}$$

and

$$[CO_3^{2-}] = \frac{K_1^* K_2^* [CO_2]}{[H^+]^2} \quad (1.2.15)$$

Replacing $[HCO_3^-]$ and $[CO_3^{2-}]$ in Eq. (1.2.9) with the right hand-side of Eqs. (1.2.14) and (1.2.15),

$$DIC = [CO_2](1 + \frac{K_1^*}{[H^+]} + \frac{K_1^* K_2^*}{[H^+]^2}) \quad (1.2.16)$$

The CO_2 concentration is therefore

$$[CO_2] = \frac{DIC}{(1 + \frac{K_1^*}{[H^+]} + \frac{K_1^* K_2^*}{[H^+]^2})} \quad (1.2.17)$$

Replacing $[CO_2]$ in Eqs. (1.2.14) and (1.2.15) with the right-hand side of Eq. (1.2.17)

$$[HCO_3^-] = \frac{DIC}{(1 + \frac{[H^+]}{K_1^*} + \frac{K_2^*}{[H^+]})} \quad (1.2.18)$$

$$[CO_3^{2-}] = \frac{DIC}{(1 + \frac{[H^+]}{K_2^*} + \frac{[H^+]^2}{K_1^* K_2^*})} \quad (1.2.19)$$

Using Eqs. (1.2.17), (1.2.18), and (1.2.19), with K_1^* and K_2^* equal to $10^{-5.86}$ and $10^{-8.92}$, respectively (S=35 and T=25°C), and assuming DIC in equilibrium with the atmosphere (approximately 2.1 mmol kg^{-1}), we can draw a Bjerrum diagram (Figure 1.3) which shows the log of the concentrations of the various carbonate species vs. pH. pK_1^* and

pK_2^* represent the pH at which equal concentrations of HCO_3^- and CO_2 and equal concentrations of HCO_3^- and CO_3^{2-} exist, respectively[1].

As is shown in Figure 1.4, the relative importance of the carbonate species is dependent on pH. As pH decreases, carbonate and bicarbonate proportions decrease and carbon dioxide contribution to the inorganic carbon pool increases (relative to bicarbonate and carbonate). At high pH, CO_3^{2-} is the dominant carbonate species. At normal seawater pH (about 8.1), HCO_3^- dominates the carbonate system (86.5% of the DIC), and CO_2 only represent 0.5% of the DIC (the difference being CO_3^{2-}). Under natural conditions, because the carbonate system is the most important contributor to the buffering capacity of seawater, changes in DIC and alkalinity generally control the pH. However, in isotopic disequilibrium experiments, pH is used to control the relative proportions of the various inorganic carbon species. In the case of a $^{14}CO_2$ pulse (discussed below), the pH is lowered well below the pK_1^*, in a region of pH dominated by CO_2.

Kinetics of the carbonate system

This section presents the reaction pathways by which equilibrium (Eq. (1.2.4)) is reached.

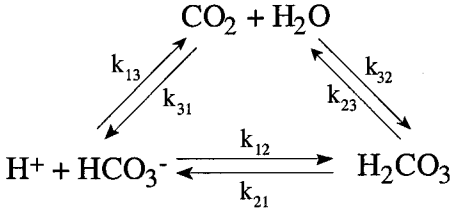

(1.2.20)

[1] $K = \frac{[A^-][H^+]}{[HA]}$. Taking the negative logarithmic on both sides, and rearranging, $pH = pK + \log(\frac{[A^-]}{[HA]})$, which is the Henderson-Hasselbalch equation. When pK=pH, $[A^-]=[HA]$.

The nomenclature in Eq. (1.2.20) follows the one in Johnson (1982). Being an ionic reaction, the acid-base association-dissociation reaction (interconversion between HCO_3^- and carbonic acid) is very rapid and can be considered instantaneous relative to the hydration-dehydration reaction, which is up to seven orders of magnitude slower (Eigen et al. 1961; Johnson 1982). For kinetic purposes, the carbonic acid and the HCO_3^- can consequently be considered in constant equilibrium,

$$K^*_{H_2CO_3} = \frac{[H^+][HCO_3^-]}{[H_2CO_3]} \tag{1.2.21}$$

The rate of CO_2 "disappearance" (k_{CO_2}) is thus a combination of CO_2 hydrations to carbonic acid (k_{32}) and to HCO_3^- (k_{31}). In other words,

$$k_{CO_2}[CO_2] = k_{31}[CO_2] + k_{32}[CO_2] \tag{1.2.22}$$

or,

$$k_{CO_2} = k_{31} + k_{32} \tag{1.2.23}$$

The rate of "formation" of CO_2 (k_d) is also a combination of two rates, the rates of dehydration of H_2CO_3 (k_{23}) and HCO_3^- to CO_2 (k_{13}) (Eq. (1.2.20)) or,

$$k_d[H^+][HCO_3^-] = k_{13}[H^+][HCO_3^-] + k_{23}[H_2CO_3] \tag{1.2.24}$$

Combining Eqs. (1.2.21) and (1.2.24),

$$k_d = k_{13} + \frac{k_{23}}{K^*_{H_2CO_3}} \tag{1.2.25}$$

As the pH of a solution increases, the hydroxyl concentration ($[OH^-]$) increases, which leads to a rise in the importance of the hydroxylation/dehydroxylation reaction relative to the hydration/dehydration reactions (k_{31}/k_{13}),

$$CO_2 + OH^- \underset{k_{HCO_3^-}}{\overset{k_{OH^-}}{\rightleftharpoons}} HCO_3^- \qquad (1.2.26)$$

The overall rate of CO_2 change is therefore the sum of the dehydration and dehydroxylation minus the hydration and hydroxylation reactions:

$$\frac{d([CO_2])}{dt} = (k_d[H^+][HCO_3^-] + k_{HCO_3^-}[HCO_3^-]) - (k_{CO_2}[CO_2] + k_{OH^-}[OH^-][CO_2]) \qquad (1.2.27)$$

Since $[OH^-] = \frac{K_W^*}{[H^+]}$, where K_W^* is the stoichiometric dissociation constant of water, and rearranging Eq. (1.2.27),

$$\frac{d([CO_2])}{dt} = (k_d[H^+] + k_{HCO_3^-})[HCO_3^-] - (k_{CO_2} + k_{OH^-}\frac{K_W^*}{[H^+]})[CO_2] \qquad (1.2.28)$$

Eq. (1.2.28) is essentially identical to Eq. (6) in Johnson (1982), the only difference being that the proton concentration and stoichiometric constants have been used instead of the proton activity and the thermodynamic constant in Johnson (1982). Johnson (1982) also used apparent constants for the dissociation of carbonic acid.

Equilibrium is reached when the rates of the forward and reverse reactions are equal. At equilibrium, the rates of the hydration and hydroxylation are hence equal to the rates of dehydration and dehydroxylation, respectively. In other words,

$$k_{CO_2}[CO_2] = k_d[H^+][HCO_3^-] \qquad (1.2.29)$$

and

$$k_{OH^-}[OH^-][CO_2] = k_{HCO_3^-}[HCO_3^-] \qquad (1.2.30)$$

The stoichiometric first dissociation constant of carbonic acid is therefore given by

$$K_1^* = \frac{k_{CO_2}}{k_d} = \frac{k_{OH^-}}{k_{HCO_3^-}}K_W^* = \frac{[H^+][HCO_3^-]}{[CO_2]} \qquad (1.2.31)$$

Reaction rates are temperature dependent and generally follow the Arrhenius equation:

$$k = Ae^{-E_a/RT} \tag{1.2.32}$$

where k is the rate constant, A is called the preexponential or frequency factor (i.e., collision frequency between reactant molecules), E_a is the activation energy, R is the gas constant, and T is the absolute temperature. This equation essentially denotes that as the temperature increases, the frequency of molecular collisions with kinetic energy equal or greater than E_a increases, increasing the rate constant. In the case of the isotopic disequilibrium experiments, it is preferable to keep the temperature of the experiments as low as possible for a given species, hence decreasing the rate of hydration of $^{14}CO_2$ to $H^{14}CO_3^-$ (see below).

Enzymes, such as CA or Rubisco, lower the E_a (Eq. (1.2.32)), and consequently increase the rate constant. However, an enzyme will not change the equilibrium concentration of the reactants and products, only the rate at which the equilibrium is reached. This is because an enzyme, as any catalyst, increases both the forward and reverse reaction rates to the same extent. As a result, an enzyme such as CA, which decreases the equilibration time of the carbonate species, cannot alter a carbonate species concentration to a concentration different from the one predicted based on thermodynamic equilibrium.

The above theoretical discussion of the carbonate system's equilibrium and kinetic properties will now be used to explain the principles behind the isotopic disequilibrium experiments and to model the kinetics of isotopic equilibration. The actual experimental protocol for these experiments is presented in Chapters 2 and 3.

1.3. Isotopic disequilibrium experiment

An analytical model of the ^{14}C uptake by phytoplankton during the isotopic disequilibrium experiments is presented in Appendix A. Appendix B is a MATLAB® m-file program of the analytical model presented in Appendix A. A Stella box-model of the isotopic disequilibrium experiments is presented in Figure 1.5. The box-model analytical equations are given in Appendix C. The conclusions presented below on the scope and the limitations of the isotopic disequilibrium experiments are based on these models.

The main purpose of the isotopic disequilibrium experiments is to estimate the relative contribution of HCO_3^- and CO_2 to the overall photosynthetic inorganic carbon uptake and to understand quantitatively the functioning of CCMs. An isotopic disequilibrium is created by the addition of tracer levels of ^{14}C to phytoplankton cultures. The ^{14}C pulse is sufficient to perturb the isotopic equilibrium but not enough to perturb the overall chemical equilibrium. The initial temporary isotopic disequilibrium allows differentiation between CO_2 and HCO_3^- uptake. The radioactive signal at some time t is the temporally integrated accumulation of ^{14}C tracer into the organic matter. The accumulation of ^{14}C into cells is dependent on the kinetic variation in specific activity of ^{14}C with respect to time (change in time in radioactive carbonate species distribution) and on chemical fractionation by phytoplankton (i.e., cells may preferentially take up CO_2 or HCO_3^-). The latter is the parameter under study. In the next section, an equation is derived that describes the kinetics of the change in the $^{14}CO_2$ activity after a $^{14}CO_2$ pulse.

Kinetics of the isotopic disequilibrium experiment $^{14}CO_2$ pulse

Because the equilibration between HCO_3^- and CO_3^{2-} is fast relative to the CO_2 and HCO_3^- equilibration, we can assume that HCO_3^- and CO_3^{2-} are in constant equilibrium. Hence, we can assume that the isotopic equilibrium in the HCO_3^--CO_3^{2-} system after the $^{14}CO_2$ pulse is reached instantaneously and that:

$$[H^{14}CO_3^-]/([H^{14}CO_3^-]+[^{14}CO_3^{2-}]) = [HCO_3^-]/([HCO_3^-]+[CO_3^{2-}]) = \Omega_b \qquad (1.3.1)$$

Similar to Eq. (1.2.9), the sum of all the inorganic radiocarbon is

$$[DI^{14}C] = [^{14}CO_2]+[H^{14}CO_3^-]+[^{14}CO_3^{2-}] \qquad (1.3.2)$$

Eq. (1.2.28) also holds for the radiocarbon

$$\frac{d([^{14}CO_2])}{dt} = k_2[H^{14}CO_3^-]-k_1[^{14}CO_2] \qquad (1.3.3)$$

where

$$k_1 = (k_{CO_2} + k_{OH^-}\frac{K_W^*}{[H^+]}) \qquad (1.3.4)$$

and

$$k_2 = (k_d[H^+]+k_{HCO_3^-}) \qquad (1.3.5)$$

From Eqs. (1.3.1), (1.3.2) and (1.3.3),

$$\frac{d([^{14}CO_2])}{dt} = k_2\Omega_b([DI^{14}C]-[^{14}CO_2])-k_1[^{14}CO_2] \qquad (1.3.6)$$

or

$$\frac{d([^{14}CO_2])}{dt} + (k_2\Omega_b + k_1)[^{14}CO_2] = k_2\Omega_b[DI^{14}C] \qquad (1.3.7)$$

which is a first-order linear differential equation with the solution

$$[^{14}CO_2] = \frac{k_2\Omega_b[DI^{14}C]}{(k_2\Omega_b + k_1)} + ce^{-(k_2\Omega_b + k_1)t} \quad (1.3.8)$$

At t=0, $[^{14}CO_2]_o = \frac{k_2\Omega_b[DI^{14}C]}{(k_2\Omega_b + k_1)} + c$. However, at time=0, $[^{14}CO_2]_o = [DI^{14}C]$, and therefore

$$c = [DI^{14}C]\left(\frac{1}{(k_2\Omega_b/k_1 + 1)}\right) \quad (1.3.9)$$

From Eqs. (1.3.8) and (1.3.9),

$$[^{14}CO_2] = \frac{[DI^{14}C]}{(k_1 + k_2\Omega_b)}(k_2\Omega_b + k_1e^{-(k_2\Omega_b + k_1)t}) \quad (1.3.10)$$

Eq. (1.3.10) is similar to the one derived by Lehman (1978). A comparable equation is also derived in Appendix A for the modeled isotopic disequilibrium experiments. In the next section, a discussion is presented that describes the importance of controlling the temperature and the pH during the isotopic disequilibrium experiments.

Dependence of $^{14}CO_2$ equilibration on temperature and pH

As discussed in the section on kinetics of the carbonate system, because of the temperature dependence of the kinetic rates (Eq. (1.2.32)), low temperatures are preferable for the isotopic disequilibrium experiments since the initial slope is estimated based on the 10-second point, at which time some of the $^{14}CO_2$ may already be converted to $H^{14}CO_3$. Slowing down the kinetics of CO_2 to HCO_3^- conversion by decreasing the temperature of the experiments allows a more accurate estimate of the initial slope. A correction factor to the % CO_2 can be applied to account for the decrease in CO_2 uptake

associated with the conversion of CO_2 to HCO_3^- in the first 10 seconds (see Chapter 2). Figure 1.6 shows the change in CO_2 specific activity (after a $^{14}CO_2$ spike) over time as a function of temperature. The rate of CO_2 conversion to HCO_3^- is greatly reduced at 4°C. Figure 1.7a presents a theoretical model of ^{14}C uptake (in the case of a $^{14}CO_2$ pulse and 100% CO_2 uptake) over 12 minutes as a function of temperature. Figure 1.7b is a magnification of the 0-10 seconds portion of Figure 1.7a. The measurement of the initial slope is, in some of the experiments, only based on a linear regression of two points, the time 0 (^{14}C in the organic pool at time zero is theoretically 0), and 10 seconds. In some of the cold-water experiments (Chapter 3), estimates of the initial slopes were based on a linear-least-squares fit of a few points up to 40 to 60 seconds. An estimate of the initial slope based solely on the 10-second point underestimates the true initial slope by about 3% in the case of a 4°C experiment, and by almost 40% at 28°C. It is therefore preferable to perform isotopic disequilibrium experiments at low temperatures such as on Southern Ocean phytoplankton species (Chapter 3). Ten seconds was the earliest sampling time to allow for complete mixing of the $^{14}CO_2$ spike and for other technical reasons. Because the specific activity of the CO_2 initially decreases exponentially (Figure 1.6), the initial slope determined by a linear model is likely to underestimate the true initial slope. For this reason, the estimate of the ratio of carbon dioxide uptake to total inorganic uptake is regarded as a lower limit.

The rate of $^{14}CO_2$ disappearance after a $^{14}CO_2$ pulse (Eq. (1.3.10)) is also dependent on the proton concentration, as k_1 and k_2, are dependent on the $[H^+]$ (Eqs. (1.3.4) and (1.3.5), respectively). Figure 1.8 shows the dependence of the equilibration time of $^{14}CO_2$ on pH. The analytical and numerical solutions (Figure 1.8 a and b,

respectively) give identical results (see Appendix D for derivation). The isotopic equilibrium is reached when $H^{14}CO_3^-$ dehydration and dehydroxylation rates become equal to the $^{14}CO_2$ hydration and hydroxylation rates, respectively. Graphically, isotopic equilibrium is reached when there is no more change in the $^{14}CO_2$ activity (i.e., the slope becomes parallel to the x-axis). Between the pH values of 7 and 8, the isotopic equilibration time is the longest (Figure 1.8). Figure 1.9 illustrates the dependence of the $^{14}CO_2$ equilibration, represented by the relaxation time (τ), on pH and temperature (see Appendix E). τ is the time it takes for the substrate (in this case $^{14}CO_2$) to reach (1/e) of its original concentration and is equal to the inverse of the rate constant (τ=1/k) (Zeebe and Wolf-Gladrow 2001). For example, at a pH of 9, τ is approximately 46 seconds at 5°C and less than 4 seconds at 25°C. In other words, the % CO_2 uptake based on a 4-second sampling time (initial slope estimate) at a pH of 9 and temperature of 25°C would be underestimated by about 63% (1-1/e). This again stresses the temperature dependence of the $^{14}CO_2$ equilibration time, but also emphasizes the importance of keeping the pH of the isotopic disequilibrium experiments between 7.5 and 8.5, where the isotopic equilibration time is the longest. Accordingly, one should be careful in interpreting the results of isotopic disequilibrium experiments on batch cultures with pH values that exceed 9 because of the depletion of the CO_2 pool.

<u>$^{14}CO_2$ vs. $H^{14}CO_3^-$ pulse</u>

If $^{14}CO_2$ is injected and the cells assimilate only CO_2, the initial uptake of the radioactive carbon will be fast relative to the isotopic steady-state uptake. As the $^{14}CO_2$ equilibrates with the bicarbonate pool, the rate of assimilation of ^{14}C will slow down. If

the cells assimilate only bicarbonate, the uptake will initially be zero and will increase as the $^{14}CO_2$ is converted to $H^{14}CO_3^-$. If instead $H^{14}CO_3^-$ is injected, and the cells assimilate only CO_2, the initial uptake rate will be zero, and as the $H^{14}CO_3^-$ equilibrates with the carbon dioxide pool, the uptake rate will increase. If the cells assimilate only HCO_3^-, the change in uptake rate relative to the equilibrium uptake rate would be small since the specific activity of a 100% $H^{14}CO_3^-$ injection is very close to the specific activity of bicarbonate in seawater. This is because, as discussed in the thermodynamic equilibrium of the carbonate system section, HCO_3^- represents 86.5 % of the DIC in normal seawater. Because HCO_3^- and CO_3^{2-} equilibrate almost instantaneously, they can be regarded as one pool, and they jointly correspond to 99.5 % of the DIC of seawater at equilibrium. Hence, because the change in specific activity in the case of a $H^{14}CO_3^-$ pulse is small, it is very difficult if not impossible (especially if the cells are taking up only bicarbonate) to draw any conclusions from a $H^{14}CO_3^-$ pulse only. Figure 1.10 shows that the change in specific activity in both the HCO_3^- and the CO_2 pool is much greater in the case of a pH=3.2 ($^{14}CO_2$) injection than in the case of a pH=8.7 ($H^{14}CO_3^-$) injection. Hence, one cannot draw conclusions based on bicarbonate uptake, as has been done in the past (Tortell et al. 1997), solely on the basis of a labeled $H^{14}CO_3^-$ pulse because the specific activity in the tracer fraction is almost the same as the one in seawater at equilibrium. This topic is discussed in more detail in Chapter 2.

In both the $H^{14}CO_3^-$ and the $^{14}CO_2$ injections, when isotopic equilibrium is reached, the accumulation of ^{14}C is linear since the specific activity in the HCO_3^- pool is the same as in the CO_2 pool at isotopic equilibrium. The proportion of DIC uptake that is CO_2 uptake after a $^{14}CO_2$ pulse is given by

$$f = (\frac{I}{F})(\frac{CO_2}{DIC}) \qquad (1.3.11)$$

where I is the initial ^{14}C uptake, right after the pulse, and F is the final ^{14}C uptake, after the isotopic equilibrium is reached (see Chapter 2 for derivation). By definition, the bicarbonate uptake will be (1-*f*).

Another important aspect to take into consideration when performing the isotopic disequilibrium experiments is the presence of extracellular CA. In the next section, we will discuss CA and its effect on the isotopic disequilibrium experiments.

Effect of external carbonic anhydrase on the isotopic disequilibrium experiments

CA is a potent zinc metalloenzyme (Molecular weight=30 000) which catalyses the reversible interconversion of carbon dioxide and bicarbonate ($HCO_3^- + H^+ \leftrightarrow CO_2 + H_2O$). It is believed to be an important physiological sink for zinc. For this reason, it has been argued that algal growth could sometimes be zinc-limited (Morel et al. 1994).

Some phytoplankton species are believed to use extracellular CA to convert bicarbonate to CO_2 for passive CO_2 diffusion. However, extracellular CA activity is only helpful to the algal cells if the CO_2 concentration in the diffusive boundary layer is lower than the equilibrium concentration. This is because CA can only bring the carbonate system to equilibrium, i.e., it cannot increase the CO_2 to a concentration greater than that of the thermodynamic predictions. Hence, if the CO_2 concentration in the vicinity of the cell is greater than the equilibrium value, the presence of extracellular CA may actually hinder inorganic carbon uptake because of the catalyzed hydration of the excess CO_2 to the less-membrane permeable HCO_3^- molecule. A CO_2 concentration in the diffusive boundary layer greater than that predicted based on chemical equilibrium could arise from

a large CO_2 efflux from the cell, as has been observed in *Synechococcus* (Tchernov et al. 1997). Moreover, if extracellular CA and mediated HCO_3^- transport are both active within the same algal cell, the two processes should be either temporally or spatially distinct, since both compete for the same substrate.

In the case of the isotopic disequilibrium experiments, extracellular CA activity increases the rate at which isotopic equilibrium in the immediate vicinity of the cell is reached. Hence, depending on CA activity, isotopic equilibrium could be reached almost instantaneously. Under such conditions, there will be no apparent surge in ^{14}C uptake and consequently one could not differentiate between CO_2 and HCO_3^- uptake. The addition of extracellular CA inhibitors, prior to the ^{14}C pulse, will maintain the isotopic disequilibrium for a longer period of time and hence allow distinction between the two types of uptake (CO_2 vs. HCO_3^-).

Carbonic anhydrase inhibitors

Most sulfonamides (e.g. ethoxyzolamide (EZA), acetazolamide (AZA), dextran-bound sulfonamide (DBS)) are potential inhibitors of CA function. EZA is a membrane permeable CA inhibitor and hence has the potential to inhibit both internal and external CA activity. AZA and DBS are presumed to be membrane impermeable and should therefore only inhibit extracellular CA. Because of its large molecular weight (approximately 6000), DBS cannot easily cross biological membranes and is accordingly probably the most reliable extracellular CA inhibitor.

The specificity of these inhibitors is still poorly understood. For instance, EZA could potentially inhibit photosystem II (PSII) activity (Stemler 1985; Badger et al. 1998)

and could also have an effect on internal carbon transport because of the similarity between carbon transport and the CA reaction mechanisms (Price and Badger 1989; Price and Badger 1989). The active sites of the proteins involved in bicarbonate transport and in bicarbonate conversion to CO_2 may be similar since their function is to bind the same molecule (HCO_3^-). In addition, there seems to be interspecific variability in the effects of EZA because of species differences in permeability of plasmalemmas (Palmqvist et al. 1994).

AZA and DBS are often used to study the importance of extracellular CA. Nonetheless, there are also many problems associated with these inhibitors. For instance, a decrease in cell affinity for C_i in the presence of AZA was observed in cells shown not to produce any external CA using the Wilbur and Anderson (1948) potentiometric method (Williams and Turpin 1987; Huertas and Lubian 1998). While the authors argue that it could be due to the infiltration of some of the AZA into the cells (and inhibition of internal CA) or to the inhibition of extracellular CA undetected by the potentiometric method, interference of AZA with bicarbonate transport (because of the parallelism between the CA reaction and C_i transport) would be consistent with their results. Despite all of the aforementioned uncertainties, inhibitor assays are still a widely used approach (usually in conjunction with the Wilbur potentiometric method) to test and inhibit CA activity (Haglund et al. 1992; Newman and Raven 1993; Merrett et al. 1996; Tortell et al. 1997).

The conventional electrometric/potentiometric method of Wilbur and Anderson (1948) is probably still the most commonly used approach for measuring CA activity. It is based on the time taken for the uncatalyzed and the catalyzed reaction to lower the pH of

a buffered CO_2-saturated solution. The results are usually given in protein normalized Wilbur-Anderson units (WA), which are basically time differences between uncatalyzed and catalyzed reactions (Haglund et al. 1992; Newman and Raven 1993; Nimer et al. 1997; Berman-Frank et al. 1998).

The specificity of DBS on *Phaeodactylum tricornutum* Utex 642, a strain that does not produce any extracellular CA (see Chapter 2), was investigated by injecting the CA inhibitor into a culture that was already at isotopic equilibrium (the ^{14}C was injected several minutes before injecting the inhibitor). If DBS exclusively inhibits extracellular CA activity, the rate of ^{14}C accumulation in the organic pool should not change because the ^{14}C is already at isotopic equilibrium in the solution. Because CA is a biological catalyst (enzyme), it can only increase the rate at which equilibrium is achieved by increasing the rates of both the forward (hydration) and the reverse (dehydration) reaction. Hence, once isotopic equilibrium is attained, the presence of a CA inhibitor should not affect the rate of uptake of the radioactive tracer, which is at that point evenly distributed between the HCO_3^- and the CO_2 pools. Assuming DBS specifically inhibits external CA activity, the slopes at isotopic equilibrium should be constant, regardless of whether DBS is present or not. The results obtained with *Phaeodactylum tricornutum* UTEX 642 confirm that DBS is extracellular CA specific and is further proof that the strain UTEX 642 does not have any external CA activity (John-McKay and Colman 1997; Satoh et al. 2001; Cassar et al. 2002).The slopes before and after DBS addition are not significantly different (Figure 1.11). However, since little or no bicarbonate uptake was detected in this strain (see Chapter 2), one cannot rule out the possibility that DBS

inhibits the HCO_3^- uptake mechanism. Similar experiments on species known to take up predominantly bicarbonate should be performed.

1.4. Discussion

^{14}C isotopic disequilibrium experiments similar to those presented in Chapters 2 and 3 have been performed in the past (Espie and Colman 1986; Espie et al. 1986; Korb et al. 1997; Elzenga et al. 2000). However, some of their results were semi-quantitative (Korb et al. 1997). Espie and Colman (1986) nonetheless presented equations to quantitatively predict the shape of the short-term ^{14}C experiments assuming carbon dioxide or bicarbonate uptake alone. By comparing the theoretical curve and the empirical results, they could appraise the ratio of bicarbonate to carbon dioxide uptake. According to their model, the difference between the actual and the predicted (predicted assuming 100% CO_2 uptake) intercepts represents the HCO_3^- contribution to the DIC uptake. However, because of the plateau we observed 60 seconds after the tracer injection in some experiments (Figure 2.1), we believe this method cannot be used, unless the theoretical model includes a transient slowdown in ^{14}C incorporation. If the plateaus are caused by photorespiration, the model of Espie and Colman (1986) could be used by suppressing it (e.g., increased CO_2 concentration). Here, an approach is presented based on modeling the short-term incorporation of the ^{14}C. This allows for quantitative estimation of the CO_2/ HCO_3^- uptake ratio based on the slope right after the radiocarbon injection (initial slope) and after the isotopic equilibrium is reached (final slope), therefore circumventing the problematic plateaus. In addition, as opposed to the papers mentioned above, cells were generally not centrifuged (in some of the papers cited above,

cells were also washed) prior to the isotopic disequilibrium experiments. As mentioned by Elzenga et al. (2000), cell damage and the release of intracellular CA could occur during centrifugation, which would decrease the isotopic equilibration time and consequently cause an underestimate of the contribution of CO_2 uptake to total inorganic uptake. When possible, we performed the experiments on chemostat cultures that were at steady state, in controlled, continuous growth conditions (Chapter 2). In a nutrient limited chemostat, the phytoplankton specific growth rate at steady state is equal to the dilution rate of the growth chamber. This is determined by the pumping rate of fresh growth medium. The growth rate is hence the outflow rate divided by the growth chamber volume (Laws and Bannister 1980). However, in our field study (Chapter 3), cells had to be concentrated by filtration in order to get a signal, with all the complications discussed above.

Limits on the scope of the short-term ^{14}C experiments

The short-term ^{14}C method may not work at extremely low CO_2 concentrations for several reasons:

- First, the difference between the CO_2 concentration in the bulk medium and the cell's diffusive boundary layer may not be negligible at high growth rate and low DIC (Wolf-Gladrow and Riebesell 1997; Laws et al. 1998).
- Second, at low seawater carbon dioxide concentrations ($[CO_2]_{sw}$), the ^{14}C pulse is significant relative to the $[CO_2]_{sw}$ and hence will perturb the chemical equilibrium between bicarbonate and carbon dioxide. Thus, negligible amounts of ^{14}C tracer must be added. Under conditions of high growth rate and low DIC, the tracer may represent a

significant fraction of the CO_2 present. Under such conditions, no conclusion can be drawn. Espie et al. (1986) have determined that an increase by less than 2% of the CO_2 concentration does not produce a detectable change in oxygen evolution. Hence, results of experiments where the ^{14}C pulse is more than 2% of the CO_2 concentration present in solution should be treated cautiously as the CO_2 uptake may be overestimated. Although the ^{14}C addition is insignificant relative to the [DIC], it is non-negligible when the $[CO_2]_{sw}$ is of the same order of magnitude as the $^{14}CO_2$ initial concentration (approximately 0.4 μM). Under such conditions, the assumption of chemical equilibrium is not satisfied. The use of high specific activity ^{14}C (50-62 mCi/mmol) allows one to partially circumvent this problem. The decay constant of the carbon nuclei is [ln(2)/5730] yr^{-1} ($t_{1/2_{^{14}C}}$ = 5730 years), or 1.21×10^{-4} yr^{-1}, or 2.30×10^{-10} $(min)^{-1}$. Radioactivities of 50-62 mCi are equivalent to decay rates (dN/dt) of 1.11×10^{11}-1.3764×10^{11} dpm. Since dN/dt = λN, N=4.82×10^{20}-5.98×10^{20}, and since there are 6.02217×10^{20} atoms of carbon per mmol, the ratio of radiocarbon to total carbon in the ^{14}C pulse is 4.82×10^{20}-5.98×10^{20}/6.022×10^{20} or 80-99%. Most of the CO_2 in the injection is therefore radiolabeled, which lowers the chemical perturbation associated with the ^{14}C addition since less sodium bicarbonate ^{14}C is required to increase signal to noise ratio.

- Third, the high pH generally associated with a low $[CO_2]_{sw}$ significantly decreases the isotopic equilibration time, making it difficult to estimate the initial slope (see discussion above).

- Fourth, at low $[CO_2]_{sw}$ or high $\mu/[CO_2]_{sw}$ (μ is the growth rate), the uptake rate of CO_2 by the phytoplankton is of the same order of magnitude as the CO_2 chemical

turnover rate. Under these conditions, biological uptake becomes important, and the equilibrium is between bicarbonate, carbon dioxide, and the biological pool. For instance, assuming carbon dioxide uptake only, a culture taking up 0.008 μM C s^{-1} (e.g., a culture growing at 1/day, 100 μM nitrate limited, and assuming a Redfield ratio of 106:16:1), could assimilate the equivalent of the whole carbon dioxide pool every minute if $[CO_2]_{sw}$ = 0.46 μM. Such an uptake rate is nevertheless small compared to the rate of carbon dioxide chemical formation: assuming a proton ionic activity (a_H) of $1x10^{-9}$ m (pH=9) and $[HCO_3^-]$= 1.3 mM, the rate of CO_2 formation is: $(k_d a_H + k_{HCO3-})HCO_3^-$ = 0.198 μM s^{-1}, where k_d and k_{HCO3-} are kinetic rate constants and are equal to $3.52x10^4$ dm^3 mol^{-1} s^{-1} and $1.17x10^{-4}$ s^{-1}, respectively, at 25°C and 33.77 salinity (Johnson 1982). In this case, the $[CO_2]_{sw}$ approximately equals 0.43 μM.

Nonetheless, the CO_2 in the environment rarely reaches such low concentrations, except in rare cases of extreme blooms. Hence, although there is a clear limitation to the application of the short-term ^{14}C experiments, they can be used to understand carbon limitation stresses to which phytoplankton are exposed under most environmental conditions. One way to overcome some of the problems associated with low CO_2 conditions is to concentrate the cells, assuming centrifugation or filtration does not create any artifacts.

Several factors may explain the variability in the isotopic disequilibrium experimental results such as errors in the estimate of the initial and final slopes. Factors that could lower the estimate of the CO_2 contribution to carbon uptake is the time it takes for the CO_2 to reach the site of fixation (see Figures 1.1 and 1.2 for the diffusion paths in

eukaryotic microalgae and in cyanobacteria, respectively) and the time for complete mixing of the ^{14}C.

Conclusion

The isotopic disequilibrium experiments are a powerful tool to understand quantitatively CCMs in marine algae. One of the considerable advantages to performing these experiments on chemostat cultures is that the environment and the cultures are not perturbed. In the next chapter, isotopic disequilibrium experiments in conjunction with stable isotope analyses are performed on a chemostat culture in order to understand the relative contribution of CO_2 and HCO_3^- uptake to the carbon isotopic signature of marine phytoplankton. Furthermore, these experiments were performed under a wide range of CO_2 concentrations to assess the responsiveness of the CCM to environmental factors. CO_2 availability was altered by changing the carbon demand (i.e., growth rate) and the carbon supply (i.e., CO_2 concentration).

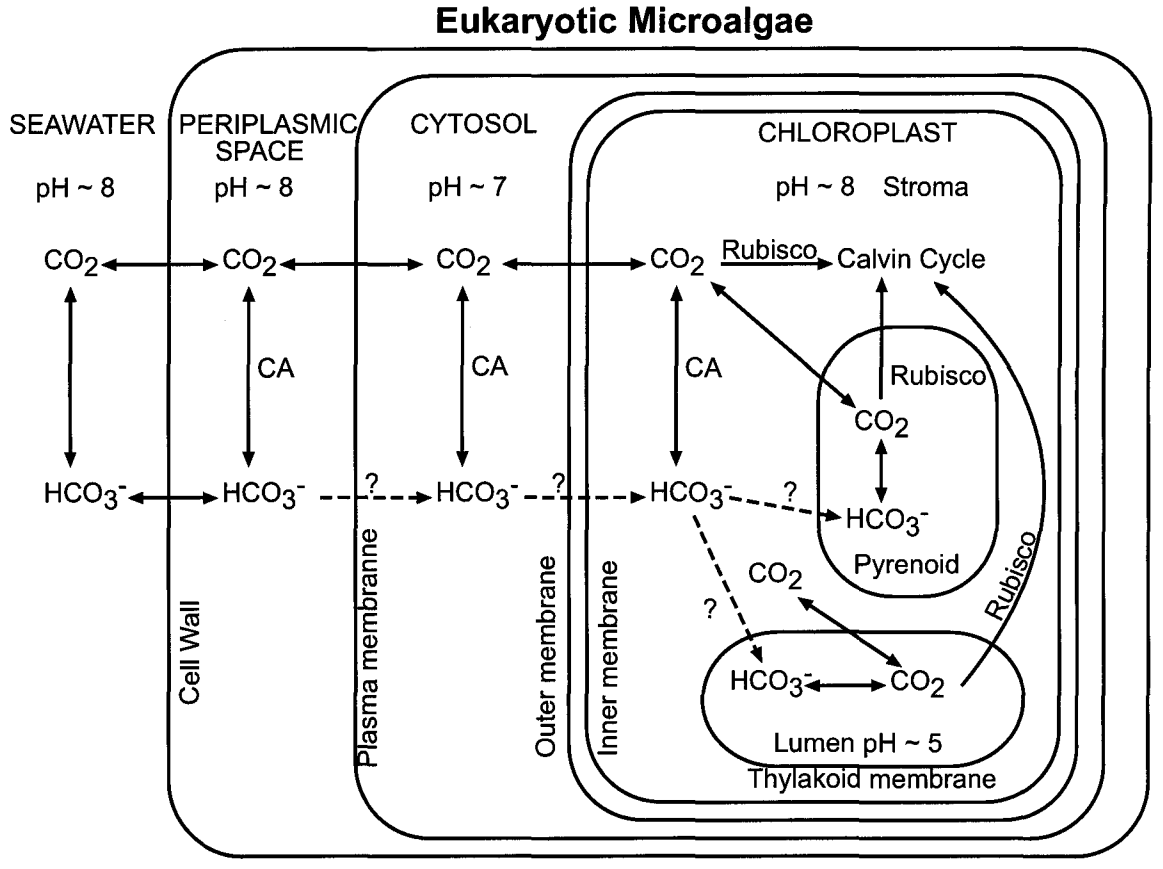

Figure 1.1. Putative CCMs in eukaryotic microalgae

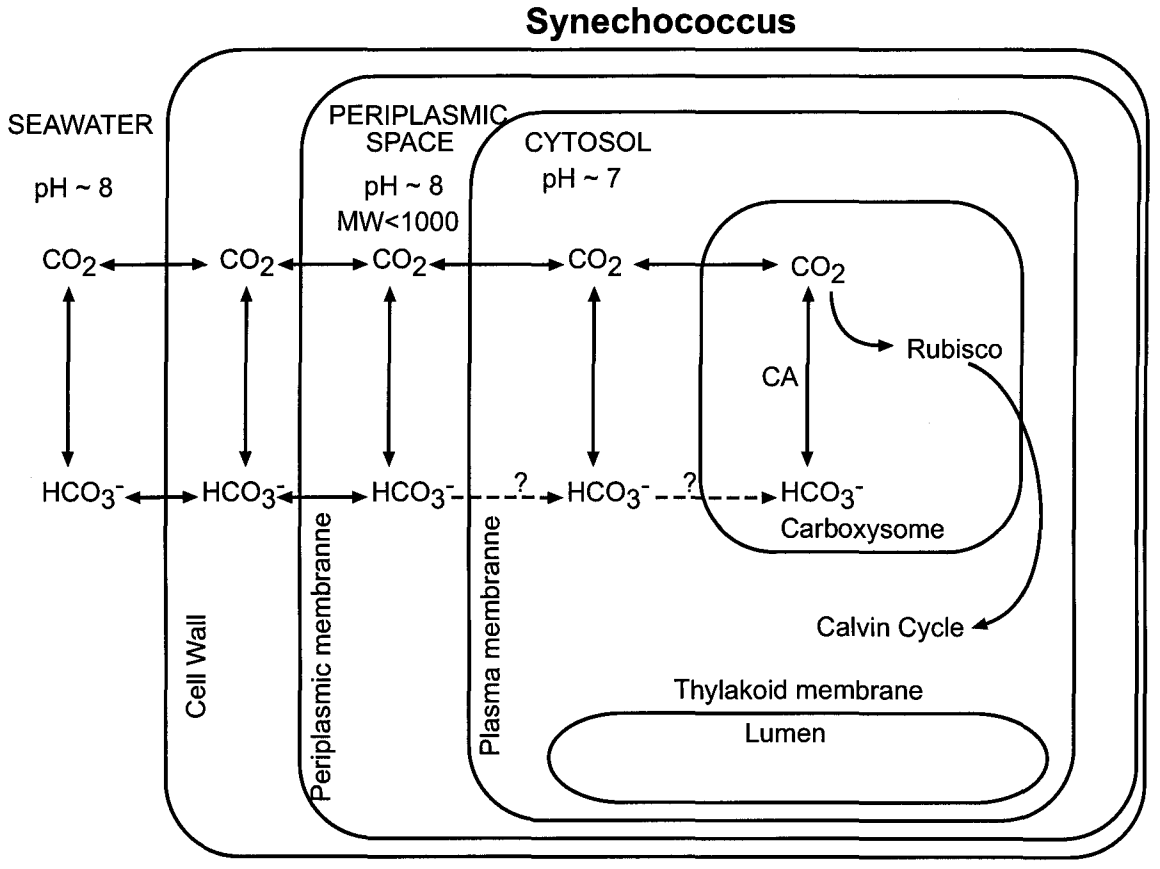

Figure 1.2. Putative CCMs in prokaryotic microalgae

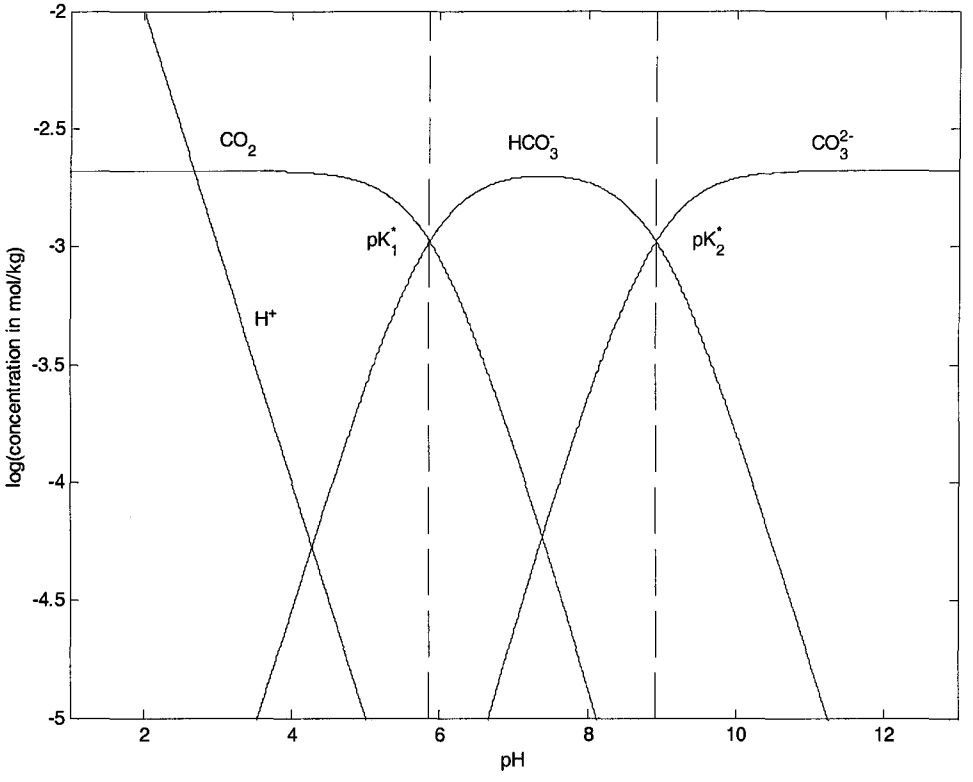

Figure 1.3. Bjerrum diagram of the carbonate system in seawater. The stoichiometric constants are for S=35 and T=25°C. DIC=2.1 mmol kg^{-1}.

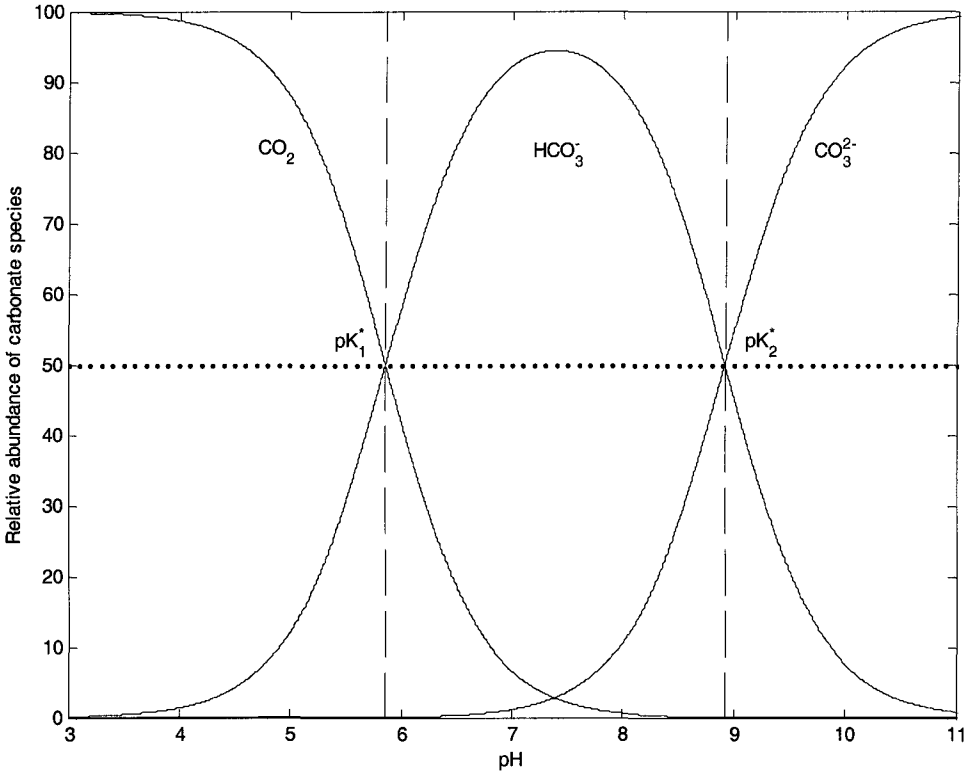

Figure 1.4. Bjerrum diagram with relative abundance of the carbonate species. The dotted line is the 50% relative abundance of HCO_3^- and CO_2 and HCO_3^- and CO_3^{2-} at pK_1^* and pK_2^*, respectively.

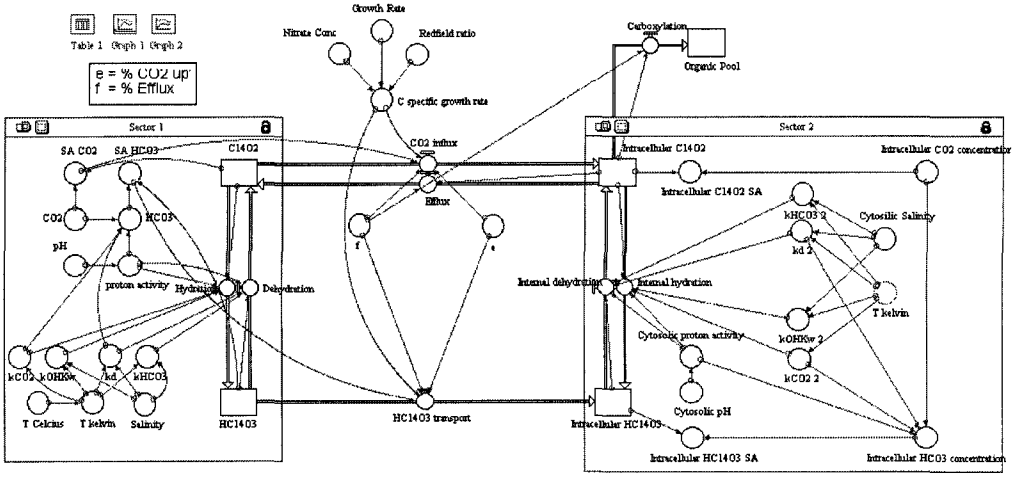

Figure 1.5. Stella box-model of the ^{14}C uptake by phytoplankton during the isotopic disequilibrium experiments. The kinetic constants are from Johnson (1982). See Appendix C for the box-model equations.

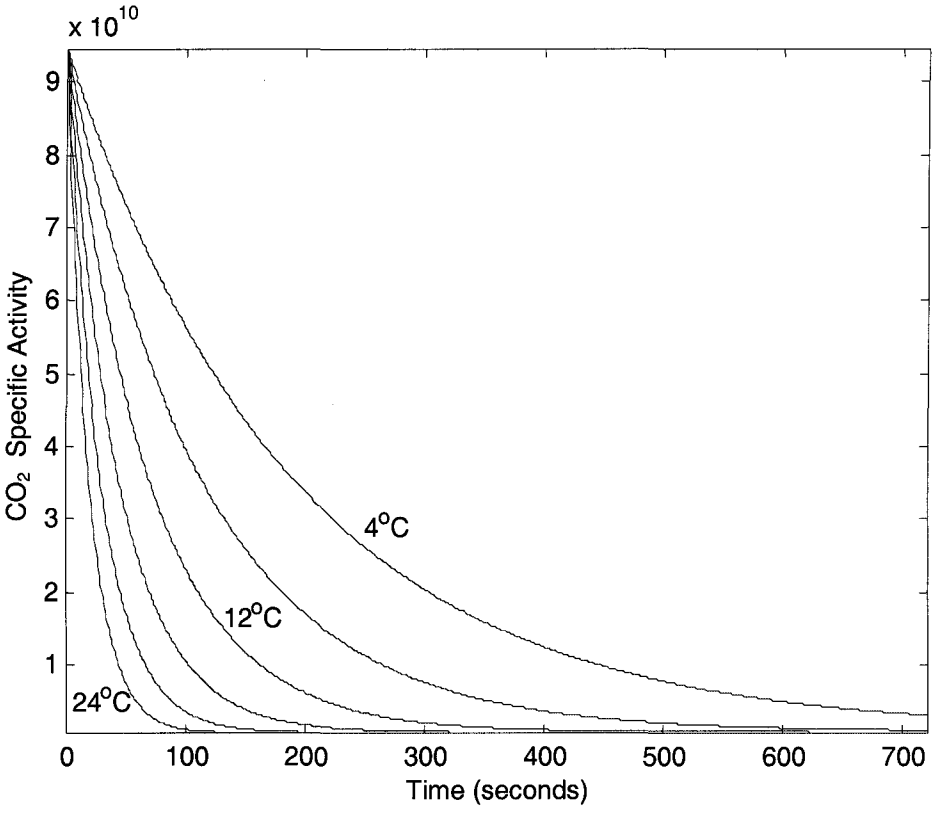

Figure 1.6. Change in CO_2 specific activity after a $^{14}CO_2$ injection in seawater as a function of temperature.

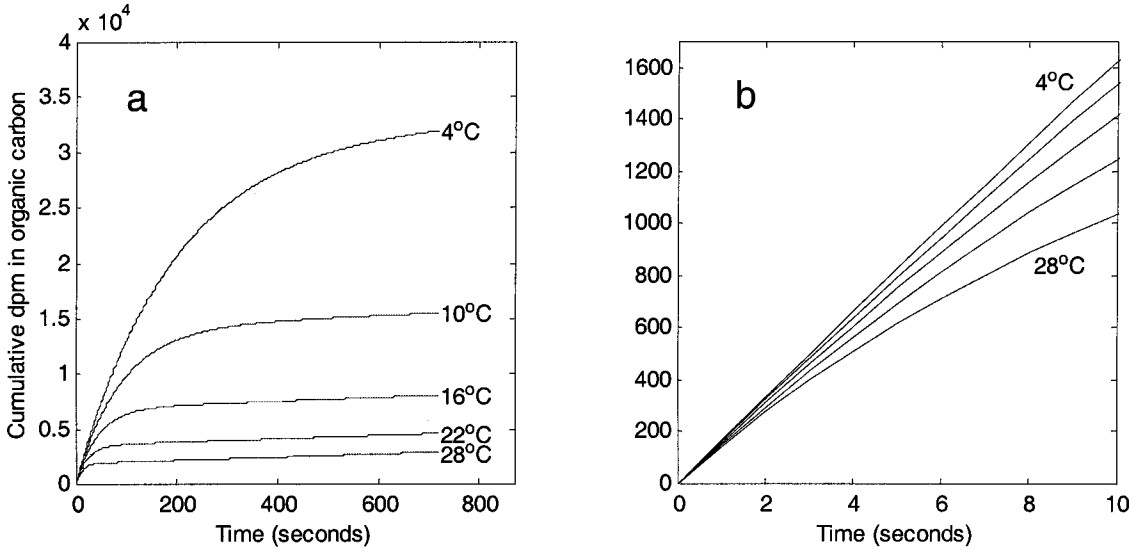

Figure 1.7. a) Theoretical radioactive carbon uptake after a $^{14}CO_2$ injection during the isotopic disequilibrium experiments assuming 100% CO_2 uptake at various temperatures. b) magnification of the 0-10 second portion of a).

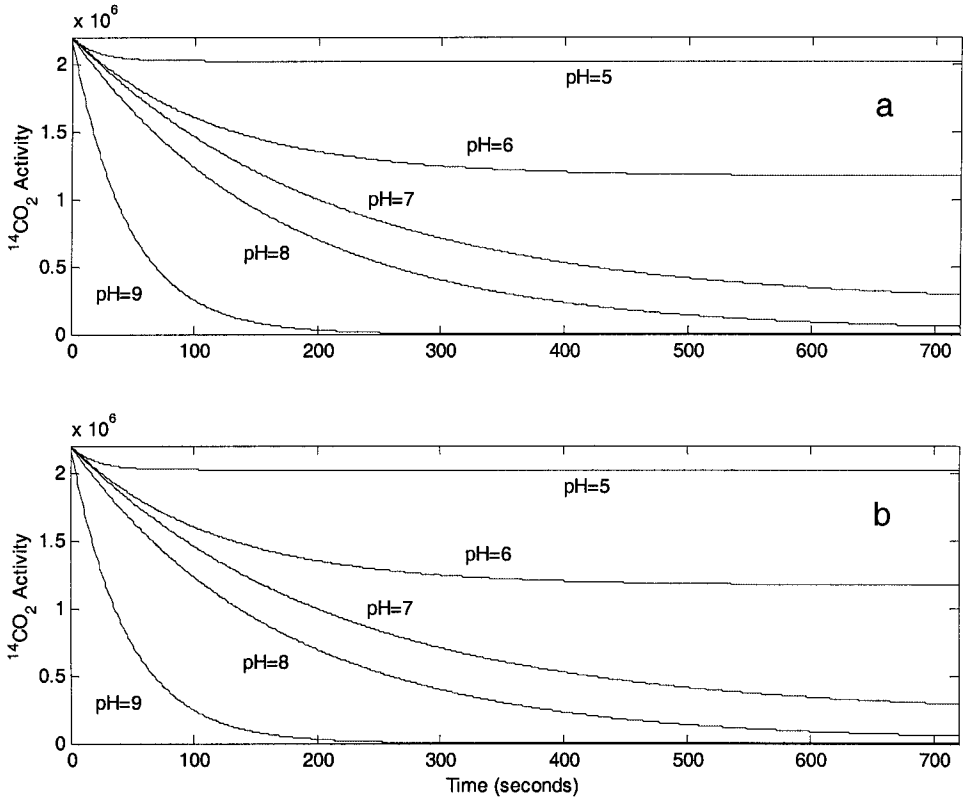

Figure 1.8. Analytical (a) and numerical (b) solutions to the equilibration time of $^{14}CO_2$ after a 1 microcurie injection of $^{14}CO_2$ at a temperature of 5°C (see Appendix D for the m-file).

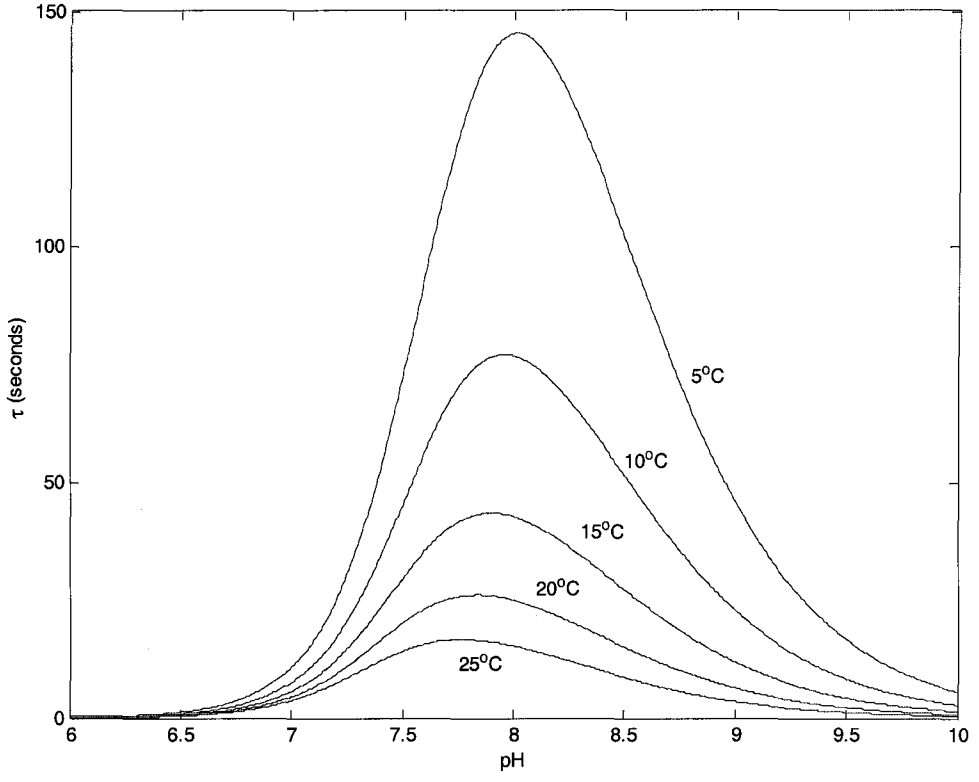

Figure 1.9. CO_2 equilibration's time (shown as τ, the relaxation time) as a function of temperature and pH (see Appendix E for the m-file).

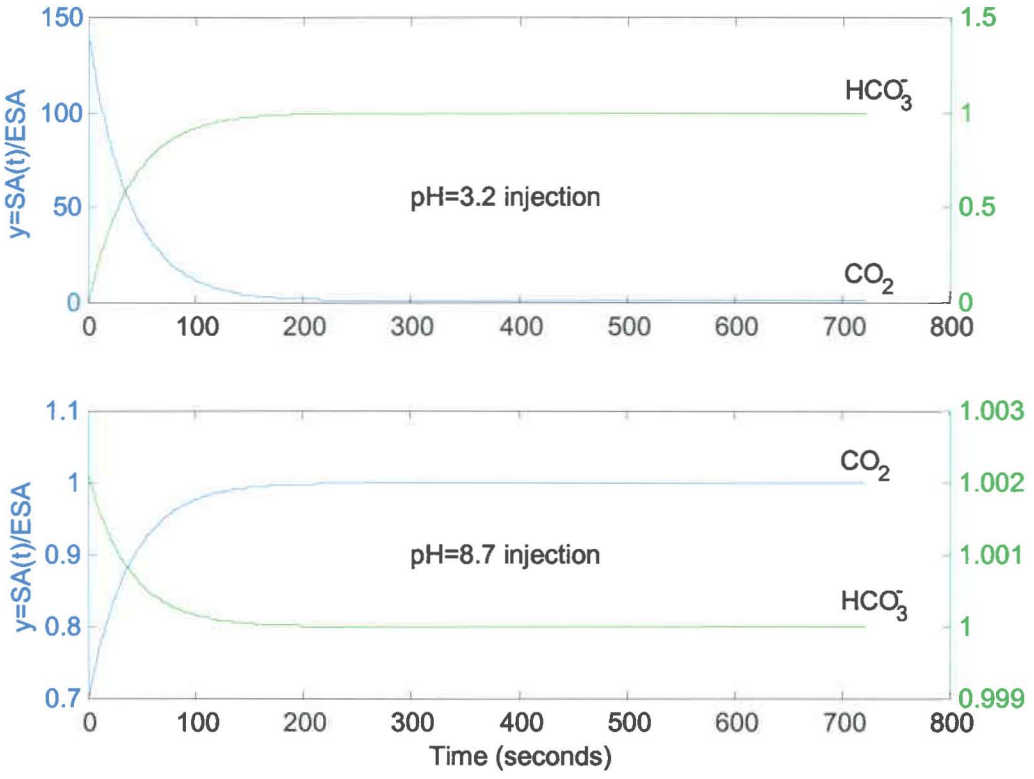

Figure 1.10. Change in specific activity over time of HCO_3^- and CO_2 after a $^{14}CO_2$ (pH=3.2) and a $H^{14}CO_3^-$ (pH=8.7) injections. The y-axes represent the specific activity at time t (SA(t)) divided by the equilibrium specific activity (ESA). The primary and secondary y-axes are for CO_2 and HCO_3^-, respectively.

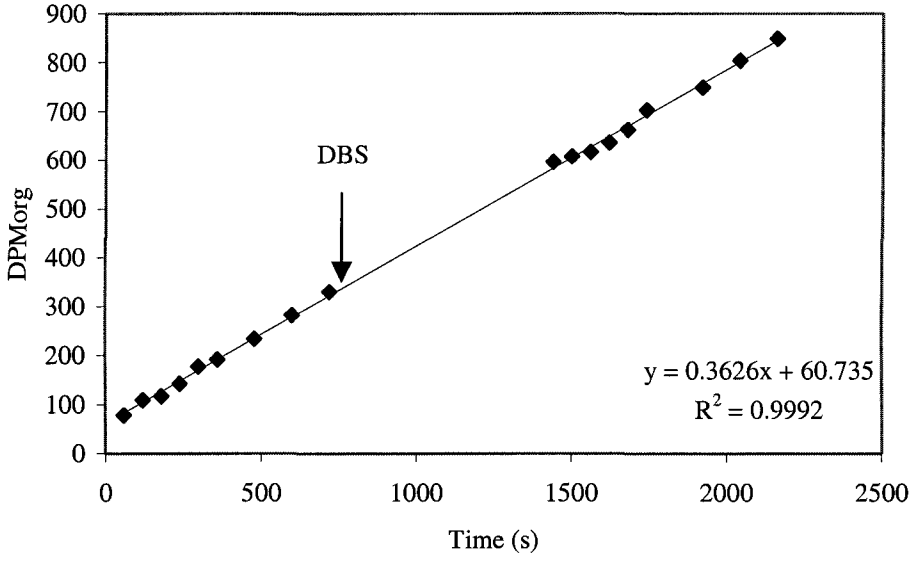

Figure 1.11. The specificity of the extracellular CA inhibitor DBS. Y-axis represents the cumulative ^{14}C in the organic phase. The vertical arrow indicates the time point at which DBS was added.

CHAPTER 2. SOURCES OF INORGANIC CARBON FOR PHOTOSYNTHESIS IN A STRAIN OF *PHAEODACTYLUM TRICORNUTUM*

Cassar, N., Edward A. Laws, Brian N. Popp, Robert R. Bidigare (2002). "Sources of inorganic carbon for photosynthesis in a strain of *Phaeodactylum tricornutum.*" Limnology and Oceanography **47**: 1192-1197.

2.1. Abstract

Diatoms are an important functional group of marine phytoplankton because of their role in the fixation of atmospheric carbon dioxide (CO_2) and transfer of organic carbon to deep waters. Carbon-concentrating-mechanisms (CCMs), such as active CO_2 and bicarbonate (HCO_3^-) uptake and carbonic anhydrase activity, are believed to be essential to marine photosynthesis, since the main carbon fixing enzyme, ribulose-1,5- bisphosphate carboxylase-oxygenase (Rubisco), is less than half saturated at normal seawater CO_2 concentrations. Based on short-term inorganic ^{14}C uptake experiments, Tortell et al. (1997, Nature 390, pp. 243-244) recently argued that marine diatoms are capable of HCO_3^- uptake. However, as discussed here, the extent of HCO_3^- uptake cannot be assessed on the basis of these experiments. Using short-term $^{14}CO_2$-disequilibrium experiments, we show that a clone of the marine diatom *Phaeodactylum tricornutum* takes up little or no HCO_3^- even under conditions of severe CO_2 limitation. Predicting the response of the oceans to increased CO_2 concentrations will require, among other things, a careful assessment of the extent to which marine algae take up HCO_3^- or CO_2. Because the plasmalemma of microalgae is gas permeable, all phytoplankton exchange CO_2 with the growth medium. Experimental results that are merely consistent with

HCO_3^- uptake are insufficient to prove that HCO_3^- uptake is occurring. Our results are in accord with predictions based on stable carbon isotopic fractionation data. Combining isotopic disequilibrium experiments with continuous growth cultures and stable isotope fractionation experiments is a powerful tool for understanding the response of oceanic primary producers to anthropogenic CO_2 emissions as well as for interpreting paleoceanographic carbon isotope data.

2.2. Introduction

Because of the effect of atmospheric CO_2 on global climate, there is increasing scientific interest in the ocean and its biota as potential sinks for anthropogenic CO_2 (Falkowski et al. 2000). An increase in atmospheric CO_2 could be buffered by a stimulation of marine photosynthesis. However, this negative feedback mechanism relies on the assumption that marine photoautotrophs are CO_2 limited and that an increase in dissolved CO_2 concentrations will intensify algal productivity (Riebesell et al. 1993).

Inorganic carbon has rarely been considered a limiting factor to marine phytoplankton growth because of its high concentration in seawater. However, less than 1% of the dissolved inorganic carbon (DIC) in seawater exists as CO_2 (Millero 1995), the substrate for ribulose-1,5-bisphosphate carboxylase/oxygenase (Rubisco). The activity of Rubisco is less than half-saturated at normal seawater CO_2 concentrations (Badger et al. 1998). To circumvent the catalytic inefficiency of Rubisco, aquatic photoautotrophs have evolved ways to actively increase the CO_2 concentration in the vicinity of Rubisco through processes called carbon-concentrating mechanisms (CCMs). Active transport of

CO_2 and/or HCO_3^-, and active conversion of HCO_3^- to CO_2 by carbonic anhydrase (CA) are putative CCMs (Badger et al. 1998).

The process by which phytoplankton acquire DIC is still the subject of debate (Laws et al. 1995; Keller and Morel 1999) and remains a methodological challenge because of the difficulty in distinguishing between HCO_3^- and CO_2 uptake. Here, we present an approach that combines the isotopic disequilibrium technique (Espie and Colman 1986) with continuous culture methodology (Laws and Bannister 1980). Combining these methods allowed us to perform short-term isotopic disequilibrium experiments directly on axenic cultures without concentrating the cells (cell damage and the release of intracellular CA could occur during the concentration of cells by centrifugation) and to estimate directly the percentage of DIC uptake accounted for by CO_2 under a variety of environmental conditions. In conjunction with the isotopic disequilibrium experiments, stable carbon isotope analyses were used to determine how changes in inorganic carbon supply and demand influenced carbon isotopic fractionation (ε_p) (Laws et al. 1995). The short-term disequilibrium results can therefore better constrain carbon isotope fractionation models used to estimate ancient CO_2 concentrations (Jasper and Hayes 1990; Bidigare et al. 1999). We chose to study *Phaeodactylum tricornutum* because, although not ecologically significant, this species has been the subject of numerous inorganic carbon uptake studies (Rees 1984; Patel and Merrett 1986; Burns and Beardall 1987; Dixon and Merrett 1988; Colman and Rotatore 1995; Rotatore et al. 1995; Iglesias-Rodriguez and Merrett 1997; Burkhardt et al. 2001).

2.3. Materials and Methods

Culture conditions

Axenic cultures of the marine diatom *Phaeodactylum tricornutum* Bohlin (Clone UTEX 642, Culture Collection of Algae MCDB, School of Biological Sciences, The University of Texas at Austin, Austin, TX 78712 USA) were grown on modified (100, or 200 μM nitrate) f/2 medium using 0.2 μm sterile filtered surface seawater collected from the Hawaii Ocean Time-series, Station ALOHA (Karl and Lukas 1996). The cultures were maintained in nitrate-limited chemostats at constant temperature (T=22°C and 16°C), salinity (34.8‰) and irradiance (21.6 mol quanta m^{-2} s^{-1}). Light was provided by a bank of daylight fluorescent bulbs. The dissolved CO_2 concentration was controlled by mixing CO_2-free air with air containing 2% CO_2 using mass flow controllers. Cell concentrations in the chemostats were approximately 10^6 cells ml^{-1} but varied depending on the growth rate.

Chemical and stable isotope analyses

Cultures were considered in steady state when the day-to-day variability in the DIC isotopic signature was within ± 0.1 ‰. Sampling for particulate organic carbon (POC) isotopic analysis and for isotopic disequilibrium experiments was not begun until the culture had completed at least four doublings at a given growth rate.

DIC and $\delta^{13}C_{DIC}$ were determined as previously described (Kroopnick 1985; Laws et al. 1995). The distribution of carbonate species was determined from temperature, salinity, total alkalinity, DIC, and phosphate and silicate concentrations (Roy et al. 1993; Millero 1995). Total alkalinity was determined by computer-controlled Gran titration.

Precision and accuracy of alkalinity and DIC measurements were less than 8 μeq kg^{-1} and 10 μM, respectively. Analytical uncertainty for the carbon isotopic analyses was less than 0.1‰.

Samples (25 ml) for isotopic analysis of POC were filtered on pre-combusted Whatman GF/F glass-fiber filters and were kept frozen until analysis. Samples were vacuum dried and oxidized (with cupric oxide at 700°C overnight) in precombusted vicor tubes. The CO_2 released from the oxidation of the POC was cryogenically distilled. The amount of CO_2 was manometrically measured to determine the POC concentration. The CO_2 isotopic signature was then measured on a MAT 252 mass spectrometer (Santrock et al. 1985).

Short-term ^{14}C disequilibrium experiments

^{14}C assays were performed on 50 ml samples taken from the chemostat at steady state. Experiments were performed at growth temperature in temperature-controlled jacketed glass beakers with magnetic stirrers. Floating semi-transparent plastic covers were used to decrease CO_2 exchange with the atmosphere.

Sodium bicarbonate ^{14}C with a specific activity of 50-62 Ci mol^{-1} (Amersham Pharmacia Biotech; code number CFA3) was diluted to a final concentration of 2 μCi ml^{-1} in deionized water that had been previously aerated with nitrogen gas (grade 5; BOC gases) overnight and boiled for one hour to remove inorganic carbon. To create the ^{14}C isotopic disequilibrium, 0.5 ml (1 μCi) of the final solution was added to the 50-ml sample in the form of $^{14}CO_2$. The $^{14}CO_2$ was prepared immediately before the short-term ^{14}C experiments by acidifying $NaH^{14}CO_3$ to a pH of about 3.2 with a 0.1% HCl solution.

The ^{14}C injection increased the dissolved CO_2 concentration by less than 5% (0.32 to 0.40 μM increase) in most cases and in no case by more than 15%. The injection decreased the pH by less than 0.1.

Samples (2 ml) were taken at timed intervals, with the first sample taken at 10 seconds. The samples were directly transferred to scintillation vials containing 0.5ml of 10% HCl to terminate ^{14}C incorporation, and left overnight in a fume hood to degas inorganic ^{14}C (carbon that had not been fixed). Overnight degassing was experimentally shown to be sufficient to eliminate the unfixed inorganic radiocarbon. Twelve ml of the liquid scintillation cocktail Aquasol-2 (Packard Bioscience) were added to each sample and the radioactive signal, which represents acid-resistant organic matter, was then measured in a Packard Tri-Carb 4640 scintillation counter.

Analytical model for the isotopic disequilibrium experiments

Carbonate (CO_3^{2-}) and HCO_3^- were considered as one pool, the HCO_3^- pool, because CO_3^{2-}/HCO_3^- interconversion is nearly instantaneous (Johnson 1982). Carbonic acid (H_2CO_3) is negligible at seawater pH (less than 1% of CO_2 concentration). Hence, in this model, DIC is the sum of HCO_3^- and CO_2. The concentrations of carbonate species (CO_2, HCO_3^-, CO_3^{2-}, and H_2CO_3) were determined from total alkalinity and total CO_2.

The initial rate of ^{14}C accumulation in the organic matter pool after addition of a $^{14}CO_2$ spike reflects only CO_2 uptake, since more than 99% of the ^{14}C is added in the form of CO_2. Hence:

$$\text{Initial rate} = R \times SA^{o}_{CO_2} = R \times SA_{DIC} \times \frac{DIC}{CO_2} \qquad (2.3.1)$$

where R is the rate of CO_2 uptake, $SA^{o}_{CO_2}$ is the initial specific activity of the CO_2, and SA_{DIC} is the specific activity of the DIC.

Once the ^{14}C spike has equilibrated with the seawater, the specific activities of all forms of inorganic carbon are identical, and the final rate of ^{14}C uptake is given by the equation

$$\text{Final rate} = U \times SA_{DIC} \qquad (2.3.2)$$

where U is the uptake rate of all forms of DIC. Hence, the ratio of the initial to final ^{14}C uptake rate is

$$\left(\frac{\text{Initial rate}}{\text{Final rate}}\right) = \frac{R \times DIC}{U \times CO_2} = f \times \frac{DIC}{CO_2} \qquad (2.3.3)$$

where f is the fraction of DIC uptake accounted for by CO_2. Hence

$$f = \left(\frac{\text{Initial rate}}{\text{Final rate}}\right) \times \left(\frac{CO_2}{DIC}\right) \qquad (2.3.4)$$

The initial rate was estimated from the activity of ^{14}C in organic carbon after 10 seconds after correcting for the temperature dependent kinetic conversion of $^{14}CO_2$ to $^{14}HCO_3^-$ using equations from Johnson (1982).

2.4. Results

Figure 2.1 shows the pattern of ^{14}C uptake during short-term isotopic disequilibrium experiments with *P. tricornutum*. The uncatalysed half-isotopic equilibration time between 16°C and 22°C at a pH of 8 is on the order of 30 seconds (Espie and Colman 1986). As expected in the case of CO_2 uptake, the initial rate of ^{14}C

uptake was much greater than the rate following isotope equilibration. Differences between curves are due to differences in growth rate, algal biomass and in the specific activity of the ^{14}C in solution. Hence, one cannot determine the relative proportion of CO_2 to HCO_3^- uptake simply by looking at the temporal increase in ^{14}C activity in the organic phase. The ratio of the initial slope to final slope and the DIC and CO_2 concentrations must be known. The values of f calculated using Eq (2.3.4) indicate that HCO_3^- uptake in *P. tricornutum* clone UTEX 642 is small (Figure 2.2a, Table 2.1). CO_2 uptake is at least 84% of the total inorganic carbon uptake, even under conditions of severe CO_2 limitation (i.e., high algal growth rate and low CO_2 concentration). Because of finite mixing and sampling times and the time required for $^{14}CO_2$ to reach the site of carbon fixation within the cell, the initial rate of uptake in Eq. (2.3.4) tends to be underestimated. Hence the figure of 84% must be regarded as a lower bound on the percentage of inorganic carbon uptake accounted for by CO_2. HCO_3^- transport could be non-existent in this clone of *P. tricornutum*, and if present, is minor and most likely constitutive.

Table 2.1. Sources of inorganic carbon for photosynthesis in a strain of *Phaeodactylum tricornutum*. Summary of the experimental results

Experiment	Temperature (°C)	μ/CO_2	DIC (μmol kg^{-1})	CO_2 (μmol kg^{-1})	ε_p (‰)	$\%CO_2$ Uptake
1	22	0.008	2329	31.3	23.42	84
2	16	0.027	1987	8.9	26.56	97
3	16	0.076	2012	12.2	19.65	88
4	22	0.123	1951	8.5	16.74	92
5	22	0.619	1654	2.3	13.80	88

No experiments with carbonic anhydrase inhibitors were performed. Since extracellular CA would decrease the time required to reach isotopic equilibrium and would therefore lower the estimate of the initial slope, isotopic disequilibrium experiments with CA inhibitors would not significantly affect the $\%CO_2$ uptake, which is already close to 100%. *P. tricornutum* clone UTEX 642 has in fact been shown not to produce external CA (John-McKay and Colman 1997).

The ratio of microalgal carbon specific growth rate to CO_2 concentration (μ/CO_2) is a useful proxy for the CO_2 demand/supply ratio. Here it was used as a surrogate for the extent of CO_2 limitation to which the microalga was exposed. A more than 75 fold increase in μ/CO_2 (0.008 to 0.619 kg μmol^{-1} d^{-1}) did not significantly change the percentage of uptake accounted for by CO_2 (84 vs. 88% CO_2 uptake, respectively; Figure 2.2a). In other words, induction of HCO_3^- transport in response to CO_2 limitation was not observed. As opposed to what has recently been proposed with respect to natural

populations (Tortell et al. 1997), not only is HCO_3^- transport across the plasmalemma in *P. tricornutum* small (if any), but it is not inducible over the range of μ/CO_2 reported in field studies (Tortell et al. 2000).

2.5. Discussion

Theoretical models predict that if passive diffusion of CO_2 accounts for all DIC uptake, the relationship between ε_p and μ/CO_2 should be linear, and indeed this is the case for *P. tricornutum* when $\mu/CO_2 \leq 0.15$ kg μmol^{-1} d^{-1} (Figure 2.2b). However, the relationship becomes distinctly nonlinear at higher μ/CO_2 (Figure2.2b), as previously reported in several laboratory and field studies on various microalgal species (Tortell et al. 2000). Because HCO_3^- uptake appears minimal and is not inducible in this clone of *P. tricornutum*, the nonlinearity of the relationship between ε_p and μ/CO_2 must reflect active uptake of CO_2, as previously suggested by Laws et al. (1997).

It has recently been argued based on short-term inorganic ^{14}C uptake experiments that HCO_3^- is an important source of inorganic carbon for diatoms (Tortell et al. 1997). This scientific correspondence, entitled "Active uptake of bicarbonate by diatoms" has been frequently cited as evidence of bicarbonate uptake (Nimer et al. 1999; Lane and Morel 2000; Taraldsvik and Myklestad 2000; Burkhardt et al. 2001; Rau et al. 2001). In the experiments presented by Tortell et al. (1997) inorganic ^{14}C equilibrated in a seawater solution (P. D. Tortell, pers. comm.) was added to natural samples of seawater dominated by large diatoms. The fact that ^{14}C uptake was observed within 10 seconds was erroneously interpreted by the authors (p. 243) as evidence of "**active uptake of HCO_3^-** in

the field", and they argued, "Carbonic anhydrase is therefore required to catalyze intracellular dehydration of **actively imported HCO_3^-**." (our emphasis). Their conclusion was based on the fact that more than 99% of the ^{14}C activity was present in the form of HCO_3^-. However, in tracer kinetics, the uptake of a labeled substrate is determined by the substrate's specific activity (e.g., activity per mol; see Eqs. (2.3.1) and (2.3.2)), not its activity (Lambrecht and Rescigno 1983; Espie and Colman 1986). Because the inorganic ^{14}C was allowed to equilibrate in a seawater solution prior to addition to the seawater samples, the specific activities of all forms of inorganic carbon were identical throughout the experiment. Hence, contrary to the authors' conclusions, the fact that uptake was observed during the first 10 seconds proved nothing regarding the form of inorganic carbon being taken up by the microalgae.

In contrast, if the inorganic ^{14}C spike is not initially in isotopic equilibrium with the inorganic carbon in the medium, the change in the rate of ^{14}C uptake as the ^{14}C equilibrates with the inorganic carbon in the medium may provide insights about the form of inorganic carbon crossing the plasmalemma (Espie and Colman 1986). The change in uptake rate will be most apparent if the spike contains ^{14}C primarily in the form of CO_2 (Elzenga et al. 2000). Under these conditions, the initial specific activity of the CO_2 in the seawater will be roughly 100 times greater than the equilibrium specific activity. The initial uptake rate of ^{14}C will therefore be roughly 100 times greater than the final uptake rate if the microalgae are taking up CO_2 exclusively. Comparison of the initial and final ^{14}C uptake rates therefore allows a quantitative assessment of the percentage of DIC uptake accounted for by CO_2 (Eq. (2.3.4) and Figure 2.1). To the extent that HCO_3^- was being taken up, a $H^{14}CO_3^-$ injection would produce only a small change in ^{14}C uptake

kinetics over time, as the change in specific activity of $H^{14}CO_3^-$ would be small (i.e., most inorganic carbon in seawater is in the form of HCO_3^-).

Our results by no means preclude the possibility that some photosynthetic eukaryotes utilize HCO_3^- as an inorganic carbon source. In some cases, HCO_3^- conversion to CO_2 is catalyzed by an external carbonic anhydrase, and CO_2 is the form of inorganic carbon that crosses the plasmalemma (Elzenga et al. 2000). Some eukaryotic microalgae may in fact actively transport HCO_3^- across the plasmalemma (Elzenga et al. 2000), but reports that microalgae take up bicarbonate to the exclusion of CO_2 must be viewed with caution (Elzenga et al. 2000), since there is no microalga whose plasmalemma is known to be impermeable to CO_2. Indeed, the fact that carbon isotopic fractionation is always observed implies that some of the internal inorganic carbon leaks out of the cell and therefore that the plasmalemma is permeable to CO_2.

Conflicting reports on carbon uptake mechanisms in *P. tricornutum* seem to be attributable to the use of different clones and growth conditions in culture studies. John-McKay and Colman (1997) found that *P. tricornutum* clone UTEX 642 lacks external CA activity. Our results are consistent with their work. Other strains of *P. tricornutum* show different levels of external CA activity (John-McKay and Colman 1997). In contrast to the work of Rees (1984), Dixon and Merrett (1988), Colman and Rotatore (1995), and Rotatore et al. (1995), we could not find evidence of direct bicarbonate transport across the plasmalemma. Burkhardt et al. (2001) recently showed that a different strain of *P. tricornutum*, also with low external CA activity, demonstrated a preference for CO_2 uptake, although HCO_3^- uptake was observed. They also found that *Thalassiosira*

weissflogii, another marine diatom, preferentially takes up HCO_3^- and concurrently has a high external CA activity. This result seems counterintuitive, since these two physiological processes (HCO_3^- transport and HCO_3^- conversion to CO_2) compete for the same substrate. Because of the apparently large intraspecific and interspecific variations in inorganic carbon uptake mechanisms among microalgae, extrapolation of our results from a single clone to natural populations or even to other clones of *P. tricornutum* is unjustified.

The methodological approach we present in this paper can be used to better understand carbon uptake in marine photoautotrophs. At issue is whether the form of inorganic carbon that crosses the plasmalemma is HCO_3^- or CO_2. There is no question that some active transport is required in almost all cases. The fact that we did not observe an increase in HCO_3^- uptake in response to CO_2 limitation does not preclude the presence of an inducible active CO_2 uptake mechanism. The short-term disequilibrium experiments only tell which form of inorganic carbon crosses the plasmalemma, not whether this transport is active or passive. Hence, it is probable that as μ/CO_2 became large, the cells were actively taking up CO_2. In fact, Rotatore et al. (1995) found evidence of active CO_2 transport in this particular strain of *P. tricornutum* (UTEX 642).

To predict the response of the biological pump and oceanic carbon sequestration to increases in dissolved CO_2 concentrations, it will be important to perform definitive experiments to determine what forms of inorganic carbon are transported in various phytoplankton species. Isotopic disequilibrium experiments carried out on continuous

growth cultures in combination with stable isotope fractionation experiments provide a powerful mechanism for addressing this question.

2.6. Acknowledgements

We wish to thank Terri Rust and David Hashimoto for help with isotopic analyses and laboratory cultures. We are also grateful to the HOT program and its personnel for their assistance in collecting the seawater for media. This research was partially supported by National Science Foundation grants OCE-9633091 (BNP, RRB, EAL and Stuart G. Wakeham), OCE-9521332 (BNP and EAL) and OCE-9725966 (EAL) and by a NSERC scholarship to N. C. This is SOEST contribution number 5932

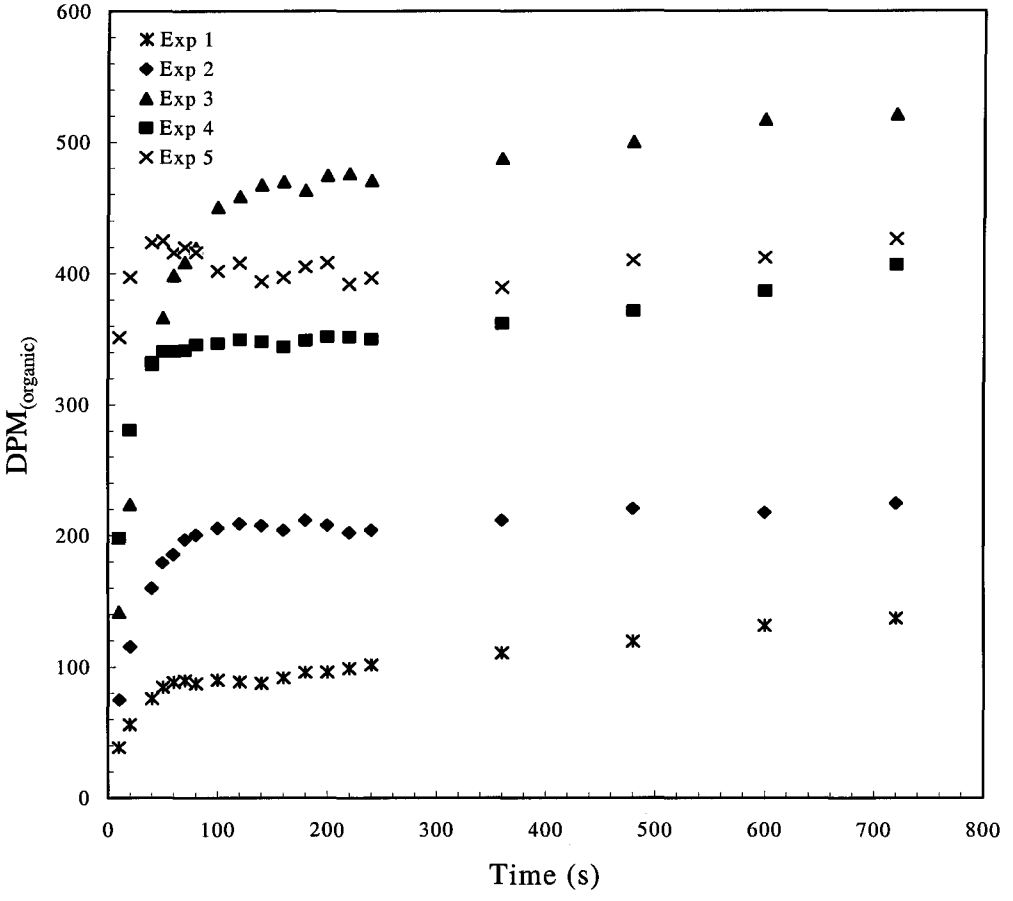

Figure 2.1. Examples of the results of short-term ^{14}C experiments with *P. tricornutum* (clone UTEX 642). Each curve represents the average of 2 to 4 experiments. $DPM_{(organic)}$ is the activity in the acid-resistant organic matter. The variations between curves are due to differences in specific activity, algal growth and density.

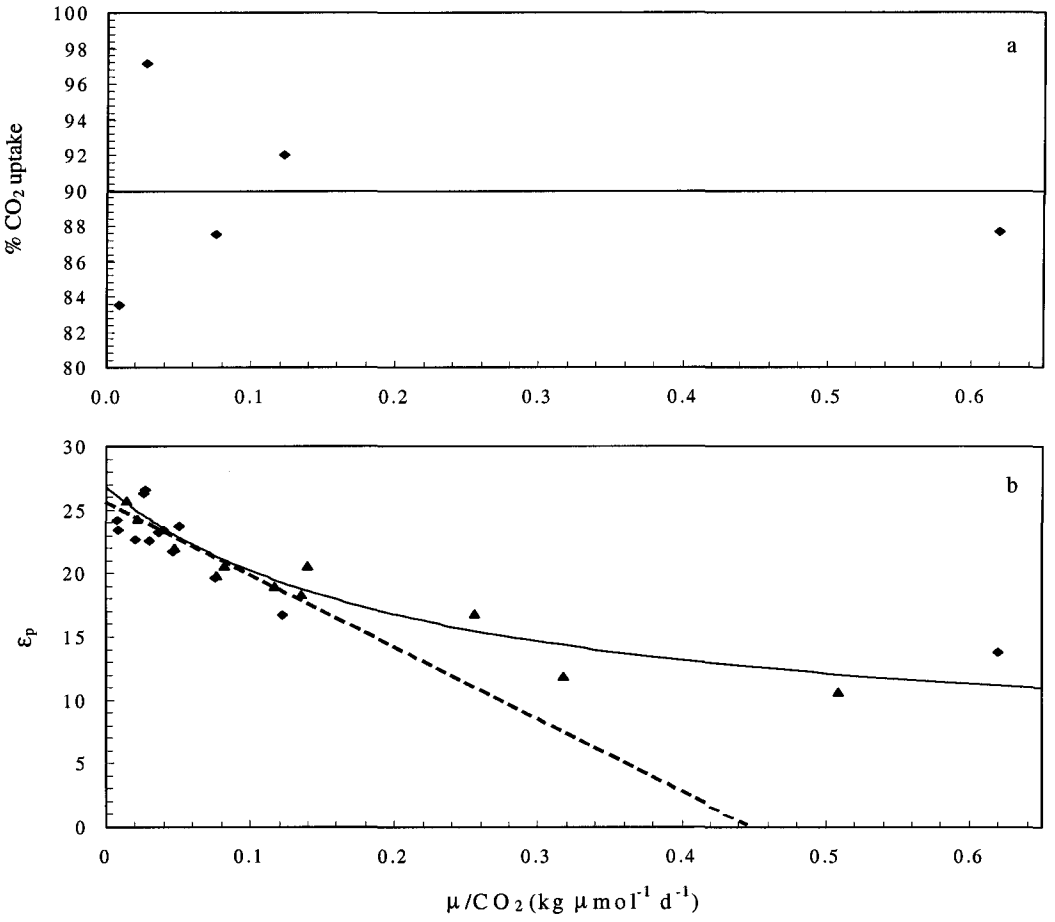

Figure 2.2. CO_2 uptake and isotopic fractionation by *Phaeodactylum tricornutum*. **a)** Percent CO_2 uptake, as determined by the isotopic disequilibrium experiments, versus μ/CO_2 for *P. tricornutum* (clone UTEX 642). Each point is the average of 2 to 4 experiments. The horizontal line is the average $\%CO_2$ uptake (90%). The standard errors vary from 2.6 % ($\mu/CO_2 = 0.619$) to 16.7 % ($\mu/CO_2 = 0.027$). **b)** Carbon isotope fractionation (ε_p) versus μ/CO_2 for *P. tricornutum* (diamonds, this study). The standard error of the ε_p is $\pm$ 0.05‰, and the standard error of the μ/CO_2 measurements is about $\pm$ 5% of the mean value at the given growth rate. Triangle symbols are *P. tricornutum* (clone CCMP1327) data from Laws et al. (1997). Diamond symbols are from this study. The dashed line is the relationship between ε_p and μ/CO_2 predicted by the passive diffusion model of Laws et al. (1995). The continuous line is a non-linear fit to the data (see Laws et al. 1997).

CHAPTER 3. BICARBONATE UPTAKE BY SOUTHERN OCEAN PHYTOPLANKTON

Cassar, N., Edward A. Laws, Robert R. Bidigare, Brian N. Popp. "Bicarbonate uptake by Southern Ocean phytoplankton". Submitted to Global Biogeochemical Cycles.

3.1. Abstract

Marine phytoplankton have the potential to significantly buffer future increases in atmospheric carbon dioxide levels. However, in order for CO_2 fertilization to have an effect on carbon sequestration to the deep ocean, the increase in dissolved CO_2 must stimulate primary productivity, i.e., marine phototrophs must be CO_2 limited (Riebesell et al. 1993). Estimation of the extent of bicarbonate (HCO_3^-) uptake in the oceans is therefore required to determine whether the anthropogenic carbon sources will enhance carbon flux to the deep ocean. Using short-term $^{14}CO_2$-disequilibrium experiments during the Southern Ocean Iron Experiment (SOFeX), we show that HCO_3^- uptake by Southern Ocean phytoplankton is significant. Since the majority of dissolved inorganic carbon (DIC) in the ocean is in the form of bicarbonate, the biological pump may therefore be insensitive to anthropogenic CO_2. Approximately half of the DIC uptake observed was attributable to direct HCO_3^- uptake, the other half being direct CO_2 uptake mediated either by passive diffusion or active uptake mechanisms. The increase in growth rates and decrease in CO_2 concentration associated with the iron fertilization did not trigger any noticeable changes in the mode of DIC acquisition, indicating that under most environmental conditions the carbon concentrating mechanism (CCM) is constitutive. A low-CO_2 treatment induced an increase in uptake of CO_2, which we attributed to increased extracellular carbonic anhydrase activity, at the expense of direct HCO_3^-

transport across the plasmalemma. Isotopic disequilibrium experiments results are consistent with Southern Ocean carbon stable isotope fractionation data from this and other studies. Although iron fertilization has been shown to significantly enhance phytoplankton growth and may potentially increase carbon flux to the deep ocean, an important source of the inorganic carbon taken up by phytoplankton in this study was HCO_3^-, whose concentration is negligibly affected by the anthropogenic rise in CO_2. We conclude that biological productivity in this region of the world's ocean is unlikely to be directly regulated by natural or anthropogenic variations in atmospheric CO_2 concentrations because of the presence of a constitutive CCM.

3.2. Introduction

Polar regions of the world's ocean are thought to play a critical role in the control of atmospheric CO_2 because of the interaction of deep-water masses with the atmosphere in these areas. Changes in primary productivity and water column stratification in these regions have been argued to regulate atmospheric CO_2 and transitions from glacial to interglacial periods (Knox and McElroy 1984; Sarmiento and Toggweiler 1984; Siegenthaler and Wenk 1984; Francois et al. 1997).

Increases in atmospheric iron deposition to the Southern Ocean may have been partly responsible for these changes in phytoplankton productivity (Martin 1990; Martin et al. 1990), which in turn may have regulated paleo-atmospheric CO_2 concentrations. The principal objective of the Southern Ocean Iron Experiment (SOFeX) cruise (January 5 – February 26, 2002) was to better understand the role of iron in the transfer of organic carbon to the deep sea, i.e., the role of the biological carbon pump, which is a crucial

component of the global carbon cycle (Sarmiento and Le Quere 1996). Understanding the carbon uptake mechanisms in Southern Ocean algal communities and their response to iron fertilization is crucial to elucidating the role of phytoplankton in the regulation of atmospheric CO_2.

CO_2 limitation has been shown to be significant in terrestrial environments (Porter and Grodzinski 1985; Idso and Kimball 1991; Long and Drake 1991). Riebesell et al. (1993) hypothesized that CO_2 could also regulate productivity in the oceans. However, in the marine realm, the presence of CCMs, which play a role similar to C_4 and CAM pathways in terrestrial plants, could alleviate CO_2 limitation. Direct transport of HCO_3^- and CO_2 and extracellular conversion of HCO_3^- to CO_2 through the catalytic activity of carbonic anhydrase are believed to be important carbon concentrating mechanisms (CCMs) in marine phytoplankton (see review by Raven 1997).

Although the dissolved inorganic carbon pool (DIC) may be large (~ 2 mM under ambient conditions), $CO_2(aq)$, the substrate for ribulose-1,5-bisphosphate carboxylase/oxygenase (Rubisco) during marine microalgal photosynthesis, is less than 1% of the DIC (Skirrow and Whitfield 1975; Millero 1995). Under these conditions, the activity of Rubisco is less than half-saturated (Badger et al. 1998). In order for marine primary producers to significantly respond to changes in atmospheric CO_2, whether due to short-term anthropogenic emissions or long-term geological cycles, their uptake of inorganic carbon must involve passive CO_2 diffusion primarily. Concentrations of HCO_3^-, the other potential photosynthetic substrate, are relatively large and not significantly affected by changes in atmospheric CO_2. In this study, we performed *in vivo* studies to investigate the ability of Southern Ocean phytoplankton communities to actively take up

DIC and the CCM response to changes in phytoplankton biomass/composition and carbonate system parameters associated with iron enrichment. The algal assemblage in this region of the world's ocean is typically dominated by diatoms, which are more likely to be CO_2 limited than smaller cells (Riebesell et al. 1993) and which are responsible for much of the deep ocean carbon export in the Southern Ocean (Bathmann 1998; Buesseler et al. 2001; Daly et al. 2001; Anadon et al. 2002).

3.3. Material and Methods

Sampling and field experiments were conducted during the Southern Ocean Iron Experiment (SOFeX) expedition onboard the R/V *Revelle* and R/V *Melville* in the Pacific sector of the Southern Ocean during January - February 2002. Stations were occupied along 172°W longitude, north (56°S) and south (66 °S) of the Antarctic Polar Frontal Zone (APFZ). This region of the Southern Ocean is considered to be a high-nitrate low-chlorophyll (HNLC) area. However, silicate concentrations (<3 μM) north of the APFZ are distinctly lower than south (~64 μM) of the APFZ. During this expedition, *in situ* iron enrichment experiments were performed in both locations and designated as the Northern Patch (NP) and Southern Patch (SP), respectively (Figure 3.1). Iron (1.2 nM) was initially added to the northern site on year day (YD) 13 (designated as t_o), and two subsequent infusions were performed 3 (1.2 nM) and 27 (1.5 nM) days after the initial enrichment. Iron (0.7 nM) was initially added to the southern site on YD 25 (designated as t_o), and three additional infusions (0.7 nM Fe each) were performed 4, 8 and 11 days after the initial addition. Additional details regarding the SOFeX expedition can be found at http://www.mbari.org/expeditions/SOFeX2002/.

Large-volume particulate organic matter (POM) samples (85-130 L) were collected on 142 mm combusted Whatman GF/F glass fiber filters aboard the R/V *Melville* at control (n = 4) and experimental (n = 7) SP stations using a McLane or Challenger Oceanic *in situ* pumping system. POM samples were collected from within the mixed layer at depths ranging from 20 to 25 m. Sub-samples (1 cm^2 each) of each filter were taken for particulate organic carbon (POC), stable carbon isotopic ($\delta^{13}C$) and phytoplankton pigment analyses. Isotopic analyses of bulk particulate organic carbon were determined on acid-fumed samples (Hedges and Stern 1984) using an on-line CHN analyzer (Verardo et al. 1990) coupled with isotope ratio mass spectrometer (ConFlo II/MAT Delta-Plus). Multiple analysis of samples and well-characterized laboratory standard materials indicated precision and accuracy using this technique were better than ±0.2‰. Phytoplankton pigment distributions were determined by reverse-phase high-performance liquid chromatography (RP-HPLC) following the methods described in Bidigare et al. (2003). Fucoxanthin (FUCO), 19'-hexanoyloxyfucoxanthin (HEX), 19'-butanoyloxyfucoxanthin (BUT), peridinin (PER), and total chlorophyll *a* (TCHLA, chlorophyllide *a* plus chlorophyll *a*) concentrations (ng L^{-1}) were used as proxies for diatom, haptophyte, pelagophyte, dinoflagellate and phytoplankton biomass, respectively (Bidigare et al. 1996).

Short-term disequilibrium experiments were performed "inside" and "outside" (control stations) of the Northern and Southern patches (Figure 3.1). Discrete samples (CTD and bucket) of 10 to 30 L were collected at several stations and gently filtered (<80 mm Hg vacuum) onto 3 μm Poretics, polycarbonate membrane filters (142 mm diameter) at a temperature <4°C. Phytoplankton cells were then gently resuspended in 50 mL of

seawater collected at the same sample location, and the short-term disequilibrium experiments were started immediately after sampling for DIC and alkalinity. The photochemical efficiency of the cells did not significantly change following filtration and resuspension (Jill Peloquin, per. comm.), which suggests that the manipulations did not adversely stress the algal cells. In some of the experiments, dextran-bound sulfonamide (DBS) or acetazolamide (AZA) at final concentrations of 200 and 20 μM, respectively, were injected 20 minutes prior to the onset of the isotopic disequilibrium experiments to determine the importance of the extracellular carbonic anhydrase activity. DBS and AZA are potent CA inhibitors that are characterized by their inability to cross the plasmalemma. DIC and alkalinity samples for each isotopic disequilibrium experiment were preserved with $HgCl_2$ for later analysis. The short-term disequilibrium experiments were performed in a transparent ice bath incubator. The sample water was gently mixed with a magnetic stirrer. Experiments were performed in front of a bank of daylight fluorescent lamps (21.6 mol quanta m^{-2} s^{-1}). Floating semi-transparent plastic covers were used to decrease CO_2 exchange with the atmosphere. DIC was determined barometrically as previously described (Kroopnick 1985; Laws et al. 1995). The distribution of carbonate species was determined from knowledge of temperature, salinity, total alkalinity, DIC, and phosphate and silicate concentrations (Roy et al. 1993; Millero 1995). Total alkalinity was determined by computer-controlled Gran titration (Edmond 1970). Precision and accuracy of alkalinity and DIC measurements were less than 8 μeq kg^{-1} and 10 μM, respectively. High specific activity sodium bicarbonate ($NaH^{14}CO_3$) was first diluted to a final concentration of 8 μCi mL^{-1} in a basic (pH = 9) solution. To ensure a high specific

activity, the distilled water used to make the basic solution had been previously boiled for three hours to remove all DIC.

Cassar et al. (2002) give a detailed description of the ^{14}C isotopic disequilibrium methodology, as modified from that described in Espie and Colman (1986) and Lehman (1978), and only a brief summary is included here. To initiate the ^{14}C isotopic disequilibrium experiment, 0.5 mL (4 μCi) of the final solution was added to the 50-mL sample in the form of $^{14}CO_2$. The $^{14}CO_2$ was prepared immediately before the short-term ^{14}C experiments by acidifying $NaH^{14}CO_3$ to a pH of ~ 3.1 with a 0.1% HCl solution. Samples (2 mL) were collected at timed intervals, with the first sample taken at 10 seconds. The samples were directly transferred to scintillation vials containing 0.5 mL of 10% HCl to terminate ^{14}C incorporation and left overnight in a fume hood to degas the $DI^{14}C$ that had not been fixed. Twelve mL of Aquasol-2 (Packard Bioscience) liquid scintillation cocktail were added to each sample and the radioactive signal, which represents acid-resistant organic matter, was measured using a Packard TRI-CARB 2770 TR/SL Liquid Scintillation Analyzer.

The relative importance of HCO_3^- and CO_2 as sources of inorganic carbon for photosynthesis was determined using the equation

$$\%\ CO_2\ \text{uptake} = \left(\frac{\text{Initial rate}}{\text{Final rate}}\right) \times \left(\frac{CO_2}{DIC}\right) \times 100 \qquad (3.3.1)$$

(Cassar et al. 2002), where % CO_2 uptake is the fraction of inorganic carbon fixation that is attributable to direct CO_2 uptake. The initial rate was estimated from the activity of ^{14}C in organic carbon immediately after the onset of the isotopic disequilibrium experiments (i.e. after 10 seconds). Due to the slow interconversion of bicarbonate and CO_2 at the

experimental temperature of ~0°C, this initial rate is due almost entirely to uptake of $^{14}CO_2$. The final rate is the uptake rate at isotopic equilibrium (i.e., ^{14}C has equilibrated with all inorganic carbon species), and represents a combination of $H^{14}CO_3^-$ and $^{14}CO_2$ uptake. Figure 3.2 shows uptake response curves with the origin as the time of injection. By comparing the steady-state (i.e. isotopic equilibrium) uptake of inorganic carbon with and without external CA inhibitors, we determined the relative importance of external CA activity. Steady-state uptake of inorganic carbon without any external CA inhibitor represents a combination of CO_2, HCO_3^-, and extracellular CA-mediated CO_2 uptake whereas with the external CA inhibitor, only CO_2 and HCO_3^- uptake are measured. The ratio of the two gives a measure of the relative importance of extracellular CA activity in the uptake of carbon.

3.4. Results and Discussion

The addition of iron to the northern site produced a phytoplankton bloom that was comprised of small (5-20 μm) phytoflagellates (dinoflagellates, pelagophytes and haptophytes) on day 12 of the NP experiment (Brown et al. 2002). The NP was re-visited 27 days following the initial iron infusion and microscopic observations revealed a dramatic shift in community composition to larger (>20 μm) chain-forming pennate diatoms. By comparison, the southern site was initially populated (t_o) with a relatively high biomass (~5 μM C) of large centric diatoms (Landry et al. 2002). The iron enrichments at the southern site yielded increases in the biomass of all resident phytoplankton groups with only small changes in phytoplankton community structure. RP-HPLC pigment analyses revealed that the phytoplankton community in the SP was

dominated (in order of decreasing biomass) by diatoms, haptophytes, pelagophytes and dinoflagellates (Figure 3.3A). A 7-fold increase in TCHLA concentration (190 to 1,300 ng L^{-1}) was observed during the 3-week period following initial enrichment. Diatoms displayed the largest "relative" increase in pigment biomass ($t_{21d}/t_o = 6.1$), followed by pelagophytes ($t_{21d}/t_o = 5.4$), dinoflagellates ($t_{21d}/t_o = 4.5$) and haptophytes ($t_{21d}/t_o = 1.5$). The ratio of FUCO-to-TCHLA (w:w) at control and patch stations was relatively constant and averaged 0.56 $\pm$ 0.08 (n = 11, CV = 14%). The use of a FUCO-to-TCHLA ratio of 0.69 for Southern Ocean diatoms (Bidigare et al. 1996) suggests that diatoms accounted for 80-90% of the TCHLA biomass at the southern site. A linear increase in POC concentration was observed during the 17-day period following the initial addition of iron to the southern site (Figure 3.3B). $\delta^{13}C$ values of the POC sampled at control and patch stations were not statistically different (P = 0.578) and averaged –28.70 $\pm$ 0.26‰ (n = 4) and –28.61 $\pm$ 0.23‰ (n = 7), respectively (grand mean = -28.64 $\pm$ 0.23, n = 11). To estimate $\delta^{13}C_{DIC}$, we derived a multiparametric linear regression (MLR) based on data from the World Ocean Circulation Experiment (WOCE) cruise P15S along 170°W from 63°S to 67°S. Several water properties (oxygen (O_2), phosphate (PO_4^{3-}), potential temperature (θ), salinity (S) and DIC) were included in the $\delta^{13}C_{DIC}$-predicting-MLR (Sonnerup et al. 2000). The predicted $\delta^{13}C_{DIC}$=-0.6847+0.0044(O_2)-0.2025(PO_4^{3-})+0.0625(θ)+0.2369(S)-0.0034(DIC) with a mean square error (mean error sum of squares) of 0.0047. Applying the mean hydrographic properties observed during the SOFeX cruise in the southern sites to this equation leads to an average $\delta^{13}C_{DIC}$ of 1.21 $\pm$ 0.07‰. The isotopic composition of CO_2 was determined, based on the $\delta^{13}C_{DIC}$ and the carbonate species relative abundances, to be about –9.64$\pm$ 0.07‰, consistent with values

reported in the literature (Francois et al. 1993; Lynch-Stieglitz et al. 1995; Popp et al. 1999; McNeil et al. 2001). In the Southern patch, the overall isotopic fractionation (ε_p) relative to CO_2 is therefore on average $19.56 \pm 0.07‰$. This is not significantly different from the ε_p observed by Popp et al. (1999) along the World Ocean Circulation experiment (WOCE) SR3 south of 61°S ($19.63 \pm 0.97‰$).

Differences in the % CO_2 uptake results (Table 3.1) could be attributed to variations in the algal community composition at the various stations, and/or to variability inherent to the isotopic disequilibrium experiments. Results were more variable when the final slope was small, i.e., when the photosynthetic rate of the sample was slow, emphasizing the importance of concentrating the collected seawater to increase the volumetric photosynthetic rate. A comparison of the coefficients of variation of the final slopes and of the inter-station % CO_2 uptake revealed that most of the variability in the latter could be accounted for by errors in the estimation of the final slopes, suggesting there may be no real difference in % CO_2 uptake between stations.

Table 3.1. Bicarbonate uptake by Southern Ocean phytoplankton. Isotopic disequilibrium experimental results with external carbonic anhydrase inhibitor (AZA or DBS, as specified). The averages are given with the standard deviation of the means. All samples were collected at the sea surface with the exception of station 28 which also included a 20 m sample (identified with an asterisk). The samples at station 29 (with/without CA inhibitors) were bubbled for several hours with nitrogen gas to decrease the CO_2 concentration. In/Out and Northern/Southern refer to the location of sampling, inside or outside the iron enriched patch, and North or South of the APFZ, respectively.

	Station	Latitude (°S) Longitude (°W)	Time since initial Fe infusion (days)	CO_2 (μmol kg^{-1})	% CO_2 uptake
Northern Patch					
OUT	31 (AZA)	54.10, 169.53		22	46
IN	33 (AZA)	54.21, 169.24	28	18	33
Southern Patch					
OUT	14 (DBS)	66.40, 170.38		23	34
	23 (DBS)	66.60, 171.78		18	54
			Average	21±2.5	44±10
IN	20 (AZA)	66.47, 171.90	1	26	34
	26 (DBS)	66.32, 171.90	6	24	78
	28 (AZA)	66.21, 172.00	9	16	71
	28* (DBS)	66.21, 172.00	9	21	33
			Average	22±2.2	54±12
Low-CO_2 treatment	29 (DBS)	66.31, 172.16	11	3	96

The steady-state (i.e., isotopic equilibrium) uptake of DIC was 16% greater without the external CA-inhibitor, indicating that a small portion of the DIC uptake may have been associated with an extracellular CA-mediated conversion of bicarbonate to CO_2, although the difference was not statistically significant ($p=0.34$). The % CO_2 uptake estimated from the isotopic disequilibrium experiments with extracellular CA-inhibitors should reflect direct CO_2 transport (passive and/or active). On average direct

uptake of CO_2 (passive and/or active) accounted for approximately 50% of inorganic carbon uptake, the other half being direct bicarbonate transport across the plasmalemma.

There were no significant differences in the percentage of direct CO_2 uptake inside and outside of the iron-enriched patches (Table 3.1). Such results imply that the increase in growth rates and decrease in CO_2 concentration associated with iron enrichment did not trigger any discernible changes in the carbon uptake mechanisms, indicating that under most environmental conditions the CCM is constitutive (Figure 3.4).

In one of the experiments (station 29), a concentrated algal sample was first bubbled with CO_2-free nitrogen gas for several hours to decrease the CO_2 concentration before initiating the disequilibrium experiments. The CO_2 and DIC concentrations decreased to 3 and 1720 μM, respectively. In this treatment, the percentage of inorganic carbon uptake accounted for by CO_2 uptake was 96% (i.e. direct and extracellular-CA mediated CO_2 uptake). The steady-state radiocarbon uptake without CA was more than twice (227%) that obtained with the CA inhibitor. Stated another way, the external CA activity increased significantly at the expense of HCO_3^- uptake, which implies the presence of a CO_2-regulated CCM. The photochemical efficiency of the cells, measured with a pulse-amplitude-modulation (PAM) fluorometer, was not affected by the decrease in CO_2 (Jill Peloquin, per. comm.), which would indicate that the availability of CO_2 is not a limiting growth factor in this area of the Southern Ocean. Why the phytoplankton increased the extracellular CA activity at the expense of direct bicarbonate transport, which could not be detected under the low CO_2 treatment conditions, is unclear. One possible explanation is that an active CO_2 transport, supplied with CO_2 from the catalytic dehydration of HCO_3^- by extracellular CA is energetically more efficient than active

HCO_3^- transport across the plasmalemma under low CO_2 conditions. If the CO_2 concentration in the diffusive boundary layer is lower than that in the bulk medium due to active uptake, extracellular CA activity would help increase the CO_2 concentration in the vicinity of the cell to equilibrium values and thereby reduce the CO_2 chemical gradient across the plasmalemma and diffusional loss of CO_2 due to efflux. Such a mechanism may increase the energetic efficiency of the CCM. Unfortunately, the isotopic disequilibrium experiments do not allow differentiation of active and passive CO_2 uptake.

The presence of extracellular CA activity would indicate the necessity to increase the kinetic conversion of HCO_3^- to CO_2 in the diffusive boundary layer which, without the presence of external CA activity, would probably be in chemical disequilibrium due to the constant uptake of CO_2. This surface boundary layer chemical disequilibrium in the absence of an external CA would be likely considering that large diatoms dominated the phytoplankton biomass in the southern patch. Interestingly, the extracellular CA activity in the southern stations (stations 14, 20, 23, 26, 28, 29), where large diatoms dominated the community, was not greater than that observed at the northern stations, where smaller species prevailed. Assuming the effective thickness of the diffusive boundary layer is dependent on cell size (Wolf-Gladrow and Riebesell 1997), one would expect that the southern stations would display higher extracellular CA activity.

Comparison with carbon isotopic fractionation

Under conditions where CO_2 is abundant and growth rate is slow, Laws et al. (1997) empirically demonstrated that photosynthetic isotopic fractionation (ε_p) follows the equation

$$\varepsilon_p = \varepsilon_{up} + (\varepsilon_{fix} - \varepsilon_{diff})(1 - \frac{\mu Q_c}{[CO_2]PA}) \quad (3.4.1)$$

where ε_{up}, ε_{diff}, and ε_{fix} are the isotopic discriminations associated with whatever process brings DIC across the plasmalemma into the cell, diffusion back into the surrounding water, and enzymatic carboxylation, respectively, μ is the growth rate, P is the permeability of the plasmalemma to CO_2, "A" is the plasmalemma surface area, and Q_c is the organic carbon content of the cell. This equation essentially denotes the linear dependence of ε_p on the ratio of the carbon demand (μQ_c) to the carbon supply ($[CO_2]PA$). Several studies have in fact pointed toward a strong dependence of ε_p on the CO_2 concentration (Arthur et al. 1985; Rau et al. 1989; Jasper and Hayes 1990; Hollander and McKenzie 1991; Laws et al. 1995). Obviously, this model (Eq. (3.4.1)) assumes that under any conditions, the main source of inorganic carbon for photosynthesis will be passive diffusion.

Subsequent studies, however, have demonstrated that a passive diffusion model could not explain empirical results obtained under extreme CO_2 limiting conditions (i.e. high growth rate, low CO_2). Under such conditions, the relationship between ε_p and μ/CO_2 becomes non-linear (Laws et al. 1997). It is now believed that the upward curvature of the relationship relative to the linear passive diffusion model is due to the activation of an active carbon transport mechanism (Laws et al. 1997; Keller and Morel 1999). Keller and Morel (1999) have demonstrated that a combination of passive diffusion and active uptake of either HCO_3^- or CO_2 can explain the non-linear dependence of ε_p on μ/CO_2.

If we assume that carbon isotope fractionation in marine algae in the Southern Ocean follows the Keller and Morel model (1999), then

$$\varepsilon_P = \varepsilon_t + f_a(\delta^{13}C_{CO_2} - \delta^{13}C_{source}) + f_{eff}(\varepsilon_{fix} - \varepsilon_{diff}) \quad (3.4.2)$$

where

$$f_a = \frac{\gamma}{\frac{[CO_2]PA}{\mu Q_c} + \gamma} \quad (3.4.3)$$

and,

$$f_{eff} = \frac{1 + (\gamma - 1)\frac{\mu Q_c}{[CO_2]PA}}{1 + \gamma\frac{\mu Q_c}{[CO_2]PA}} \quad (3.4.4)$$

where ε_t is the carbon isotope fractionation associated with active transport mechanisms, $\delta^{13}C_{CO_2}$ and $\delta^{13}C_{source}$ are the isotopic signatures of the CO_2 in the medium and of the substrate for carbon transport, respectively, γ is the ratio of active transport to carboxylation, f_a is the proportion of uptake that is active, and f_{eff} is the ratio of efflux to influx. This model assumes that active transport is a constant proportion of fixation and is independent of the CO_2 concentration in the medium. According to our results, and assuming that CO_2 uptake is based on diffusion, the proportion of CO_2 diffusion to total transport across the plasmalemma, $[CO_2]PA/ (\gamma \mu Q_c + [CO_2]PA)$, is about 0.5 (with a range of 0.33 to 0.78; range in parentheses hereafter), and the ratio of passive to active transport, $[CO_2]PA/ \gamma \mu Q_c$, is 1 (0.49 to 3.55). The "f_a" and "f_{eff}" terms in Eq. (3.4.2) are therefore equal to 0.5 (0.22 to 0.67) and (1-0.5 γ) ((1-0.67γ) to (1-0.22 γ)), respectively.

Also according to our results, the majority of active utilization (i.e., HCO_3^- transport plus extracellular CA activity) is attributable to direct HCO_3^- transport (the steady-state ^{14}C uptake is not significantly higher without CA inhibitors). Assuming a $\delta^{13}C_{DIC}$ of 1.7 ‰ and a $\delta^{13}C_{CO_2}$ of −10 ‰ (Francois et al. 1993), the $\delta^{13}C_{source}$ and ($\delta^{13}C_{CO_2}$ - $\delta^{13}C_{source}$) are approximately equal to 1.7 ‰ and −11.7 ‰, respectively. Considering carbon fixation at the studied stations was predominantly performed by eucaryotic Rubisco, which has a carbon isotope discrimination of 29 ‰ (Roeske and O'Leary 1984; Raven and Johnston 1991), and an isotope fractionation associated with dissolved CO_2 diffusion in aqueous solutions of 0.7 ‰ (O'Leary 1984), and following Keller and Morel's (1999) assumption that ε_t is equal to ε_{diff}, Eq. (3.4.2) becomes

$$\varepsilon_P = 0.7 + 0.5(-11.7) + (1 - 1/(2\gamma))(28.3) \qquad (3.4.5)$$

Because of efflux in the mass balance, γ must be ≥ 0.5. However, according to Eq. (3.4.5), and considering ε_p can only be positive, γ must be greater than 0.61. With an isotopic fractionation of about 15 to 20 ‰ in the Southern Ocean (Francois et al. 1993; Popp et al. 1999), γ should be between 1.75 and 4.5 (Figure 3.5). Such a range is consistent with the model fits for various species by Keller and Morel (1999) except for *Porosira glacialis*, for which they obtain no active HCO_3^- uptake (γ=0), a result they attribute to its low specific growth rate (i.e., diffusion rate is sufficient for the low carbon fixation rate). Our results indicate that even under low growth rates, $\gamma > 0$. Following this reasoning, and using a f_{eff} of (1-0.5 γ) (see above), the ratio of efflux to influx would be 86% to 94% (62% to 85% with (1-0.67 γ) and 87% to 95% with (1-0.22 γ)). Such high efflux is consistent with results in the literature (Rotatore et al. 1995; Sukenik et al. 1997;

Tchernov et al. 1997; Tchernov et al. 1998). According to this result, to maintain a high CO_2 concentration in the vicinity of Rubisco, the CCM must constantly maintain a concentration gradient (higher intracellular DIC concentration), one of the consequences of which would be a significant efflux of CO_2. In other words, efflux and carbon fixation are competing processes for the intracellular inorganic pool, and because of Rubisco's low catalytic efficiency, efflux may be dominant.

From Eqs. (3.4.3) and (3.4.4), it is easy to show that f_{eff} is equal to $1-f_a/\gamma$ and therefore that

$$\varepsilon_P = \varepsilon_t + f_a(\delta^{13}C_{CO_2} - \delta^{13}C_{source} - \frac{(\varepsilon_{fix} - \varepsilon_{diff})}{\gamma}) + \varepsilon_{fix} - \varepsilon_{diff} \qquad (3.4.6)$$

Assuming that all factors other than f_a are constants, the carbon isotope fractionation, ε_p, should be a linear function of the proportion of uptake that is active, f_a. If no active uptake is present (f_a=0), $\varepsilon_P = \varepsilon_t + \varepsilon_{fix} - \varepsilon_{diff}$. However, if all uptake is active (f_a=1), $\varepsilon_P = \varepsilon_t + (\delta^{13}C_{CO_2} - \delta^{13}C_{source}) + (1-\frac{1}{\gamma})(\varepsilon_{fix} - \varepsilon_{diff})$. Assuming *Phaeodactylum tricornutum*'s isotopic fractionation (Laws et al. 1997) to be representative of marine phytoplankton, ε_p should be 26.8 when f_a=0 and 5.5 when f_a=1. In other words,

$$\varepsilon_P = -21.3 \times f_a + 26.8 \qquad (3.4.7)$$

Popp et al. (1999) tested the dependence of ε_p on CO_2 in the Southern Ocean, where the concentration of CO_2 is relatively high and the phytoplankton's growth rate is suppressed because of the low ocean surface temperature (Six and Maier-Reimer 1994). Along the WOCE SR3 transect (Hobart to Antarctica), they found a strong linear dependence of the carbon isotopic fractionation on CO_2 concentration. Popp et al. (1999)

observed an average isotopic fractionation of 17.22 ‰, with a range of 12.94 to 21.18 ‰, which would correspond, according to Eq. (3.4.7), to an average percent CO_2 uptake of 55 %, with a range of 35 % to 74%, which is in good agreement with our mean of 48 %, with a range of 33 to 78%, obtained using isotopic disequilibrium experiments.

Several authors have in fact argued that carbon isotopic discrimination in the Southern Ocean is controlled mainly by the CO_2 concentrations (Fischer 1991; Rau et al. 1991; Rau et al. 1991; Dunbar and Leventer 1992; Rogers and Dunbar 1993; Kopczynska et al. 1995; Dehairs et al. 1997; Rosenthal et al. 2000). Francois et al. (1993) and Popp et al. (1999) however found areas where the isotopic signature of the organic matter varied independently of the CO_2 concentration, indicating that factors other than the concentration of CO_2 may play an important role in determining fractionation. The presence of carboxylases other than Rubisco, such as phosphoenolpyruvate carboxylase (PEPC), and phosphoenolpyruvate carboxykinase (PEPCK), which have distinctive isotopic discriminations (Raven 1997) could explain some of the variability in ε_p (Guy et al. 1989; Le Roux-Swarthout et al. 2000).

3.5. Conclusion

Because of the low-permeability of biological membranes to charged molecules, HCO_3^- assimilation can only occur through active uptake or extracellular conversion to CO_2 through carbonic anhydrase activity. Consequently, one would expect the HCO_3^- source to be utilized only when CO_2 becomes limiting. Our results indicate that even under conditions that should favor a passive diffusion mode of carbon transport, i.e., low carbon requirement (low growth rate) and high CO_2, HCO_3^- is an important substrate for

photosynthesis. Under most natural conditions, although CCM plasticity associated with changes in CO_2 and growth rate may be present, such plasticity is not expressed naturally in this area of the Southern Ocean.

Assuming that the uptake of DIC was only by diffusion, Riebesell et al. (1993) hypothesized that CO_2 could limit algal growth rates in the oceans. This would be especially true for large phytoplankton, such as those observed in this region of the Southern Ocean, because of the long diffusion path in the cell boundary layer. However, as observed by Goldman (1999), we could not find evidence that CO_2 availability limits growth rate. Caperon and Smith (1978) have shown that the DIC half saturation constant is between 67 and 442 $\mu mol\ L^{-1}$ for various axenic algal cultures and natural phytoplankton populations, which is well below the DIC concentrations the algae were exposed to in our experiments, even under the low-CO_2 treatment. In our experiments, the availability of DIC did not affect the phytoplankton's photochemical energy conversion efficiency, which suggests that carbon was not limiting growth rate, presumably because of the presence of an active CCM. In contrast, based on growth rate, phosphate and nitrate utilization and photochemical efficiency measurements at various CO_2 concentrations, Huertas et al. (2000) found evidence that inorganic carbon could limit growth rate in some marine macroalgae.

While there is a plethora of evidence of CCM in the laboratory, very few studies have shown the presence of a CCM in the marine realm in the field. Tortell et al. (2000) and Tortell and Morel (2002) recently found unequivocal evidence of a CCM in the coastal and eastern subtropical and equatorial Pacific. In one of the areas studied, which was dominated by diatoms, Tortell and Morel (2002) found that extracellular dehydration

of HCO_3^- to CO_2 by CA was the main source of carbon uptake and that direct HCO_3^- could also have potentially been present. Although they were successful in demonstrating the presence of various CCMs, they were unable to quantify the relative importance of each mode of transport. Our study confirms their observation of the importance of CCM *in vivo*, and is, to our knowledge, the first quantitative assessment of the relative importance of the various photosynthetic carbon uptake mechanisms in the field. In contrast to the diatom assemblages studied by Tortell and Morel (2002), diatoms in this region of the Southern Ocean acquire roughly half of their DIC through direct bicarbonate transport, the other half being active or passive CO_2 uptake. Extracellular carbonic anhydrase activity, although present, is minor relative to other pathways. The percentage of CO_2 uptake did not respond to any of the changes associated with iron enrichment. We did see an inducible CCM response in the low CO_2 treatment (Figure 3.4), but such low CO_2 concentrations in the marine environment are rare, even during intense algal blooms.

Considering that we observed HCO_3^- uptake under relatively low growth rates and high CO_2 conditions, which should theoretically favor a passive CO_2 mode of uptake, HCO_3^- uptake could potentially be even more important in warmer areas of the ocean, where growth rates can be higher (Eppley 1972) and CO_2 solubility lower. The large size of the cells observed in this region of the world's ocean may however explain their requirement for active uptake of carbon. Although the Southern Ocean has the greatest potential to sequester carbon, we conclude that CO_2 fertilization is unlikely to effect much response from Southern Ocean phytoplankton. CO_2 fertilization may produce a significant response from terrestrial plants (Curtis 1996; Curtis and Wang 1998; Fan et al. 1998; Phillips et al. 1998; DeLucia et al. 1999; Pacala et al. 2001; Schimel et al. 2001),

but even in the terrestrial environment, CO_2 fertilization may not be as important as previously believed. Changes in land use may account for a large proportion of the terrestrial carbon sink (Fang et al. 2001; Pacala et al. 2001). On a geological time scale, productivity and organic carbon sequestration to the deep ocean by the biological pump in the Southern Ocean is unlikely to have been stimulated by the increase in surface water CO_2 concentrations observed during interglacial periods. On the human-time scale, the increase in temperature associated with the anthropogenic release of CO_2 is more likely to increase thermal stratification of the surface oceans and therefore decrease primary productivity through reduced upwelling of nutrient rich waters. Hence, the negative feedback of increased biological pumping rate through marine CO_2 fertilization is probably negligible relative to the positive feedback of a reduction in the former associated with a CO_2-mediated decline in conveyor belt activity.

3.6. Acknowledgments

We thank Richard T. Barber for kindly providing the sodium bicarbonate ^{14}C and the space in the rad-van on the R/V *Revelle* to perform the short-term disequilibrium experiments. We also wish to acknowledge Susan Brown, Karen Selph and Michael Landry for providing floristic information, and Jill Peloquin for performing the photochemical efficiency measurements. We also would like to thank Rolf Sonnerup for helpful discussions on the use of MLRs for the determination of $\delta^{13}C_{DIC}$. This work was supported by National Science Foundation grants OCE-0094637 (BNP, RRB, and EAL) and OCE-0094272 (BNP) and a NSERC scholarship awarded to NC.

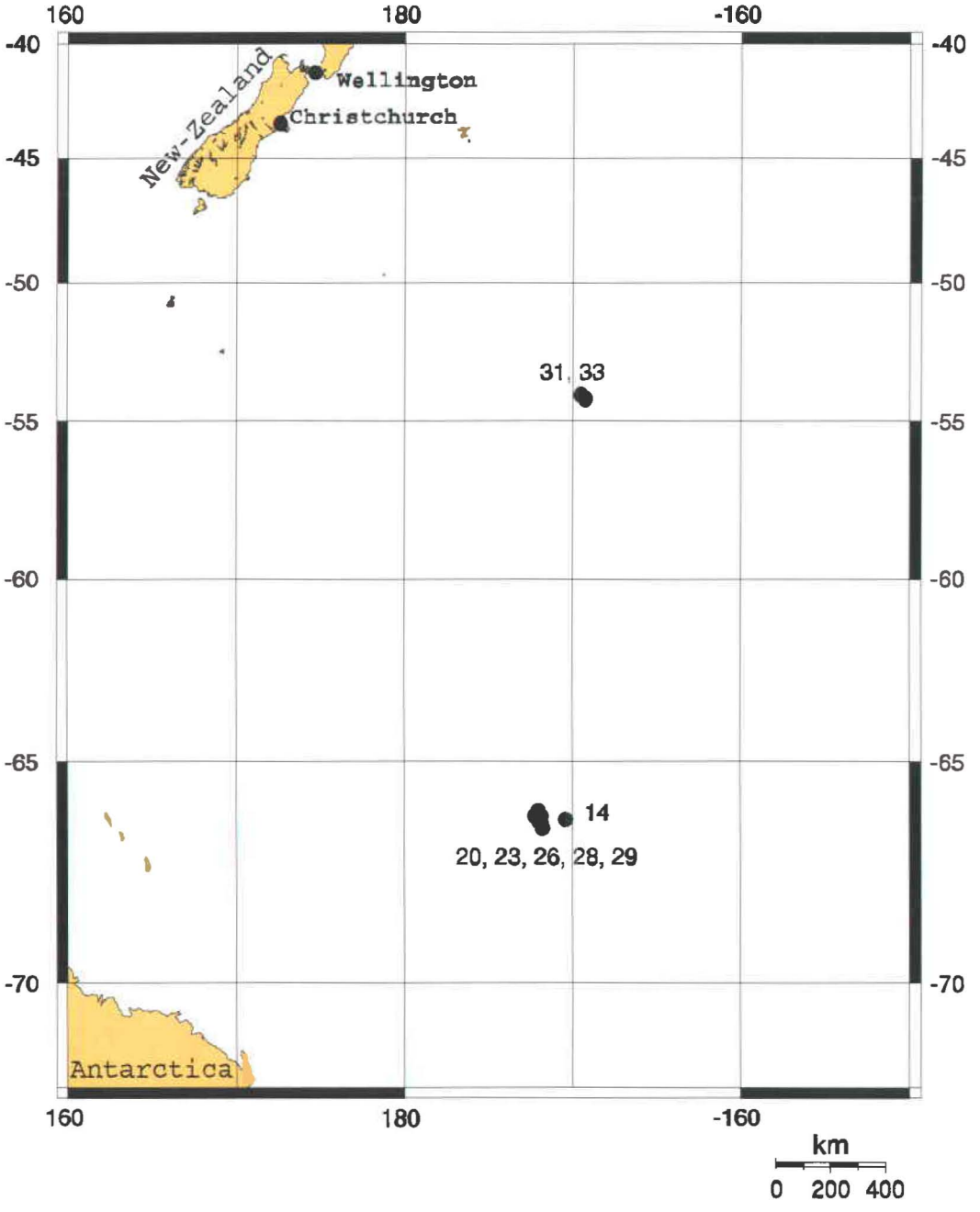

Figure 3.1. Southern Ocean sampling locations for the short-term isotopic disequilibrium experiments. The numbers refer to the station numbers used on the *R/V Revelle* during the SOFeX cruise.

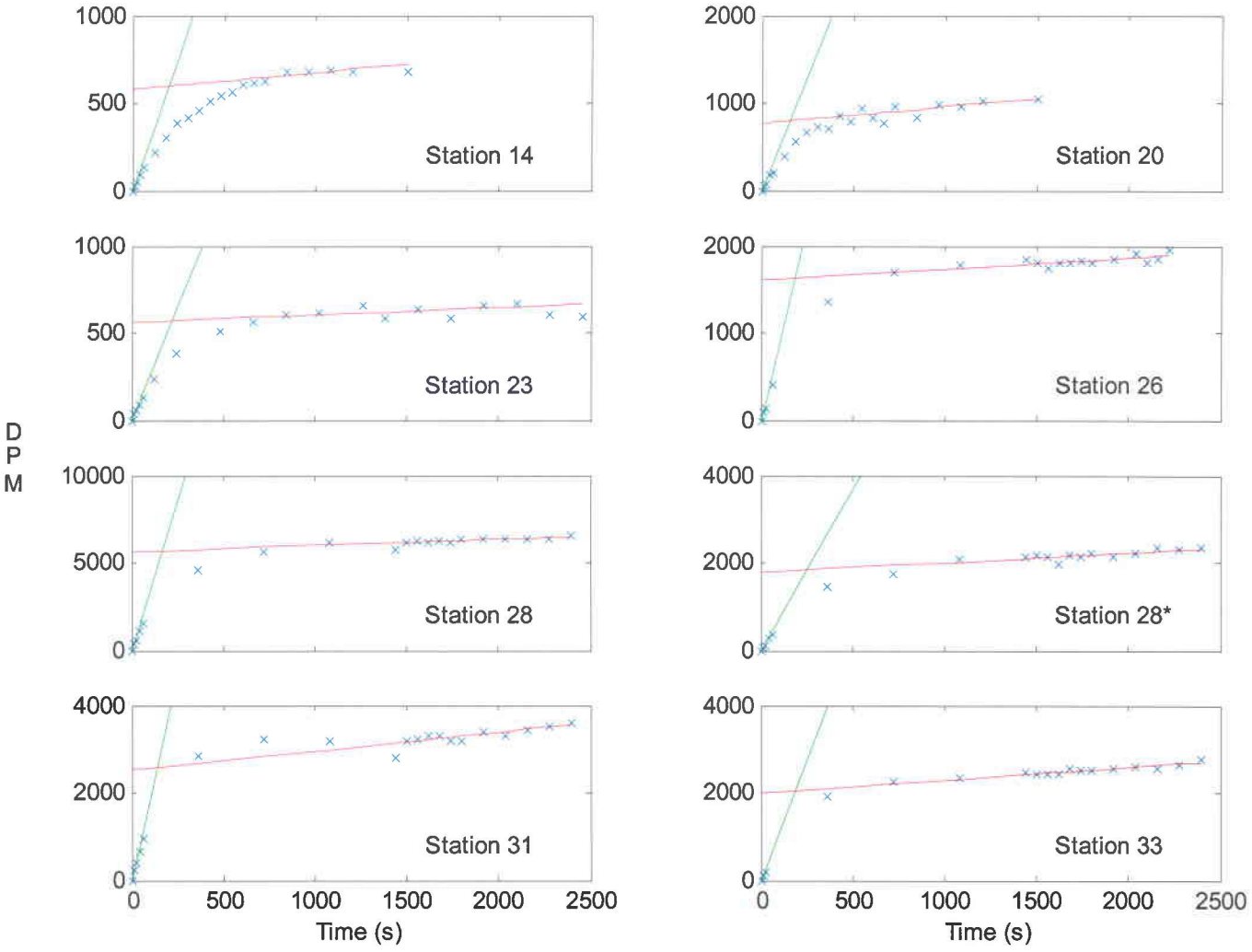

Figure 3.2. Isotopic disequilibrium experimental results in the Southern Ocean (excluding station 29). The y-axis represents the cumulative ^{14}C activity in the organic phase. Station 28* was collected from a depth of 20 m.

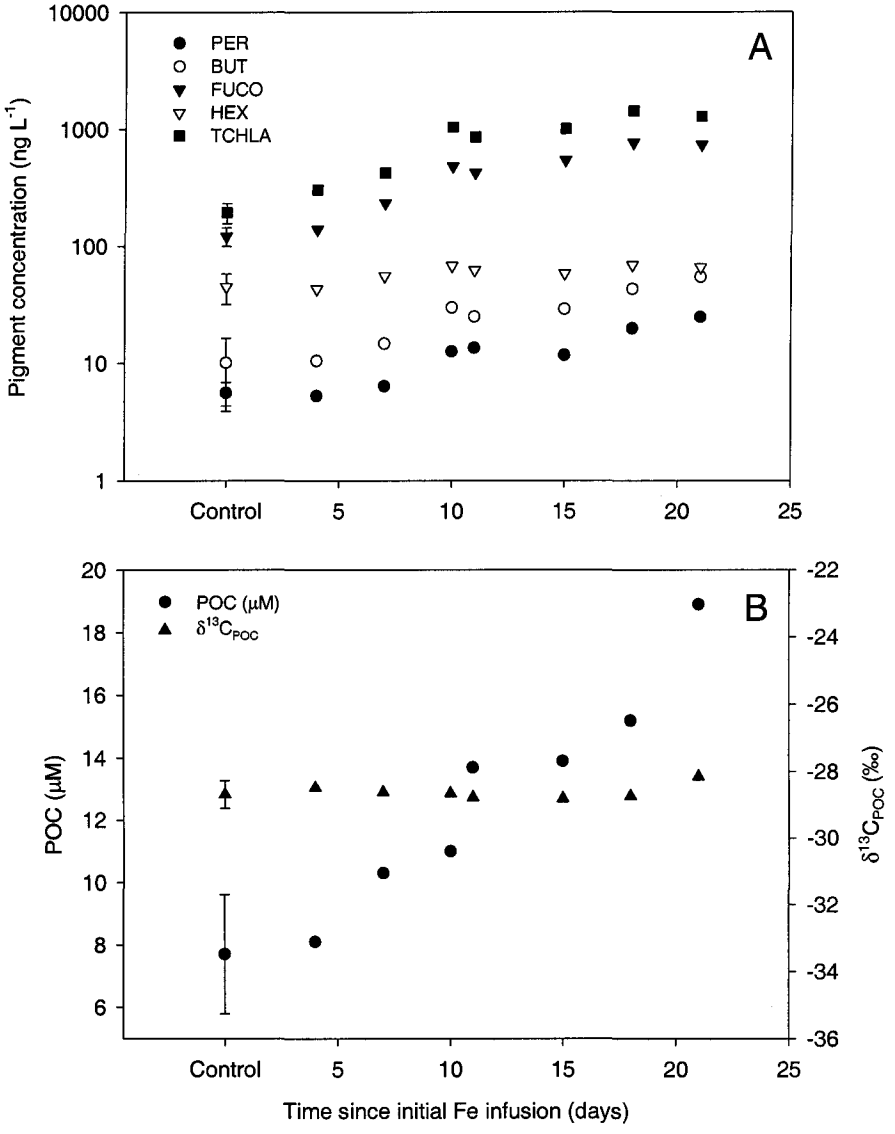

Figure 3.3. Temporal variations in POM parameters measured within the mixed layer (20-25 m) at control and experimental SOFeX Southern Patch stations: (A) phytoplankton biomarker concentrations (note the log scale on the ordinate) and (B) POC concentrations and stable carbon isotopic compositions. Means of the controls and their 95% confidence limits are shown.

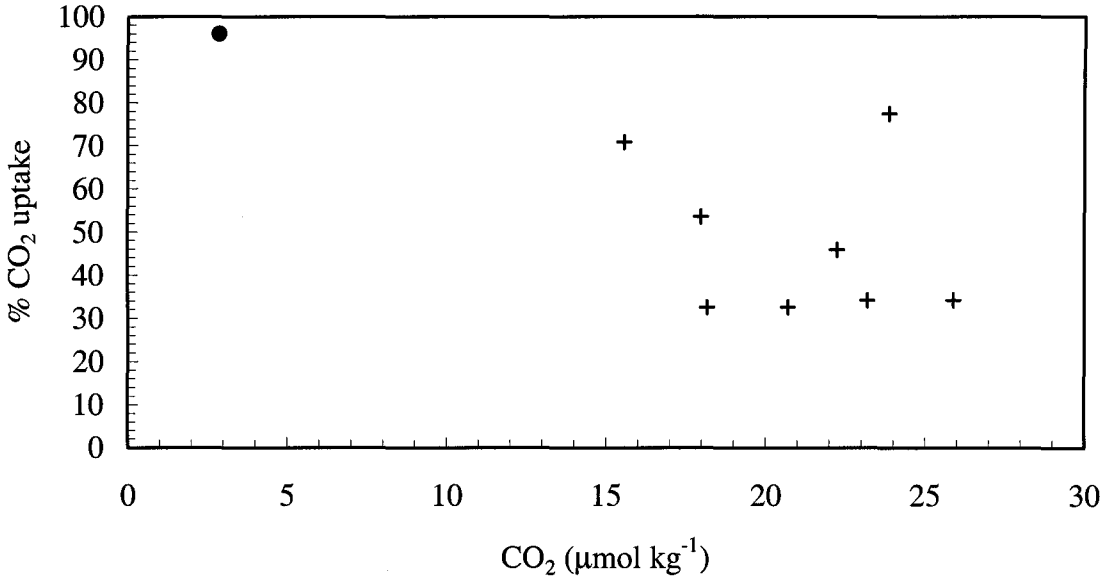

Figure 3.4. The contribution of CO_2 uptake (with the difference equal to HCO_3^- uptake) to total carbon assimilation vs. CO_2 concentration. The low-CO_2 treatment is represented by the solid circle.

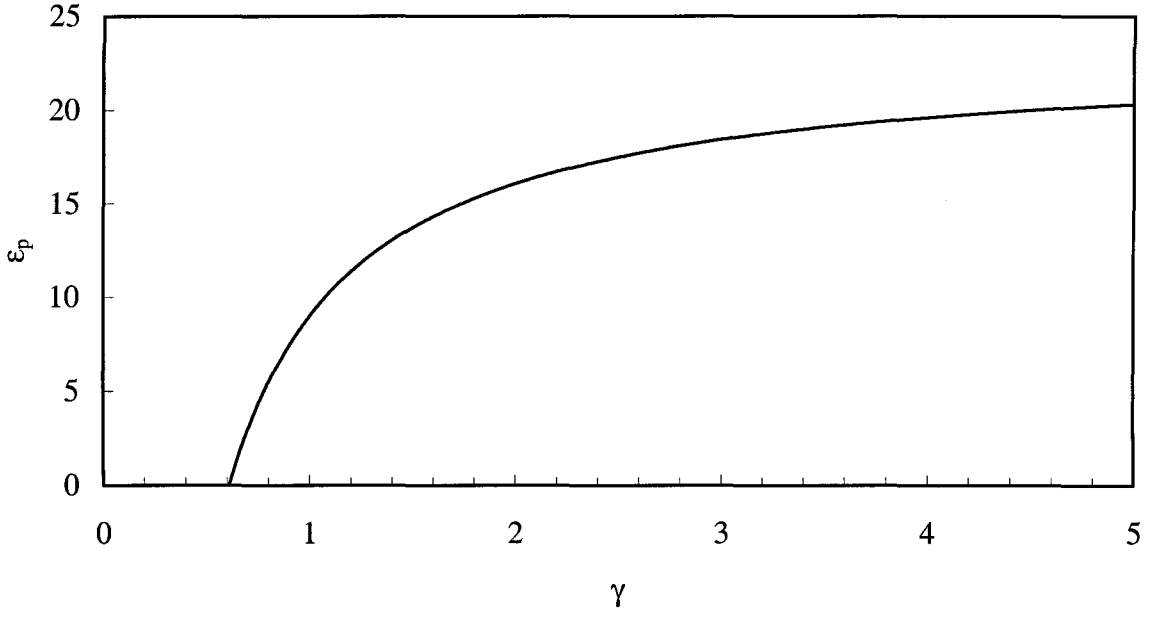

Figure 3.5. ε_p vs. γ following the Keller and Morel model (1999) fitted with our experimental results.

CHAPTER 4. PHOTOSYNTHETIC STABLE CARBON ISOTOPE FRACTIONATION

4.1. Introduction

Ultimately, one of the main goals of the study of carbon isotope fractionation is the use of the sedimentary photosynthetic organic matter isotopic record as a paleoceanographic proxy for CO_2. Unfortunately, a multitude of confounding factors may affect the dependence of ε_p on CO_2. A quantitative understanding of these factors is therefore mandatory before ε_p can be used for paleo-CO_2 reconstruction.

François et al. (1993) showed that

$$\varepsilon_P = \varepsilon_{up} + f_{eff}(\varepsilon_{fix} - \varepsilon_{diff}) \tag{4.1.1}$$

where

$$\varepsilon_P = \frac{\delta^{13}C_{CO_2} - \delta^{13}C_p}{1 + (\frac{\delta^{13}C_p}{1000})} \tag{4.1.2}$$

and

$$\delta^{13}C = \frac{(^{13}C/^{12}C)_{sample}}{(^{13}C/^{12}C)_{PDB}} - 1 \tag{4.1.3}$$

where $\delta^{13}C_{CO_2}$ and $\delta^{13}C_p$ are the $\delta^{13}C$ of the aqueous CO_2 and the phytoplankton carbon, respectively. ε_{up}, ε_{diff}, and ε_{fix} are the isotopic discriminations associated with the processes that bring inorganic carbon through the plasmalemma into the cell, diffusion back into the surrounding medium, and enzymatic carboxylation, respectively, and f_{eff} is the fraction of the inorganic carbon taken up by the cell that diffuses back into the water (see Appendix F for derivation of Eq.(4.1.1); Appendix G is a four-box model with two intracellular inorganic carbon pools). Hence, the overall carbon isotopic signature of a

phototroph is a function of the carbon source, the transport mechanism from the medium to the site of carboxylation, and the carboxylating enzyme (Figure 4.1). Another potentially important factor, not included in Eq. (4.1.1) but which will also be discussed, is the fractionation associated with carbon losses such as photorespiratory processes. Additionally, the possibility that the size of the internal inorganic carbon pool (and therefore efflux) may vary according to the ambient CO_2 concentration may considerably complicate carbon isotope fractionation models (see section 4.3). For instance, Nimer et al. (1999) found that the chloroplast and cytosolic pH in the marine dinoflagellate *Prorocentrum micans* vary depending on the DIC availability.

The notion that photosynthetic carbon isotope fractionation (ε_p) is controlled by the ratio of growth rate to CO_2 concentration (μ/CO_2), which is an estimate of the carbon supply vs. demand was first introduced by Laws et al. (1995) with the equation:

$$\varepsilon_P = \varepsilon_{up} + (\varepsilon_{fix} - \varepsilon_{diff})(1 - \frac{\mu C}{PCO_2}) \qquad (4.1.4)$$

where P is the permeability of the plasmalemma to CO_2 and C is the organic carbon content of the cell. The supply/demand model assumes the phytoplankton physiology to be static and passive. However, phytoplankton species have been shown to alter their gross carbon uptake (i.e., carbon uptake through the plasmalemma, which is a function of both passive influx and active transport of inorganic carbon) and their carbon fixation efficiency in response to CO_2 limitation.

4.2. ε_p vs. Gross carbon influx

At some level of CO_2 deprivation, many marine phytoplankton species are capable of inducing the production of Carbon Concentrating Mechanisms (CCMs) to alleviate

CO_2 limitation (Raven 1997). At low CO_2 levels, ε_p will therefore be greater than expected from a passive diffusion model because the CO_2 concentration does not adequately represent the supply, which is increased by CCMs (Figure 2.2). As discussed in Chapter 2, the increasing divergence of empirical data from a passive diffusional model may be due to the induction of CCMs under CO_2 limitation.

μ/CO_2 may in fact not be a good proxy for carbon demand vs. supply. At low levels of CO_2, CCMs are induced, and the transport of carbon is no longer passive. Under these conditions, a model that uses the CO_2 concentration as a surrogate for supply would be inaccurate because the actual CO_2 supply is increased by the CCMs. Such physiological plasticity greatly complicates the reconstruction of paleo-CO_2 from the sedimentary isotopic record. In addition, ε_p becomes increasingly insensitive to changes in μ/CO_2 as CO_2 limitation increases. The correlation between the isotopic signature of a certain sedimentary record and paleo-CO_2 is consequently obscured if the CO_2 availability prevalent when the photosynthetic organic matter was formed was low.

4.3. ε_p vs. Carbon fixation efficiency

Another possibility, which has to our knowledge not yet been explored, is that carbon isotopic fractionation is influenced by the ability of cells to fix inorganic carbon, which is proportional to the availability of nitrogen (production/regeneration of Rubisco). Thus far, most carbon isotope fractionation models have focused on the influence of the gross inorganic carbon influx (i.e., carbon transport mechanisms from the periplasmic space to the site of carboxylation) on ε_p. This modeling strategy is driven by the inability to constrain the intracellular CO_2 concentration ($[CO_2]_{in}$) and its response to changes in

growth conditions. Such an approach however fails to take into account the influence of the carbon fixation ability (i.e, changes in Rubisco abundance and enzymatic efficiency) on efflux (and on f_{eff}, see Eq. (4.1.1)).

A large proportion of the nitrogen assimilated by plants is used for Rubisco production. For example, Rubisco may represent more than 50% of the total soluble proteins in multicellular C_3 plants (Ku et al. 1979) and may account for up to 10% of the total organic nitrogen in algal cells (Beardall and Giordano 2002). The dependence of Rubisco activity on nitrogen availability has been demonstrated in a variety of species including *Laminaria hyperborean* (Küppers and Weidner 1980), *Ulva rigida* (Jimenez del Rio et al. 1995), *Elodea Canadensis* (Madsen and Baattrup-Pedersen 1995) and *Dunaliella tertiolecta* (Sciandra et al. 1997). Changes in chlorophyll *a* specific light-saturated net photosynthesis in response to variations in N per cell in *P. tricornutum* is also consistent with a nitrogen control on Rubisco activity (Osborne and Geider 1986). The availability of nitrogen (and the forms of nitrogen) could therefore influence ε_p by constraining the amount of Rubisco present. Because gross photosynthesis is a linear function of the nitrogen-based growth rate (Osborne and Geider 1986), it is expected that as the growth rate increases, the requirement for Rubisco total activity increases (Shuter 1979).

The inorganic carbon uptake rate into the cytoplasm must equal the sum of the efflux and the carboxylation rates. In other words,

$$A_t + k_1[CO_2]_{out} = \mu_g C + k_2[CO_2]_{in} \qquad (4.3.1)$$

where A_t and $\mu_g C$ refer to any active transport through the plasmalemma, and gross carbon carboxylation rate (in moles C per unit time per unit volume), respectively.

$[CO_2]_{out}$ is the extracellular CO_2 concentration, and k_1 and k_2 are the CO_2 diffusional rate constants in and out of the cell, respectively.

If F_1 is the gross inorganic carbon influx rate (i.e., $A_t + k_1[CO_2]_{out}$) and F_{-1} is the efflux rate (i.e., $k_2[CO_2]_{in}$), then the cellular inorganic carbon balance can be expressed as:

$$F_1 = F_{-1} + \mu_g C \tag{4.3.2}$$

or,

$$\mu_g C = F_1(1 - f_{eff}) \tag{4.3.3}$$

where f_{eff} is defined as F_{-1}/F_1 (see Eq. (4.1.1)). Algal physiology could therefore respond in several ways to an increase in growth rate: (1) increase in F_1, (2) decrease in f_{eff}, (3) combination of (1) and (2), (4) both F_1 and f_{eff} increase, but the overall $[F_1(1\text{-}f\ f_{eff})]$ increases, and (5) both F_1 and f_{eff} decrease, but the overall $[F_1(1\text{-}f_{eff})]$ increases.

One possible scenario would be that as the growth rate increases, both the gross carbon influx and the carbon fixation could increase. Although the efflux may also increase in response to the increased carbon influx, the f_{eff} would decrease because of the larger rate of carbon fixation. Alternatively, as the growth rate increases, the gross carbon influx could remain constant, but Rubisco abundance/efficiency would increase, which would lower the proportion of the inorganic carbon that is actively pumped into the cell that leaks out (i.e., f_{eff}). This is because an increase in Rubisco's efficiency and/or abundance would lower the intracellular CO_2 concentration required for efficient carboxylation. These scenarios are not mutually exclusive (i.e., both the gross carbon

influx and Rubisco cellular abundance and enzymatic efficiency could increase). They are both consistent with a decrease in isotopic fractionation with increased growth rate.

At high growth rates, the diffusion into the cells of CO_2 becomes an insignificant source of inorganic carbon relative to the active uptake. If we assume, like Keller and Morel (1999), that the active uptake is regulated in a constant ratio (γ) to the carbon fixation rate, the cellular carbon balance at high growth rates would be:

$$\gamma\mu_g C = \mu_g C + k_2[CO_2]_{in} \tag{4.3.4}$$

Again, this equation assumes that the contribution of passive diffusion to inorganic carbon influx becomes negligible at high growth rates. Under these high-growth conditions, the f_{eff} becomes constant and equal to $(\gamma\text{-}1)/\gamma$. This may explain why, at high μ/CO_2, ε_p becomes insensitive to CO_2 (Laws et al. 1997). Again, assuming diffusional influx is negligible under high growth rate conditions, and from Eq. (4.3.2),

$\frac{F_{-1}}{F_1} = (1 - \frac{\mu_g C}{F_1})$, and since f_{eff} is constant, F_{-1}, F_1 $\mu_g C$ must change in direct proportion at high growth rates. Following this reasoning, because F_{-1} is a function of the intracellular CO_2 concentration ($k_2[CO_2]_{in}$), $\mu_g C$ must also be a function of the latter. Explicitly,

$$F_{-1} \propto [CO_2]_{in} \Rightarrow \mu_g C \propto [CO_2]_{in} \tag{4.3.5}$$

Assuming Michaelis-Menten kinetics,

$$v_c = \mu_g C = \frac{V_{CO_2}[CO_2]_{in}}{K_{1/2_{CO_2}} + [CO_2]_{in}} \propto [CO_2]_{in} \tag{4.3.6}$$

where v_c is the carboxylase rate, V_{CO_2} is the maximal rate of Rubisco's carboxylase activity, and $K_{1/2_{CO_2}}$ is the half-saturation constant of Rubisco for CO_2 (see Chapter 1 for

more details). The fact that the gross carbon fixation is a function of $[CO_2]_{in}$ indicates that Rubisco is not fully CO_2 saturated (otherwise, $\mu_g C = V_{CO_2}$). Rubisco's activity is a linear function of $[CO_2]_{in}$. Hence, at high growth rates, Rubisco's enzymatic efficiency (which is among other things CO_2 dependent) must increase with the increase in carboxylation rate associated with the increase in growth rate. The cellular Rubisco concentration may also potentially increase with the increase in growth rate. If the $[CO_2]_{in}$ is a function of $[CO_2]_{out}$, we also predict a dependence of Rubisco's kinetics on the CO_2 concentration in the medium.

Total cellular enzymatic activity is a function of both enzyme abundance and specific catalytic efficiency. In the case of Rubisco,

$$\xi_{Rubisco} = B_{Rubisco} \times \eta_{Rubisco} \tag{4.3.7}$$

where $\xi_{Rubisco}$ is the total cellular enzymatic activity, $B_{Rubisco}$ is the cellular Rubisco biomass, and $\eta_{Rubisco}$ is the enzymatic efficiency (carbon fixed per enzyme per unit time; this enzymatic efficiency should not be confused with V_{max}/K_m which is also often referred to as "enzymatic efficiency"). Two extreme scenarios are possible: a Rubisco enzymatic pool that is invariant in size and independent of growth rate, but with a specific catalytic activity that is linearly proportional to growth rate, or vice versa. Obviously, there is an array of possible combinations between these two limits. Assuming that most of the carboxylation is performed by Rubisco (which may not be the case, see Chapter 5),

$$\mu_g C = \xi_{Rubisco} \times [\#C] = B_{Rubisco} \times \eta_{Rubisco} \times [\#C] = \mu_g \times [N] \times (C/N) \tag{4.3.8}$$

where C is the cellular carbon content, [#C] is the concentration of cells, [N] represents the concentration of the growth limiting nutrient, and C/N is the molar ratio of organic

carbon to the limiting nutrient. The gross carbon specific growth rate (μ_g) can be estimated from the carbon specific growth rate (μ) since the specific rate of dark respiration is a linear function of growth rate (Laws 1975). In fact, the use of μ as a surrogate of the carbon demand may be inaccurate, since μ is reflective of net photosynthesis.

The enzymatic efficiency is dependent on the chemical and physiological conditions at the carboxylation site. For instance, high CO_2 concentration around Rubisco (through the induction of CCM for example) will allow saturation of the active site and activation of Rubisco through carbamylation of a lysine residue on Rubisco (Hartman and Harpel 1994). Changes in pH in the stroma or in the pyrenoids (eukaryotes) and in the carboxysomes (cyanobacteria) may also affect Rubisco's enzymatic efficiency, which is optimal at a pH of ~ 8. Other factors, such as Mg^{2+} concentration and the presence of Rubisco activase, will also have an impact on the Rubisco's catalytic efficiency.

To test whether carbon isotopic fractionation could be a function of both Rubisco's abundance and specific catalytic activity, Rubisco enzymatic assays were performed on chemostat cultures of *Phaeodactylum tricornutum* at various growth conditions (Table 4.1). The enzymatic assay protocols are presented in Chapter 5. As discussed in the previous paragraph, the *in vivo* enzymatic activity is a function of both the cellular enzymatic biomass (i.e., abundance of Rubisco per cell) and its catalytic efficiency. In our enzymatic assays, although the *in vitro* conditions could potentially not be optimal for Rubisco activity, they were kept identical. The enzymatic assays cannot therefore be used to directly estimate the *in vivo* enzymatic efficiency ($\eta_{Rubisco}$), or the

total cellular enzymatic activity ($\xi_{Rubisco}$) for that matter, since the *in vitro* conditions may not be representative of *in vivo* conditions. However, the *in vitro* enzymatic activity (EA_{vitro}) should be proportional to $B_{Rubisco}$,

$$EA_{vitro} \propto B_{Rubisco} \times V_{filtered} \times [\#C] \tag{4.3.9}$$

where $V_{filtered}$ is the volume of sample filtered for the assay. Again, assuming that most of the carboxylation is performed by Rubisco,

$$\eta_{Rubisco} = \frac{\mu_g \times [N] \times (C/N)}{B_{Rubisco} \times [\#C]} \tag{4.3.10}$$

or,

$$\eta_{Rubisco} \propto \frac{\mu_g \times [N] \times (C/N) \times V_{filtered}}{EA_{vitro}} \tag{4.3.11}$$

Falkowski et al. (1989) have in fact found that (Rubisco nitrogen)/(total cellular nitrogen pool) rises with increasing growth rates in *Isochrysis galbana*. In agreement with Falkowski et al. (1989) findings, our results show that an increase in growth rate is associated with an increase in both the abundance of Rubisco ($B_{Rubisco}$) and its catalytic efficiency ($\eta_{Rubisco}$) (Table 4.1). This is the case if we compare both the high-growth-rate high-CO_2 and high-growth-rate low-CO_2 NO_3^- limited chemostats to the low-growth-rate chemostat (Table 4.1). In a batch culture of the same species (stationary phase), the cellular Rubisco biomass was less than 20% of the high-growth rate nitrate limited chemostat. The increase in catalytic efficiency at a higher growth rate means that a larger proportion of the inorganic carbon that enters the cell will actually be fixed before having a chance to leak out of the cell. The increase in Rubisco abundance and efficiency at high growth rates lowers the intracellular CO_2 concentration required for efficient

photosynthesis and therefore lowers efflux. Hence, such a result is consistent with the lower fractionation at higher growth rates observed by several authors (Laws et al. 1995; Bidigare et al. 1997; Laws et al. 1997; Popp et al. 1998).

Table 4.1. Effect of growth conditions (Nitrate (NO_3^-) vs. Phosphate (PO_4^{3-}) limited chemostats at high and low CO_2 levels) on Rubisco's kinetics. Ratios of $B_{Rubisco}$ and $\eta_{Rubisco}$ were calculated based on Eqs. (4.3.9) and (4.3.10), respectively (both have arbitrary units). Shown are comparisons of Rubisco biomass (in percent; $[(B_{Rubisco_{COLUMN}}/B_{Rubisco_{ROW}})\times 100]$) and, in parentheses, of the catalytic efficiencies (also in percent; $[(\eta_{Rubisco_{COLUMN}}/\eta_{Rubisco_{ROW}})\times 100]$.

(Column/Row)×100	NO_3^- (μ=0.93; high CO_2)	NO_3^- (μ=0.93; low CO_2)	NO_3^- (μ=0.18)	PO_4^{3-} (μ=1.02; high CO_2)	PO_4^{3-} (μ=1.02; low CO_2)
NO_3^- (μ=0.93; high CO_2)	-	48 (396)	155 (876)	412 (31)	39 (303)
NO_3^- (μ=0.93; low CO_2)		-	222 (350)	877 (8)	83 (78)
NO_3^- (μ=0.18)			-	429 (2)	41 (24)
PO_4^{3-} (μ=1.02; high CO_2)				-	9.5 (986)
PO_4^{3-} (μ=1.02; low CO_2)					-

In addition to nitrogen control on Rubisco levels, a negative correlation between Rubisco concentration and CO_2 availability has already been reported for aquatic plants (Garcia-Sanchez et al. 1994; Madsen et al. 1996; Andria et al. 1999; Andria et al. 2001). Our results are consistent with those studies and document that CO_2 modulates cellular Rubisco abundance. $[(B_{Rubisco_{highCO_2}}/B_{Rubisco_{lowCO_2}})\times 100]$ of the high-growth-rate nitrate limited chemostat is 48%. In other words, as CO_2 concentration increases, the increase in catalytic efficiency of Rubisco enzymes (as shown by the $[(\eta_{Rubisco_{highCO_2}}/\eta_{Rubisco_{lowCO_2}})\times 100]$ of 396%), allows the cells to allocate less of their organic nitrogen to Rubisco synthesis and regeneration (as shown by the $[(B_{Rubisco_{highCO_2}}/B_{Rubisco_{lowCO_2}})\times 100]$). The same is true for

the phosphate limited chemostats (Table 4.1), in which case the discrepancies of Rubisco biomasses and catalytic efficiencies at high and low CO_2 concentrations are even more dramatic ($[(B_{Rubisco_{highCO_2}}/B_{Rubisco_{lowCO_2}})\times100]=9.5$ and $[(\eta_{Rubisco_{highCO_2}}/\eta_{Rubisco_{lowCO_2}})\times100]=$ 986). Assuming that the increase in catalytic efficiency is associated with an increase in Rubisco CO_2 saturation state, an increase in isotopic fractionation would follow because of the larger f_{eff} coupled to the increase in size of the intracellular inorganic carbon pool.

Several conclusions can be drawn from this study, the most pivotal being the importance of the contribution of several factors to f_{eff}. The influx of inorganic carbon inside the cell may respond to changes in growth conditions. For instance, CCM activity may be regulated in response to inorganic carbon availability. Several authors have in fact modeled the effect of active carbon uptake (A_t) on isotopic fractionation (see Chapters 2 and 3, section 4.2 and Laws et al. 1997; Keller and Morel 1999). However, ε_p is not only a function of changes in the pumping rate of inorganic carbon into the cell, but also a function of the competition between the carboxylation rate and efflux. Carbon fixation efficiency, which has hitherto been ignored, may also respond to variations in growth conditions and consequently influence isotopic fractionation. In fact, a plot of ε_p and μ/CO_2 vs. the amount of Rubisco activity in the enzymatic assays clearly shows a trend (Figure 4.2). The results presented in Figure 4.2 include both phosphate and nitrate limited chemostats of *Phaeodactylum tricornutum*. Assuming $\varepsilon_{rubisco}$ (i.e., isotopic fractionation associated with carbon fixation by Rubisco) to be constant may in fact be incorrect. $\varepsilon_{rubisco}$ could potentially be a function of Rubisco's enzymatic efficiency. The

dependence of Rubisco's enzymatic efficiency on both the CO_2 concentration and the growth rate (see above) may explain the trend observed in Figure 4.2.

ε_p under nitrate vs. phosphate limitation

Because of the intrinsic dependence of the CCMs on energy (i.e., ATP), it is likely that phosphorus limited growth will have an effect on the isotopic signature of the organic matter. Assuming Rubisco is the largest sink of organic nitrogen, nitrogen limitation is likely to affect Rubisco availability (phosphorus may however also affect Rubisco activity). Hence, at the same growth rate, phosphorus limitation would limit the ability of cells to manufacture CCM and harvest the inorganic carbon, whereas nitrogen limitation would decrease the ability to fix the inorganic carbon. Both should affect the carbon isotope fractionation in the same direction, but not necessarily to the same extent. A decrease in CCM activity due to phosphorus limitation will decrease the rate at which inorganic carbon is provided to Rubisco, and a decrease in Rubisco activity/abundance will increase the proportion of the internal inorganic carbon that leaks out of the cell before being fixed. Consequently, increases in phosphorus and in nitrogen limitation will both increase the carbon isotope fractionation. A phosphorus-limited chemostat culture of *Phaeodactylum tricornutum* (CCMP 1327) was grown at low and high μ/CO_2 to test the effect of phosphorus availability on carbon isotope fractionation. The results of these experiments indicate that the isotopic fractionations under phosphate and nitrate limitations are similar at low μ/CO_2. Surprisingly, our results are different from those obtained by Laws et al. (1997) (Figure 4.3). We did not see the upward curvature in fractionation at low μ/CO_2 that Laws et al. (1997) observed with the same algal strain.

Based on our results, one could actually predict a linear dependence of fractionation on μ/CO_2. The reason for the discrepancy is unclear, but a mutation in this algal strain may have occurred since the experiments of Laws et al. (1997) were performed. At high μ/CO_2, we found that the fractionation is significantly smaller under phosphate than under nitrate limitation. However, this difference could also be accounted for by a mutation in this strain. Repeating the isotopic fractionation measurements on the original cultures studied by Laws et al. (1997) and the ones used for these phosphate-limited experiments would help to determine if the discrepancy is real. Because of the limited number of data points for these experiments, the difference may not be statistically significant. More work on the effect of phosphorus limitation on carbon isotopic fractionation is necessary.

Interestingly, our results show that Rubisco is less efficient under nitrate limitation than under phosphate limitation. Assuming most of the variability in the enzymatic assays between the phosphate and nitrate limited chemostats is not due to a difference in growth rate (μ=1.02 vs. 0.93, respectively), a lower enzymatic efficiency is observed in the nitrate-limited chemostat both under high and low CO_2 conditions than in the phosphate-limited chemostat ($[(\eta_{Rubisco_{NO_3^-}} / \eta_{Rubisco_{PO_4^{3-}}}) \times 100] = 31$ and 78, respectively). However, the effect of the nutrient limitation (nitrate vs. phosphate) on the Rubisco biomass is opposite at low and high CO_2 concentrations (Table 4.1). Why the Rubisco enzymes are more efficient under phosphate limitation is unclear. One possibility is that there is a higher CO_2 saturation under phosphate limitation (CCMs more active) than under nitrate limitation. However, such a control would imply that nitrogen availability is more

important in regulating CCM activity than phosphorus, a result contradictory to what had been originally hypothesized (see previous paragraph).

4.4. ε_p vs. C/N

A strong dependence of C/N on μ/CO_2 was observed (Figure 4.4a). In fact, the C/N ratio may be a better proxy for carbon demand/supply since the organic carbon reflects the carbon demand, and the organic nitrogen levels dictate the ability of phototrophs to harvest (CCMs) and fix (Rubisco) the DIC pool. This is shown by the strong linear dependence of ε_p on the C/N factor (Figure 4.4b) down to the Redfield ratio whereas the dependence of ε_p on μ/CO_2 is non-linear.

The increase in C/N could also be associated with luxury uptake of carbon (carbohydrate accumulation). Burkhardt et al. (1999) also observed a decrease in ε_p associated with an increase in C/N during a time course photoperiod experiment, which they attributed to an increase in carbon fixation. This indicates that there is a close physiological link between C/N and ε_p. This may explain why ε_p seems insensitive to changes in light-controlled growth rates (Riebesell et al. 2000). The dependence of C/N on growth rate is much smaller (and opposite) under light limitation than under nutrient limitation. The unresponsiveness of ε_p to changes in light-controlled growth rates would hence be consistent with C/N being a surrogate for a factor controlling ε_p. Ironically, ε_p could potentially be a better predictor of paleo C/N than paleo CO_2.

An inverse correlation between the nitrate concentration and the isotopic discrimination has in fact been observed (Riebesell et al. 2000). The authors argue that under nitrate limitation (as opposed to nitrate-replete conditions), excess energy may

support enhanced CCM activity, which would lead to an increase in the active carbon uptake to carbon fixation ratio and therefore increase isotopic fractionation (Keller and Morel 1999). However, a decrease in Rubisco levels could also explain their results. As the nitrate decreases, less Rubisco can be maintained, increasing the proportion of inorganic carbon effluxing the cell. In fact, any change in the factors controlling the ability of marine phytoplankton to induce the production and the maintenance of CCMs and Rubisco will potentially influence f_{eff}, and consequently ε_p. For instance, the availability of zinc, an important component of carbonic anhydrase, could influence ε_p.

C/N vs. growth rate and CO_2

However, the correlation between ε_p and C/N could simply be an indirect result of the correlation between C/N and growth rate, or CO_2 for that matter. C/N has been shown to be inversely related to nutrient-limited growth rates (Laws and Bannister 1980). Light level and nutrient concentration effects on the phytoplankton elemental molar ratio are in fact well known (Caperon 1972; Caperon and Meyer 1972; Thomas and Dodson 1972; Caperon and Ziemann 1976; Laws and Caperon 1976; Perry 1976; Sakshaug and Holm-Hansen 1977; Goldman 1986). Figure 4.5 however clearly shows that the dependence of ε_p on C/N (Figure 4.5a) is greater than on μ (Figure 4.5b). Consequently, the dependence of ε_p on C/N is probably not only an outcome of the growth rate.

More recently, Burkhardt and Riebesell (1997) and Burkhardt et al. (1999) found evidence that CO_2 availability also influences the C:N:P of phytoplankton. These authors observed only significant changes in C/N/P at CO_2 concentrations not typically encountered in the oceans and concluded that CO_2 availability is unlikely to have a

significant impact on the elemental composition of phytoplankton under natural conditions. As pointed out by the authors, the experiments were performed under high light and nutrient replete conditions, which are uncharacteristic of modern oceans. Burkhardt et al. (1999) saw most of the elemental stoichiometry changes below a CO_2 concentration of 10 μmol kg^{-1} and hypothesized that such behavior was correlated to a CO_2-related decrease in algal growth rates. The use of chemostats allowed us to study the CO_2 effect on elemental ratios under nutrient limited conditions. Our results indicate that the C/N of the marine diatom *Phaeodactylum tricornutum*, grown under nitrate limitation, is affected by the CO_2 concentration. In our experiments, cultures were maintained at a constant growth rate. Hence, a decrease in growth rate due to CO_2 limitation could not explain the change in elemental ratio we observed. However, the dependency seems to be growth-rate dependent. As the growth rate increases, the C/N dependency on the CO_2 concentration decreases (Figure 4.6). As algal growth progresses from a log to a stationary phase, the CO_2 effect on the elemental molar ratio increases. This is probably due to the increased uncoupling of the carbon and nitrogen physiological cycles at low growth rates. At low growth rates, most of the inorganic carbon fixed goes into storage carbohydrates (luxury uptake). As the availability of nitrogen increases, the possibility for luxury uptake decreases as most of inorganic carbon fixed goes into functional biomolecule synthesis (Shuter 1979; Laws and Chalup 1990). This is to our knowledge the first time that such an observation has been made. This would indicate that, as opposed to what is generally believed, the elemental ratio of phytoplankton is dependent on the CO_2 concentration. The decrease in CO_2 concentration at the end of a bloom should therefore partially counter the effect of the decreased growth rate (senescence

associated with the end of a bloom) on the C/N. In addition, the atmospheric CO_2 (and its rise due to anthropogenic activity) could influence the C/N ratio of sinking organic matter in the oceans.

Overall, there seems to be a significant non-linear negative correlation between μ/CO_2 and C/N (Figure 4.4a).

4.5. ε_p vs. SA/V

Popp et al (1998) demonstrated that species with higher surface area:volume ratios (SA/V), which are proportional to plasmalemma permeability:organic carbon content (carbon supply:demand), have a higher ε_p at a given μ/CO_2.

Porosira glacialis carbon isotopic fractionation (ε_p) shows a large dependency on μ/CO_2 (i.e., steep slope, see Popp et al. 1998). Popp et al. (1998) hypothesized that the strong dependence of ε_p on cell geometry (SA/V) could be explained by a passive diffusion CO_2 uptake model. However, as demonstrated by the isotopic disequilibrium experiments (this study, Figure 4.7 and Table 4.2), this Southern Ocean centric diatom's ability to actively transport bicarbonate would indicate that the diffusion of CO_2 inside the cell should not affect the carbon uptake, an indication that the mode of carbon transport may not be the factor controlling ε_p. Our results indicate that, under batch growth, direct HCO_3^- transport accounts for more than 90% of the inorganic carbon uptake in *Porosira glacialis* (CCMP 651). This is opposite to what is predicted by Keller and Morel (1999). Based on a carbon isotopic fractionation model, they argue that no active HCO_3^- uptake (γ=0, see Chapter 3) is present in *Porosira glacialis*. They

hypothesized that this is probably due to the low growth rate achievable by *Porosira glacialis* (i.e., low carbon requirement).

Our laboratory isotopic disequilibrium experiments (Table 4.2) confirm our field study (Chapter 3) that demonstrates that cold-water species also have CCMs. Table 4.2 also shows the results of isotopic disequilibrium experiments on *Synechococcus*. Experiments with the presence of DBS were not performed on *Synechococcus* since extracellular carbonic anhydrase activity is not present in this species (Elzenga et al. 2000). The ratio of final slope with DBS ($Final_{(DBS)}$) vs. without DBS ($Final_{(DBS\text{-}absent)}$) is a good indicator of extracellular carbonic anhydrase activity. A ratio of 1 indicates that the inhibitor had no effect on carbon uptake and therefore that extracellular carbonic anhydrase activity is not involved in the carbon uptake mechanism.

Table 4.2. Isotopic disequilibrium Experiments on batch cultures of various cold-water species and the cyanobacterium *Synechococcus*. NA stands for not available. The forth column is the ratio of the final slopes with DBS vs. without DBS.

Species	CO_2 ($\mu mol\ kg^{-1}$)	% CO_2 uptake	$Final_{(DBS)}/Final_{(DBS\text{-}absent)}$
Chaetoceros brevis	1	49.9	1.04
Nitzschia curta	4.2	86	0.68
Porosira glacialis	0.8	8.1	0.98
Thalassiosira antarctica	2.2	62	0.99
Pseudo-nitzschia	3.5	76	0.92
Synechococcus	0.18	2	NA

In the case of *Porosira glacialis*, HCO_3^- transport is the main inorganic carbon uptake pathway. The dependence of μ/CO_2 on SA/V is however indisputable (Popp et al. 1998). Hence, other factors, dependent on SA/V, may indirectly control ε_p. Looking back

at equation (4.1.1), assuming the isotopic discrimination factors ε_{up}, ε_{diff}, and ε_{fix} to be constant, f_{eff} is the only factor that may affect ε_p. The relative importance of efflux and carbon fixation, two processes competing for the internal inorganic carbon pool, should control f_{eff} and therefore ε_p (see (4.5.1)).

$$DIC_{external} \underset{CCM}{\overset{Efflux}{\rightleftarrows}} DIC_{internal} \xrightarrow{Rubisco} C_{org} \qquad (4.5.1)$$

A large cell like *Porosira glacialis*, with a small SA/V, is likely to have a lower ε_p at a given μ/CO_2 than a species with a larger SA/V, such as *Phaeodactylum tricornutum*, because of the lower efflux (f_{eff}). The strong dependence of ε_p on SA/V observed in several studies (Laws et al. 1995; Rau et al. 1996; Popp et al. 1998; Burkhardt et al. 1999) is probably not directly caused by the mode of transport of inorganic carbon inside the cell, because most cells have active transport mechanisms, but by the efflux, which is likely to be strongly dependent mostly on SA/V. Since the gross uptake of inorganic carbon across the plasmalemma is equal to the sum of carbon fixation and efflux ($A_t + k_1[CO_2]_{out} = \mu_g C + k_2[CO_2]_{in}$), the active transport mechanisms are indirectly dependent on SA/V. However, the CCMs could be directly dependent on SA/V if the abundance of active transporters in the plasmalemma is limited by density. In that case, a larger cell would have less active transporters per unit volume. A lower potential for gross inorganic carbon uptake and efflux would follow. Both the efflux and the active transporters' dependence on SA/V are consistent with a decrease in isotopic fractionation with cellular size.

The initial slope of the isotopic disequilibrium experiments on *Porosira glacialis* are influenced by the presence of the extracellular carbonic anhydrase inhibitor DBS,

whereas the final slope is not significantly different with and without the inhibitor (Figure 4.7). The ratio of the final slopes with and without the inhibitor is 98%. The fact that the final slopes in the *Porosira glacialis* experiments are the same with or without DBS indicates that there is a chemical equilibrium in the vicinity of the cell (there should be a decrease in uptake at isotopic equilibrium after the addition of the DBS if CA is used for carbon uptake). Immunological analyses have in fact established that the extracellular CA may be present whether CO_2 is limiting or not, even though the CA activity could only be detected when inorganic carbon was limiting (Nimer et al. 1999). This may explain why DBS slowed the rate at which the isotopic equilibrium was reached (greater initial slope with the inhibitor) but did not affect the carbon uptake once the isotopic equilibrium is reached (similar slope with and without CA inhibitor). This would indicate that the extracellular CA during these experiments was present, but that the carbonate system in the diffusive boundary layer was at chemical equilibrium. Thus, as opposed to what has been recently suggested (Elzenga et al. 2000; Tortell and Morel 2002), an increase in initial slope with the addition of extracellular CA inhibitors in isotopic disequilibrium experiments is only indicative of the presence of CA and does not necessarily denote CA activity (i.e., chemical disequilibrium in the diffusive surface boundary layer). One needs to compare the slopes with and without the external CA inhibitor at isotopic equilibrium to tell whether the CA is active or not (i.e., chemical disequilibium is present or not). Surprisingly, the large size of *Porosira glacialis*, up to 70 μm in diameter (Priddle and Fryxell 1985), would be favorable to a chemical disequilibrium in the periplasmic space since the effective thickness of the diffusional boundary layer around a cell is approximately equal to the cell radius (Wolf-Gladrow and Riebesell 1997).

Synechococcus ε_p seems insensitive to changes in μ/CO_2 (Popp et al. 1998). *Synechococcus* has a high SA/V ratio (which would indicate large efflux), and the main carbon supply is through bicarbonate transport (Table 4.2). Hence, while a large SA/V may be an advantage of small cells in the uptake of other nutrients, it is a disadvantage for the uptake of inorganic carbon because of the permeability of the membrane to CO_2. Consistent with previous results (Badger and Andrews 1982; Badger et al. 1985; Badger et al. 1994; Espie and Kandasamy 1994; Salon et al. 1996; Li and Canvin 1998; Popp et al. 1998; Price et al. 1998; Sueltemeyer et al. 1998; Omata et al. 1999; Maeda et al. 2000), our isotopic disequilibrium experiments indicate that *Synechococcus* (strain WH7803), a marine cyanobacterium, takes up primarily HCO_3^-. Other cyanobacteria have also been found to take up HCO_3^- (Miller and Colman 1980; Volokita et al. 1984). Figure 1.2 shows the potential inorganic carbon uptake mechanisms in *Synechococcus*. This result is at first quite surprising considering the fact that biological membranes are more permeable to CO_2 than to HCO_3^- (Gutknecht et al. 1977) and that *Synechococcus* has a high surface area to volume ratio (Popp et al. 1998), which should favor passive diffusion. The carbon isotopic composition of *Synechococcus* and the fact that fractionation is virtually independent of μ/CO_2 (Popp et al. 1998) clearly points toward a rapid exchange of inorganic carbon across the plasmalemma and indicates that *Synechococcus* is probably fighting a concentration gradient to keep Rubisco saturated and that most bicarbonate actively transported leaks out before being fixed. This is consistent with the *Synechococcus* study by Tchernov et al. (1997) who found that a large proportion of the inorganic carbon actively transported into the cell during photosynthesis effluxes. Hence, the large SA/V of *Synechococcus*, an advantage for the uptake of other nutrients (e.g.,

NO_3^-, PO_4^{3-}), which are generally charged and therefore plasmalemma impermeable, is a disadvantage in carbon assimilation because it favors efflux of the internal inorganic carbon pool over carbon fixation, forcing *Synechococcus* to spend energy on actively transporting bicarbonate. The requirement for HCO_3^- uptake is probably explained by the high $K_{1/2(CO2)}$ and low τ of cyanobateria (see review by Raven 1997). The large efflux hypothesis is also consistent with results obtained in Chapter 3 on Southern Ocean algal communities.

4.6. Environmental cues for CCM regulation

CCMs are believed to respond to environmental cues. Several environmental factors have been put forward as the main signal that induces changes in CCM activity, such as CO_2 concentration (Matsuda and Colman 1995; Matsuda et al. 2002), the ratio of CO_2/O_2 in the medium (Kaplan et al. 1990; Marek and Spalding 1991; Kaplan et al. 1994), DIC (or C_i) (Sueltemeyer et al. 1998), and μ/CO_2 (Laws et al. 1995 and this study). However, which of these factors is the primary signal remains enigmatic. One possibility that should not be ignored is that the CCMs response to external signals is species specific. Assuming that the carbon isotope fractionation is reflective of the CCM activity (which may not be the case, see section 4.3), we can indirectly test the relative contribution of these environmental cues. In the next section, the sensitivity of the photosynthetic isotope fractionation to some of these factors is assessed.

ε_p vs. DIC

As discussed in the previous paragraph, DIC has been hypothesized to be an environmental cue for the induction of CCMs (Sueltemeyer et al. 1998). To test this

hypothesis, *Phaeodactylum tricornutum* (UTEX 642) was grown in a chemostat on a low DIC medium (398μM DIC, 0.6 μM CO_2, μ/CO_2=1.28). The low DIC medium was prepared by acidifying seawater and bubbling it with nitrogen gas and buffering the solution to a final pH of 8.6 with sodium borate. This had the effect of drastically changing the bicarbonate concentration, but keeping the CO_2 concentration and the μ/CO_2 in the range previously studied by Laws et al. (1997). Because ε_p (10.49) was in agreement with the observed data under normal DIC concentration (Laws et al. 1997), this result is further evidence that CO_2 and not HCO_3^- controls the divergence of the observed carbon isotopic fractionation from a passive diffusion model in *Phaeodactylum tricornutum* (Cassar et al. 2002). Because HCO_3^- is the main inorganic carbon pool in seawater, the result also shows that the DIC is not a major control on the isotope fractionation. Again, assuming that the carbon isotope fractionation reflects CCM activity, the experiment demonstrates that DIC is not an induction signal for CCM activity in this particular diatom.

ε_p vs. CO_2 and μ/CO_2

The quantity of membrane transport proteins is generally regulated according to both the concentration of the nutrient in the medium and the metabolic needs of the cell for that nutrient. In short, transporter activity is often regulated by the bioeconomical concept of demand vs. supply. One possible surrogate for the inorganic carbon demand/supply is μ/CO_2. The inorganic carbon demand should be proportional to the photosynthetic rate (μC), and the CO_2 availability is obviously well represented by its concentration. For an analysis of the dependence of ε_p on μ/CO_2, see Laws et al. (1995;

1997). Growth rate influences ε_p through the rate of consumption of the intracellular inorganic carbon. A higher μ increases the proportion of the internal inorganic carbon pool that is fixed relative to efflux, therefore decreasing ε_p. Hence, CCM activity, like for instance active HCO_3^- transport, may be regulated by μ/CO_2 (Laws et al. 1995).

As discussed above, Matsuda and Colman (1995) theorized that the CCMs are induced by changes in CO_2 concentration. However, if this is correct, the CO_2 concentration covers only part of the equation and does not take into account the inorganic carbon metabolic need. With the exception of Burkhardt et al. (1999; 1999), in most carbon isotope experimental studies, CO_2 and μ vary concurrently. Such an approach does not allow an assessment of the specific impact of each of these factors on ε_p. Here, we isolated the contribution of CO_2 to ε_p by keeping a constant growth rate (μ=1 d^{-1}) in continuous-growth cultures and regulating the CO_2 concentration using an infrared CO_2 Analyzer (LI-COR LI-6262 CO_2/H_2O analyzer). Figure 4.8 shows that CO_2 does have an impact on fractionation, independent of growth rate (which was kept constant). However, as was mentioned earlier, a factor other than CO_2 may ultimately control isotopic fractionation.

<u>ε_p vs. CO_2/O_2</u>

In the current literature, photorespiration in marine algae and cyanobacteria is believed to be significantly less than in terrestrial C_3 plants because of the presence of a CCM in microalgae which, in theory, should suppress the oxygenase activity of Rubisco in a fashion similar to C_4 plants (Beardall 1989; Burns and Beardall 1987; Kerby and Raven 1985; Spalding 1989). It is also believed that, as opposed to higher plant Rubisco,

microalgae Rubisco has little potential for photorespiration even when carbon dioxide is limiting (Badger et al. 1998).

Phaeodactylum tricornutum was grown under various CO_2/O_2 to assess this ratio's potential as an environmental induction cue of CCM activity. Most carbon isotopic fractionation models including the original Farquhar et al. (1982) model assume that there is little or no intrinsic discrimination by dark respiration and photorespiration. Although there is little evidence supporting this statement, it has been widely accepted, and most carbon isotopic fractionation models do not incorporate the potential effect of photorespiration and dark respiration (Francois et al. 1993; Laws et al. 1995; Keller and Morel 1999). Recent evidence suggests that photorespiration and dark respiration could have a significant effect on carbon isotopic discrimination (Gillon and Griffiths 1997; Berner et al. 2000; Ghashghaie et al. 2001).

Studies of the effect of oxygen on carbon isotopic fractionation could provide a better understanding of CCMs and marine photorespiration. For instance, photorespiration could potentially explain the inflection in the carbon isotopic fractionation vs. μ/CO_2 relationship. Increased O_2/CO_2 would increase the competitive advantage of O_2 for the active site of Rubisco (being a competitive inhibitor, an increase in O_2 should increase the apparent $K_{1/2}$ of Rubisco for CO_2, but not alter the V_{max} of the carboxylation reaction- see Chapter 1). Because carbon isotope fractionation during photosynthesis is believed to be dependent on the ratio of carbon efflux to carbon fixation (Farquhar et al. 1982), an increase in oxygen should affect the isotopic signature of the organic carbon by increasing the ratio of efflux to fixation (increase f_{eff}). Assuming the model appropriately depicts carbon uptake, an increased O_2 concentration (and therefore

increased carbon efflux) would theoretically increase carbon isotope fractionation. Another possible outcome of increased O_2 is increasing the proportion of photorespired CO_2 in the internal inorganic carbon pool (and therefore increasing the proportion of photorespired CO_2 fixation) which, assuming the photorespired CO_2 is isotopically lighter than the internal inorganic pool, would also increase the apparent carbon isotope fractionation.

For a given marine phytoplankton species, the unresponsiveness of the carbon isotope fractionation signal to varying O_2 concentration would indicate an efficient suppression of photorespiration, i.e., an efficient CCM (Rubisco sufficiently saturated with CO_2 to hinder Rubisco's oxygenase activity), or a highly discriminative Rubisco (high CO_2 specificity factor). Preliminary results indicate that carbon isotopic fractionation is not affected by oxygen concentration. Two *Phaeodactylum tricornutum* chemostats were grown under almost identical growth conditions except for the oxygen concentration (13 % vs. 245 % of normal atmospheric O_2 levels, i.e., approximately 2.7 and 51.5 % O_2, respectively). DIC and CO_2 were almost identical to avoid the confounding effect of the CO_2 concentration on ε_p (1.548 mmol/kg, 1.3 μmol/kg and 1.565 mmol/kg, 1.7 μmol/kg, respectively). Experiments were conducted at high growth rates (0.98 d^{-1}) to increase the carbon demand, and low carbon dioxide (to favor the oxygenase reaction). Nitrate was the limiting factor. The carbon isotope fractionations at 13 and 245 % O_2 were almost undistinguishable (12.73 and 12.75‰, respectively), and in agreement with the observed carbon isotopic fractionation data at normal O_2 concentrations used by Laws et al. (1997). In contrast to Berner et al. (2000), we did not find an effect of oxygen on photosynthetic carbon isotopic fractionation.

Since Rubisco's CO_2 specificity factor for diatoms is not much greater than that of C_3 terrestrial plants (Raven 1997; Badger et al. 1998, approximately 108 vs. 80-100, respectively), which are known to be susceptible to oxygen, the fact that we did not observe an effect of oxygen on carbon isotope fractionation indicates the presence of an efficient CCM in diatoms. The ratio of the carboxylase to oxygenase activities of Rubisco is controlled not only by Rubisco's ability to discriminate between CO_2 and O_2 but also the ability of phototrophs to saturate the active site of Rubisco with CO_2 to suppress the oxygenase activity. The relative importance of the two catalytic reactions of Rubisco is dependent on the relative concentrations of O_2 and CO_2 at the site of fixation. Marine phototrophs, like terrestrial C_4 and CAM plants, have found a way to compensate for the catalytic inefficiency of Rubisco by saturating it with CO_2.

These results also show that the CO_2/O_2 ratio is not an environmental signal that induces CCM, as opposed to what has been established in previous studies (Kaplan et al. 1990; Marek and Spalding 1991; Kaplan et al. 1994). The CCM inducing factor(s) could however be species specific, which would explain differences in results between studies. Further studies on the effect of oxygen on the carbon isotopic fractionation in various algal species are needed to clarify this dilemma.

Alternatively, these results could indicate that there is no intrinsic isotopic discrimination associated with photorespiration. Photorespiration may have been present during these experiments but did not leave any isotopic signal. In the next section, we will present evidence based on the isotopic disequilibrium experiments in support of the latter hypothesis.

Isotopic disequilibrium Experiments in the study of marine photorespiration

We performed isotopic disequilibrium experiments on continuous growth-cultures under various O_2 levels to assess the importance of photorespiration in *Phaeodactylum tricornutum* strain UTEX 642. This algal species was grown in a chemostat under nitrate limitation at a growth rate of 0.6 d^{-1}. Results of the isotopic disequilibrium experiments are presented in Figure 4.9 and Table 4.3. The % CO_2 uptake is on average approximately 45% and does not change with variations in oxygen levels. Interestingly, the % CO_2 uptakes are significantly different from the ones presented in Chapter 2 on the same algal strain. This could indicate that when algae switch from one CCM pattern to another and "adopt it", the new CCM becomes constitutive. However, the possibility that another strain of *Phaeodactylum tricornutum* was accidentally used cannot be ruled out.

Table 4.3. Potential importance of photorespiration. Isotopic disequilibrium experiments on *Phaeodactylum tricornutum* strain UTEX 642 (μ=0.6 d^{-1}). The % O_2 is the oxygen concentration under which the continuous-growth culture was grown. The % CO_2 uptake is the relative contribution of the CO_2 uptake to total inorganic carbon uptake (see Chapters 2 and 3). The initial and final slopes are the slopes right after the ^{14}C injection (Initial) and after the isotopic equilibrium is reached (Final). They are normalized to the CO_2 and DIC concentrations that were prevalent in the chemostats, respectively. The slopes have arbitrary units. The estimates of the % CO_2 uptake and the initial and final slopes are based on averages of triplicate experiments.

% O_2	3.6	22.3	26.5	31.5	37.8
O_2/CO_2	21.1	15.2	21.7	33.1	1.3
% CO_2 uptake	44.7	45.6	44	42.6	46.2
Initial	153.2	158.5	78.2	76.7	58.5
Final	342.3	393.9	177.6	180.2	126.8

The lack of response of the % CO_2 uptake to changes in oxygen levels is consistent with the results presented above that indicate that the CO_2/O_2 is not a CCM inducing cue. Examination of the initial and final slopes of the isotopic disequilibrium experiments may also reveal how significant photorespiration is in marine algae. Because the initial slope represents CO_2 uptake, and assuming that the uptake of CO_2 is passive (may not be the case in some microalgae which are believed to have active CO_2 uptake mechanisms), the response of the initial slope to changes in oxygen concentration is a direct estimate of the competition between O_2 and CO_2 for the active site of Rubisco. Hence, the isotopic disequilibrium experiments could be used to assess the *in vivo* oxygen suppression of Rubisco's carboxylase activity, without having to suppress the CCM activity. Increasing the oxygen concentration will increase the concentration of the Rubisco-oxygen intermediate complex (whether Rubisco's oxygenase reaction is completed or not) and hence increase the probability of the internal inorganic carbon effluxing before being fixed. The oxygen could therefore affect the initial slope without having an effect on the final slope because the latter is representative of inorganic carbon uptake facilitated by CCM (if CCMs are present). As opposed to the initial slope, the final slope reflects the effect of oxygen both upstream (CCM activity) and downstream of Rubisco (photorespiratory carbon loss). Such a measurement however relies on two assumptions. First, that the uptake of CO_2 is purely passive. Second, either that CA is not present or that its activity does not change in response to changes in oxygen levels. This is to our knowledge the first time that the isotopic disequilibrium experiments have been employed for photorespiration measurements. They could prove to be an efficient method

to estimate the *in vivo* kinetic properties of Rubisco (such as Rubisco's selectivity factor for CO_2 over O_2- see Chapter 1).

Based on the % CO_2 uptake (Table 4.3), we can safely say that a CCM is active. Nonetheless, our results indicate that both the initial and the final slopes are affected by the oxygen concentration. Carboxylation is decreased at oxygen concentrations greater than 22 %. It therefore seems that the CCM activity is not sufficient to suppress photorespiration. Interestingly, only an increase in oxygen concentration above normal atmospheric concentration affects the carbon uptake kinetics. In other words, an oxygen concentration below normal atmospheric levels does not seem to increase the carboxylase efficiency (little difference in both initial and final slopes between 3.6 and 22.3 % oxygen). A change in algal physiology at oxygen concentrations above normal atmospheric levels would be consistent with this step-like function. This physiological behavior is evocative of the biphasic response of C_3-C_4 intermediates to oxygen concentration. C_3-C_4 intermediates are only slightly inhibited by an increase in O_2 concentration up to some O_2 concentration. At that point, the inhibitory response to any additional increase in O_2 concentration becomes more significant. The reduced photorespiration in C_3-C_4 intermediates is predominantly attributable to a recycling of photorespiratory CO_2. The biphasic response is due to a saturation of the mechanism involved in the capture of the photorespiratory CO_2 at some oxygen concentration. β-carboxylases, present in this algal strain (see Chapter 5), could potentially be involved in the capture of the photorespiratory CO_2 before it effluxes from the cell.

The atmospheric oxygen during the Phanerozoic period varied between approximately 15 and 30% (Berner 1999). The lack of response of the carboxylase to the

oxygen below current atmospheric concentrations may be explained by an evolutionary adaptation and maximal fit to an oxygen concentration that has changed very little over the last 550 million years. The fact that phototrophs were rarely exposed to oxygen concentrations much greater than present day levels may account for the apparently strong inhibition of Rubisco's carboxylase activity when the oxygen concentration is greater than normal current atmospheric values. There has been little selective pressure over geologic time for Rubisco to evolve a greater O_2-CO_2 discriminatory capability since the oxygen has rarely risen above present day values. It could however also mean that photorespiration has limited the oxygen level in the atmosphere to current values (James Lovelock Gaia hypothesis, see also Chapter 6 on "the world is a wine cask"). Isotopic disequilibrium experiments on species that have evolved strictly in oxygen deficient and anoxic environments, such as *Rhodospirillum rubrum*, would provide more insight into the evolutionary selective pressures on Rubisco's kinetic properties.

Interestingly, the initial and the final slopes are more dependent on the oxygen concentration than on the O_2/CO_2 ratio, as shown by a test of significance of the regression coefficients. For the sake of argument, let us assume the effect of the oxygen concentration on the carboxylation efficiency is linear at and above the 22.3% oxygen concentration. Unless physiological processes (such as CCMs) are initiated in response to changes in O_2 or in O_2/CO_2, there is no reason to believe that the competition between CO_2 and O_2 for the active site of Rubisco should not be linear. In this regard, our results indicate that CCMs are constitutive in this particular species (see Chapter 2; no change in % CO_2 uptake in the experiments presented in Table 4.3). The slopes of the "initial and final slopes vs. the O_2 concentrations" are statistically more significant (P=0.165 and

0.169, respectively) than the slopes of the "initial and final slopes vs. the O_2/CO_2 concentration" (P=0.664 and 0.666, respectively). Thus, the CO_2 concentration in the surrounding medium does not seem to be an important factor in regulating the inhibitory effect of oxygen on Rubisco's carboxylase activity. This can only be explained if the CO_2 concentration in the vicinity of Rubisco is not dictated by the CO_2 concentration in the surrounding medium. This is consistent with results presented above that demonstrate that the CCMs constantly provide Rubisco with inorganic carbon (approximately 45% CO_2 uptake). If this is correct, these results could have important implications for the interpretation of stable isotope data since it would indicate that stable isotope fractionation is not controlled by the CO_2 concentration in the water in which the algal cell is growing. Again, factors other than the CO_2 concentration, such as the factor(s) controlling the C/N ratio of algal cells (see above), may be more significant contributors to the isotopic signature of photosynthetic organic matter. For instance, carboxylases other than Rubisco, with an isotopic discrimination factor different from Rubisco, and unaffected by the presence of oxygen, could contribute relatively more to the carbon assimilation as the oxygen increases and Rubisco is inhibited (see Raven 1997 for a review of the various carboxylation pathways). At high O_2/CO_2 conditions (when Rubisco's carboxylase activity is reduced), fixation of HCO_3^- by β-carboxylases could become relatively more important (see Chapter 6).

The plateau area observed at about 60 seconds (Figure 4.9) in the isotopic disequilibrium experiments suggests that there is a significant loss of ^{14}C from the organic pool at that time (or that ^{14}C stops being fixed at that time, which is unlikely). This ^{14}C loss is consistent with photorespiratory loss of labeled inorganic carbon

(*downstream* O_2 inhibition of carbon fixation). The time required for the ^{14}C to be fixed, to go through the Calvin cycle, and to be photorespired as ^{14}C labeled ribulose 1,5-bisphosphate cycles through the photorespiratory carbon oxidation cycle (PCOC) could explain the delay in the onset of the plateau. Because the specific activity of the inorganic carbon that is photorespired was higher when it was fixed than the one that is being fixed when photorespiration of labeled carbon starts (plateau), the fact that the plateau is parallel to the x-axis does not mean that the rate of photorespiration is equal to the rate of photosynthesis. The specific activity of the carbon that is photorespired is different from the one that is fixed at any time t. This result however suggests that the proportion of carbon fixed that is converted to ribulose 1,5-bisphosphate is high, as was to be expected: theoretically, out of 36 atoms fixed by Rubisco (12 molecules of 3-phosphogycerate), 6 atoms are converted to 2 molecules of glyceraldehyde 3-phosphate (and leave the Calvin cycle) and 30 atoms are converted to 6 molecules of ribulose 1,5-bisphosphate. A portion of the carbon in ribulose 1,5-bisphosphate is being photorespired.

Determining the photorespiration rate from the $^{14}CO_2$-injection experiment would require knowing the difference in specific activity of what is being fixed vs. what is being photorespired at any time. A simpler way to measure the photorespiration rate would be to inject the labeled carbon at seawater pH (isotope equilibrium experiment): the initial slope (before 60 seconds) would be the *gross photosynthetic rate* and the slope after the onset of the photorespiration of the labeled carbon would be the *net photosynthetic rate* (gross-total respiration). Preliminary experiments indicate that photorespiration at 21% O_2 is negligible. Further isotope equilibrium experiments at oxygen concentrations greater than 21% should however be performed. Our results indicate that photorespiration

in marine ecosystems could be important when the O_2 concentration is greater than 21%. Such would be the case in sea ice brines, where photosynthetically active ice algae can dramatically decrease the CO_2 concentration with a parallel increase in the O_2 concentration (Gleitz et al. 1995).

4.7. Conclusions

There has been a long debate over carbon isotopic fractionation results. Keller and Morel (1999) have mathematically shown that active transport of both CO_2 and HCO_3^- can explain the upward curvature of ε_p as a function of μ/CO_2. Hence, the carbon transport mechanism cannot be inferred from the stable isotope fractionation data. The isotopic disequilibrium experiments with *Phaeodactylum tricornutum*, which predominantly takes up CO_2 (Cassar et al. 2002), and *Emiliania huxleyi*, which has the ability to harvest the bicarbonate pool (Dong et al. 1993; Laws et al. 1998; Dong et al. 1999) indicate that both bicarbonate and CO_2 transport can explain the inflection in the ε_p vs. μ/CO_2 model observed with these two species.

On the other hand, these results could also mean that isotopic fractionation during photosynthesis is *not* controlled by the mode of inorganic carbon transport and that the onset of CCMs may *not* be responsible for the divergence of the observed data from a passive diffusion model of ε_p vs. μ/CO_2 (linear model). Another factor(s), which influences C/N, may control the ε_p. Changes in total cellular enzymatic activity of Rubisco may explain the carbon isotopic fractionation data. Our results show that the dependence of ε_p on μ/CO_2 may be indirect, and that the latter may not be the primary factor controlling isotopic fractionation in marine algae.

Several authors have attributed the dependence of ε_p on μ/CO_2 to changes in the carbon transport mechanisms (Francois et al. 1993; Laws et al. 1995; Rau et al. 1996; Bidigare et al. 1997; Laws et al. 1997; Rau et al. 1997; Popp et al. 1998; Keller and Morel 1999; Riebesell et al. 2000; Rau et al. 2001) and may have failed to take into account variations in the carbon fixation ability in response to growth conditions. Although some of the variability in ε_p may in fact be credited to changes in the carbon supply (i.e., carbon demand/supply model, diffusion and active transport mechanism), the dependence of the carboxylation kinetics of Rubisco on both CO_2 and growth rate (see section 4.3) is also consistent with the ε_p on μ/CO_2 correlation cited in the literature. The ε_p vs. μ/CO_2 would be an indirect dependence on Rubisco kinetics. In the next chapter, we will discuss the potential contribution of β-carboxylase activity to the overall photosynthetic carbon isotope fractionation.

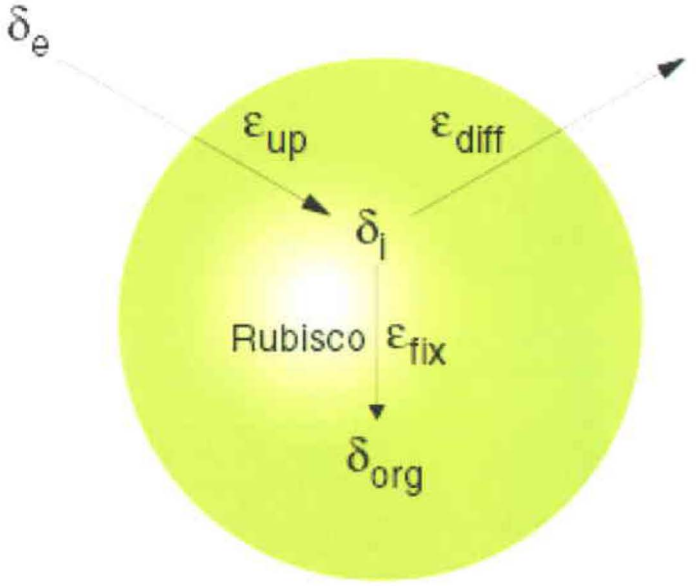

Figure 4.1. Graphical representation of the carbon isotope fractionation model. δ_e, δ_i and δ_{org} are the isotopic signatures of the external source of carbon (CO_2 and/or HCO_3^-), of the internal inorganic carbon pool, and of the organic carbon pool. ε_{up} is the fractionation associated with uptake (passive and active), relative to CO_2. ε_{diff} is the fractionation associated with diffusion out of the cell, or efflux, and ε_{fix} is the fractionation associated with carboxylation.

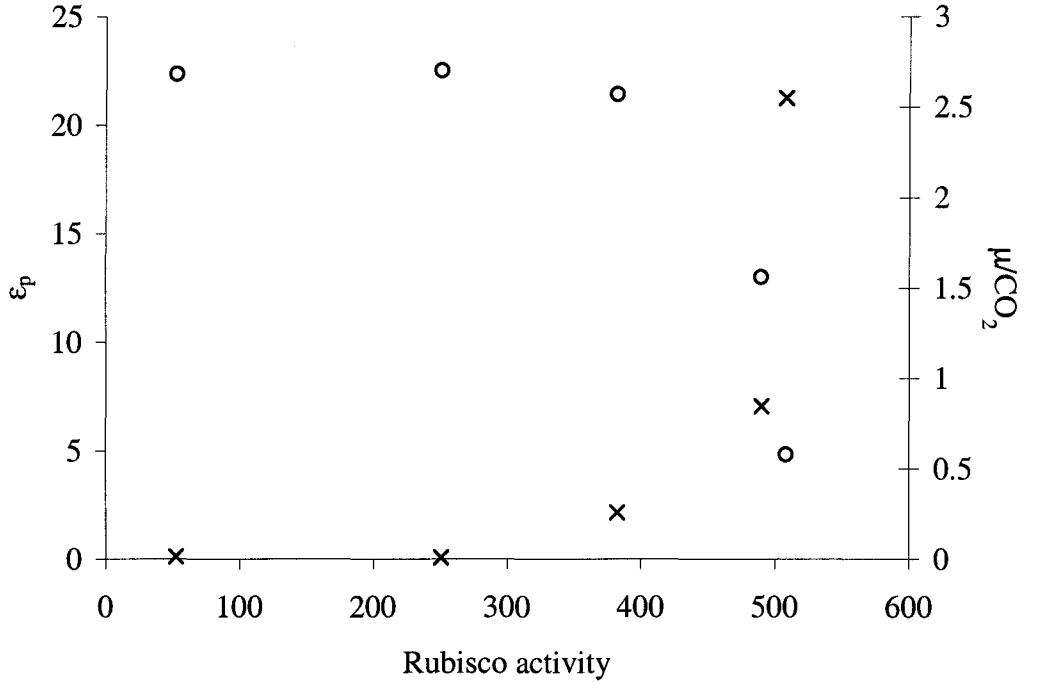

Figure 4.2. ε_p (circles) and μ/CO_2 (crosses) vs. Rubisco activity (nmol C (μg Chl) $^{-1}$(hr)$^{-1}$).

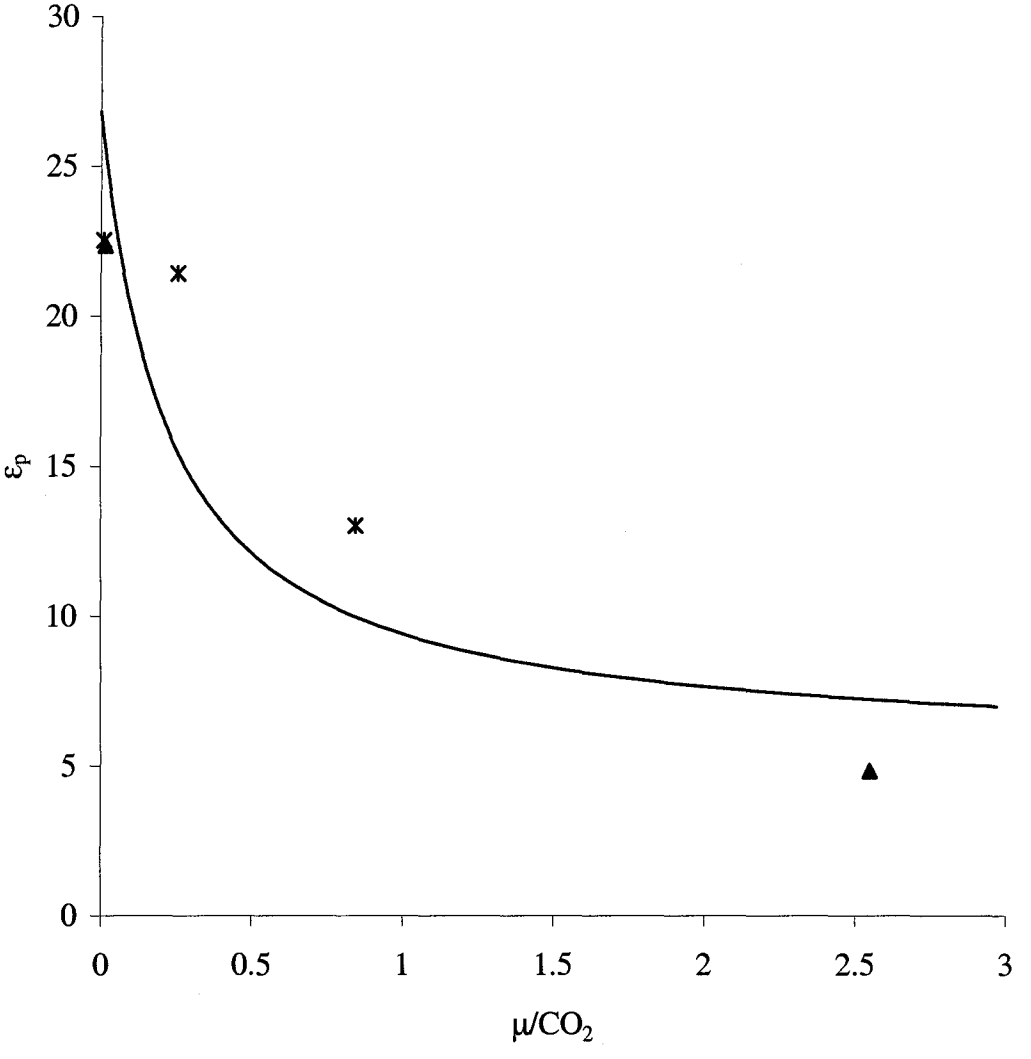

Figure 4.3. ε_p vs. μ/CO_2 in a phosphate-limited *Phaeodactylum tricornutum* (CCMP 1327) chemostat. The star and triangle symbols are nitrate and phosphate-limited experiments, respectively. The continuous line is a nonlinear fit to the data of Laws et al. (1997).

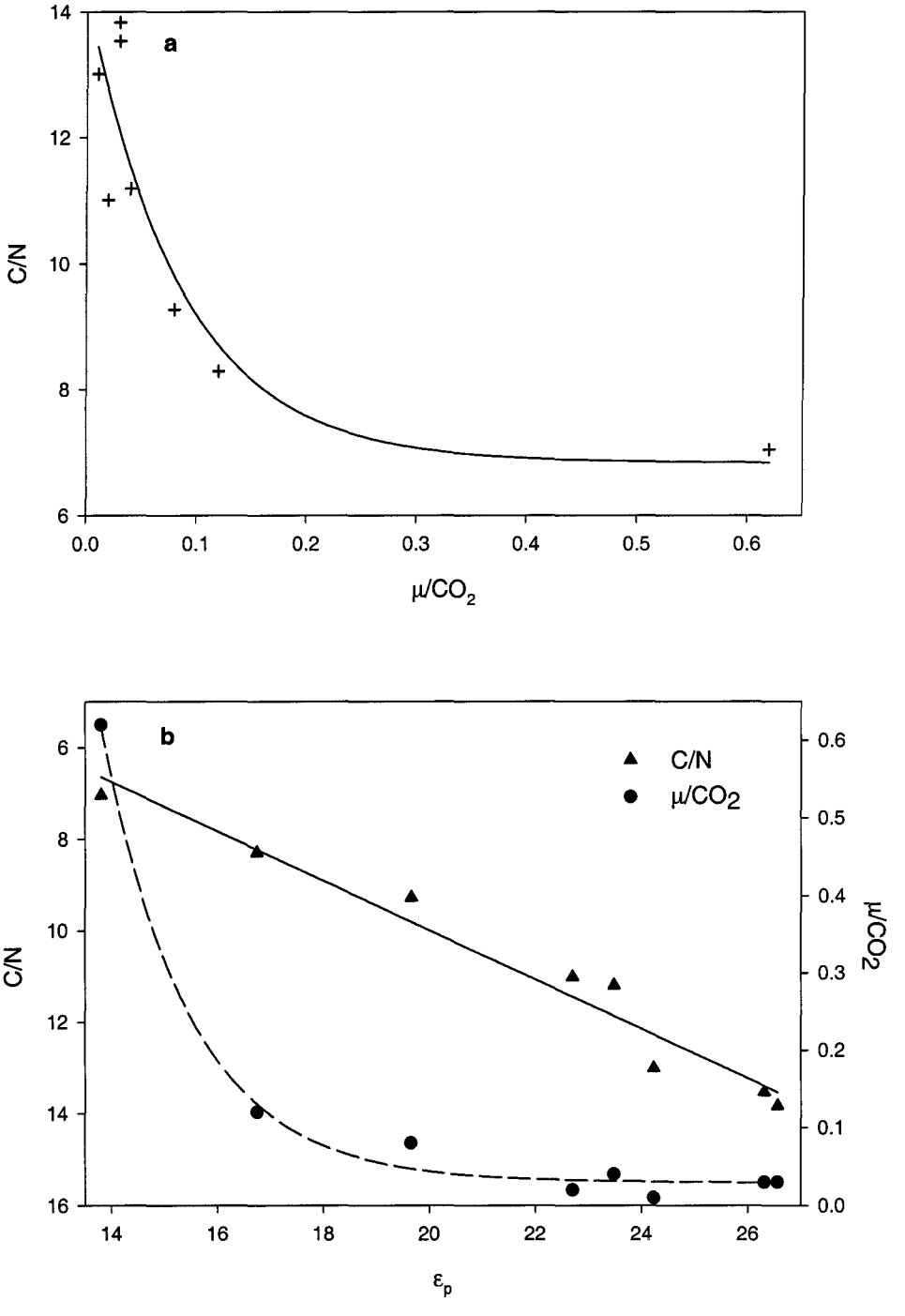

Figure 4.4. a) C/N vs. μ/CO_2. b) ε_p vs. C/N and μ/CO_2.

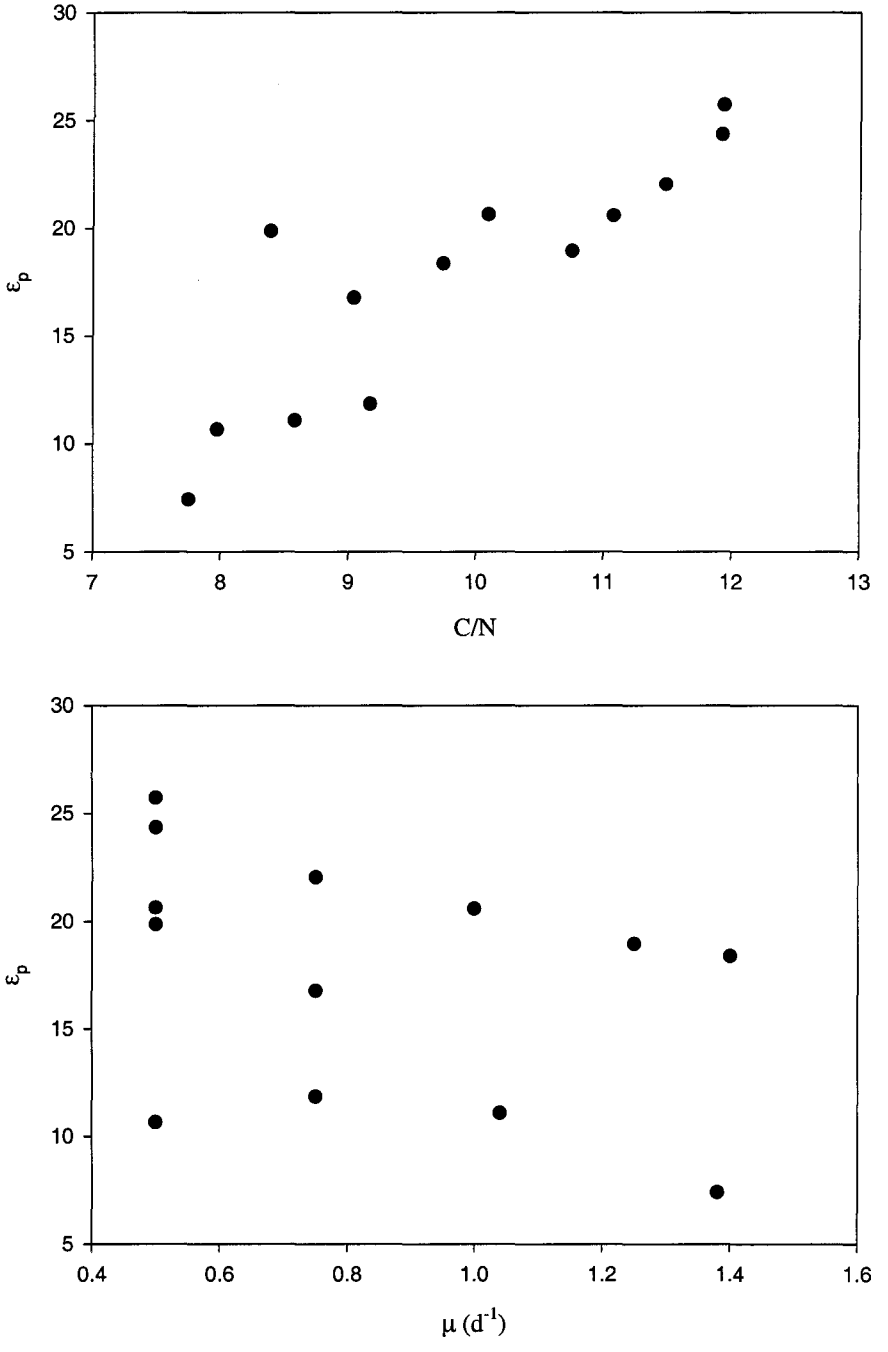

Figure 4.5. a) ε_p vs. C/N (ε_p= 3.3137(C/N) - 15.042; R^2 = 0.7539) b) ε_p vs. μ (ε_p= -6.6971 μ + 23.129; R^2 = 0.1677). Data is from Laws et al. (1997).

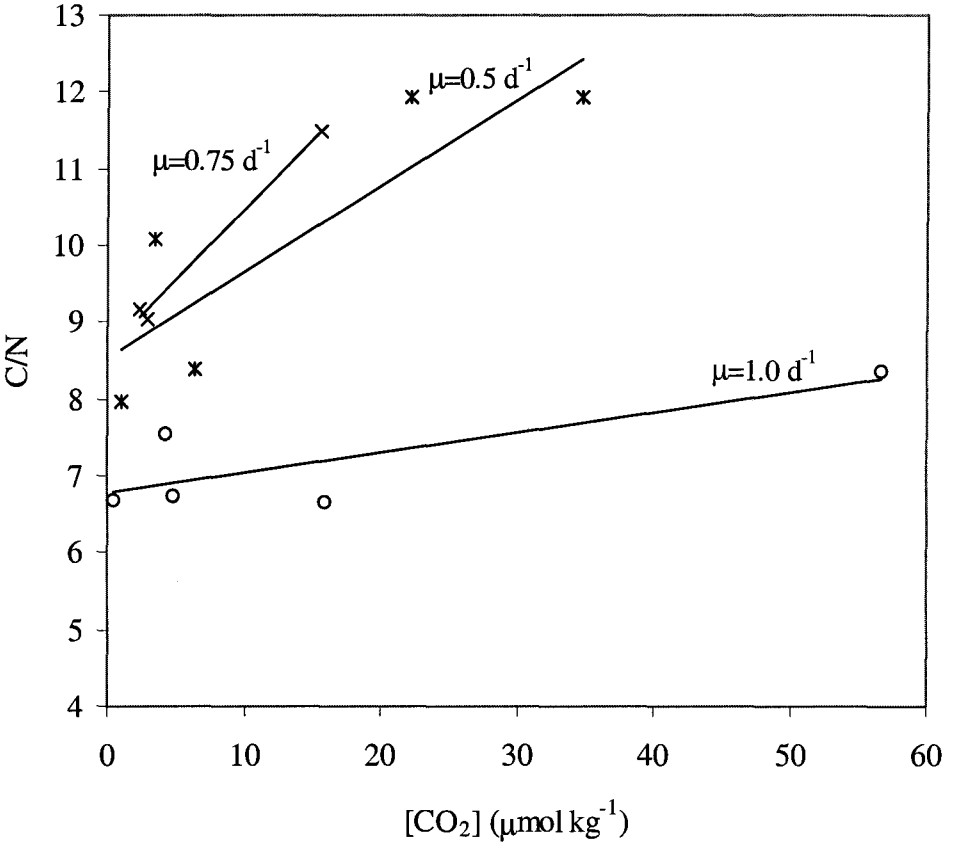

Figure 4.6. C/N vs. CO_2 for *Phaeodactylum tricornutum* at various growth rates. Star, cross, and circle symbols indicate growth rates of 0.5, 0.75, and 1 d^{-1}, respectively. The lines are linear least-square regressions for each growth rate (for μ=0.5, C/N = 0.1125[CO_2]+8.5304, R^2 = 0.7452; for μ=0.75, C/N = 0.1826[CO_2]+8.6246, R^2 = 0.9927; and for μ=1.0, C/N = 0.026[CO_2]+6.7772, R^2 = 0.6526). The results for the growth rates of 0.5 and 0.75 are from Laws et al. (1997). The results for the growth rate of 1 are from this study.

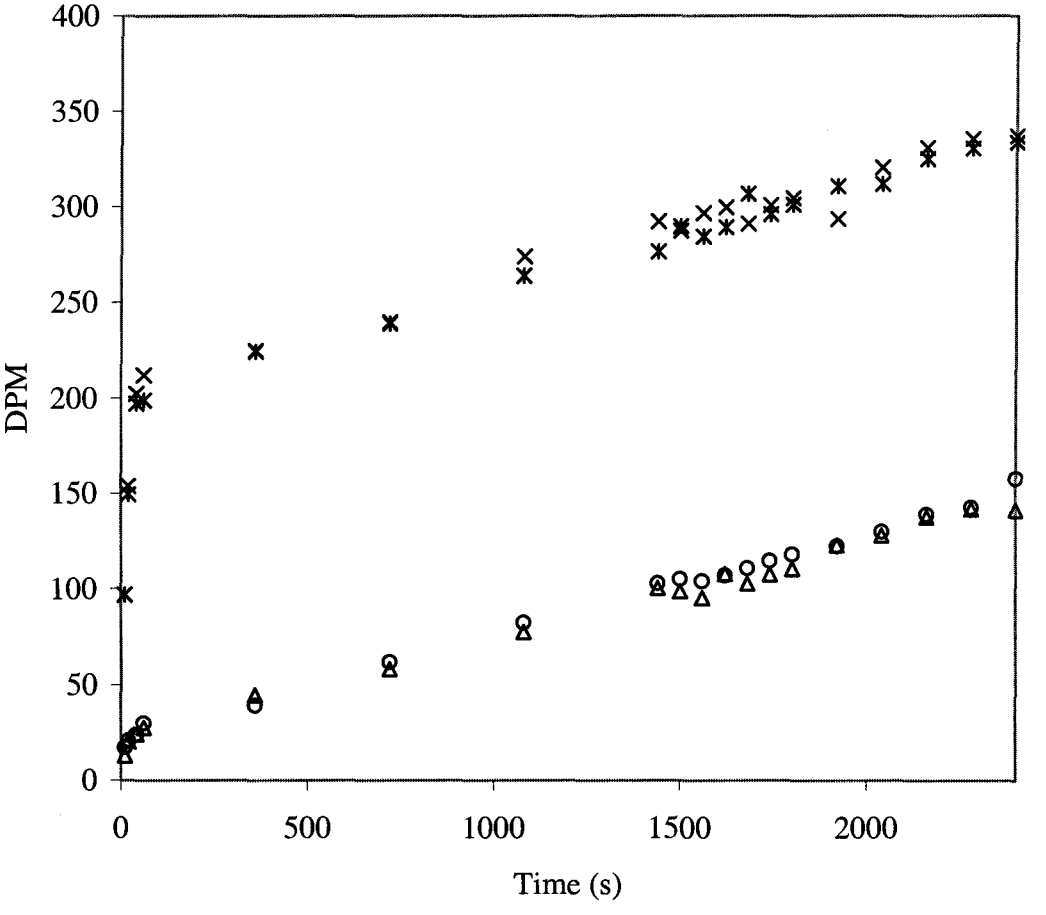

Figure 4.7. Isotopic disequilibrium experiment on *Porosira glacialis*. The y-axis is the cumulative ^{14}C activity in the organic phase. The star and cross symbols represent duplicate experiments in the presence of 200 μM DBS. The circle and triangle symbols represent duplicate experiments without the presence of the extracellular carbon anhydrase inhibitor.

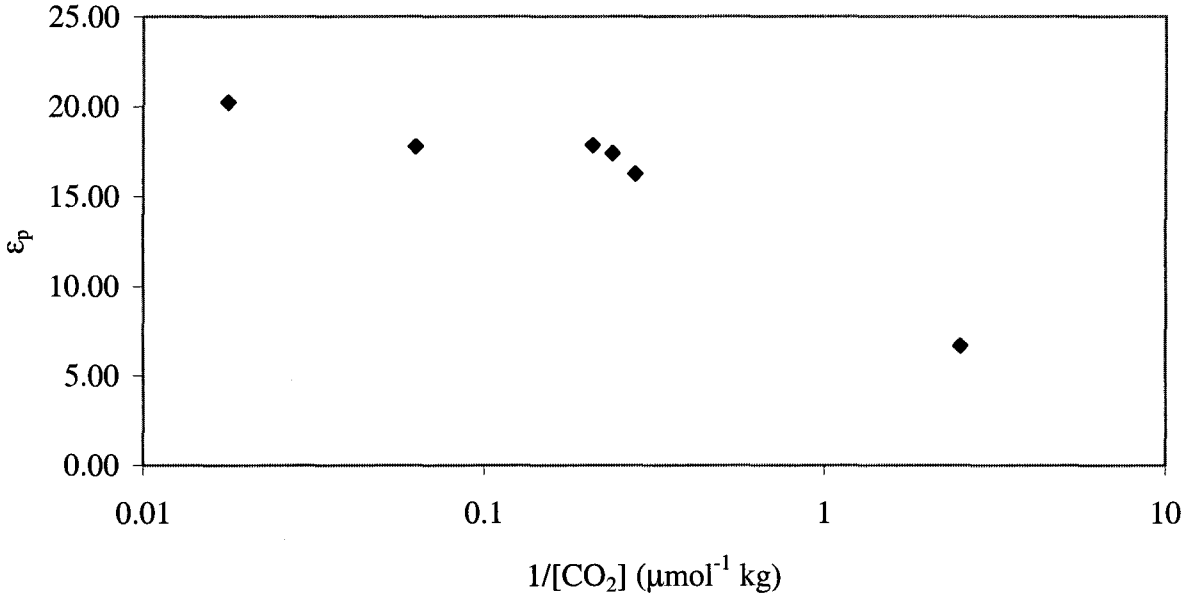

Figure 4.8. Carbon isotopic fractionation (ε_p) as a function of the CO_2 concentration, at a constant growth rate of 1 d^{-1} (*Phaeodactylum tricornutum*, nitrate limited chemostat).

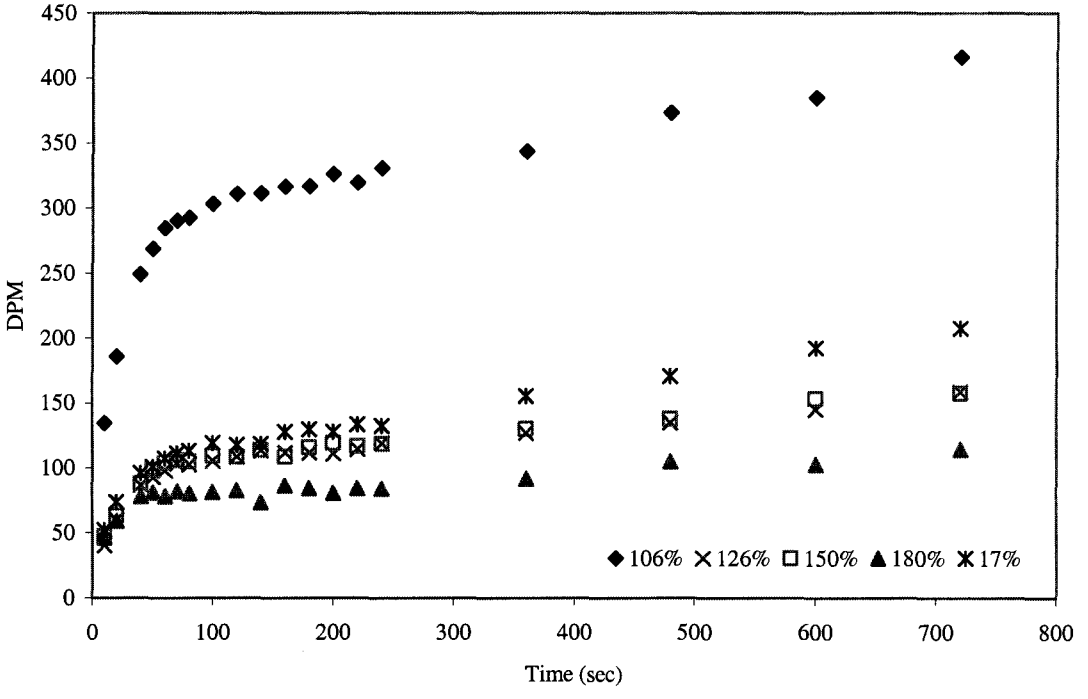

Figure 4.9. Isotopic disequilibrium experiments at various oxygen concentrations (17, 106, 126, 150, and 180 % of current atmospheric O_2 concentration).

CHAPTER 5. THE β-CARBOXYLASES AND THEIR POTENTIAL CONTRIBUTION TO PHOTOSYNTHETIC CARBON ISOTOPE FRACTIONATION IN MARINE PHYTOPLANKTON

5.1. Introduction

Let's assume photosynthetic carbon isotope fractionation (ε_p) follows the model:

$$\varepsilon_P = \varepsilon_t + f_a(\delta^{13}C_{CO_2} - \delta^{13}C_{source}) - f_{eff}(\varepsilon_{diff} - \varepsilon_{fix}) \qquad (5.1.1)$$

where ε_t, ε_{diff}, and ε_{fix} are the isotopic discriminations associated with the active transport mechanisms, diffusion and enzymatic carboxylation, respectively. $\delta^{13}C_{CO_2}$ and $\delta^{13}C_{source}$ are the isotopic signatures of the CO_2 in the medium and of the substrate for the carbon transport, respectively. f_a is the proportion of uptake that is active and f_{eff} is the ratio of efflux to influx (see Appendix F for its derivation). This model is similar to the one presented by Keller and Morel (1999). Assuming a box model where the inorganic carbon entering the cell, i.e., diffusion (D_i) + active uptake (A_t), is equal to efflux (D_o) + carbon fixation (G),

$$f_a = 1 - \frac{1}{\frac{D_o}{D_i} + \frac{G}{D_i}} \qquad (5.1.2)$$

where

$$D_i = k_1[CO_2]_{out} \qquad \text{and} \qquad D_o = k_2[CO_2]_{in}$$

where $[CO_2]_{in}$ and $[CO_2]_{out}$ are the intra and extracellular CO_2 concentrations, respectively. Assuming that there is symmetrical diffusional resistance of the plasmalemma to CO_2 (k_1=k_2), and that the intracellular inorganic carbon concentration (C_i) is identical to the extracellular one (C_o), which is probably a lower bound on the

C_i/C_o because most marine algae have been shown to have $C_i/C_o > 1$ (Raven 1997; Badger et al. 1998), and using a cytosilic pH of 7.1, an external carbon concentration of 2.1 mmol kg^{-1}, and assuming thermodynamic equilibrium of the carbonate species in the intracellular inorganic carbon pool (unlikely but would probably be a lower bound estimate of the intracellular CO_2 concentration), the ratio of D_o/D_i should be approximately 20.

For instance, Beer et al. (1990) found C_i/C_o that ranged from 6 to 78, depending on the growth condition, in *Ulva fasciata*. Similar results were obtained by Burns and Beardall (1987) in four microalgae with an average C_i/C_o of 7. Badger et al. (1998) also presents C_i/C_o for a variety of microalgae that ranges from 5 to 75. Hence, a D_o/D_i ratio of 20 is probably an underestimate, since we assumed $C_i/C_o=1$. Whether the intracellular inorganic carbon pool is at thermodynamic equilibrium remains a source of debate, as can be attested by the conflicting evidences in *Synechococcus* (Price and Badger 1989; Miller et al. 1997; Salon and Canvin 1997). If our model is correct, efflux >> diffusional influx. Hence, active transport is the dominant source of uptake under most conditions, and f_a, the proportion of uptake that is active, does not vary much, from 95 to 100%. This is consistent with the results obtained by Cassar et al. (submitted, Chapter 3) who found 86 to 94% efflux/influx in the Southern Ocean based on stable carbon isotope fractionation data and isotopic disequilibrium experiments.

Interestingly, if efflux is truly greater than influx, the periplasmic CO_2 concentration may be greater than the CO_2 concentration in the cytoplasm. Hence, although the overall effect of photosynthesis is to lower the CO_2 concentration in the bulk medium, microenvironments with elevated CO_2 levels may be present in the vicinity of

the cell (Falkowski 1997; Tchernov et al. 1997; Tchernov et al. 1998). Such a condition would defeat the purpose of having extracellular CA activity in the periplasmic space, since such activity would lower the CO_2 concentration to its thermodynamic equilibrium concentration. This reasoning however does not hold if the CA is released into the seawater, away from the vicinity of the cell. Since turbulent mixing is negligible at the cellular level and since the effective diffusional boundary layer thickness is essentially equal to the radius of the cell in spherical geometry, one would expect larger species to express less extracellular CA activity. Carbon isotope fractionation models may wrongly assume that the CO_2 concentration to which the photosynthetic organism is exposed is at equilibrium. A thermodynamic disequilibrium in the CO_2 concentration in the diffusional boundary layer due to efflux of CO_2 (from the CA mediated dehydration of actively imported HCO_3^-) would greatly complicate the interpretation of these models.

Assuming the substrate for the carbon transport is HCO_3^- (and that the actively transported inorganic carbon species does not change with growth conditions), which represents the largest potential ($\delta^{13}C_{CO_2} - \delta^{13}C_{source}$) (roughly 10 ‰), the maximum contribution of variations in f_a to variations in ε_p would be on the order of 0.5 ‰ (i.e., 10 ‰ x 0.05). In the extreme case where an algal cell would switch from 100 % active CO_2 uptake to 100 % active HCO_3^- uptake, the maximum contribution of variations in $f_a(\delta^{13}C_{CO_2} - \delta^{13}C_{source})$ to variations in ε_p would be on the order of 10 ‰. Such a range is not sufficient to account for natural variability in the isotopic signatures of photosynthetic organic matter. Moreover, such a drastic change in actively transported inorganic carbon species is unlikely. Hence, the overall contribution of $[f_a(\delta^{13}C_{CO_2} - \delta^{13}C_{source})]$ to ε_p is

probably much smaller than 10 ‰. These results imply that the isotopic fractionation during photosynthesis (ε_p) is *not* controlled only by the mode of inorganic transport and that the induction of CCMs may *not* be solely responsible for the divergence of the observed data from a passive diffusion model of ε_p vs. μ/CO_2 (linear model). If the ratio of actively transported species does not change with growth conditions (i.e., ($\delta^{13}C_{CO_2}$ - $\delta^{13}C_{source}$) constant), the contribution of changes in CCM activity to ε_p would be insignificant.

Following this reasoning, we can simplify Eq. (5.1.1) to

$$\varepsilon_P = \varepsilon_t - f_{eff}(\varepsilon_{diff} - \varepsilon_{fix}) + \delta^{13}C_{CO_2} - \delta^{13}C_{source} \qquad (5.1.3)$$

Assuming the mode of active transport to be invariant, one may argue that ε_t should be constant. ε_{diff} is probably also constant (O'Leary 1984). According to this analysis, the two parameters that may influence ε_p are f_{eff} and ε_{fix}. In the last chapter, we discussed the role of f_{eff}, and how changes in cellular Rubisco levels could affect this parameter. In this chapter, we will tackle the potential contribution of changes in ε_{fix} to the overall carbon isotopic fractionation.

Most carbon isotope fractionation models assume ε_{fix} to be constant and equal to $\varepsilon_{rubisco}$. This assumption could potentially lead to misinterpretation of fractionation data (see below), since other carboxylases, with different intrinsic carbon isotope discrimination factors, fix inorganic carbon in parallel (TCA cycle) and potentially upstream (C_4 photosynthesis) of Rubisco. In the next sections, we will look at β-carboxylases in marine algae, their importance in the Krebs cycle, and their potential

contribution to ε_p. We will also explore the possibility that some marine diatoms may possess the ability for C_4 photosynthesis.

5.2. Alternative carboxylation pathways

The tricarboxylic acid (TCA) cycle (also known as the Krebs cycle or the citric acid cycle) plays an important role in amino acid biosynthesis. Some of the key enzymes involved in the replenishment of TCA cycle intermediates are phosphoenolpyruvate carboxylase (PEPC) and phosphoenolpyruvate carboxykinase (PEPCK) (Latsko and Kelly 1983), which catalyse the anaplerotic carboxylation of PEP to oxaloacetate (OAA), and pyruvate carboxylase (PC), which catalyses the carboxylation of pyruvate also to OAA. OAA is then converted to aspartate or malate (species variable) by aspartate aminotransferase or malate dehydrogenase, respectively. Table 5.1 shows the reactions catalyzed by these various enzymes. This is not an exhaustive list of enzymes involved in carbon fixation. For extensive reviews of carboxylases, see Falkowski and Raven (1997) and Raven (1997).

Table 5.1. PEPC, PEPCK, and Pyruvate β-carboxylases and their catalytic functions

PEPC reaction
$PEP + HCO_3^- \rightarrow OAA + P_i$ (metallic activator: Mg^{2+}/Mn^{2+})
PEPCK reaction
$PEP + CO_2 + ADP \rightarrow OAA + ATP$ (metallic activator: Mn^{2+})
PC reaction
$Pyruvate + HCO_3^- + ATP \rightarrow OAA + ADP + P_i$ (metallic activator: Mg^{2+})

The presence of these enzymes in algae is well known (Morris 1980; Reinfelder et al. 2000). Factors controlling the importance of anaplerotic carbon fixation by β-carboxylases are however poorly understood. Various environmental factors may affect the βC/R (i.e., (β–carboxylation/Rubisco activities)x100). For instance, Guy et al. (1989) found that an ammonium pulse increased significantly the contribution of PEPC activity to total carbon fixation. The contribution of β-carboxylases to total carbon fixation has also been shown to increase at subsaturating light levels (Glover et al. 1975; Glover and Morris 1979; Guy et al. 1989; Zimba et al. 1990). Morris (1980), Descolas-Gros and Fontugne (1990) and Descolas-Gros and Oriol (1992) also showed that the βC/R is greater in the stationary than in the exponential phases. Assuming the increase in βC/R observed with the transition from the exponential to the stationary phase is due to a decline in growth rate, one could argue that the dependence of ε_p on μ/CO_2 is indirect. This would indicate that as cells evolve from an exponential stage of growth to a stationary phase, the TCA cycle contribution to carbon flow increases relative to the photosynthetic carbon reduction cycle (PCRC).

Because the synthesis rate of the TCA cycle metabolites is generally higher in the light, β-carboxylase may be higher during the photoperiod (Raven 1976). In fact, β-carboxylase can be stimulated by light (Raven 1970; Raven 1974; Morris 1980). Jiao and Chollet (1988; 1989) and Bakrim et al. (1993) have established that the covalent seryl-phosphorylation of PEPC during the transition from dark to light is responsible for its increase in catalytic efficiency. Phosphorylation by a PEPC kinase (Jiao et al. 1991; Vidal and Chollet 1997; Hartwell et al. 1999; Nimmo et al. 2001) decreases the sensitivity of PEPC to the allosteric inhibitor L-malate (Chollet et al. 1996; Vidal and Chollet 1997;

Nimmo 2000). Although most of the work on the influence of light on PEPC activity has been performed on C_4 plants, light-induced phosphorylation of the anaplerotic PEPC has also been shown in C_3 terrestrial plants (Duff and Chollet 1995; Li et al. 1996; Smith et al. 1996).

Theoretically, because β-carboxylation mainly provides carbon skeletons for amino acid synthesis (Mortain-Bertrand et al. 1988), the isotopic signature of proteins should reflect the isotopic fractionation associated with the β-carboxylase processes, unless there is an isotopic homogenization of elementary biomolecules. Increased ^{14}C labeling of the protein pool has in fact been associated with an increase in βC/R (Mukerji et al. 1978).

Hypothetically, if β-carboxylases assume only an anaplerotic role, the contribution of β-carboxylation to gross carbon fixation in continuous light should be 25% or less because in the anaplerotic β-carboxylase process, one carbon is added to the photosynthetic carbon reduction cycle (PCRC) derived 3-carbon PEP (Beardall 1989). βC/total carboxylation activities greater than 0.25 (or βC/R > 1/3) would imply an external source of PEP (e.g., mixotrophy, and/or provisional increase in βC/total carboxylation from consumption of carbohydrate reserves) and/or PEP recycling such as C_4 photosynthesis. A temporally sustained ratio greater than 0.25, such as in a steady-state continuous growth culture, would necessarily imply mixotrophy or PEP recycling (i.e., C_4 photosynthesis).

When grown under nutrient-limited conditions, nitrogen assimilation and photosynthetic CO_2 fixation dynamics become "uncoupled", and the starch content increases (Stevens and Van Baalen 1973; Syrett 1988; Turpin and Vanlerberghe 1991).

Under such conditions, the carbon requirement for amino acid synthesis can be provided by starch glycolysis. Under nutrient replete conditions, the nitrogen uptake and the production of amino acids are dependent on the supply of new photosynthates rather than stored carbohydrates. Hence, the extent of the uncoupling between the nitrogen assimilation and carboxylation is dictated by the nutrient availability. The growth rate can be regarded as a degree of nutrient limitation, i.e., the lower the growth rate (in the case of a chemostat the dilution rate), the greater the nitrogen limitation, the greater the luxury uptake of carbon. This may explain the dependence of the C/N ratio on μ and also potentially the strong linear correlation between ε_p and C/N we observed (see Chapter 4 and Figure 4.4). As nutrient-limited growth rate decreases, the C/N increases, which indicates a larger cellular proportion of carbohydrates relative to amino acids at low growth rates. Since β-carboxylases are involved in amino acid biosynthesis, one would expect a lower βC/R at low growth rates. Because Rubisco is isotopically more discriminatory than PEPC, a higher fractionation due to a smaller βC/R would ensue. However, a lower βC/R at low growth rates is opposite to observations performed in various studies (see above).

Under nutrient limitation, phosphoenolpyruvate, the substrate for the PEPC enzymatic reaction, will most likely come from stored carbohydrate. As growth rate increases, the luxury storage of carbohydrates decreases, and the contribution of the Calvin-Benson derived 3-PGA to PEP for β-carboxylation increases. In short, as growth rate increases, more of the Rubisco-fixed carbon is directly funneled to β-carboxylation instead of being initially stored as carbohydrates.

Because the rates of photosynthetic carbon fixation and nitrogen assimilation are uncoupled, Rubisco's carboxylase activity is not a direct positive function of growth rate (otherwise, the C/N would be independent of growth rate). On the other hand, PEPC activity has been shown to be a linear function of nitrogen assimilation (growth rate) (Vanlerberghe et al. 1990). Consequently, PEPC/R should theoretically vary with growth rate.

5.3. The contribution of β–carboxylation reactions to photosynthetic carbon isotope fractionation

Assuming the above reasoning is correct, i.e., that β–carboxylase activity does not vary in a constant proportion to Rubisco activity (variable βC/R) and that it is a significant contribution to total carbon fixation, as shown by Morris (1980), ε_{fix}, the isotopic fractionation associated with carbon fixation should vary with growth rate. Most carbon isotope fractionation models may therefore incorrectly assume ε_{fix} to be constant and equal to $\varepsilon_{rubisco}$. To allow for variations in (anaplerotic βC)/R,

$$\varepsilon_{fix} = \frac{1}{(1+\beta C/R)}\varepsilon_{rubisco} + (1-\frac{1}{(1+\beta C/R)})\varepsilon_{\beta} \qquad (5.3.1)$$

and the overall photosynthetic carbon isotope fractionation would therefore be

$$\varepsilon_P = \varepsilon_t + f_{eff}(\frac{1}{(1+\beta C/R)}\varepsilon_{rubisco} + (1-\frac{1}{(1+\beta C/R)})\varepsilon_{\beta} - \varepsilon_{diff}) \qquad (5.3.2)$$

where ε_β is the carbon isotope fractionation associated with β–carboxylase activities. The kinetic isotope fractionations associated with fixation of HCO_3^- by PEPC (in terms of dissolved CO_2) is 4.7 ‰ (O'Leary et al. 1992) and fixation of CO_2 by phosphoenolpyruvate carboxykinase (PEPCK) is 24-40 ‰ (Arnelle and O'Leary 1992). In

order to explain the linear dependence of ε_p on C/N, the latter should be inversely proportional to the PEPC/R. A recent study has in fact demonstrated the importance of the ratio of PEPC to total carboxylase activities in the control of carbon isotope discrimination in terrestrial C_3 plants (Le Roux-Swarthout et al. 2000).

The potential role of β–carboxylation in the control of ε_p has been postulated in the past (Beardall et al. 1976; Falkowski 1991), but it is nowadays generally dismissed based on the lack of correlation between interspecific isotopic composition and βC/R activity (Leboulanger et al. 1995) and also based on measurements of anaplerotic carbon fixation in marine algae (Holdsworth and Colbeck 1976; Mortain-Bertrand et al. 1988; Falkowski and Raven 1997; Raven 1997). β–carboxylation is generally assumed to represent no more than 10-15% of total carbon fixation, which would not provide enough leverage to account for the large changes observed in photosynthetic carbon isotope fractionation. There is however evidence that under some conditions, PEPC activity can account for a larger proportion of carbon fixation.

The dependence of fractionation on the length of the photoperiod (Burkhardt et al. 1999) may also be due to the importance of the β-carboxylases during the scotophase. Burkhardt et al. (1999) showed that several species, including *P. tricornutum*, showed lower isotopic fractionation during a 16:8 h light:dark cycle than under continuous light. They attribute this difference to changes in the instantaneous growth rates. However, variation in the PEPC/Rubisco activity associated with adaptation to the diel cycle could also explain such isotopic behavior.

We performed enzymatic assays on continuous-growth cultures of *Phaeodactylum tricornutum* under various growth conditions (nitrate vs. phosphate limited, high vs. low

growth rate, high vs. low CO_2) to examine the contribution of β-carboxylases to the overall carbon isotope fractionation signal and to investigate the potential of marine diatoms (in this case, *Phaeodactylum tricornutum*) for C_4 photosynthesis. We performed Rubisco, PEPC, and PEPCK enzymatic assays according to the methods of Descolas-Gros and Oriol (1992), Reinfelder et al. (2000), and Grzymski et al. (2002). Discrepancies in the results obtained with these different methods are discussed in section 5.5. In the next section, we will focus our analysis on the results obtained with the Reinfelder et al. (2000) method, unless stated otherwise. Results are presented in Table 5.2. We define βC/R as [((PEPC+PEPCK)/Rubisco)x100], which is a good approximation of the contribution of β-carboxylase activity to carbon fixation in marine diatoms. PEPC activity is the rate in the absence of ADP, and PEPCK activity is the difference between this rate and that obtained in the presence of ADP (see Tables 5.1 and 5.2).

Table 5.2. The influence of growth conditions on Rubisco, PEPC, and PEPCK activity. PEPC/R is equal to (PEPC/Rubisco)×100. PEPCK activity is equal to $(\frac{\text{Rubisco}}{100}\times\frac{\beta C}{R})-\text{PEPC}$. The enzymatic activities were determined according to the methods presented in Reinfelder (2000).

Limiting Nutrient	μ (d^{-1})	Chl a ($mg\ m^{-3}$)	[CO_2] ($\mu mol\ kg^{-1}$)	μ/[CO_2]	ε_p	Rubisco	PEPC	PEPC/R	βC/R
Phosphate	1.02	44.93	70.1	0.0146	22.35	52.6	26.4	50.2	155.0
Phosphate	1.02	37.75	0.40	2.55	4.84	508.5	18.6	3.7	6.5
Nitrate	0.93	15.6	96.4	0.0096	22.52	250.6	116.4	46.5	105.5
Nitrate	0.93	13.74	1.10	0.846	13.01	489.9	116.3	23.8	21.5
Nitrate	0.18	7.95	0.70	0.257	21.42	382.3	202.2	52.9	62.4
Batch	-	15.89	-	-	-	98.9	81.3	82.1	119.0

We observed PEPC activity and βC/R much greater than generally reported in the literature for diatoms (Appleby et al. 1980; Descolas-Gros and Fontugne 1985; Descolas-Gros and Oriol 1992). PEPC is commonly not considered to be significant in *Phaeodactylum tricornutum* or in diatoms in general (Holdsworth and Colbeck 1976; Holdsworth and Bruck 1977; Kremer and Berks 1978; Appleby et al. 1980; Descolas-Gros and Fontugne 1985; Descolas-Gros and Fontugne 1990; Descolas-Gros and Oriol 1992; Johnston et al. 2001). However, our results are consistent with Glover and Morris (1979) who found PEPC activity (enzymatic assays without the presence of $MnCl_2$ and ADP) in *Phaeodactylum tricornutum.* The differences in results between these studies may be due to strain-specific variations in β-carboxylases. However, part of the discrepancies can be attributed to differences in enzymatic assay conditions employed in these research papers (see section 5.5). Our results indicate that the contribution of β-carboxylase activity to carbon fixation in marine diatoms may currently be underestimated (the *in vitro* enzymatic assays may however not be representative of *in vivo* conditions). In addition, the results show that simultaneous activities of PEPC and PEPCK can occur within a given species, as opposed to what had been observed in other studies (Appleby et al. 1980; Descolas-Gros and Fontugne 1990).

Previous studies have mostly focused on the effect of growth rate (stationary vs. log phase) on β-carboxylases activities (Morris 1980; Descolas-Gros and Fontugne 1990; Descolas-Gros and Oriol 1992). Our results are consistent with these studies. The βC/R activity increased as the nitrate-limited *Phaeodactylum tricornutum* culture evolved from a rapid growth (μ=0.93; βC/R=21.5) to a slower growth (μ=0.18; βC/R=62.4) to a final

stationary phase (βC/R=119). Since the change in CO_2 concentration between the growth rates of 0.93 and 0.18 is minimal (1.1 and 0.70 μmol kg^{-1}, respectively), the increase in βC/R with the decrease in growth rate is solely due to a decrease in growth rate. A decrease in CO_2 concentration is actually expected to lower the βC/R (see section 5.4). Hence, as algal cells evolve from a log phase to a stationary phase of growth, βC/R increases.

However, our results are inconsistent with our original hypothesis that a decrease in isotopic fractionation at high μ/CO_2 is due to an increase in PEPC/R. In fact, PEPC/R actually decreases as μ/CO_2 increases, both in the phosphate and in the nitrate-limited chemostats (Table 5.2). It is however possible that PEPC carboxylates respired CO_2, as has been demonstrated in C_3 terrestrial plants (Latsko and Kelly 1983). Such a mechanism would increase the apparent isotopic discrimination factor associated with PEPC activity. It could also be due to the fact that a significant fraction of the PEPC-fixed CO_2 may be decarboxylated within the TCA cycle. Its residence time in the organic phase would therefore not be long enough to contribute to the isotopic signature of the organic matter. On the other hand, our results clearly establish that PEPC/R varies with growth conditions and that it may be a significant contribution to total carbon fixation. Hence, assuming ε_{fix} in Eq. (5.1.1) to be constant may be incorrect.

As discussed in the previous paragraph, although changes in isotopic fractionation cannot be explained by a change in β-carboxylase activity, we did find a strong correlation between the PEPC/R (and βC/R) and ε_p and μ/CO_2 (Figure 5.1). This correlation is much stronger than if PEPC/R and βC/R are compared to the growth rate

and the CO_2 concentration independently, which suggests that there may be a physiological reason for the change in cellular carboxylase activity in response to changes in CO_2 demand/supply. However, most of this correlation is probably driven by the dependence of Rubisco levels on μ/CO_2 (see Chapter 4). Many physiological pathways are expected to respond to changes in CO_2 availability. This is further evidence that the dependence of isotopic fractionation on μ/CO_2 may be indirect or even perhaps fortuitous.

As discussed above, phosphorylation of a serine residue on PEPC increases its catalytic efficiency. The PEPC activity would therefore be expected to be lower under phosphate limitation than under nitrate limitation. As expected, under approximately the same growth rate (and identical light and temperature) the PEPC activity is greater under nitrate than under phosphate limitation. We attribute this difference to a greater activation of PEPC by phosphorylation under nitrate limitation than under phosphate limitation.

5.4. C_4 Photosynthesis in marine diatoms

It has recently been argued that the β-carboxylase activity in a marine diatom may be upstream and in series with Rubisco (i.e., C_4 pathway) (Reinfelder et al. 2000) in addition to the more commonly accepted β-carboxylase activity parallel to Rubisco activity (i.e., anaplerotic function). This would suggest that marine algae have evolved two compensatory metabolic processes upstream of Rubisco, the C_4 pathway and CCMs. The first steps of the C_4-dicarboxylic acid pathway is the carboxylation of the C_3 monocarboxylate PEP to oxaloacetate by PEPC, which is insensitive to O_2. The C_4 molecule is then transported to the site of Rubisco carboxylation where it is decarboxylated to release and concentrate the CO_2 in the vicinity of Rubisco. C_4

photosynthesis is believed to be a competitive advantage under certain circumstances (e.g., low CO_2, high O_2) because it minimizes photorespiration by spatially concentrating CO_2 around Rubisco. The most direct evidence of C_4 photosynthesis is by pulse-chase ^{14}C-inorganic carbon-labeling experiments (Reiskind et al. 1988; Reiskind and Bowes 1991; Reinfelder et al. 2000). The evidence provided by Reinfelder (2000) that C_4 photosynthesis occurs in *Thalassiosira weissflogii* has however received some criticism (Johnston et al. 2001), and the dispute is yet to be resolved.

Assuming the C_4 photosynthetic pathway is present in marine diatoms and that it responds to the same environmental cues as the CCM, such as low inorganic carbon availability, β-carboxylase activity should increase at low CO_2 concentration. Hence, a negative correlation between CO_2 concentration and β-carboxylase activity would be consistent with C_4 photosynthesis, which functions in an analogous fashion to CCMs, spatially concentrating CO_2 around Rubisco when passive CO_2 diffusion is not sufficient to saturate Rubisco. A lack of response would indicate that either marine C_4 photosynthesis is constitutive or that the β-carboxylase activity is simply anaplerotic. In short, a lack of response would not resolve the issue. A positive correlation between the β-carboxylase activity and the CO_2 concentration would be incompatible with marine diatom C_4 photosynthesis theory and would indicate that, assuming β-carboxylases are mainly involved in the anaplerotic replenishment of metabolites in the TCA cycle, a larger proportion of the inorganic carbon would be channeled through the Krebs cycle instead of the photosynthetic carbon reduction cycle when CO_2 availability increases. Another alternative is that PEPC and PEPCK are involved in some other pathway that is responsive to the CO_2 concentration.

Our results show that βC/R drastically responds to changes in CO_2 levels. β-carboxylation contribution to total carbon fixation increases with CO_2 availability, which implies that under CO_2-replete conditions, a larger proportion of the inorganic carbon is fixed anaplerotically. The increase in β-carboxylase with CO_2 concentration we observed is therefore inconsistent with the hypothesized C_4 photosynthesis in marine diatoms (Reinfelder et al. 2000). The results presented in Chapter 4 indicate that the decrease in Rubisco activity is partly responsible for this increase in βC/R associated with an increase in CO_2 levels. However, irrespective of the effect of CO_2 on Rubisco's kinetic efficiency (see Chapter 4), an increase in β-carboxylases is observed with increased CO_2 concentration both for the nitrate and the phosphate limited *Phaeodactylum tricornutum* chemostats (Table 5.2). Most of this increase is attributable to an increase in PEPCK activity (PEPC activity does not respond in the nitrate-limited chemostat). This is to our knowledge the first time a dependency of β-carboxylases activities on CO_2 concentration has been observed. The CO_2 regulation of β-carboxylase activity is considerable, as is attested by the large increase in βC/R associated with the transition from low CO_2 to high CO_2 conditions (24 and 4 fold increases in βC/R for the phosphate and the nitrate limited chemostats, respectively). Since the anaplerotic carboxylations associated with PEPC and PEPCK are essential for the biosynthesis of certain amino acids, porphyrins, and pyrimidines (Reinfelder et al. 2000), an increase in CO_2 should boost the synthesis of some of these biomolecules. For instance, a rise in tetrapyrrole (in chlorophylls) synthesis in response to increased CO_2 availability may occur (luxury uptake and fixation of inorganic carbon necessitates energy). In addition, since the TCA cycle is the final stage of carbohydrate and lipid oxidation, an increase in the activity of these anaplerotic

carboxylases would imply an increase in metabolism. Alternatively, the change in intracellular pH associated with variations in CO_2 concentration may affect these β-carboxylases efficiencies.

5.5. Enzymatic assay protocols

Theoretically, if the carboxylation rate obtained by enzymatic assay analysis is representative of the *in vivo* rate, the sum of Rubisco, PEPC, and PEPCK activities should equal the short-term *in vivo* ^{14}C uptake (long-term would be a measure of net photosynthesis). With the C:N ratio, the nitrate concentration of the medium, and the dilution rate, one can estimate the net photosynthesis of the nitrate limited steady-state continuous growth culture. Gross photosynthesis will be greater. The fact that the sum of the enzymatic assays carboxylations is smaller than the net photosynthetic rate derived from the chemostat's dilution rate (difference would be even larger with the gross photosynthetic rate) indicates that either some or all of the enzymatic assays (Rubisco, PEPC, PEPCK) underestimated the true *in vivo* enzymatic activities or that other enzymes may significantly contribute to carbon fixation. Hence, one should be careful in interpreting enzymatic assay results since they may not be representative of the *in vivo* enzymatic rates.

Comparison of enzymatic assay protocols

We found large discrepancies in results between the enzymatic assays presented by Descolas-Gros and Oriol (1992), Reinfelder et al. (2000), and Grzymski et al. (2002) (Figure 5.2). Generally, the method of Descolas-Gros and Oriol (1992) tends to underestimate the enzymatic activities relative to the other two methods except in the

case of the Rubisco assays. Interestingly, in the latter case, the Descolas-Gros and Oriol (1992) method gives results consistent with the other two methods, except when the CO_2 concentration in the growth cultures is high (both in the case of the phosphate and nitrate limited chemostats). In these cases, the Rubisco activities based on the Descolas-Gros and Oriol (1992) method are higher than those with the other two methods. Why such a discrepancy exists only when the culture was grown under high CO_2 conditions is unclear and an answer requires further experiments. A kinetic profile study of the influence of several factors on Rubisco activity in marine diatoms would be necessary. However, we can speculate that some Rubisco activator or inhibitor may be induced in response to the CO_2 treatment and react differently to various reaction mixtures. For example, Mg^{2+}, $NaHCO_3$, and glycerol are absent from the extraction solution of the Descolas-Gros and Oriol (1992) method but present in the other two methods. Alternatively, some of the chemicals in the reaction mixture of these various methods may directly inhibit or activate Rubisco under certain growth conditions. For instance, we observed that adding glycerol to the Descolas-Gros and Oriol (1992) method considerably lowered the Rubisco and (PEPC+PEPCK) activities of a batch culture of *Phaeodactylum tricornutum*. However, the removal of glycerol from the Reinfelder et al. (2000), and Grzymski et al. (2002) methods did not significantly affect the Rubisco activity but greatly lowered the PEPC activity estimates (Figure 5.3).

The large difference in the enzymatic assays for PEPC and PEPCK by Descolas-Gros and Oriol (1992), Reinfelder et al. (2000), and Grzymski et al. (2002) may result from the glycerol present in the latter two methods (Figures 5.2 and 5.3). Glycerol is believed to increase the affinity of PEPC for its substrate by stabilizing the quaternary

structure of the enzyme (Gekko and Timasheff 1981; Gekko and Timasheff 1981; Selinioti et al. 1987; Stamatakis et al. 1988; Podesta and Andreo 1989). PEPC's oligomeric structure is a tetramer (400 kDa). However, in the absence of PEP, or cosolutes like glycerol, it is rapidly dimerized, losing most of its catalytic efficiency. Glycerol is thought to prevent unfolding of the enzyme and to promote self-association of the enzyme to form aggregates (i.e., the exclusion of glycerol from the protein's domain forces the enzyme to adopt a hydrated low volume profile), hence reproducing the *in vivo* physiological conditions where the enzyme is highly concentrated. This is known as the exclusion volume theory. A cosolute such as glycerol therefore dramatically increases the kinetic rate of the catalyzed reaction under suboptimal conditions (low substrate concentration, suboptimum pH). Glycerol decreases the $S_{0.5}$ ($=K_m$) and the Hill coefficient of PEP without affecting the V_{max} of PEPC. The Hill coefficient is a measure of cooperative interactions of substrate with proteins with multiple subunits. The rate curve (i.e., enzymatic rate against substrate concentration) of an allosteric enzyme is sigmoidal, as opposed to the hyperbolic function (Michaelis-Menten kinetics) of a non-allosteric enzyme. In essence, the cosolute has a similar allosteric stabilization effect on the protein by positive cooperative binding (Hill coefficient > 1) as the substrate. PEPC activity is in fact understood to be homotropically regulated by PEP.

The oligomeric state (tetramer vs. dimer) and catalytic efficiency of PEPC are highly dependent on PEPC's concentration. Therefore, under the dilute conditions of *in vitro* enzymatic assays, the catalytic efficiency of PEPC is greatly reduced unless glycerol is present. This is because the diluted enzyme samples are initially incubated for a certain time in the absence of the substrate. Glycerol prevents the dimerization of PEPC prior to

the addition of PEP. The absence of glycerol from some enzymatic assay protocols such as the one presented in Descolas-Gros and Oriol (1992) may explain why PEPC activity is commonly underestimated in the current literature.

In maize leaves, the PEPC dimer:tetramer ratio was shown to be greater at a pH of 7 than at 8 (Podesta and Andreo 1989). Assuming PEPC in marine algae behaves the same as its equivalent in C_4 plants, the difference in incubation pH may explain the discrepancy in PEPC estimates between the various methods studied. The Grzymski et al. (2002) method had the highest PEPC activity estimate (incubation pH=8.0), followed by the Reinfelder et al. (2000) method (incubation pH=7.5), and finally the Descolas-Gros and Oriol (1992) method had the lowest PEPC activity estimate (incubation pH=6.8) (Figure 5.2).

Mg^{2+} has been shown to be inhibitory to PEPCK activity (Burnell 1986; Chen et al. 2002). This may explain some of the difference in PEPCK+PEPC activity between the Descolas-Gros and Oriol (1992) (10 mM $MgCl_2$ in the PEPCK+PEPC assay reaction mixture) and the Reinfelder et al.(2000) and Grzymski et al. (2002) methods (no $MgCl_2$ present). As Chen et al. (2002) point out, "it is also clear that measurements of the maximum activity of PEPCK in plant extracts should still be made under conditions of saturating Mn^{2+} in the absence of Mg^{2+}."

The disagreement between the results of these various methods suggests a current lack of understanding of the kinetics of these enzymes. These assays are most probably not representative of the *in vivo* conditions, or even of these enzymes' V_{max} for that matter. A quantitative understanding of the numerous factors (e.g., inhibitors, activators, pH) affecting these carboxylases will help to better constrain their relative contribution to

photosynthetic carbon fixation. However, since we systematically used the same methods under the various growth conditions tested, we believe that the general trends we observed are truly representative of physiological adaptations.

Although tremendous progress has been accomplished in the last two decades in the study of these enzymes, most particularly from C_4 terrestrial plants and agricultural studies, our results offer an appreciation of how little is known and how much is yet to be discovered about these carboxylases and their physiological regulation. If we aspire to unravel the complexity of the multitude of interacting factors in the regulation of these enzymes, a more fluid exchange of information between enzyme biochemists, molecular biologists, and algal physiologists will first and foremost be required.

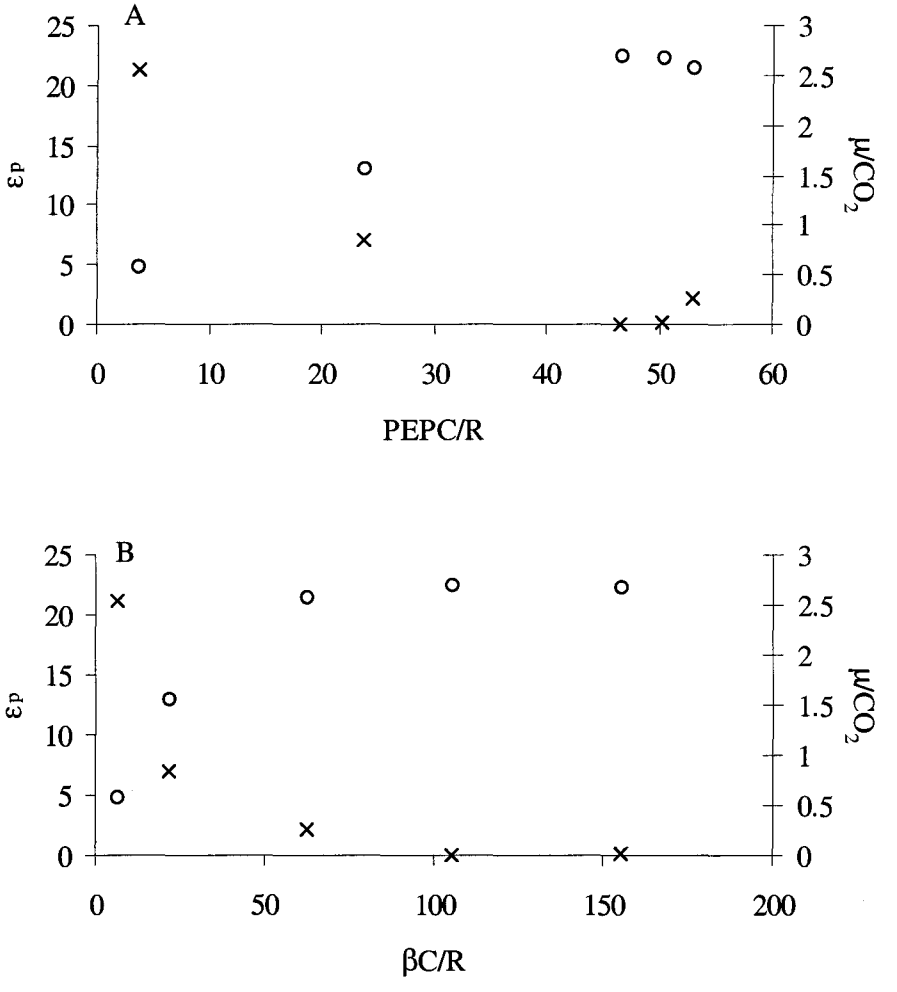

Figure 5.1. ε_p (circles) and μ/CO_2 (crosses) vs. PEPC/R and $\beta C/R$ (panels A and B, respectively).

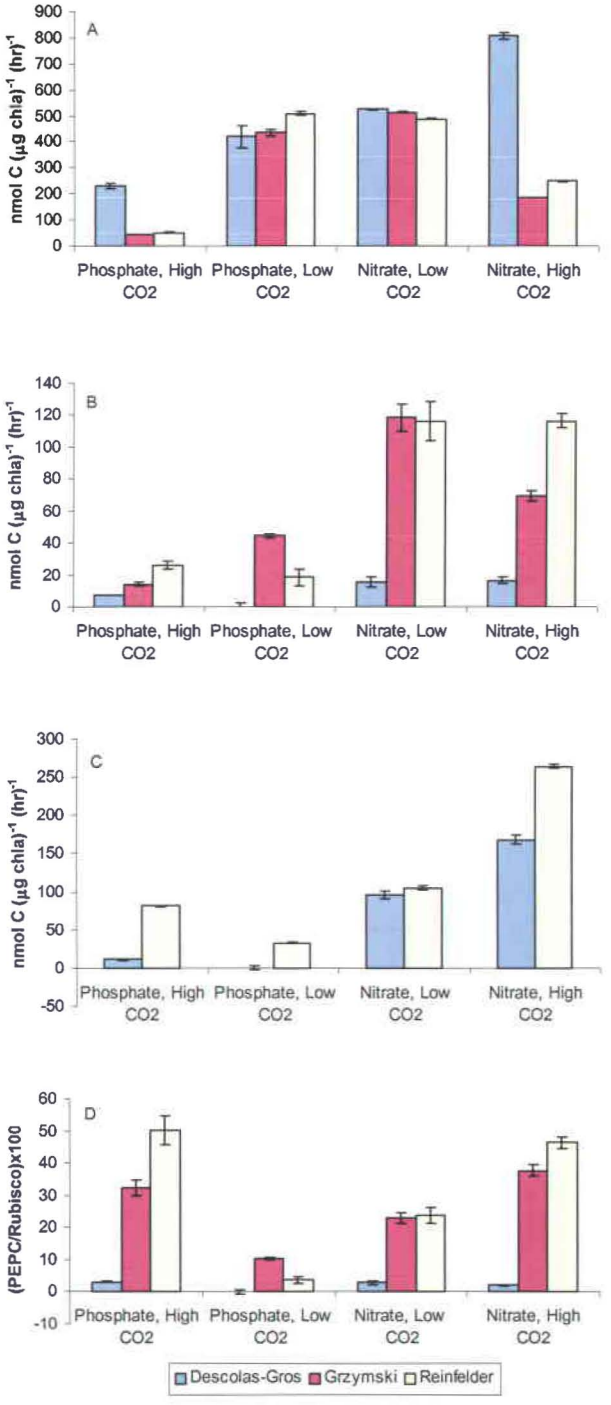

Figure 5.2. Comparison of Rubisco (Panel A), PEPC (Panel B), PEPCK+PEPC (Panel C) activities and [(PEPC/Rubisco)x100 (Panel D)] based on several protocols (Descolas-Gros and Oriol (1992), Reinfelder et al. (2000), and Grzymski et al. (2002)). These experiments were performed on nitrate and phosphate limited *Phaeodactylum tricornutum* chemostats (Nitrate, Phosphate, respectively) at low and high CO_2 concentrations (Low, High CO_2, respectively). The error bars represent the means ± their standard errors. Carboxylase assays were performed in triplicates.

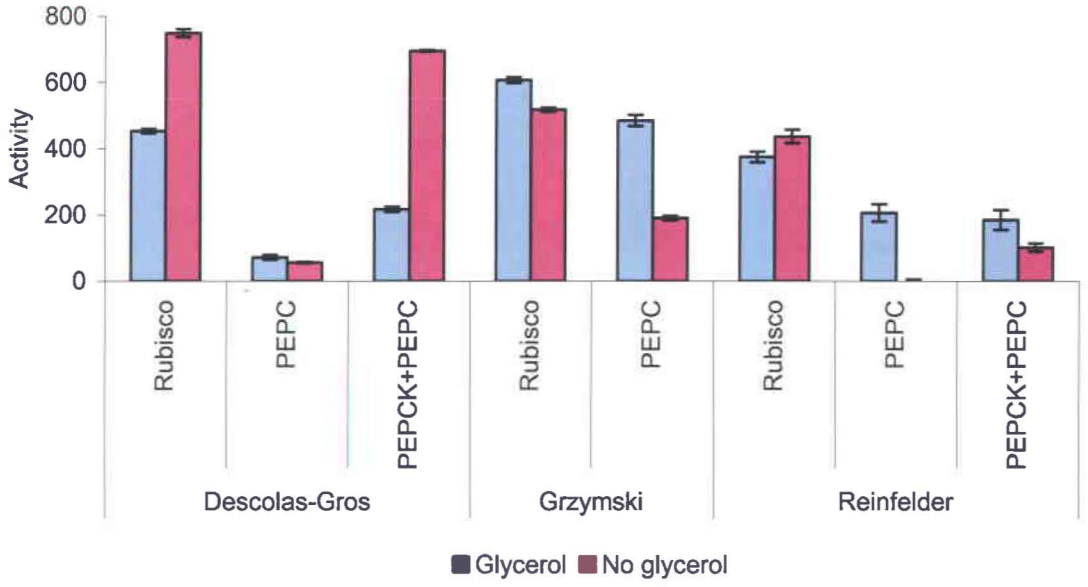

Figure 5.3. The effects of glycerol addition to the Descolas-Gros and Oriol (1992) method and glycerol removal from the Reinfelder et al. (2000), and Grzymski et al. (2002) methods on the enzymatic assay measurements. These experiments were performed on a batch culture of *Phaeodactylum tricornutum*. The error bars represent the means ± their standard errors. Carboxylase assays were performed in triplicates. Activity is in (nmol C (μg Chla)$^{-1}$ (hr)$^{-1}$).

CHAPTER 6. CONCLUSIONS AND IMPLICATIONS

6.1. Preamble

In this study, the potential contribution of several factors to the overall photosynthetic carbon isotopic fractionation factor was explored upstream (CCMs, C_4 photosynthesis), downstream (photorespiration), and in parallel to Rubisco (β-carboxylases in the TCA cycle). In Chapters 2 and 3, bicarbonate transport and its influence on ε_p was studied both in the laboratory on an algal strain and in the field on an algal community. This was accomplished mainly using isotopic disequilibrium experiments, which are presented in Chapter 1. Chapter 4 presents several of the factors that may potentially affect isotopic fractionation. For instance, a change in Rubisco kinetics in response to growth conditions could potentially influence the isotopic signature of organic matter. In Chapter 5, the importance of β-carboxylation in marine algal photosynthesis and its contribution to ε_p were examined. Figure 6.1 presents a summary of the biochemical-physiological pathways investigated in this study. Appendix H presents the original data sets of selected Figures from Chapters 1 to 5.

The evolutionary advantages provided by the metabolic processes that compensate for the enzymatic inefficiency of Rubisco (i.e., C_4 photosynthesis, CCM, photorespiratory carbon oxidation cycle) are likely to lessen as the atmospheric CO_2 increases due to anthropogenic activity. A shift in species composition may also take place. However, the increase in temperature coupled to global warming and caused by the release of greenhouse gases such as CO_2 will probably increase photorespiration, and therefore partially oppose the increase in catalytic efficiency of Rubisco associated with the rise in

CO_2. Photorespiration is affected by temperature in two ways. First, the differential temperature solubility dependency of oxygen and carbon dioxide favors the former at higher temperatures. For instance, assuming oxygen saturation, a DIC concentration of 2.1 mmol kg^{-1}, and a pH of 8.1, the ratio of O_2/CO_2 at 10°C is 17.83 and 20.96 at 30°C. Second, the oxygenase reaction increases more rapidly with increasing temperature than the carboxylase activity of Rubisco. A larger activation energy (E_a) for the oxygenase reaction relative to the carboxylase reaction could explain the greater dependency of the former on temperature than the latter (see Eq. (1.2.32)). In short, the increase in Rubisco's carboxylase efficiency associated with the rise in CO_2 may be countered by the increase in Rubisco's oxygenase activity due to a CO_2- dependent rise in temperature.

6.2. "Byproduct accumulation" as a limiting factor OR the world is a wine cask

As the yeasts in a wine cask ferment the sugar into alcohol, the latter will reach a point at which it is lethal to the yeast cells. Any remaining sugar that is left unfermented will stay in the wine. Hence, it is not the lack of substrate but the accumulation of waste products that is the limiting factor in most fermentation processes. Heat (and the associated increase in temperature), another byproduct of the exothermic fermentation process, may also prematurely kill the yeast cells. Likewise, some ecological systems may not be substrate limited. The accumulation of waste products could control growth, from the cellular level, to the ecosystem level (algal bloom crash), to the planetary level (oxygen accumulation in the atmosphere).

Bottom up (nutrients) and top down (predation) factors are commonly believed to be the most important controls on population dynamics. The availability of nutrients

(including intra and interspecific competition for resources) and predation pressures are considered the main constraints on population growth. In regard to the results obtained at various oxygen concentrations with the ^{14}C experiments, photorespiration in marine ecosystems may be underestimated in the current literature. Photorespiration represents a large energy sink for plants. Many pathways have evolved to reduce it. Hence, in some instances, not the nutrient availability nor the predation pressures but the accumulation of toxic byproducts or waste products may be growth limiting. If diffusion into the cell of certain elements is limiting to growth, diffusion out of the cell of toxic wastes may also be limiting.

Photorespiration

Since oxygen decreases the affinity of Rubisco for CO_2, oxygen could limit growth rate. On a geological time scale, oxygen could also explain iron limitation by reducing the availability of iron to photoautotrophs (reduced iron is more soluble). Iron is an important component of Fe-S and heme proteins involved in electron transport (redox reactions) in the photosynthetic and respiratory pathways. These proteins account for most of the cellular iron (Raven 1988). In addition, the dominant fraction of the nitrogen pool switched from ammonia to nitrate as oxygen increased in the atmosphere, thereby increasing cellular Fe requirements (nitrate reduction may account for about 60% of biological Fe requirements, Raven 1990).

It has been argued that photorespiration is beneficial to plants as a protective mechanism against photoinhibition (Kozaki and Takeba 1996). This was demonstrated with enriched chloroplastic glutamine synthetase (GS2) transgenic tobacco plants, which

had an increased tolerance to high light intensity relative to the wild type. In the PCOC, ammonia is released in the conversion of two molecules of glycine to one molecule of serine by the mitochondrial glycine decarboxylase complex. GS2 fixes the photorespiratory ammonia by reacting it with glutamate to form glutamine in an energy dependent reaction. This reaction is important since a large amount of the nitrogen fixed in plants goes through the photorespiratory pathway and can be lost to the environment if not refixed. The fact that the enriched GS2 mutants are better adapted to high light intensity conditions does not necessarily indicate that the oxygenase activity of Rubisco is useful to the plant. The PCOC (photorespiratory pathway) function is most probably to decrease the damage concurrent with the oxygenase reaction and to recycle most of the carbon in 2-phosphoglycolate. In photosynthetic organisms, photorespiration is responsible for most if not all the glycolate synthesis. Hence, the mutant's resistance to high light conditions does not necessarily indicate that photorespiration has a physiological function but rather suggests that the recycling of the elements that go through the photorespiratory pathway is critical. In other words, the physiological function of the PCOC is only relevant to the phototroph because of the ineffectiveness of Rubisco in discriminating between carbon dioxide and oxygen.

In addition, if photorespiration was an evolutionary adaptation, species that evolved in low-oxygen environments should have a Rubisco with lower oxygenase activity (relative to the carboxylation activity) than species that evolved in a high-oxygen environment. This is not what is actually observed. Cyanobacteria, for instance, have a high half saturation constant for CO_2 and a low CO_2 specificity factor (τ; see Chapter 1) (Jordan and Ogren 1981; Read and Tabita 1994; Tortell 2000). In addition, phototrophic

obligate anaerobic prokaryotes, like *Rhodospirillum rubrum*, have Rubisco that has a high oxygenase activity (Jordan and Ogren 1981). The fact that these bacteria cannot photosynthesize in oxic conditions precludes the idea that photorespiration could have a beneficial physiological function. The dual affinity of Rubisco may be an evolutionary constraint ("dead-end evolution") but is more likely a physical/chemical intrinsic constraint on the structure of the active site of Rubisco and on the specificity of enzymatic reactions for certain gases.

Another piece of unambiguous evidence that photorespiration has no physiological role other than a partial remedy for Rubisco's inefficiency is the presence of CCMs in phototrophs. Several mechanisms and structures (phosphoenolpyruvate carboxylase in C_4 terrestrial plants, pyrenoids and carboxysomes in microalgae, active inorganic carbon transports, carbonic anhydrase, etc.), that are energy dependent have evolved both in terrestrial and marine photoautotrophs to increase the efficiency of Rubisco at fixing carbon but also to favor the carboxylation over the oxygenase reaction of Rubisco. Several of these compensatory physiological pathways have been examined in this study.

6.3. Chemical factors colimitation or biological limitation

An old but still current dogma in the scientific literature is that ecosystems follow the "Liebig's law of the minimum" (Liebig 1840): population growth is limited by only one factor at a time (e.g., carbon, nitrate, iron limitations). According to this theory, the concentration of a certain nutrient will be the limiting factor. Brandt (1899) was the first one to transpose this "law" from agriculture (Liebig 1840) to oceanic communities and to

suggest that planktonic growth is limited by a single factor, nitrogen. Liebig's law was later restated by Blackman (1905).

Another theory, introduced by Nathansohn (1908), has unfortunately received much less attention and is still today underappreciated. It states that systems may be rate-limited rather than being concentration limited (see Mills 1989 ; De Baar 1994 for presentation of these opposing concepts). The presence of enzymes in organisms, in fact, indicates that often the limiting growth factor is not a quantity but a rate. Enzymes are biological catalysts. What limits life is often not an amount but kinetics (e.g., diffusion and conversion rates). Obviously, kinetic rates are often proportional to concentrations. Nathansohn (1908) and Gebbing (1910) also introduced the notion of multifactorial controls on production rates.

The Nathansohn theory may in fact be more accurate to describe growth limitation in certain marine environments. Several chemical factors could be colimiting to one limiting biological factor. For instance, the biological process of carbon fixation by Rubisco may in some cases be the limiting factor to productivity (Sukenik et al. 1987). Other rate (e.g., CO_2 diffusion rate) and concentration (e.g., nitrogen) limiting factors control this rate-limiting biological factor. This theory supports Liebig's law of the minimum, except the limiting factor is biological rather than being chemical. However, it also agrees with the Nathansohn theory since several chemical factors could be colimiting at the same time, and the ultimate limiting factor is a rate (carbon fixation) rather than being a concentration.

For instance, what is considered a nitrogen limitation could actually be a Rubisco limitation, since a large portion of the organic nitrogen is sequestered in Rubisco. To

compensate for the enzymatic inefficiency of Rubisco, plants produce large amounts of it (Rubisco accounts for a large proportion of plants' proteins). In addition, because the PCOC's function is intrinsically linked to Rubisco's inability to discriminate between carbon dioxide and oxygen, it is a major sink of energy and nitrogen (nitrogen of the enzymes involved in this pathway, and nitrogen losses due to photorespiratory ammonia production), for which the catalytic inefficiency of Rubisco would be indirectly responsible. Iron could also be indirectly limiting to carbon fixation by limiting the rate of nitrate reduction and therefore Rubisco production. The photorespiratory phosphorus cycle, a necessary outcome of the enzymatic inefficiency of Rubisco, could also be a major sink of phosphorus. In the PCOC, phosphoglycolate is hydrolyzed to phosphate and glycolate. Growth would not be limited by carbon, nitrogen or iron, but by carbon fixation. In marine phototrophs, inorganic carbon assimilation and reduction can consume more than 60% of the ATP and approximately 95% of the NADPH (Falkowski and Raven 1997).

Nitrogen limitation has been shown to activate the CCM in phytoplankton (Beardall et al. 1982). This is probably because nitrogen limits the amount of Rubisco available. Hence, lower nitrogen concentrations would mean lower Rubisco concentrations. Phytoplankton compensate for the lack of the carbon-fixing enzyme by increasing the concentration of carbon dioxide around the available Rubisco and hence increase the apparent efficiency of photosynthesis. By doing so, they also decrease the oxygenase reaction of Rubisco, and therefore the loss of photorespiratory ammonia (higher nitrogen-use efficiency). CCMs would therefore relieve the nitrogen limitation.

The ratio of several colimiting chemical factors may therefore be more appropriate to describe the controls on growth rate. The ratio of inorganic nitrogen to inorganic carbon to oxygen may be more accurate than simply looking at nitrate concentration. Increasing nitrogen concentration will allow more Rubisco synthesis, and increasing the carbon dioxide concentration or decreasing the oxygen concentration will increase the apparent efficiency of Rubisco. Other chemical factors, such as the ones involved in the carbon concentrating mechanisms may also play an important role. By increasing the carbon dioxide concentration in the vicinity of Rubisco, the carbon concentrating mechanisms artificially increase Rubisco carboxylation's reaction efficiency. Hence, zinc, for instance, which is found in CA (Morel et al. 1994), could also indirectly limit growth by affecting the carbon dioxide concentration around Rubisco. Even temperature could be a limiting factor by changing the carboxylation/oxygenase activity ratio of Rubisco, although this is more difficult to prove since temperature affects many physiological (e.g., cell metabolic activity) and chemical (e.g., CO_2 solubility and carbonate species equilibrium constants) processes. The oxygenase and the carboxylase reactions of Rubisco also have a different pH optimum (8.6-8.8 and 8.2-8.3, respectively, Jensen and Bahr 1976; see also Chen and Durbin 1994; Ritchie et al. 1996). Other environmental factors, such as light intensity (light stimulated CA activity, Merrett et al. 1996) and Na^+ concentration could influence the carbon fixation rate (bicarbonate transport, Miller and Canvin 1985; Espie et al. 1988). But again, the importance of these factors is difficult to appraise because they are likely to affect other physiological and chemical processes.

However, the limiting factor in all the cases mentioned above is always biological, and any macro or micronutrients that will directly or indirectly increase the efficiency of

the limiting biological process are colimiting chemical factors. Areas considered nitrogen limited could actually be "carbon fixation limited."

Because of the strong intricate interdependency of metabolic pathways, life is likely to be colimited by a variety of nutrients. A reductional segregation of regions of the oceans according to one limiting factor shows an underappreciation of biological plasticity. Life may have evolved to maximize its potential with available resources, or it might have evolved the ability to constrain these resources to maximize itself (James Lovelock "Gaia" hypothesis). In both cases, life is unlikely to be limited by a single resource.

At the basis of life is Rubisco. It is quite perplexing that the most abundant protein in the world (Ellis 1979), and definitely one of the most important, is ill-adapted to its present environment (high oxygen, low CO_2 conditions). Rubisco is fascinating in many ways. First and foremost, it is the primary route of inorganic carbon from the geosphere to the biosphere. In addition, it is one of the largest enzymes in nature with a molecular mass of 560 kDa. Finally, it is catalytically slow and inefficient (oxygenase activity), which may explain why it is the most abundant protein in the world, why it is the largest organic sink of nitrogen in some photoautotrophs, and also why some terrestrial plants have evolved C_4 pathways and aquatic algae have evolved CCMs. Some of these compensatory pathways have been the focus of our interest in this study. Overall, because Rubisco is the ultimate limiting factor to photosynthesis and because the latter is the most important bridge for carbon into the organic world, this ancient enzyme of monophyletic origin could potentially be the bottleneck of most forms of life.

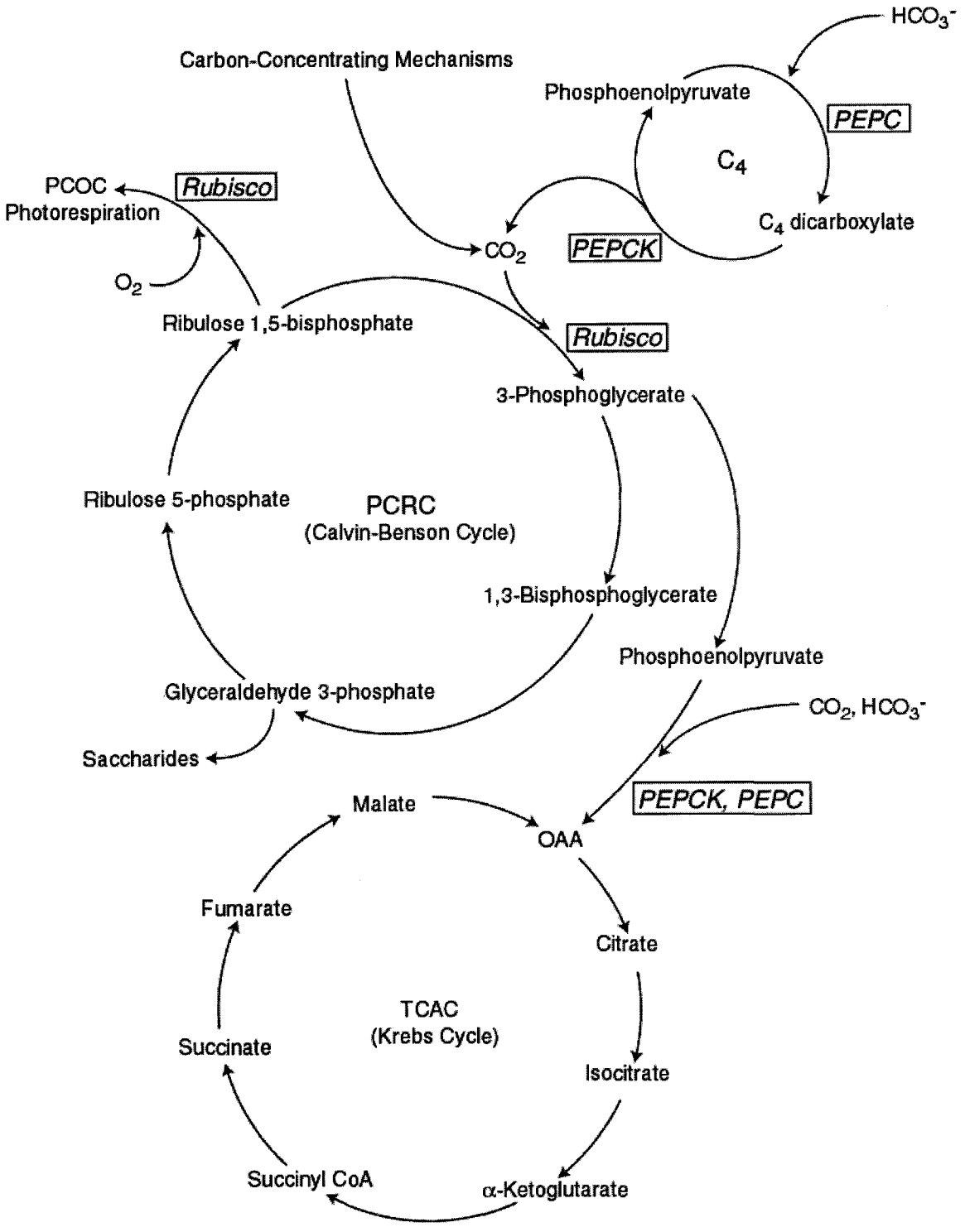

Figure 6.1. Investigated physiological pathways (CCM, C_4 photosynthesis, PCOC, TCAC) and enzymes (Rubisco, PEPC, PEPCK).

APPENDIX A. ANALYTICAL MODEL FOR THE ISOTOPIC DISEQUILIBRIUM EXPERIMENTS

$^{14}CO_2$ kinetic variation over time

Parameters

A = CO_2 (carbon dioxide)
B = HCO_3^- (bicarbonate)
C = CO_3^{2-} (carbonate)

A* = Activity in the CO_2 form
B* = Activity in the HCO_3^- form
C* = Activity in the CO_3^{2-} form

Kinetics

$A^* \leftrightarrow B^*$

At equilibrium $k_1A = k_2B$

$dA^*/dt = -k_1A^* + k_2B^*$
where $k_1=(k_{CO2}+k_{OH^-}K_W^*/[H^+])$, and $k_2=(k_d[H^+]+k_{HCO3^-})$ (Johnson 1982)

$T^* = A^* + B^* + C^*$
$T^* - A^* = B^* + C^*$

Because $B \leftrightarrow C$ equilibrium is reached almost instantaneously

$B^*/(B^*+C^*) = B/(B+C)$ (1)

$B^*+C^*=T^*-A^*$ (2)

(2) in (1)

$B^*/(T^*-A^*) = B/(B+C)$ (3)

Isolate B*

$B^* = (T^* - A^*)\ B/(B+C)$ (at equilibrium, a constant fraction of the bicarbonate-carbonate pool is in the form of bicarbonate (b/(b+c)), because the bicarbonate-carbonate equilibrium is reached instantaneously, the fraction $b^*/(b^*+c^*) = b/(b+c)$).

$dA^*/dt = -k_1A^* + k_2\ (T^* - A^*)\ B/(B+C)$

$dA^*/dt + k_1A^* - k_2\ (T^* - A^*)\ B/(B+C) = 0$

$dA^*/dt + k_1A^* + k_2\ A^*\ B/(B+C) - k_2\ T^*\ B/(B+C) = 0$

$dA^*/dt + k_1A^* + k_2\ A^*\ B/(B+C) = k_2\ T^*\ B/(B+C)$

Let's define $k_2' = k_2\ B/(B+C)$

$dA^*/dt + k_1A^* + k_2'\ A^* = k_2'\ T^*$

$dA^*/dt + (k_1 + k_2')\ A^* = k_2'\ T^*$

First Order Linear Differential Equation

$A^* = (k_2'\ T^*/ (k_1 + k_2')) + ce^{-(k1 + k2')\ t}$ where c is a constant (4)

$k_2'/ (k_1 + k_2') = 1/ ((k_1 + k_2')/ k_2') = 1/((k_1/k_2')+1)$ (5)

$k_1A = k_2B$ (at equilibrium)

$k_1/k_2 = B/A$

$k_2' = k_2\ B/(B+C)$ (see above)

$k_1/k_2' = (k_1/k_2)(k_2/k_2') = (B/A)\ (B+C)/B = (B+C)/A = (T-A)/A$ because T=A+B+C

$k_1/k_2' = (T-A)/A$ (6)

(6) in (5) and (5) in (4)

$A^* = T^*A/T + ce^{-(k1 + k2')\ t}$

Find the c constant

At t=0

$A_o^* = c + T^*A/T \Rightarrow c = A_o^* - AT^*/T = (A_o^*T - AT^*)/T = A_o^*T/T - AT^*/T = A_o^* - AT^*/T$

If 100% of spike is CO_2, $A_o^* \approx T^*$

Hence, $c = A_o^* - AT^*/T = T^* - AT^*/T = T^*\ (1- (A/T)) = T^*\ (T-A)/T$

Therefore, the equation that describes the variation of $^{14}CO_2$ over time is:

$$A^* = T^*\ [((T-A)/T)\ e^{-(k1 + k2')\ t} + A/T] \qquad (7)$$

Influx rate of ^{14}C through the plasma membrane

Influx rate

R = uptake rate (through the cell plasma membrane; this is not a fixation rate but the rate at which the labeled carbon influx through the plasma membrane)

R = f R + (1-f) R where f is the proportion of the uptake that is CO_2 influx and (1-f) is the proportion that is HCO_3^- influx

R* = influx rate of labeled inorganic carbon (^{14}C)

$R^* = fRA^*/A + (1-f)RB^*/B$

(A^*/A and B^*/B are proportions because the uptake rate of ^{14}C is dependent on the encounter rate of labeled carbon)

$T^*=A^* + B^* + C^*$
$B^* + C^* = T^* - A^*$

$B/(B+C) = B/(T-A)= B^*/(B^*+C^*) = B^*/(T^*- A^*)$ (because equilibrium of labeled carbon is reached instantaneously)

$B/(T-A)= B^*/(T^*- A^*)$

$\Rightarrow B^*/B = (T^*-A^*)/(T-A)$

$R^* = fRA^*/A + (1-f)R\ (T^*-A^*)/(T-A)$

$R^* = fRA^*/A + (1-f)R\ T^*/(T-A)- (1-f)RA^*)/(T-A)$

$R^* = (1-f)R\ T^*/(T-A) + A^*\ (fR/A - (1-f)R/(T-A))$

$R^* = (1-f)R\ T^*/(T-A) + A^*(fR(T-A)-(1-f)RA)/((T-A)A))$

$R^* = (1-f)R\ T^*/(T-A) + A^*(fRT-AR)/((T-A)A))$

$R^* = (1-f)R\ T^*/(T-A) + A^*R((fT-A)/((T-A)A))$

Replace A* by (7)

$R^* = [(1-f)RT^*/(T-A) + R(fT-A)/(A(T-A))\ T^*\ [((T-A)/T)\ e^{-(k1 + k2')\ t} + A/T]$

After simplification

$$R^* = RT^*/T + R(fT-A)/(AT)\, e^{-(k1 + k2')\, t}\, T^* \qquad (8)$$

Or,

$$R^* = RT^*/T\, (1 + (fT/A-1)\, e^{-(k1 + k2')\, t}) \qquad (9)$$

Integration over time (from time 0 to time t)

Time dependent term integration

$$\int_0^t R(fT-A)/(AT)\, e^{-(k1 + k2')\, t}\, T^* dt$$

$$= T^*R(fT-A)/(-AT(k_1+k_2'))\, e^{-(k1 + k2')\, t} \text{ from 0 to t}$$

$$= T^*R(fT-A)/(AT(k_1+k_2'))\, (1- e^{-(k1 + k2')\, t})$$

Time independent term integration

$$\int_0^t (RT^*/T)dt = (RT^*/T)t$$

Hence, the time integrated influx (^{14}C accumulation) is

$$C^* = T^*R(fT-A)/(AT(k_1+k_2'))\, (1- e^{-(k1 + k2')\, t}) + (RT^*/T)t \qquad (10)$$

Ratio of initial to final slope

The slope of DPM vs time is R*. R* is the slope of C* vs time ($dC^*/dt = R^*$)

Initial slope ($t \rightarrow 0$)

$$\lim_{t\to 0} (RT^*/T + R(fT-A)/(AT)\, e^{-(k1 + k2')\, t}\, T^*) = RT^*/T + RT^*(fT-A)/(AT)$$

Final slope ($t \rightarrow \alpha$)

$$\lim_{t\to \alpha} (RT^*/T + R(fT-A)/(AT)\, e^{-(k1 + k2')\, t}\, T^*) = RT^*/T$$

Initial slope = $RT^*/T + RT^*(fT-A)/(AT)$
Final slope = RT^*/T

Initial/Final = fT/A

Ratio of intercept to final slope

Final slope = RT*/T

Intercept: when $t \rightarrow \alpha$, $C^* = T^*R(fT-A)/(AT(k_1+k_2'))) + (RT^*/T)t$
This equation is in the form y=mx+b where m = (RT*/T) (which is actually equal to R* at α, final slope) and b is $T^*R(fT-A)/(AT(k_1+k_2'))$

The ratio of intercept to final slope is, after simplification (and after replacing k_2'/k_1 by (T-A)/A):

Intercept/final slope = $(fT-A)\ (T-A)/Atk_1$

^{14}C uptake with efflux model

Variation rate of internal labeled inorganic carbon

A_i^* = internal inorganic ^{14}C activity

DA_i^* = loss of intracellular inorganic ^{14}C activity (loss trough fixation and efflux)

$DA_i^* = (1-f_2)\ A_i^* + f_2\ A_i^*$

Where f_2 is the fraction that is loss through efflux, $(1-f_2)\ A_i^*$ is the $^{14}CO_2$ fixed and $f_2\ A_i^*$ is the $^{14}CO_2$ lost through leakage.

$dA_i^*/dt = R^* - DA_i^*$ (the variation in intracellular $^{14}CO_2$ is equal to the difference between the uptake (R*) and the losses through efflux and fixation (DA_i^*)

$dA_i^*/dt + DA_i^* = R^*$

First-order ordinary differential equation

Hence, $(e^{Dt}\ A_i^*)' = e^{Dt}R^*$

$e^{Dt}\ A_i^* = T^*R/T\ ((e^{Dt}-1)/D + (fT/A-1)\ (e^{(D-k1-k2')\,t}-1)/(D-k_1-k_2'))$

$$A_i^* = T^*R/T\ ((1-e^{-Dt})/D + (fT/A-1)\ (e^{-(k1+k2')\,t} - e^{-Dt})/(D-k_1-k_2') \qquad (11)$$

Time integrated variation of A_i* (internal labeled inorganic carbon)

Y = Time integrated variation of A_i*

$$\int_0^t A_i^* \, dt = T^*R/T \, (t/D + (e^{-Dt}-1)/D^2 + (fT/A - 1) \, (1/(D-k_1-k_2')) \, ((e^{-Dt}-1)/D - (e^{-(k1+k2')\,t}-1)/(k_1+k_2')))$$

$$Y = T^*R/T \, (t/D + (e^{-Dt}-1)/D^2 + (fT/A - 1) \, (1/(D-k_1-k_2')) \, ((e^{-Dt}-1)/D - (e^{-(k1+k2')\,t}-1)/(k_1+k_2'))) \quad (12)$$

Net uptake of ^{14}C

Rate

Z = Net uptake of ^{14}C

$Z = R^* - f_2 DA_i^*$ (Net uptake = fixation rate = gross uptake – loss through efflux)

$Z = RT^*/T \, (1 + (fT/A-1) \, e^{-(k1 + k2')\,t}) - f_2 DA_i^*$

Replace A_i* by (11)

$$Z = RT^*/T \, (1 + (fT/A-1) \, e^{-(k1 + k2')\,t}) - f_2 D[T^*R/T \, ((1-e^{-Dt})/D + (fT/A - 1) \, (e^{-(k1+k2')\,t} - e^{-Dt})/(D-k_1-k_2')]$$

Let $a=(fT/A-1)$, and $k=k_1+k_2'$

$$Z = RT^*/T \, [\, 1 + ae^{-k\,t} - f_2 D \, ((1- e^{-Dt})/D) - f_2 Da \, (e^{-kt} - e^{-Dt})/(D-k_1-k_2')]$$

$$Z = RT^*/T \, [\, 1 + ae^{-k\,t} - f_2 Dae^{-kt}/(D-k_1-k_2') + f_2 e^{-Dt} + f_2 Dae^{-Dt}/(D-k_1-k_2') - f_2]$$

$$Z = RT^*/T \, [\, 1 + ae^{-k\,t}(1- f_2 D/(D-k_1-k_2')) + f_2 e^{-Dt}(1+Da/(D-k_1-k_2'))- f_2]$$

Time integrated variation of Z

X = time integrated variation of Z

$$X = \int_0^t RT^*/T \, [\, 1 + ae^{-k\,t}(1- f_2 D/(D-k_1-k_2')) + f_2 e^{-Dt}(1+Da/(D-k_1-k_2'))- f_2] \, dt$$

$$X = RT^*/T \, [\, t + a(1- f_2 D/(D-k_1-k_2'))e^{-k\,t}/-k + f_2(1+Da/(D-k_1-k_2'))e^{-Dt}/-D - f_2 t] \text{ from 0 to t}$$

$X = RT^*/T\ [t - f_2t - a/k\ (1- f_2D/(D-k_1-k_2'))\ e^{-k\,t} - f_2/D(1+Da/(D-k_1-k_2'))e^{-Dt}]$ from 0 to t

$X = RT^*/T\ [t - f_2t - a/k\ (1- f_2D/(D-k_1-k_2'))\ e^{-k\,t} - f_2/D(1+Da/(D-k_1-k_2'))e^{-Dt} + a/k(1- f_2D/(D-k_1-k_2')) + f_2/D(1+Da/(D-k_1-k_2'))]$

$X = RT^*/T\ [(1- f_2)t + a/k(1- f_2D/(D-k_1-k_2'))\ (1- e^{-k\,t}) + f_2/D(1+Da/(D-k_1-k_2'))\ (1- e^{-Dt})]$

Replace "a" by (fT/A-1), and "k" by (k_1+k_2')

$X = RT^*/T\ [(1- f_2)t + ((fT/A-1)/(k_1+k_2'))(1- f_2D/(D-k_1-k_2'))\ (1- e^{-(k1+k2')\,t}) + f_2/D(1+D(fT/A-1)/(D-k_1-k_2'))(1- e^{-Dt})]$

APPENDIX B. MATLAB PROGRAM FOR THE ANALYTICAL MODEL IN APPENDIX A.

```
% This is to model C14 uptake by phytoplankton (taking into account
% C14 efflux)

clear;

% Rate constants from Johnson (1982), Limnol. Oceanogr. 27: 849-855
%

A=[1246.98 -930.13 1346.24 -2225.22];
B=[0 0.11 -.126 -.049];
D=[-6.19 3.1 -6.44 8.91]*10^(4);
E=[-183 140.9 -196.4 336.6];

% Assume dissociation constant of water is 10^(-14);

kw=10^(-14);

% Specify temperature (T)

T=input('Enter Temperature (oC) (default=22) : ');
if isempty(T)==1;
  T=22;
else
 T=T;
end

% Convert from Centigrade to Kelvin

T=T+273.16;

% Specify salinity and pH of seawater

pHsw=input('Enter pH (default=8.15) : ');
if isempty(pHsw)==1;
  pHsw=8.15;
else
 pHsw=pHsw;
end

Hsw=10^(-pHsw);

Ssw=input('Enter salinity (default=35) : ');
```

```
if isempty(Ssw)==1;
  Ssw=35;
else
 Ssw=Ssw;
end

% Calculate constants from Johnson paper

lnk=A+B*sqrt(Ssw)+D/T+E*log(T);
k=exp(lnk);

k1=k(1)+k(2)/Hsw;
k2=k(3)*Hsw+k(4);
fprintf('k1= %f\n',k1);fprintf('k2= %f\n',k2);


% Net uptake rate = R-fDA where A is internal activity
% a=(fT/A - 1)
% zp=net time integrated accumulation of C14 into organic tissues
% f=fraction of D (e.g., f=0.4 means 40% of gross internal activity loss is due to efflux)

% Specify Total DIC and CO2 concentration in chemostat

TCO2=input('Enter TCO2 (mM) (default=2.8) : ');
if isempty(TCO2)==1;
  TCO2=2.8;
else
  TCO2=TCO2;
end

CO2=input('Enter CO2 (uM) (default=20) : ');
if isempty(CO2)==1;
  CO2=20;
else
  CO2=CO2;
end

% Convert CO2 (uM) to CO2 (mM)

CO2=CO2/1000;

t=0:720;
k=k1+k2;
D=1.1*k;
f=0;
```

```
% f1 is the fraction of inorganic carbon uptake that is CO2 uptake

for f1=[0:.2:1];
  a=(f1*TCO2/CO2)-1;
  zp=t-f*t-(a/k)*(1-(f*D/(D-k)))*exp(-k*t)-(f/D)*(1+((D*a)/(D-k)))*exp(-D*t)+...
    (a/k)*(1-(f*D/(D-k)))+(f/D)*(1+(D*a/(D-k)));
  plot(t,zp);xlabel('Time (seconds)'); ylabel('DPM');...
    ;zoom on;
hold on;
end;
hold off;
```

APPENDIX C. STELLA BOX-MODEL ANALYTICAL EQUATIONS

Sector 1
C14O2(t) = C14O2(t - dt) + (Dehydration + Efflux - Hydration - CO2_influx) * dt
INIT C14O2 = 2.2^12

INFLOWS:
Dehydration = (kd*proton_activity+kHCO3)*HC14O3
Efflux (Not in a sector)
OUTFLOWS:
Hydration = (kCO2+kOHKw/proton_activity)*C14O2
CO2_influx (Not in a sector)
HC14O3(t) = HC14O3(t - dt) + (Hydration - Dehydration - HC14O3_transport) * dt
INIT HC14O3 = 0

INFLOWS:
Hydration = (kCO2+kOHKw/proton_activity)*C14O2
OUTFLOWS:
Dehydration = (kd*proton_activity+kHCO3)*HC14O3
HC14O3_transport (Not in a sector)
CO2 = 9.9
HCO3 = (CO2/proton_activity)*(kCO2/kd)
kCO2 = EXP(1246.98+0-(61900/T_kelvin)-(183*LOGN(T_kelvin)))
kd = EXP(1346.24-0.126*SQRT(Salinity)-64400/T_kelvin-196.4*LOGN(T_kelvin))
kHCO3 = EXP((-2225.22)-
(0.049*SQRT(Salinity))+(89100/T_kelvin)+(336.6*LOGN(T_kelvin)))
kOHKw = EXP(-
930.13+(0.11*SQRT(Salinity))+(31000/T_kelvin)+(140.9*LOGN(T_kelvin)))
pH = 8.1
proton_activity = 10^(-pH)
Salinity = 35
SA_CO2 = C14O2/CO2
SA_HCO3 = HC14O3/HCO3
T_Celcius = 30
T_kelvin = T_Celcius+273.15

Sector 2
Intracellular_C14O2(t) = Intracellular_C14O2(t - dt) + (CO2_influx +
Internal_dehydration - Efflux - Internal_hydration - Carboxylation) * dt
INIT Intracellular_C14O2 = 0

INFLOWS:
CO2_influx (Not in a sector)

Internal_dehydration =
(kd_2*Cytosolic_proton_activity+kHCO3_2)*Intracellular_HC14O3
OUTFLOWS:
Efflux (Not in a sector)
Internal_hydration =
(kCO2_2+kOHKw_2/Cytosolic_proton_activity)*Intracellular_C14O2
Carboxylation (Not in a sector)
Intracellular_HC14O3(t) = Intracellular_HC14O3(t - dt) + (Internal_hydration +
HC14O3_transport - Internal_dehydration) * dt
INIT Intracellular_HC14O3 = 0

INFLOWS:
Internal_hydration =
(kCO2_2+kOHKw_2/Cytosolic_proton_activity)*Intracellular_C14O2
HC14O3_transport (Not in a sector)
OUTFLOWS:
Internal_dehydration =
(kd_2*Cytosolic_proton_activity+kHCO3_2)*Intracellular_HC14O3
Cytosilic_Salinity = 0
Cytosolic_pH = 7.1
Cytosolic_proton_activity = 10^(-Cytosolic_pH)
Intracellular_C14O2_SA = Intracellular_C14O2/Intracellular_CO2_concentration
Intracellular_CO2_concentration = 50
Intracellular_HC14O3_SA = Intracellular_HC14O3/Intracellular_HCO3_concentration
Intracellular_HCO3_concentration =
(Intracellular_CO2_concentration/Cytosolic_proton_activity)*(kCO2_2/kd_2)
kCO2_2 = EXP(1246.98+0-(61900/T_kelvin)-(183*LOGN(T_kelvin)))
kd_2 = EXP(1346.24-0.126*SQRT(Cytosilic_Salinity)-64400/T_kelvin-
196.4*LOGN(T_kelvin))
kHCO3_2 = EXP((-2225.22)-
(0.049*SQRT(Cytosilic_Salinity))+(89100/T_kelvin)+(336.6*LOGN(T_kelvin)))
kOHKw_2 = EXP(-
930.13+(0.11*SQRT(Cytosilic_Salinity))+(31000/T_kelvin)+(140.9*LOGN(T_kelvin)))

Not in a sector
Organic_Pool(t) = Organic_Pool(t - dt) + (Carboxylation) * dt
INIT Organic_Pool = 0

INFLOWS:
Carboxylation = Intracellular_C14O2*(1-f)
CO2_influx = SA_CO2*e*(C_specific_growth_rate/(1-f))

OUTFLOW FROM: C14O2 (IN SECTOR: Sector 1)

INFLOW TO: Intracellular_C14O2 (IN SECTOR: Sector 2)

Efflux = f*Intracellular_C14O2

OUTFLOW FROM: Intracellular_C14O2 (IN SECTOR: Sector 2)

INFLOW TO: C14O2 (IN SECTOR: Sector 1)
HC14O3_transport = SA_HCO3*(1-e)*(C_specific_growth_rate/(1-f))

OUTFLOW FROM: HC14O3 (IN SECTOR: Sector 1)

INFLOW TO: Intracellular_HC14O3 (IN SECTOR: Sector 2)
C_specific_growth_rate = Growth_Rate*Nitrate_Conc*Redfield_ratio/(24*60*60)
e = 0.6
f = 0.8
Growth_Rate = 0.2
Nitrate_Conc = 100
Redfield_ratio = 6.625

APPENDIX D. ANALYTICAL AND NUMERICAL SOLUTION FOR THE EQUILIBRATION OF $^{14}CO_2$ AFTER A $^{14}CO_2$ INJECTION

```
% Calculates the equilibration time of CO2
% Equations are from Table 2.3.1 in Zeebe and Wolf-Gladrow's book (2001) and from
      Johnson (1982)
% k1=kco2; k_1=kd; k2=k32; k_2=k23; k3=k12; k_3=k21; k4=koh-; k_4=khco3-

clear;
clf;
T=5;
T=T+273.15;
S=35;
Kw=exp(148.96502-13847.26/T-23.6521*log(T)+(118.67/T-
      5.977+1.0495*log(T))*sqrt(S)-0.01615*S);
K1=exp(2.83655-(2307.1266/T)-(1.5529413*log(T))-
      (0.207608410+4.0484/T)*sqrt(S)+0.0846834*S-0.00654208*(S^1.5)+log(1-
      0.001005*S));
K2=exp(-9.226508-3351.6106/T-0.2005743*log(T)-
      (0.106901773+23.9722/T)*sqrt(S)+0.1130822*S-0.00846934*(S^1.5)+log(1-
      0.001005*S));
k1=exp(1246.98-(6.19*10^4/T)-183*log(T))
k_1=k1/K1
lnk_1b=1346.24-0.126*sqrt(S)-(6.44*10^4/T)-196.4*log(T);
k_1b=exp(lnk_1b);
k4=(4.70*10^7)*exp(-23200/(8.3145*T))
k4b=exp(-930.13+0.110*sqrt(S)+3.10*10^4/T+140.9*log(T));
k4bb=k4b/10^-14;
k_4=k4*Kw/K1;

% Analytical Solution to the Equilibration of 14CO2 after a 1 microcurie 14CO2
      injection
% ka=k1, kb=k2
DIC=0.002;
DI14C=2.2e6
z=0
for pH=5:9
z=z+1;
h=10^(-pH);
co2=DIC/(1+K1/h+K1*K2/h^2);
hco3=DIC/(1+h/K1+K2/h);
co3=DIC/(1+h/K2+h^2/(K1*K2));
ka=(k1+k4*Kw/h);
kb=(k_1*h+k_4);
alpha=hco3/(hco3+co3);
```

```
t=[0:720];
c14o2=(DI14C/(ka+kb*alpha))*(kb*alpha+ka*exp(-(kb*alpha+ka)*t));
c14o2f=(DI14C/(ka+kb*alpha))*(kb*alpha+ka*exp(-(kb*alpha+ka)*30000));
subplot(2,1,1)
plot(t,c14o2')
axis([0 720 0 2.2e6])
hold on
ylabel('^1^4CO_2 Activity')
end
hold off
text(400,1.9e6,'pH=5'),text(320,1.4e6,'pH=6'),text(240,1e6,'pH=7')
text(140,0.6e6,'pH=8'),text(20,0.3e6,'pH=9')
text(650,1.7e6,'a','fontsize',16)

% Numerical Solution to the Equilibration of 14CO2 after a 1 microcurie 14CO2
      injection
z=0;
for pH=5:9;
z=z+1;
h=10^(-pH);
co2=DIC/(1+K1/h+K1*K2/h^2);
hco3=DIC/(1+h/K1+K2/h);
co3=DIC/(1+h/K2+h^2/(K1*K2));
dco2dt=(k_1*h+k_4)*hco3-(k1+k4*Kw/h)*co2;
% Activity of CO2 = SAa (arbitrary units) 2.2*10^6
tlim=720;
SAa(1)=2.2e6;
SAb(1)=0;
for m=1:tlim
SAdco2dt=(k_1*h+k_4)*SAb(m)-(k1+k4*Kw/h)*SAa(m);
SAa(m+1)=(SAa(m)+SAdco2dt);
SAb(m+1)=(SAb(m)-SAdco2dt);
end
x=[0:720];
subplot(2,1,2);
plot(x,SAa);axis([0 720 0 2.2e6])
hold on
xlabel('Time (seconds)')
ylabel('^1^4CO_2 Activity')
end
hold off
text(400,1.9e6,'pH=5'),text(320,1.4e6,'pH=6'),text(240,1e6,'pH=7')
text(140,0.6e6,'pH=8'),text(20,0.3e6,'pH=9')
text(650,1.7e6,'b','fontsize',16)
```

APPENDIX E. CO_2 EQUILIBRATION'S TIME (SHOWN AS τ, THE RELAXATION TIME) AS A FUNCTION OF TEMPERATURE AND PH

```
% Calculates the relaxation time for the equilibration of CO2 based on Equations and
      Constants in Zeebe and Wolf-Gladrow (2001)

clear;
clf;
for T=5:5:25;
T=T+273.15;
S=35;
Kw=exp(148.96502-13847.26/T-23.6521*log(T)+(118.67/T-
      5.977+1.0495*log(T))*sqrt(S)-0.01615*S);
K1=exp(2.83655-(2307.1266/T)-(1.5529413*log(T))-
      (0.207608410+4.0484/T)*sqrt(S)+0.0846834*S-0.00654208*(S^1.5)+log(1-
      0.001005*S));
K2=exp(-9.226508-3351.6106/T-0.2005743*log(T)-
      (0.106901773+23.9722/T)*sqrt(S)+0.1130822*S-0.00846934*(S^1.5)+log(1-
      0.001005*S));
k1=exp(1246.98-(6.19*10^4/T)-183*log(T));
k_1=k1/K1;
%lnk_1b=1346.24-0.126*sqrt(S)-(6.44*10^4/T)-196.4*log(T);
%k_1b=exp(lnk_1b);
k4=(4.70*10^7)*exp(-23200/(8.3145*T));
k_4=k4*Kw/K1;
%k4b=exp(-930.13+0.110*sqrt(S)+3.10*10^4/T+140.9*log(T));
%k4bb=k4b/10^-14;
DIC=2e-3;
z=0;
for pH=6:0.01:10;
z=z+1;
h=10.^(-pH);
co2=DIC./(1+K1./h+K1*K2./h.^2);
hco3=DIC./(1+h./K1+K2./h);
co3=DIC./(1+h./K2+(h.^2)./(K1*K2));
oh=Kw./h;
alpha=Kw./(h.^2);
dsb=-((h+2*co3/(1+alpha))/(K2+h+co3/(1+alpha)));
dsh=-(dsb+2)./(1+alpha);
dsoh=alpha*(dsb+2)/(1+alpha);
rau(z)=1./(k1-k_1.*(dsb.*h+dsh.*hco3)-k_4.*dsb+k4.*oh+dsoh.*co2);
pHa(z)=pH;
end
plot(pHa,rau); xlabel('pH');ylabel('\tau (seconds)');
```

```
text(8.8,73,'5^oC');text(8.5,55,'10^oC');text(8.3,40,'15^oC');text(8.1,28,'20^oC');text(7.75
        ,12,'25^oC')
hold on
end
hold off
```

APPENDIX F. DERIVATION OF A THREE-BOX CARBON ISOTOPE FRACTIONATION MODEL

$$\delta_e \underset{\varepsilon_{diff}}{\overset{\varepsilon_{up}}{\rightleftarrows}} \delta_i \xrightarrow{\varepsilon_{fix}} \delta_{org}$$

Let's define δ_e, δ_i and δ_{org} as the isotopic signatures of the external source of carbon (CO_2 and/or HCO_3^-), of the internal inorganic carbon pool, and the organic carbon pool. ε_{up} is the fractionation associated with uptake (passive and active), relative to CO_2. ε_{diff} is the fractionation associated with diffusion out of the cell, or efflux, and ε_{fix} is the fractionation associated with carboxylation (see Figure 4.1).

$$\delta_i = \delta_e - \varepsilon_{up} + f_{eff}\varepsilon_{diff} + (1 - f_{eff})\varepsilon_{fix}$$

where f_{eff} is the fraction of the internal inorganic carbon pool that leaks out of the cell.

$$\delta_{org} = \delta_i - \varepsilon_{fix}$$

Hence,

$$\delta_{org} = \delta_e - \varepsilon_{up} + f_{eff}\varepsilon_{diff} + (1 - f_{eff})\varepsilon_{fix} - \varepsilon_{fix}$$
$$\delta_{org} = \delta_e - \varepsilon_{up} + f_{eff}\varepsilon_{diff} - f_{eff}\varepsilon_{fix}$$
$$\delta_{org} = \delta_e - \varepsilon_{up} + f_{eff}(\varepsilon_{diff} - \varepsilon_{fix})$$

and therefore, ε_p, the overall fractionation is

$$\varepsilon_p = \delta_e - \delta_{org} = \varepsilon_{up} - f_{eff}(\varepsilon_{diff} - \varepsilon_{fix}) \qquad (1)$$

This is a model similar to the one presented by Francois et al. (1993). Up to now, no assumptions were made on the source of inorganic carbon. The only assumption is the number of compartments in the box model.

ε_p, ε_{diff}, and ε_{fix} are supposedly known. Let's look at ε_{up}

Derivation of ε_{up}

Let's define f_a and f_p as the proportions of the uptake across the plasmalemma, which are active and passive, respectively. Let's also define $\delta^{13}C_{feed}$ as the isotopic signature of the carbon that crosses the plasmalemma. $\delta^{13}C_{feed}$ is a combination of the active and passive transport mechanisms. Active transport could be HCO_3^- or CO_2 transport.

$$\delta^{13}C_{feed} = f_a(\delta^{13}C_{source} - \varepsilon_t) + f_p(\delta^{13}C_{CO_2} - \varepsilon_{diff})$$

where $\delta^{13}C_{source}$ and $\delta^{13}C_{CO_2}$ are the isotopic signatures of the external inorganic carbon source for the active uptake (HCO_3^- and/or CO_2) and of the CO_2 in the medium. ε_t is the overall fractionation associated with the active transport mechanism(s).

$$\varepsilon_{up} = \delta^{13}C_{CO_2} - \delta^{13}C_{feed} = \delta^{13}C_{CO_2} - f_a(\delta^{13}C_{source} - \varepsilon_t) - f_p(\delta^{13}C_{CO_2} - \varepsilon_{diff})$$

$$\varepsilon_{up} = \delta^{13}C_{CO_2} - f_a\delta^{13}C_{source} + f_a\varepsilon_t - f_p\delta^{13}C_{CO_2} + f_p\varepsilon_{diff}$$

$$\varepsilon_{up} = \delta^{13}C_{CO_2}(1-f_p) - f_a\delta^{13}C_{source} + f_a\varepsilon_t + f_p\varepsilon_{diff}$$

However, $f_a=1-f_p$

$$\varepsilon_{up} = f_a(\delta^{13}C_{CO_2} - \delta^{13}C_{source}) + f_a\varepsilon_t + f_p\varepsilon_{diff} \qquad (2)$$

Assuming that ε_t is equal to ε_{diff} would give us an ε_{up} identical to the one derived by Keller and Morel , i.e.,

If $\varepsilon_t = \varepsilon_{diff}$,

$$\varepsilon_{up} = f_a(\delta^{13}C_{CO_2} - \delta^{13}C_{source}) + \varepsilon_{diff}(f_a + f_p)$$

and because $f_a+f_p=1$

$$\varepsilon_{up} = \varepsilon_{diff} + f_a(\delta_{CO_2} - \delta^{13}C_{source}) \qquad (3)$$

Replacing ε_{up} in equation 1 by the right-hand side of equation 2,

$$\varepsilon_p = f_a(\delta^{13}C_{CO_2} - \delta^{13}C_{source}) + f_a\varepsilon_t + f_p\varepsilon_{diff} - f_{eff}(\varepsilon_{diff} - \varepsilon_{fix}) \qquad (4)$$

Or, assuming $\varepsilon_t = \varepsilon_{diff}$, we obtain an equation which is very similar to equation 4 in Keller and Morel (1999),

$$\varepsilon_p = \varepsilon_t + f_a(\delta^{13}C_{CO_2} - \delta^{13}C_{source}) - f_{eff}(\varepsilon_{diff} - \varepsilon_{fix}) \qquad (5)$$

APPENDIX G. DERIVATION OF A FOUR-BOX CARBON ISOTOPE FRACTIONATION MODEL

$$\delta_e \underset{\varepsilon_{diff},f_{-1}}{\overset{\varepsilon_{up},f_1}{\rightleftarrows}} \delta_i \underset{\varepsilon_{-i},f_{-2}}{\overset{\varepsilon_i,f_2}{\rightleftarrows}} \delta_f \xrightarrow{\varepsilon_{fix},\mu C} \delta_{org}$$

In the four-box model, the intracellular inorganic carbon pool is composed of two pools, the δ_i (e.g., cytoplasm) and the δ_f (e.g., stroma/pyrenoids/carboxysomes). Intrinsic isotopic fractionation factors are associated with the transport/diffusion of the inorganic carbon from the δ_i pool to the δ_f pool (ε_i) and leakage (diffusion) of inorganic carbon from the δ_f pool to the δ_i pool (ε_{-i}). The f factors are the quantities of inorganic carbon that leave or enter a given pool (see diagram). The additional nomenclature is identical to the one presented in Appendix F. The proportion of carbon that enters the δ_f pool that actually leaks out before being fixed by Rubisco is $f_i = \frac{f_{-2}}{f_2}$.

Mass balance of the δ_f pool

$$f_2(\delta_i - \varepsilon_i) = \mu C(\delta_f - \varepsilon_{fix}) + f_{-2}(\delta_f - \varepsilon_{-i}) \qquad (1)$$

Isolate δ_i from Eq. (1)

$$\delta_i = \frac{\mu C}{f_2}(\delta_f - \varepsilon_{fix}) + \frac{f_{-2}}{f_2}(\delta_f - \varepsilon_{-i}) + \varepsilon_i$$

$$\delta_i = (1 - f_i)(\delta_f - \varepsilon_{fix}) + f_i(\delta_f - \varepsilon_{-i}) + \varepsilon_i$$

$$\delta_i = \delta_f + \varepsilon_i - \varepsilon_{fix} + f_i(\varepsilon_{fix} - \varepsilon_{-i}) \qquad (2)$$

Mass balance of the δ_i pool

$$f_1(\delta_e - \varepsilon_{up}) + f_{-2}(\delta_f - \varepsilon_{-i}) = f_{-1}(\delta_i - \varepsilon_{diff}) + f_2(\delta_i - \varepsilon_i)$$

Mass balance for the whole cell

$$f_1(\delta_e - \varepsilon_{up}) = f_{-1}(\delta_i - \varepsilon_{diff}) + \mu C(\delta_f - \varepsilon_{fix}) \qquad (3)$$

Since,

$$f_{-1} = f_1 - \mu C \qquad (4)$$

We can replace f_{-1} in Eq. (3) by the right-hand-side of Eq. (4) and rearrange

$$f_1(\delta_e - \varepsilon_{up} + \varepsilon_{diff} - \delta_i) = \mu C(\delta_f - \varepsilon_{fix} + \varepsilon_{diff} - \delta_i) \qquad (5)$$

The proportion of the inorganic carbon that enters δ_i that leaks out to the periplasmic space is $f = \frac{f_1 - \mu C}{f_1}$ (since $f_1 = f_{-1} + \mu C$). Hence, Eq. (5) can be simplified to

$$\delta_e - \varepsilon_{up} + \varepsilon_{diff} - \delta_i = (1-f)(\delta_f - \varepsilon_{fix} + \varepsilon_{diff} - \delta_i) \qquad (6)$$

Replacing δ_i in Eq. (6) by the right-hand side of Eq. (2)

$$\delta_e - \varepsilon_{up} + \varepsilon_{diff} - \delta_f - \varepsilon_i + \varepsilon_{fix} - f_i(\varepsilon_{fix} - \varepsilon_{-i})) = (1-f)(\varepsilon_{diff} - \varepsilon_i - f_i(\varepsilon_{fix} - \varepsilon_{-i})) \qquad (7)$$

And since

$$\delta_{org} = \delta_f - \varepsilon_{fix} \text{ and } \varepsilon_p = \delta_e - \delta_{org}$$

Eq. (7) can be simplified to

$$\varepsilon_p - \varepsilon_{up} + \varepsilon_{diff} - \varepsilon_i - f_i(\varepsilon_{fix} - \varepsilon_{-i})) = (1-f)(\varepsilon_{diff} - \varepsilon_i - f_i(\varepsilon_{fix} - \varepsilon_{-i})) \qquad (8)$$

Rearranging and simplifying Eq. (8)

$$\varepsilon_p = \varepsilon_{up} + f(f_i(\varepsilon_{fix} - \varepsilon_{-i}) + \varepsilon_i - \varepsilon_{diff}) \qquad (9)$$

If $\varepsilon_{-i} = \varepsilon_i$ and f_i=1, Eq. (9) is identical to Eq. (1) in Appendix F.

APPENDIX H. ORIGINAL DATA SETS OF SELECTED FIGURES

Figure 1.11

Time	DPM_{org}
60	107.29
120	137.77
180	146.12
240	171.21
300	205.85
360	220.33
480	262.79
600	311.21
720	359.25
1440	625.12
1500	636.53
1560	645.57
1620	664.52
1680	691.57
1740	731.37
1920	777.35
2040	832.6
2160	877.04

Figure 2.1

	Exp 1	Exp 2	Exp 3	Exp 4	Exp 5
Time (s)	$DPM_{(organic)}$	$DPM_{(organic)}$	$DPM_{(organic)}$	$DPM_{(organic)}$	$DPM_{(organic)}$
10	38.67	75.01	141.60	198.08	351.33
20	56.07	115.57	223.84	280.36	397.23
40	76.38	160.10	331.27	332.67	423.77
50	85.07	179.44	366.25	340.76	425.14
60	88.65	185.87	398.70	340.76	416.01
70	89.70	197.14	408.64	341.35	419.75
80	87.34	200.73	419.34	345.81	415.99
100	90.15	205.84	450.20	346.57	401.95
120	88.70	209.30	458.29	349.82	408.01
140	87.68	207.75	467.33	347.94	393.82
160	91.71	204.22	469.71	344.04	397.01
180	95.73	211.59	462.94	348.99	405.06
200	96.11	207.93	474.32	351.60	408.22
220	98.98	202.46	476.05	351.56	391.89
240	101.77	204.46	470.76	350.04	396.58
360	110.95	212.06	487.44	361.93	389.51
480	119.45	220.56	500.00	371.09	409.86
600	131.53	217.72	517.06	386.50	411.85
720	137.18	224.89	521.44	406.32	426.27

Figure 3.2

Station 14		Station 20		Station 23		Station 26	
Time (s)	DPM	Time (s)	DPM	Time (s)	DPM	Time (s)	DPM
0	0	0	0	0	0	0	0
10	30.7	10	53	12	31.63	10	88.6
20	50.26	20	78.5	22	58.09	20	145.6
40	93.01	40	170.3	40	90.08	60	407.1
60	127.68	60	202.6	60	126.75	360	1367.8
120	217.32	120	380.8	120	233.57	720	1689.6
180	299.95	180	559.1	240	383.86	1080	1781.6
240	388.75	240	657.2	480	514.28	1440	1849.1
300	417.14	300	735.5	660	561.15	1500	1799.5
360	462.97	360	715	840	605.89	1560	1744.8
420	513.8	420	853.1	1020	617.69	1620	1803.1
480	543.05	480	797.1	1260	658.51	1680	1806
540	567.08	540	929.1	1380	586.66	1740	1816.5
600	604.83	600	829	1560	636.93	1800	1799.7
660	616.63	660	775	1740	584.96	1920	1849.3
720	629.18	720	959.6	1920	659.99	2040	1901.9
840	678.74	840	825.1	2100	669.67	2100	1804
960	681.29	960	983.1	2280	602.49	2160	1846
1080	687.24	1080	966.7	2460	592.61	2220	1953.2
1200	683.41	1200	1013.1				
1500	678.42	1500	1042.1				

Figure 3.2 (cont'd)

Station 28		Station 28*		Station 31		Station 33	
Time (s)	DPM	Time (s)	DPM	Time (s)	DPM	Time (s)	DPM
0	0	0	0	0	0	0	0
10	336.3	10	73.8	13	244.6	10	110.1
20	575	20	121.3	23	402	20	208.9
40	1116.9	40	263.6	40	646.3	360	1900
60	1507.5	60	353.1	60	939.3	720	2264
360	4595.7	360	1437.2	360	2847.5	1080	2351
720	5673.1	720	1752.8	720	3237.2	1440	2481
1080	6120.5	1080	2091.7	1080	3176.5	1500	2413
1440	5723.5	1440	2132.3	1440	2780.2	1560	2417
1500	6173.8	1500	2158.9	1500	3162	1620	2406
1560	6244.1	1560	2119	1560	3219.1	1680	2553
1620	6185.7	1620	1949.1	1620	3318.7	1740	2526
1680	6284.9	1680	2175.1	1680	3286.9	1800	2485
1740	6166.3	1740	2109.7	1740	3183.9	1920	2551
1800	6414	1800	2208.4	1800	3187.4	2040	2599
1920	6316	1920	2146.6	1920	3408	2160	2526
2040	6373.9	2040	2205.1	2040	3321.9	2280	2652
2160	6407.4	2160	2332	2160	3444.4	2400	2772
2280	6374.1	2280	2302.6	2280	3533.7		
2400	6575.2	2400	2342.5	2400	3594.2		

Figure 4.2

See Descolas-Gros and Oriol (1992), Reinfelder et al. (2000), and Grzymski et al. (2002) for enzymatic assay conditions presented in Chapters 4 and 5. The Rubisco enzymatic assay conditions are based on enzymatic assays performed by Reinfelder et al. (2000) for PEPC activity. Enzymatic activities are normalized to (nmol C (μg Chl)$^{-1}$ (hr)$^{-1}$). Instead of PEP (5 mM), RuBP at a final concentration of 2.3 mM was used. The only distinction between the PEPC assays of Reinfelder et al. (2000) and the Rubisco and PEPC assays of Grzymski et al. (2002) is the pH of the Bicine buffer (7.5 and 8, respectively), and that bovine serum albumin (5 mg/ml) is used in the former and lysolecithin (0.2 mg/ml) is used in the latter. All other chemicals used in these 2 methods are at the same concentrations. Grzymski et al. (2002) measured PEPC and Rubisco enzymatic activities under the same in vitro conditions with the addition of PEP (2.3 mM) for the PEPC assays and RuBP for the Rubisco assays (5 mM).

x-axis	Primary y-axis			Secondary y-axis
Rubisco Activity	ε_p	μ (d^{-1})	CO_2 (μmol kg^{-1})	μ/CO_2
52.6	22.35	1.02	70.1	0.0146
508.5	4.84	1.02	0.4	2.55
250.6	22.52	0.93	96.4	0.0096
489.9	13.01	0.93	1.1	0.846
382.3	21.42	0.18	0.7	0.257

Figure 4.3

x-axis				y-axis
μ/CO_2	Limiting nutrient	μ (d^{-1})	CO_2 (μmol kg^{-1})	ε_p
0.015	Phosphate	1.02	70.1	22.4
2.55	Phosphate	1.02	0.4	4.84
0.01	Nitrate	0.93	96.4	22.5
0.846	Nitrate	0.93	1.1	13
0.257	Nitrate	0.18	0.7	21.4

Figure 4.4

Figure 4.4 a)

x-axis	Primary y-axis			Secondary y-axis
ε_p	C/N	μ (d^{-1})	CO_2 (μmol kg^{-1})	μ/CO_2
16.74	8.29	1.04	8.67	0.12
13.8	7.04	1.42	2.29	0.62
19.65	9.27	0.93	11.63	0.08
23.48	11.19	0.51	12.75	0.04
26.56	13.83	0.25	8.33	0.03
24.23	13.01	0.3	30.00	0.01
22.7	11.01	0.6	30.00	0.02
26.31	13.53	0.23	7.67	0.03

Figure 4.4 b)

x-axis			y-axis
μ/CO_2	μ (d^{-1})	CO_2 (μmol kg^{-1})	C/N
0.12	1.04	8.67	8.29
0.62	1.42	2.29	7.04
0.08	0.93	11.63	9.27
0.04	0.51	12.75	11.19
0.03	0.25	8.33	13.83
0.01	0.3	30.00	13.01
0.02	0.6	30.00	11.01
0.03	0.23	7.67	13.53

Figure 4.5

Figure 4.5 a)

x-axis	y-axis
C/N	ε_p
7.75	7.42
8.58	11.08
7.97	10.65
9.17	11.83
9.04	16.76
10.09	20.63
8.39	19.85
9.74	18.36
10.75	18.94
11.07	20.58
11.48	22.04
11.92	24.35
11.93	25.72

Figure 4.5 b)

x-axis	y-axis
μ (d^{-1})	ε_p
1.38	7.42
1.04	11.08
0.5	10.65
0.75	11.83
0.75	16.76
0.5	20.63
0.5	19.85
1.4	18.36
1.25	18.94
1	20.58
0.75	22.04
0.5	24.35
0.5	25.72

Figure 4.6

x-axis		y-axis
CO_2 (μmol kg^{-1})	μ (d^{-1})	C/N
0.40	1	6.695
4.80	1	6.73
15.90	1	6.67
4.20	1	7.56
56.60	1	8.36
0.98	0.5	7.97
3.56	0.5	10.09
6.49	0.5	8.39
22.23	0.5	11.92
34.71	0.5	11.93
2.36	0.75	9.17
2.93	0.75	9.04
15.61	0.75	11.48

Figure 4.7

x-axis Time (s)	y-axis DPM Star	y-axis DPM Cross	y-axis DPM Triangle	y-axis DPM Circle
10	96.82	96.61	12.74	17.19
20	149.46	153.8	20.39	20.81
40	197.24	202.4	24.12	23.81
60	198.68	212	27.63	30.01
360	224.23	224.7	44.59	39.11
720	238.91	239.5	58.24	61.86
1080	263.73	273.9	77.58	82.44
1440	276.35	292.3	100.34	102.82
1500	289.48	287.2	98.58	105.09
1560	284.31	296.5	95.16	104.16
1620	289.28	299.6	107.78	107.16
1680	306.75	291	102.71	110.88
1740	295.9	300.6	107.57	114.61
1800	301.07	304.6	110.57	118.12
1920	310.68	293.6	122.88	122.36
2040	311.82	320.5	127.95	130.02
2160	324.96	330.9	137.46	138.81
2280	330.54	335.6	141.81	142.63
2400	333.75	337.2	141.29	157.73

Figure 4.8

x-axis	y-axis
$1/[CO_2]$ (μmol^{-1} kg)	ε_p
0.28	16.23
2.50	6.65
0.21	17.81
0.06	17.75
0.24	17.37
0.02	20.23

Figure 4.9

x-axis Time (s)	y-axis DPM Diamond	y-axis DPM Cross	y-axis DPM Square	y-axis DPM Triangle	y-axis DPM Star
10	134.57	40.21	47.30	46.02	51.89
20	185.67	59.67	62.83	58.95	73.43
40	249.00	86.97	88.62	78.24	96.50
50	268.80	92.79	98.98	81.11	101.10
60	284.80	98.12	104.07	77.97	107.48
70	290.33	103.41	106.14	81.76	111.21
80	292.69	102.63	105.06	80.40	113.19
100	303.11	105.49	109.50	81.26	119.20
120	310.81	108.59	108.73	82.43	117.80
140	311.54	113.90	114.27	73.65	118.80
160	316.45	111.78	108.76	86.37	127.91
180	316.79	111.92	115.99	84.35	129.77
200	326.04	111.11	119.55	80.61	127.94
220	319.56	114.54	116.89	84.30	133.42
240	330.81	118.93	118.66	84.04	132.55
360	343.49	127.01	130.32	91.96	155.37
480	373.04	135.09	137.82	105.12	170.67
600	384.83	145.19	153.55	103.03	192.34
720	415.66	158.50	157.56	114.56	207.53

Figure 5.1

Figure 5.1 A
Rubisco and PEPC activities are normalized to (nmol C (μg Chl)$^{-1}$ (hr)$^{-1}$)

x-axis		Primary y-axis					Secondary y-axis
PEPC/ R	Limiting nutrient	R	PEPC	ε_p	μ (d^{-1})	CO_2 (μmol kg^{-1})	μ/CO_2
50.2	Phosphate	52.6	26.4	22.35	1.02	70.1	0.0146
3.7	Phosphate	508.5	18.6	4.84	1.02	0.4	2.55
46.5	Nitrate	250.6	116.4	22.52	0.93	96.4	0.0096
23.8	Nitrate	489.9	116.3	13.01	0.93	1.1	0.846
52.9	Nitrate	382.3	202.2	21.42	0.18	0.7	0.257

Figure 5.1 B
Rubisco and βC activities are normalized to (nmol C (μg Chl)$^{-1}$ (hr)$^{-1}$)

x-axis				Primary y-axis			Secondary y-axis
βC/R	Limiting nutrient	R	βC	ε_p	μ (d^{-1})	CO_2 (μmol kg^{-1})	μ/CO_2
155	Phosphate	52.6	81.52	22.35	1.02	70.1	0.0146
6.5	Phosphate	508.5	33.14	4.84	1.02	0.4	2.55
105.5	Nitrate	250.6	264.43	22.52	0.93	96.4	0.0096
21.5	Nitrate	489.9	105.12	13.01	0.93	1.1	0.846
62.4	Nitrate	382.3	238.57	21.42	0.18	0.7	0.257

Figure 5.2

Figure 5.2 A

Method	Phosphate High CO_2	Phosphate Low CO_2	Nitrate Low CO_2	Nitrate High CO_2
Descolas-Gros and Oriol (1992)	231.39	421.93	525.84	807.41
Grzymski et al. (2002)	43.48	436.71	515.22	184.24
Reinfelder et al. (2000)	52.58	508.52	489.89	250.55

Figure 5.2 B

Method	Phosphate High CO_2	Phosphate Low CO_2	Nitrate Low CO_2	Nitrate High CO_2
Descolas-Gros and Oriol (1992)	7.34	0.12	15.21	16.60
Grzymski et al. (2002)	14.12	44.73	118.52	69.55
Reinfelder et al. (2000)	26.38	18.58	116.35	116.42

Figure 5.2 C

Method	Phosphate High CO_2	Phosphate Low CO_2	Nitrate Low CO_2	Nitrate High CO_2
Descolas-Gros and Oriol (1992)	11.13	0.02	95.92	168.64
Grzymski et al. (2002)				
Reinfelder et al. (2000)	81.52	33.14	105.12	264.43

Figure 5.2 D

Method	Phosphate High CO_2	Phosphate Low CO_2	Nitrate Low CO_2	Nitrate High CO_2
Descolas-Gros and Oriol (1992)	3.17	0.03	2.89	2.06
Grzymski et al. (2002)	32.48	10.24	23.00	37.75
Reinfelder et al. (2000)	50.16	3.65	23.75	46.47

Figure 5.3

All activities are normalized to (nmol C (μg Chl)$^{-1}$ (hr)$^{-1}$)

	Descolas-Gros and Oriol (1992)			Grzymski et al. (2002)		Reinfelder et al. (2000)		
	Rubisco	PEPC	PEPCK +PEPC	Rubisco	PEPC	Rubisco	PEPC	PEPCK +PEPC
Glycerol	454.53	72.70	217.06	607.82	485.69	375.02	206.79	185.37
No glycerol	749.95	56.94	696.25	518.96	191.20	437.54	-0.54	102.77

REFERENCES

Anadon, R., F. Alvarez-Marques, E. Fernandez, M. Varela, M. Zapata, J. M. Gasol and D. Vaque (2002). "Vertical biogenic particle flux during Austral summer in the Antarctic Peninsula area." Deep Sea Research **49**: 4-5.

Andria, J. R., F. G. Brun, J. L. Perez-Llorens and J. J. Vergara (2001). "Acclimation Responses of *Gracilaria sp.* (Rhodophyta) and *Enteromorpha intestinalis* (Chlorophyta) to Changes in the External Inorganic Carbon Concentration." Botanica Marina **44**(4): 361-370.

Andria, J. R., J. J. Vergara and J. L. Perez-Llorens (1999). "Biochemical responses and photosynthetic performance of *Gracilaria sp.* (Rhodophyta) from Cadiz, Spain, cultured under different inorganic carbon and nitrogen levels." European Journal of Phycology **34**(5): 497-504.

Appleby, G., J. Colbeck and E. S. Holdsworth (1980). "β carboxylation enzymes in marine phytoplankton and isolation and purification of pyruvate carboxylase from *Amphidinium carterae* (dinophyceae)." Journal of Phycology **16**: 290-295.

Arnelle, D. R. and M. H. O'Leary (1992). "Binding of carbon dioxide to phosphoenolpyruvate carboxykinase from carbon kinetic isotope effect." Biochemistry **31**: 4363-4368.

Arthur, M. A., W. E. Dean and G. E. Claypool (1985). "Anomalous ^{13}C enrichment in modern marine organic carbon." Nature **315**: 216-218.

Badger, M. R. (1987). The CO_2-concentrating mechanism in aquatic photoautotrophs. The biochemistry of plants: a comprehensive treatise. New York, Academic Press. **10:** 132-218.

Badger, M. R. and T. J. Andrews (1982). "Photosynthesis and inorganic carbon usage by the marine cyanobacterium, *Synechococcus sp.*" Plant Physiology **70**(2): 517-523.

Badger, M. R., T. J. Andrews, S. M. Whitney, M. Ludwig, D. C. Yellowlees, W. Leggat and G. D. Price (1998). "The diversity and coevolution of Rubisco, plastids, pyrenoids, and chloroplast-based CO_2-concentrating mechanisms in algae." Canadian Journal of Botany/Revue Canadienne de botanique **76**(6): 1052-1071.

Badger, M. R., M. Bassett and H. N. Comins (1985). "A model for HCO_3^- accumulation and photosynthesis in the cyanobacterium *Synechococcus* sp. Theoretical predictions and experimental observations." Plant Physiology **77**(2): 465-471.

Badger, M. R., A. Kaplan and J. A. Berry (1980). "Internal inorganic carbon pool of *Chlamydomonas reinhardtii*: evidence for a carbon dioxide concentrating mechanism." Plant Physiology **66**: 407-413.

Badger, M. R., K. Palmqvist and J.-W. Yu (1994). "Measurement of CO_2 and HCO_3^- fluxes in cyanobacteria and microalgae during steady-state photosynthesis." Physiologia Plantarum **90**(3): 529-536.

Badger, M. R., G. D. Price and J. W. Yu (1991). "Selection and analysis of mutants of the CO_2 concentrating mechanism in cyanobacteria." Canadian Journal of Botany/Revue Canadienne de botanique **69**(5): 974-983.

Bakrim, N., J. L. Prioul, E. Deleens, J. P. Rocher, M. Arrio-Dupont, J. Vidal, P. Gadal and R. Chollet (1993). "Regulatory Phosphorylation of C4 Phosphoenolpyruvate Carboxylase (A Cardinal Event Influencing the Photosynthesis Rate in Sorghum and Maize)." Plant Physiology **101**(3): 891-897.

Bathmann, U. V. (1998). "Ecology and biogeochemistry in the Atlantic sector of the Southern Ocean during austral spring: The first JGOFS expedition aboard RV Polarstern." Journal of Marine Systems **17**: 1-4.

Beardall, J. (1989). "Photosynthesis and photorespiration in marine phytoplankton." Aquatic Botany **34**(1-3): 105-130.

Beardall, J. and M. Giordano (2002). "Ecological implications of microalgal and cyanobacterial CO_2 concentrating mechanisms, and their regulation." Functional Plant Biology **29**: 2-3.

Beardall, J., H. Griffiths and J. A. Raven (1982). "Carbon isotopic discrimination and the CO_2 accumulating mechanisms in *Chlorella emersonii*." Journal of Experimental Botany **33**: 729-737.

Beardall, J., D. Mukerji, H. E. Glover and I. Morris (1976). "The path of carbon in photosynthesis by marine phytoplankton." Journal of Phycology **12**(4): 409-417.

Beer, S., A. Israel, Z. Drechsler and Y. Cohen (1990). "Photosynthesis in *Ulva fasciata* . 5. Evidence for an inorganic carbon concentrating system, and ribulose-1,5-bisphosphate carboxylase/oxygenase CO_2 kinetics." Plant Physiology **94**(4): 1542-1546.

Berman-Frank, I., J. Erez and A. Kaplan (1998). "Changes in inorganic carbon uptake during the progression of a dinoflagellate bloom in a lake ecosystem." Canadian Journal of Botany/Revue Canadienne de botanique **76**: 1043-1051.

Berner, R. A. (1991). "A model for atmospheric CO_2 over Phanerozoic time." American Journal of Science **291**: 339-376.

Berner, R. A. (1994). "Geocarb II: a revised model of atmospheric CO2 over Phanerozoic time." American Journal of Science **294**: 56-91.

Berner, R. A. (1999). "Atmospheric oxygen over Phanerozoic time." Proceedings of the National Academy of Sciences of the United States of America **96**: 10955-10957.

Berner, R. A. and Z. Kothavala (2001). "Geocarb III: A revised model of atmospheric CO_2 over a Phanerozoic time." American Journal of Science **301**: 182-204.

Berner, R. A., S. T. Petsch, J. A. Lake, D. J. Beerling, B. N. Popp, R. S. Lane, E. A. Laws, M. B. Westley, N. Cassar, F. I. Woodward and W. P. Quick (2000). "Isotope Fractionation and Atmospheric Oxygen: Implications for Phanerozoic O_2 Evolution." Science **287**: 1630-1633.

Bidigare, R. R., A. Fluegge, K. H. Freeman, K. L. Hanson, J. M. Hayes, D. Hollander, J. P. Jasper, L. L. King, E. A. Laws, J. Milder, F. J. Millero, R. Pancost, B. N. Popp, P. A. Steinberg and S. G. Wakeham (1997). "Consistent fractionation of ^{13}C in nature and in the laboratory: Growth-rate effects in some haptophyte algae." Global Biogeochemical Cycles **11**(2): 279-292.

Bidigare, R. R., K. L. Hanson, K. O. Buesseler, S. G. Wakeham, K. H. Freeman, R. D. Pancost, F. J. Millero, P. Steinberg, B. N. Popp, M. Latasa, M. R. Landry and E. A. Laws (1999). "Iron-stimulated changes in ^{13}C fractionation and export by equatorial Pacific phytoplankton: Toward a paleogrowth rate proxy." Paleoceanography **14**(5): 589-595.

Bidigare, R. R., J. L. Iriarte, S.-H. Kang, M. E. Ondrusek, D. Karentz and G. A. Fryxell (1996). Phytoplankton: Quantitative and qualitative assessments. Foundations for Ecosystem Research in the Western Antarctic Peninsula Region, Antarctic Research Series. E. H. a. L. Q. R. Ross, Eds. Washington, D. C., American Geophysical Union. **70:** pp. 173-198.

Bidigare, R. R., L. Van Heukelem and C. C. Trees (2003). HPLC phytoplankton pigments: Sampling, laboratory methods, and quality assurance procedures. Ocean Optics Protocols for Satellite Ocean Color Sensor Validation, Revision 4. G. S. F. a. C. R. M. J. L. Mueller, Eds., NASA Technical Memorandum 2003-211621. **V (Chapter 2):** 5-14.

Blackman, F. F. (1905). "Optima and limiting factors." Annals of Botany **19**: 281-295.

Brandt, K. (1899). "Ueber den Stoffwechsel im meere (Rektoratsrede)." Wissenschaftliche Meeresuntersuchungen, Abteilung Kiel, Neue Folge **4**: 215-230.

Brown, S. L., M. L. Landry, K. E. Selph, R. R. Bidigare, S. Christensen, B. S. Twining, N. Cassar, Z. Johnson and C. Sheridan (2002). "Plankton community response to iron-fertilization in the "Northern Patch" at 56°S." Eos Trans. AGU, 83 (47), Fall Meet. Suppl., Abstract OS11A-0216.

Buesseler, K. O., L. Ball, J. Andrews, J. K. Cochran, D. J. Hirschberg, M. P. Bacon, A. Fleer and M. Brzezinski (2001). "Upper ocean export of particulate organic carbon and biogenic silica in the Southern Ocean along 170 degree W." Deep Sea Research **48**: 19-20.

Burkhardt, S., G. Amoroso, U. Riebesell and D. Sültemeyer (2001). "CO_2 and HCO_3^- uptake in marine diatoms acclimated to different CO_2 concentrations." Limnology and Oceanography **46**(6): 1378-1391.

Burkhardt, S. and U. Riebesell (1997). "CO_2 availability affects elemental composition (C:N:P) of the marine diatom *Skeletonema costatum*." Marine Ecology Progress Series **155**: 67-76.

Burkhardt, S., U. Riebesell and I. Zondervan (1999). "Effects of growth rate, CO_2 concentration, and cell size on the stable carbon isotope fractionation in marine phytoplankton." Geochimica et Cosmochimica Acta **63**(22): 3729-3741.

Burkhardt, S., U. Riebesell and I. Zondervan (1999). "Stable carbon isotope fractionation by marine phytoplankton in response to daylength, growth rate, and CO_2 availability." Marine Ecology Progress Series **184**: 31-41.

Burkhardt, S., I. Zondervan and U. Riebesell (1999). "Effect of CO_2 concentration on C:N:P ratio in marine phytoplankton: A species comparison." Limnology and Oceanography **44**(3): 683-690.

Burnell, J. N. (1986). "Purification and properties of phosphenolpyruvate carboxykinase from C_4 plants." Australian Journal of Plant Physiology **13**: 577-587.

Burns, B. D. and J. Beardall (1987). "Utilization of inorganic carbon by marine microalgae." Journal of Experimental Marine Biology and Ecology **107**(1): 75-86.

Caperon, J. (1972). "Nitrogen-limited growth of marine phytoplankton. I. Changes in population characteristics with steady-state growth rate." Deep Sea Research **19**(9): 601-618.

Caperon, J. and J. Meyer (1972). "Nitrogen-limited growth of marine phytoplankton. II Uptake kinetic and their role in nutrient growth of phytoplankton." Deep Sea Research **19**(9): 619-632.

Caperon, J. and D. F. Smith (1978). "Photosynthetic rates of marine algae as a function of inorganic carbon concentration." Limnology and Oceanography **23**(4): 704-708.

Caperon, J. and D. A. Ziemann (1976). "Synergistic effects of nitrate and ammonium ion on the growth and uptake kinetics of *Monochrysis lutheri* in continuous culture." Marine Biology **36**(1): 73-84.

Cassar, N., E. A. Laws, B. N. Popp and R. R. Bidigare (2002). "Sources of inorganic carbon for photosynthesis in a strain of *Phaeodactylum tricornutum*." Limnology and Oceanography **47**: 1192-1197.

Chen, C. Y. and E. G. Durbin (1994). "Effects of pH on the growth and carbon uptake of marine phytoplankton." Marine Ecology Progress Series **109**(1): 83-94.

Chen, Z. H., R. P. Walker, R. M. Acheson and R. C. Leegood (2002). "Phosphoenolpyruvate carboxykinase assayed at physiological concentrations of metal ions has a high affinity for CO_2." Plant Physiology **128**(1): 160-164.

Chollet, R., J. Vidal and M. H. O'Leary (1996). "Phosphoenolpyruvate carboxylase: a ubiquitous, highly regulated enzyme in plants." Annual Review of Plant Physiology and Plant Molecular Biology **47**: 273-298.

Coleman, J. R. (1991). "The Molecular and biochemical analyses of carbon dioxide-concentrating mechanisms in cyanobacteria and microalgae." Plant, cell and environment **14**: 861-868.

Colman, B. and C. Rotatore (1995). "Photosynthetic inorganic carbon uptake and accumulation in two marine diatoms." Plant, Cell & Environment **18**(8): 919-924.

Curtis, P. S. (1996). "A meta-analysis of leaf gas exchange and nitrogen in trees grown under elevated carbon dioxide." Plant, cell and environment **19**: 127-137.

Curtis, P. S. and X. Wang (1998). "A meta-analysis of elevated CO_2 effects on woody plant mass, form, and physiology." Oecologia **113**: 299-313.

Daly, K. L., W. O. Smith, Jr., G. C. Johnson, G. R. DiTullio, D. R. Jones, C. W. Mordy, R. A. Feely, D. A. Hansell and J. Z. Zhang (2001). "Hydrography, nutrients, and carbon pools in the Pacific sector of the Southern Ocean: Implications for carbon flux." Journal of Geophysical Research **106**(C4): 7107-7124.

De Baar, H. J. W. (1994). "Von Liebig's law of the minimum and plankton ecology (1899-1991)." Progress in Oceanography **33**: 347-386.

Dehairs, F., E. Kopczynska, P. Nielsen, C. Lancelot, D. C. E. Bakker, W. Koeve and L. Goeyens (1997). "partial differential ^{13}C of Southern Ocean suspended organic matter during spring and early summer: Regional and temporal variability." Deep-Sea Research (Part II, Topical Studies in Oceanography) **44**(1-2): 129-142.

DeLucia, E. H., J. G. Hamilton, S. L. Naidu, R. B. Thomas, J. A. Andrews, A. Finzi, M. Lavine, R. Matamala, J. E. Mohan, G. R. Hendrey and W. H. Schlesinger (1999). "Net primary production of a forest ecosystem with experimental CO2 enrichment." Science **284**: 1177-1179.

Descolas-Gros, C. and M. Fontugne (1990). "Stable carbon isotope fractionation by marine phytoplankton during photosynthesis: commissioned review." Plant, cell and environment **13**(3): 207-213.

Descolas-Gros, C. and M. R. Fontugne (1985). "Carbon fixation in marine phytoplankton: Carboxylase activities and stable carbon-isotope ratios; physiological and paleoclimatological aspects." Marine Biology **87**(1): 1-6.

Descolas-Gros, C. and L. Oriol (1992). "Variations in carboxylase activity in marine phytoplankton cultures. β-carboxylation in carbon flux studies." Marine Ecology Progress Series **85**(1-2): 163-169.

Dixon, G. K. and M. J. Merrett (1988). "Bicarbonate utilization by the marine diatom *Phaeodactylum tricornutum* Bohlin." New Phytologist **109**: 47-51.

Dong, L.-f., M. J. Merrett and C.-y. Wu (1999). "Comparative studies of inorganic carbon utilization in Emiliania huxleyi and some non-calcifying marine microalgae." Chinese Journal of Oceanology and Limnology **17**(3): 219-232.

Dong, L. F., N. A. Nimer, E. Okus and M. J. Merrett (1993). "Dissolved inorganic carbon utilization in relation to calcite production in *Emiliania huxleyi* (Lohmann) Kamptner." New Phytologist **123**(4): 679-684.

Duff, S. M. G. and R. Chollet (1995). "In vivo regulation of wheat-leaf phosphoenolpyruvate carboxylase by reversible phosphorylation." Plant Physiology **107**: 775-782.

Dunbar, R. B. and A. Leventer (1992). "Seasonal variation in carbon isotopic composition of Antarctic sea ice and open-water plankton communities." Antarctic Journal of the United States **27**(5): 79-81.

Edmond, J. M. (1970). "High precision determination of titration alkalinity and total carbon dioxide content of sea water by potentiometric titration." Deep Sea Research **17**: 737-750.

Eigen, M., K. Kustin and G. Maass (1961). "Die Geschwindigkeit der Hydration von SO_2 in wasseriges Losung." Zeitschrift für Physikalische Chemie **30**: 130-136.

Ellis, R. J. (1979). "The most abundant protein in the world." Trends in Biochemical Sciences **4**: 241-244.

Elzenga, J. T. M., H. B. A. Prins and J. Stefels (2000). "The role of extracellular carbonic anhydrase activity in inorganic carbon utilization of *Phaeocystis globosa* (Prymnesiophyceae): A comparison with other marine algae using the isotopic disequilibrium technique." Limnology and Oceanography **45**(2): 372-380.

Eppley, R. W. (1972). "Temperature and phytoplankton growth in the sea." Fishery Bulletin **70**: 1063-1085.

Espie, G. S. and B. Colman (1986). "Inorganic carbon uptake during photosynthesis. I. A theoretical analysis using the isotopic disequilibrium technique." Plant Physiology **80**: 863-869.

Espie, G. S. and R. A. Kandasamy (1994). "Monensin inhibition of Na^+-dependent HCO_3^- transport distinguishes it from Na^+-independent HCO_3^- transport and provides evidence for Na^+/HCO_3^- symport in the cyanobacterium *Synechococcus* UTEX 625." Plant Physiology **104**(4): 1419-1428.

Espie, G. S., A. G. Miller and D. T. Canvin (1988). "Characterization of the Na^+ requirement in cyanobacterial photosynthesis." Plant Physiology **88**: 757-763.

Espie, G. S., G. W. Owttrim and B. Colman (1986). "Inorganic carbon uptake during photosynthesis. II. Uptake by isolated *Asparagus* mesophyll cells during isotopic disequilibrium." Plant Physiology **80**: 870-876.

Falkowski, P. G. (1991). "Species variability in the fractionation of ^{13}C and ^{12}C by marine phytoplankton." Journal of Plankton Research **13**(suppl.): 21-28.

Falkowski, P. G. (1997). "Photosynthesis: The paradox of carbon dioxide efflux." Current Biology **7**(10): R637-R639.

Falkowski, P. G. and J. A. Raven (1997). Aquatic photosynthesis. USA, Blackwell.

Falkowski, P. G., R. J. Scholes, E. Boyle, J. Canadell, D. Canfield, J. Elser, N. Gruber, K. Hibbard, P. Hogberg, S. Linder, F. T. Mackenzie, B. I. Moore, T. Pedersen, Y. Rosenthal, S. Setzinger, V. Smetacek and W. Steffen (2000). "The global carbon cycle: a test of our knowledge of Earth as a system." Science **290**: 291-296.

Falkowski, P. G., A. Sukenik and R. Herzig (1989). "Nitrogen limitation in *Isochrysis galbana* (Haptophyceae). 2. Relative abundance of chloroplast proteins." Journal of Phycology **25**(3): 471-478.

Fan, S., M. Gloor, J. Mahlman, S. Pacala, J. Sarmiento, T. Takahashi and P. Tans (1998). "A large terrestrial carbon sink in North America implied by atmospheric and oceanic carbon dioxide data and models." Science **282**: 442-446.

Fang, J., A. Chen, C. Peng, S. Zhao and L. Ci (2001). "Changes in Forest Biomass Carbon Storage in China Between 1949 and 1998." Science **292**: 2320-2322.

Farquhar, G. D., M. H. O'Leary and J. A. Berry (1982). "On the relationship between carbon isotope discrimination and the intercellular carbon dioxide concentration in leaves." Australian Journal of Plant Physiology **9**: 121-137.

Fischer, G. (1991). "Stable carbon isotope ratios of plankton carbon and sinking organic matter from the Atlantic sector of the Southern Ocean." Marine Chemistry **35**(1-4): 581-596.

Francois, R., M. A. Altabet and R. Goericke (1993). "Changes in the $\delta^{13}C$ surface water particulate organic matter across the subtropical convergence in the SW Indian Ocean." Global Biogeochemical Cycles **7**(3): 627-644.

Francois, R., M. A. Altabet, E.-F. Yu, D. M. Sigman, M. P. Bacon, M. Frank, G. Bohrmann, G. Bareille and L. D. Labeyrie (1997). "Contribution of Southern Ocean surface-water stratification to low atmospheric CO_2 concentrations during the last glacial period." Nature **389**(6654): 929-935.

Garcia-Sanchez, M. J., J. A. Fernandez and X. Niell (1994). "Effect of inorganic carbon supply on the photosynthetic physiology of *Gracilaria tenuistipitata.*" Planta **194**(1): 55-61.

Gebbing, J. (1910). "Über den Gehalt des Meeres an Stickstoffnährsalzen. Untersuchungsergebnisse der von der Deutschen Südpolar-Expedition (1901-1903) gesammelten Meerwasserproben." Internationale Revue der gesamten Hydrobiologie **3**: 50-66.

Gekko, K. and S. N. Timasheff (1981). "Mechanism of protein stabilization by glycerol: preferential hydration in glycerol-water mixtures." Biochemistry **20**: 4667-4676.

Gekko, K. and S. N. Timasheff (1981). "Thermodynamic and kinetic examination of protein stabilization by glycerol." Biochemistry **20**(4677-4686).

Ghashghaie, J., M. Duranceau, F. W. Badeck, G. Cornic, M. T. Adeline and E. Deleens (2001). "$\delta^{13}C$ of CO_2 respired in the dark in relation to $\delta^{13}C$ of leaf metabolites: Comparison between *Nicotiana sylvestris* and *Helianthus annuus* under drought." Plant, Cell & Environment **24**: 505-515.

Gillon, J. S. and H. Griffiths (1997). "The influence of (photo)respiration on carbon isotope discrimination in plants." Plant, Cell & Environment **20**(10): 1217-1230.

Gleitz, M., M. Rutgers v.d. Loeff, D. N. Thomas, G. S. Dieckmann and F. J. Millero (1995). "Comparison of summer and winter inorganic carbon, oxygen and nutrient concentrations in Antarctic sea ice brine." Marine Chemistry **51**(2): 81-91.

Glover, H., J. Beardall and I. Morris (1975). "Effects of environmental factors on photosynthesis patterns in *Phaeodactylum tricornutum* (Bacillariophyceae) 1. Effect on nitrogen deficiency and light intensity." Journal of Phycology **11**(4): 424-429.

Glover, H. E. and I. Morris (1979). "Photosynthetic carboxylating enzymes in marine phytoplankton." Limnology and Oceanography **24**: 510-519.

Goldman, J. C. (1986). "On phytoplankton growth rates and particulate C:N:P ratios at low light." Limnology and Oceanography **31**(6): 1358-1363.

Goldman, J. C. (1999). "Inorganic carbon availability and the growth of large marine diatoms." Marine Ecology Progress Series **180**: 81-91.

Grzymski, J., O. M. Schofield, P. G. Falkowski and J. M. Bernhard (2002). "The function of plastids in the deep-sea benthic foraminifer, *Nonionella stella*." Limnology and Oceanography **47**(6): 1569-1580.

Gutknecht, J., M. A. Bisson and F. C. Tosteson (1977). "Diffusion of carbon dioxide through lipid bilayer membranes. Effects of carbonic anhydrase, bicarbonate, and unstirred layers." Journal of General Physiology **69**: 779-794.

Guy, R. D., G. C. Vanlerberghe and D. H. Turpin (1989). "Significance of phosphoenolpyruvate carboxylase during ammonium assimilation. Carbon isotope discrimination in photosynthesis and respiration by the N-limited green alga *Selenastrum minutum*." Plant Physiology **89**(4): 1150-1157.

Haglund, K., M. Bjoerk, Z. Ramazanov, G. Garcia-Reina and M. Pedersen (1992). "Role of carbonic anhydrase in photosynthesis and inorganic-carbon assimilation in the red alga *Gracilaria tenuistipitata*." Planta **187**(2): 275-281.

Hartman, F. C. and M. R. Harpel (1994). "Structure, function, regulation, and assembly of D-ribulose-1,5-bisphosphate carboxylase/oxygenase." Annual Review of Biochemistry **63**: 197-234.

Hartwell, J., A. Gill, G. A. Nimmo, M. B. Wilkins, G. I. Jenkins and H. G. Nimmo (1999). "Phosphoenolpyruvate carboxylase kinase is a novel protein kinase regulated at the level of expression." The Plant Journal **20**(3): 333-342.

Hedges, J. I. and J. H. Stern (1984). "Carbon and nitrogen determinations of carbonate-containing solids." Limnology and Oceanography **29**(3): 657-663.

Holdsworth, E. S. and K. Bruck (1977). "Enzymes concerned with β-carboxylation in marine phytoplankter. Purification and properties of phosphoenolpyruvate carboxykinase." Archives of biochemistry and biophysics **182**(1): 87-94.

Holdsworth, E. S. and J. Colbeck (1976). "The pattern of carbon fixation in the marine unicellular alga *Phaeodactylum tricornutum*." Marine Biology **38**(3): 189-199.

Hollander, D. J. and J. A. McKenzie (1991). "CO_2 control on carbon-isotope fractionation during aqueous photosynthesis: A paleo-pCO_2 barometer." Geology **19**(9): 929-932.

Huertas, E., O. Montero and L. M. Lubian (2000). "Effects of dissolved inorganic carbon availability on growth, nutrient uptake and chlorophyll fluorescence of two species of marine macroalgae." Aquacultural Engineering **22**(3): 181-197.

Huertas, I. E. and L. M. Lubian (1998). "Comparative study of dissolved inorganic carbon utilization and photosynthetic responses in *Nannochloris* (Chlorophyceae) and *Nannochloropsis* (Eustigmatophyceae) species." Canadian Journal of Botany/Revue Canadienne de botanique **76**(6): 1104-1108.

Idso, S. B. and B. A. Kimball (1991). "Downward regulation of photosynthesis and growth at high CO_2 levels." Plant Physiology **96**: 990-992.

Iglesias-Rodriguez, M. D. and M. J. Merrett (1997). "Dissolved inorganic carbon utilization and the development of extracellular carbonic anhydrase by the marine diatom *Phaeodactylum tricornutum*." New Phytologist **135**(1): 163-168.

Israel, A. and S. Beer (1992). "Photosynthetic carbon acquisition in the red alga *Gracilaria conferta* . 2. Rubisco carboxylase kinetics, carbonic anhydrase and HCO_3^- uptake." Marine Biology **112**(4): 697-700.

Jasper, J. P. and J. M. Hayes (1990). "A carbon isotope record of CO_2 levels during the late Quaternary." Nature **347**(6292): 462-464.

Jensen, R. G. and J. T. Bahr (1976). Regulation of CO_2 incorporation via the pentose phosphate pathway. CO_2 Metabolism and Plant Productivity. R. H. B. a. C. C. Black. Baltimore, University Park Press.

Jiao, J. A. and R. Chollet (1988). "Light/dark regulation of maize leaf phosphoenolpyruvate carboxylase by in vivo phosphorylation." Archives of biochemistry and biophysics **261**(2): 409-417.

Jiao, J. A. and R. Chollet (1989). "Regulatory seryl-phosphorylation of C4 phosphoenolpyruvate carboxylase by a soluble protein kinase from maize leaves." Archives of biochemistry and biophysics **269**(2): 526-535.

Jiao, J. A., C. Echevarria, J. Vidal and R. Chollet (1991). "Protein turnover as a component in the light/dark regulation of phosphoenolpyruvate carboxylase protein-serine kinase activity in C4 plants." Proceedings of the National Academy of Sciences of the United States of America **88**(7): 2712-2715.

Jimenez del Rio, M., Z. Ramazanow and G. Garcia R (1995). "Effect of nitrogen supply on photosynthesis and carbonic anhydrase activity in the green seaweed *Ulva rigida* (Chlorophyta)." Marine Biology **123**(4): 687-691.

John-McKay, M. E. and B. Colman (1997). "Variation in the occurrence of external carbonic anhydrase among strains of the marine diatom *Phaeodactylum tricornutum* (Bacillariophyceae)." Journal of Phycology **33**(6): 988-990.

Johnson, K. S. (1982). "Carbon dioxide hydration and dehydration kinetics in seawater." Limnology and Oceanography **27**(5): 849-855.

Johnston, A. M. (1991). "The acquisition of inorganic carbon by marine macroalgae." Canadian Journal of Botany/Revue Canadienne de botanique **69**(5): 1123-1132.

Johnston, A. M. and J. A. Raven (1996). "Inorganic carbon accumulation by the marine diatom *Phaeodactylum tricornutum*." European Journal of Phycology **31**(3): 285-290.

Johnston, A. M., J. A. Raven, J. Beardall and R. C. Leegood (2001). "Photosynthesis in a marine diatom." Nature **412**: 40-41.

Jordan, D. B. and W. L. Ogren (1981). "Species variation in the specificity of ribulose bisphosphate carboxylase-oxygenase." Nature **227**(513-515).

Kaplan, A., M. R. Badger and J. A. Berry (1980). "Photosynthesis and the intracellular inorganic carbon pool in the blue green alga *Anabaena variabilis*: response to external CO_2 concentration." Planta **149**: 219-226.

Kaplan, A., R. Schwarz, R. Ariel and L. Reinhold (1990). The CO_2 concentrating system in cyanobacteria: perspectives and prospects. Regulation of photosynthetic processes. S. K. R. Kanai, S. Miyachi. Bot. Mag., spec.issue.

Kaplan, A., R. Schwarz, J. Lieman-Hurwitz, M. Ronen-Tarazi and L. Reinhold (1994). Physiological and molecular studies on the response of cyanobacteria to changes in the ambient inorganic carbon concentration. The Molecular Biology of Cyanobacteria. D. Bryant. Dordrecht, Netherlands, Kluwer Academic Publishers: 469-485.

Karl, D. M. and R. Lukas (1996). "The Hawaii Ocean Time-series (HOT) Program: Background, rationale and field implementation." Deep-Sea Research (Part 2, Topical Studies in Oceanography) **43**(2-3): 129-156.

Kasting, J. F. (1987). "Theoretical constraints on oxygen evolution and carbon dioxide concentrations in the Precambrian atmosphere." Precambrian Research **34**: 205-229.

Keller, K. and F. M. M. Morel (1999). "A model of carbon isotopic fractionation and active carbon uptake in phytoplankton." Marine Ecology Progress Series **182**: 295-298.

Knox, F. and M. B. McElroy (1984). "Changes in atmospheric CO_2: Influence of the marine biota at high latitude." Journal of Geophysical Research **89**: 4629-4637.

Kopczynska, E. E., L. Goeyens, M. Semeneh and F. Dehairs (1995). "Phytoplankton composition and cell carbon distribution in Prydz Bay, Antarctica: Relation to

organic particulate matter and its $\delta^{13}C$ values." Journal of Plankton Research **17**(4): 685-707.

Korb, R. E., P. J. Saville, A. M. Johnston and J. A. Raven (1997). "Sources of inorganic carbon for photosynthesis by three species of marine diatom." Journal of Phycology **33**(3): 433-440.

Kozaki, A. and G. Takeba (1996). "Photorespiration protects C_3 plants from photooxidation." Nature **384**: 557-560.

Kremer, B. P. and R. Berks (1978). "Photosynthesis and carbon metabolism in marine and freshwater diatoms." Z. Pflanzenphysiol. **87**: 149-165.

Kroopnick, P. (1985). "The distribution of ^{13}C in $\Sigma CO2$ in the world oceans." Deep-Sea Research **32**: 57-84.

Ku, M. S. B., M. R. Schmitt and G. E. Edwards (1979). "Quantitative determination of RuBP carboxylase-oxygenase protein in leaves of several C_3 and C_4 plants." Journal of Experimental Botany **30**: 89-98.

Küppers, U. and M. Weidner (1980). "Seasonal variations of enzyme activity in *Laminaria hyperborea*." Planta **148**: 222-230.

Lambrecht, R. M. and A. Rescigno (1983). Tracer kinetics and physiologic modeling: theory to practice. New York, Springer-Verlag.

Landry, M. L., S. L. Brown, K. E. Selph, R. R. Bidigare, Z. Johnson, C. Sheridan, S. Christensen, B. S. Twining and N. Cassar (2002). "Biomass, Growth and Grazing Responses in the SOFeX Iron-Fertilized Patch at 66°S." Eos Trans. AGU, 83 (47), Fall Meet. Suppl., Abstract OS22D-07.

Lane, T. W. and F. M. M. Morel (2000). "Regulation of Carbonic Anhydrase Expression by Zinc, Cobalt, and Carbon Dioxide in the Marine Diatom *Thalassiosira weissflogii*." Plant Physiology **123**(1): 345-352.

Lasaga, A. C., R. A. Berner and R. M. Garrels (1985). The carbon cycle and atmospheric CO_2: Natural variations Archean to present. E. T. B. Sundquist, W. S. Washington, D. C., American Geophysical Union: 397-411.

Latsko, E. and G. J. Kelly (1983). "The many-faceted function of phosphoenolpyruvate carboxylase in C_3 plants." Physiologie Vegetale **21**(805-815).

Laws, E. and J. Caperon (1976). "Carbon and nitrogen metabolism by *Monochrysis lutheri*: measurement of growth-rate-dependent respiration rates." Marine Biology **36**(1): 85-97.

Laws, E. A. (1975). "The importance of respiration losses in controlling the distribution of marine phytoplankton." Ecology **56**: 419-426.

Laws, E. A. and T. T. Bannister (1980). "Nutrient- and light-limited growth of *Thalassiosira fluviatilis* in continuous culture, with implications for phytoplankton growth in the ocean." Limnology and Oceanography **25**(3): 457-473.

Laws, E. A., R. R. Bidigare and B. N. Popp (1997). "Effect of growth rate and CO_2 concentration on carbon isotopic fractionation by the marine diatom *Phaeodactylum tricornutum*." Limnology and Oceanography **42**(7): 1552-1560.

Laws, E. A. and M. S. Chalup (1990). "A microalgal growth model." Limnology and Oceanography **35**(3): 597-608.

Laws, E. A., B. N. Popp, R. R. Bidigare, M. C. Kennicutt and S. A. Macko (1995). "Dependence of phytoplankton carbon isotopic composition on growth rate and CO_2: Theoretical considerations and experimental results." Geochimica et Cosmochimica Acta **59**(6): 1131-1138.

Laws, E. A., P. A. Thompson, B. N. Popp and R. R. Bidigare (1998). "Sources of inorganic carbon for marine microalgal photosynthesis: A reassessment of $\delta^{13}C$ data from batch culture studies of *Thalassiosira pseudonana* and *Emiliania huxleyi*." Limnology and Oceanography **43**(1): 136-142.

Lazier, J. R. N. and K. H. Mann (1989). "Turbulence and the diffusive layers around small organisms." Deep Sea Research **36**: 1721-1733.

Le Roux-Swarthout, D., V. Terwilliger, M. Christianson, C. Martin and S. Madhavan (2000). "Carbon isotope discrimination correlates with a range of ratios of phosphoenolpyruvate to total carboxylase activities found in two C_3 species." Journal of Plant Physiology **157**: 489-493.

Leboulanger, C., C. Descolas-Gros, M. R. Fontugne, I. Bentaleb and H. Jupin (1995). "Interspecific variability and environmental influence on particulate organic carbon $\delta^{13}C$ in cultured marine phytoplankton." Journal of Plankton Research **17**(11): 2079-2091.

Lehman, J. T. (1978). "Enhanced transport of inorganic carbon into algal cells and its implication for biological fixation of carbon." Journal of Phycology **14**: 33-42.

Li, B., X. Q. Zhang and R. Chollet (1996). "Phosphoenolpyruvate carboxylase kinase in tobacco leaves is activated by light in a similar but not identical way as in maize." Plant Physiology **111**: 497-505.

Li, Q. and D. T. Canvin (1998). "Energy Sources for HCO_3^- and CO_2 Transport in Air-Grown Cells of *Synechococcus* UTEX 625." Plant Physiology **116**: no. 3.

Liebig, J. (1840). Chemistry in its application to agriculture and physiology. London, Taylor and Walton.

Long, S. P. and B. G. Drake (1991). "Effect of the long-term elevation of CO_2 concentration in the field on the quantum yield of photosynthesis of the C_3 sedge, *Scirpus olneyi*." Plant Physiology **96**: 221-226.

Lynch-Stieglitz, J., T. F. Stocker, W. S. Broecker and R. G. Fairbanks (1995). "The influence of air-sea exchange on the isotopic composition of oceanic carbon: Observations and modeling." Global Biogeochemical Cycles **9**: 653-665.

Madsen, T. V. and A. Baattrup-Pedersen (1995). "Regulation of growth and photosynthetic performance in *Elodea canadensis* in response to inorganic nitrogen." Functional Ecology **9**(2): 239-247.

Madsen, T. V., S. C. Maberly and G. Bowes (1996). "Photosynthetic acclimation of submersed angiosperms to CO_2 and HCO_3^-." Aquatic Botany **53**(1-2): 15-30.

Maeda, S., G. D. Price, M. R. Badger, C. Enomoto and T. Omata (2000). "Bicarbonate Binding Activity of the CmpA Protein of the Cyanobacterium *Synechococcus* sp. strain PCC 7942 Involved in Active Transport of Bicarbonate." Journal of Biological Chemistry **275**(27): 20551-20555.

Marek, L. F. and M. H. Spalding (1991). "Changes in photorespiratory enzyme activity in response to limiting CO_2 in *Chlamydomonas reinhardtii*." Plant Physiology **97**(1): 420-425.

Martin, J. H. (1990). "Glacial-interglacial CO_2 change: The iron hypothesis." Paleoceanography **5**(1): 1-13.

Martin, J. H., R. M. Gordon and S. E. Fitzwater (1990). "Iron in Antarctic waters." Nature **345**(6271): 156-158.

Matsuda, Y. and B. Colman (1995). "Induction of CO_2 and bicarbonate transport in the Alga *Chlorella ellipsoidea*. II. Evidence for induction in response to external CO_2 concentration." Plant Physiology **108**: 253-260.

Matsuda, Y., K. Satoh, H. Harada, D. Satoh, Y. Hiraoka and T. Hara (2002). "Regulation of the expressions of HCO_3^- uptake and intracellular carbonic anhydrase in response to CO_2 concentration in the marine diatom *Phaeodactylum* sp." Functional Plant Biology **29**(2-3): 279-287.

McNeil, B. I., R. J. Matear and B. D. Tilbrook (2001). "Does carbon 13 track anthropogenic CO_2 in the Southern Ocean?" Global Biogeochemical Cycles **15**(3): 597-613.

Merrett, M. J. (1991). "Inorganic carbon transport in some marine microalgal species." Canadian Journal of Botany/Revue Canadienne de botanique **69**(5): 1032-1039.

Merrett, M. J., N. A. Nimer and L. F. Dong (1996). "The utilization of bicarbonate ions by the marine microalga *Nannochloropsis oculata* (Droop) Hibberd." Plant, Cell & Environment **19**(4): 478-484.

Miller, A. G. and D. T. Canvin (1985). "Distinction between HCO_3^- and CO_2 dependent photosynthesis in the cyanobacterium *Synechococcus leopoliensis* based on the selective response of HCO_3^- transport to Na^+." FEBS Letters **187**: 29-32.

Miller, A. G. and B. Colman (1980). "Evidence for HCO_3^- transport by the blue-green alga (cyanobacterium) *Coccochloris peniocystis*." Plant Physiology **65**: 397-402.

Miller, A. G., C. Salon, G. S. Espie and D. T. Canvin (1997). "Measurement of the amount and isotopic composition of the CO_2 released from the cyanobacterium *Synechococcus* UTEX 625 after rapid quenching of the active CO_2 transport system." Canadian Journal of Botany/Revue Canadienne de botanique **75**(6): 981-997.

Millero, F. J. (1995). "Thermodynamics of the carbon dioxide system in the oceans." Geochimica et Cosmochimica Acta **59**(4): 661-677.

Mills, E. (1989). Biological Oceanography. An Early history, 1870-1960. Ithaca, Cornell University Press.

Morel, F. M. M., J. R. Reinfelder, S. B. Roberts, C. P. Chamberlain, J. G. Lee and D. Yee (1994). "Zinc and carbon co-limitation of marine phytoplankton." Nature **369**(6483): 740-742.

Morita, E., H. Kuroiwa, T. Kuroiwa and H. Nozaki (1997). "High localization of ribulose-1,5-bisphosphate carboxylase/oxygenase in the pyrenoids of *Chlamydomonas reinhardtii* (Chlorophyta), as revealed by cryofixation and immunogold electron microscopy." Journal of Phycology **33**(1): 68-72.

Morris, I. (1980). Paths of carbon assimilation in marine phytoplankton. Primary Productivity in the Sea. P. G. Falkowski. New-York, Plenum Press**:** 139-159.

Mortain-Bertrand, A., C. Descolas-Gros and H. Jupin (1988). "Pathway of dark inorganic carbon fixation in two species of diatoms: Influence of light regime and regulator factors on diel variations." Journal of Plankton Research **10**(2): 199-217.

Mukerji, D., H. E. Glover and I. Morris (1978). "Diversity in the mechanism of carbon dioxide fixation in *Dunaliella tertiolecta* (Chlorophyceae)." Journal of Phycology **14**(2): 137-142.

Nathansohn, A. (1908). "Über die allgemeinen Produktionsbedingungen im meere." Internationale Revue der gesamten Hydrobiologie **1**(Beiträge zur biologie des planktons, von H.H. Gran und Alexander Nathansohn): 38-72.

Newman, J. R. and J. A. Raven (1993). "Carbonic anhydrase in *Ranunculus penicillatus* spp. pseudofluitans: Activity, location and implications for carbon assimilation." Plant, Cell & Environment **16**(5): 491-500.

Nimer, N. A., C. Brownlee and M. J. Merrett (1999). "Extracellular Carbonic Anhydrase Facilitates Carbon Dioxide Availability for Photosynthesis in the Marine Dinoflagellate *Prorocentrum micans*." Plant Physiology **120**(1): 105-112.

Nimer, N. A., M. D. Iglesias-Rodriguez and M. J. Merrett (1997). "Bicarbonate utilization by marine phytoplankton species." Journal of Phycology **33**(4): 625-631.

Nimer, N. A., M. X. Ling, C. Brownlee and M. J. Merrett (1999). "Inorganic carbon limitation, exofacial carbonic anhydrase activity, and plasma membrane redox activity in marine phytoplankton species." Journal of Phycology **35**(6): 1200-1205.

Nimer, N. A. and M. J. Merrett (1996). "The development of a CO_2-concentrating mechanism in *Emiliania huxleyi*." New Phytologist **133**(3): 383-389.

Nimmo, G. A., M. B. Wilkins and H. G. Nimmo (2001). "Partial purification and characterization of a protein inhibitor of phosphoenolpyruvate carboxylase kinase." Planta **213**(2): 250-257.

Nimmo, H. G. (2000). "The regulation of phosphoenolpyruvate carboxylase in CAM plants." Trends Plant Sci. **5**(75-80).

O'Leary, M. H. (1984). "Measurement of the isotopic fractionation associated with diffusion of carbon dioxide in aqueous solution." Journal of Physical Chemistry **88**: 823-825.

O'Leary, M. H., S. Madhavan and P. Paneth (1992). "Physical and chemical basis of carbon isotope fractionation in plants." Plant, Cell & Environment **15**: 1099-1104.

Omata, T., G. D. Price, M. R. Badger, M. Okamura, S. Gohta and T. Ogawa (1999). "Identification of an ATP-binding cassette transporter involved in bicarbonate uptake in the cyanobacterium *Synechococcus* sp. strain PCC 7942." Proceedings of the National Academy of Sciences, USA **96**(23): 13571-13576.

Osborne, B. A. and R. J. Geider (1986). "Effect of nitrate-nitrogen limitation on photosynthesis of the diatom *Phaeodactylum tricornutum* Bohlin (Bacillariophyceae)." Plant, Cell & Environment **9**: 617-625.

Pacala, S. W., G. C. Hurtt, D. Baker, P. Peylin, R. A. Houghton, R. A. Birdsey, L. Heath, E. T. Sundquist, R. F. Stallard, P. Ciais, P. Moorcroft, J. P. Caspersen, E. Shevliakova, B. Moore, G. Kohlmaier, E. Holland, M. Gloor, M. E. Harmon, S.-M. Fan, J. L. Sarmiento, C. L. Goodale, D. Schimel and C. B. Field (2001). "Consistent Land- and Atmosphere-Based U.S. Carbon Sink Estimates." Science **292**: 2316-2320.

Palmqvist, K., J.-W. Yu and M. R. Badger (1994). "Carbonic anhydrase activity and inorganic carbon fluxes in low- and high-C sub(i) cells of *Chlamydomonas reinhardtii* and *Scenedesmus obliquus*." Physiologia Plantarum **90**(3): 537-547.

Patel, B. N. and M. J. Merrett (1986). "Inorganic-carbon uptake by the marine diatom *Phaeodactylum tricornutum*." Planta **169**(2): 222-227.

Patel, B. N. and M. J. Merrett (1986). "Regulation of carbonic-anhydrase activity, inorganic-carbon uptake and photosynthetic biomass yield in *Chlamydomonas reinhardtii*." Planta **169**(1): 81-86.

Perry, M. J. (1976). "Phosphate utilization by an oceanic diatom in phosphorus-limited chemostat culture and in the oligotrophic waters of the central North Pacific." Limnology and Oceanography **21**(1): 88-107.

Phillips, O. L., Y. Malhi, N. Higuchi, W. F. Laurance, P. V. Núñez, R. M. Vásquez, S. G. Laurance, L. V. Ferreira, M. Stern, S. Brown and J. Grace (1998). "Changes in the Carbon Balance of Tropical Forests: Evidence from Long-Term Plots." Science **282**: 439-442.

Podesta, F. E. and C. S. Andreo (1989). "Maize leaf phosphoenolpyruvate carboxylase : oligometric state and activity in the presence of glycerol." Plant Physiology **90**: 427-433.

Popp, B. N., E. A. Laws, R. R. Bidigare, J. E. Dore, K. L. Hanson and S. G. Wakeham (1998). "Effect of phytoplankton cell geometry on carbon isotopic fractionation." Geochimica et Cosmochimica Acta **62**(1): 69-77.

Popp, B. N., T. Trull, F. Kenig, S. G. Wakeham, T. M. Rust, B. Tilbrook, F. Griffiths, S. W. Wright, H. J. Marchant, R. R. Bidigare and E. A. Laws (1999). "Controls on the carbon isotopic composition of Southern Ocean phytoplankton." Global Biogeochemical Cycles **13**: no. 4.

Porter, M. A. and B. Grodzinski (1985). "CO_2 enrichment of protected crops." Hort. Rev. **7**: 345-398.

Price, G. D. and M. R. Badger (1989). "Ethoxyzolamide inhibition of CO_2 uptake in the cyanobacterium *Synechococcus* PCC7942 without apparent inhibition of internal carbonic anhydrase activity." Plant Physiology **89**: 37-43.

Price, G. D. and M. R. Badger (1989). "Ethoxyzolamide inhibition of CO_2-dependent phototsynthesis in the cyanobacterium *Synechococcus* PCC7942 without apparent inhibition of internal carbonic anhydrase activity." Plant Physiology **89**: 44-50.

Price, G. D. and M. R. Badger (1989). "Expression of human carbonic anhydrase in the cyanobacterium *Synechococcus* PCC7942 creates a high CO_2-requiring phenotype: evidence for a central role for the carboxysomes in the carbon dioxide concentrating mechanisms." Plant Physiology **91**: 505-513.

Price, G. D. and M. R. Badger (1991). "Evidence for the role of carboxysomes in the cyanobacterial CO_2 concentrating mechanism." Can. J. Bot./J. Can. Bot. **69**(5): 963-973.

Price, G. D., D. Sültemeyer, B. Klughammer, M. Ludwig and M. R. Badger (1998). "The functioning of the CO_2 concentrating mechanism in several cyanobacterial strains: a review of general physiological characteristics, genes, proteins, and recent advances." Canadian Journal of Botany/Revue Canadienne de botanique **76**(6): 973-1002.

Priddle, J. and G. A. Fryxell (1985). Handbook of the Common Plankton Diatoms of the Southern Ocean: Centrales Except the Genus *Thalassiosira*, Cambridge University Press.

Rau, G. H., F. P. Chavez and G. E. Friederich (2001). "Plankton $^{13}C/^{12}C$ variations in Monterey Bay, California: evidence of non-diffusive inorganic carbon uptake by phytoplankton in an upwelling environment." Deep Sea Research **48**(1): 79-94.

Rau, G. H., F. P. Chavez and G. E. Friederich (2001). "Plankton $^{13}C/^{12}C$ variations in Monterey Bay, California: evidence of non-diffusive inorganic carbon uptake by phytoplankton in an upwelling environment." Deep-Sea Research I **48**: 79-94.

Rau, G. H., U. Riebesell and D. Wolf-Gladrow (1996). "A model of photosynthetic ^{13}C fractionation by marine phytoplankton based on diffusive molecular CO_2 uptake." Marine Ecology Progress Series **133**(1-3): 275-285.

Rau, G. H., U. Riebesell and D. Wolf-Gladrow (1997). "CO_2 dependent photosynthetic ^{13}C fractionation in the ocean: A model versus measurements." Global Biogeochemical Cycles **11**(2): 267-278.

Rau, G. H., C. W. Sullivan and L. I. Gordon (1991). "$\delta^{13}C$ and $\delta^{15}N$ Variations in Weddell Sea particulate organic matter." Marine Chemistry **35**(1-4): 355-369.

Rau, G. H., T. Takahashi and D. J. Des Marais (1989). "Latitudinal variations in plankton ^{13}C: Implications for CO_2 and productivity in past oceans." Nature **341**(6242): 516-518.

Rau, G. H., T. Takahashi, D. J. Des Marais and C. W. Sullivan (1991). "Particulate organic matter $\delta^{13}C$ variations across the Drake Passage." Journal of Geophysical Research. C. Oceans **96**(C8): 15,131-135.

Raven, J. A. (1970). "Exogenous inorganic carbon sources in plant photosynthesis." Biological Reviews **45**: 167-221.

Raven, J. A. (1974). Carbon dioxide fixation. Algal Physiology and Biochemistry. W. D. P. Stewart. Oxford, Blackwell Scientific Publications: 434-455.

Raven, J. A. (1976). Division of labour between chloroplasts and cytoplasm. The intact chloroplast. J. Barber. Amsterdam, Elsevier: 403-443.

Raven, J. A. (1988). "The iron and molybdenum use efficiencies of plant growth with different energy, carbon and nitrogen sources." New Phytology **109**: 279-287.

Raven, J. A. (1990). "Predictions of Mn and Fe use efficiencies of phototrophic growth as a function of light availability for growth." New Phytology **116**: 1-18.

Raven, J. A. (1995). "The early evolution of land plants: aquatic ancestors and atmospheric interactions." Botanical Journal of Scotland **47**: 151-175.

Raven, J. A. (1997). "Inorganic carbon acquisition by marine autotrophs." Advances in Botanical Research **27**: 85-209.

Raven, J. A. and A. M. Johnston (1991). "Mechanisms of inorganic-carbon acquisition in marine phytoplankton and their implications for the use of other resources." Limnology and Oceanography **36**(8): 1701-1714.

Read, B. A. and F. R. Tabita (1994). "High substrate specificity factor for ribulose bisphosphate carboxylase/oxygenase from eukariotic marine algae and properties of recombinant cyanobacterial Rubisco containing "algal" residue modifications." Archives of biochemistry and biophysics **312**: 210-218.

Rees, T. A. V. (1984). "Sodium dependent photosynthetic oxygen evolution in a marine diatom." Journal of Experimental Botany **35**: 332-337.

Reinfelder, J. R., A. M. L. Kraepiel and F. M. M. Morel (2000). "Unicellular C_4 photosynthesis in a marine diatom." Nature **407**(6807): 996-999.

Reiskind, J. B. and G. Bowes (1991). "The role of phosphoenolpyruvate carboxykinase in a marine macroalga with C_4-like photosynthetic characteristics." Proceedings of the National Academy of Sciences, USA **88**(7): 2883-2887.

Reiskind, J. B., P. T. Seamon and G. Bowes (1988). "Alternative methods of photosynthetic carbon assimilation in marine macroalgae." Plant Physiology **87**(3): 686-692.

Riebesell, U., S. Burkhardt, A. Dauelsberg and B. Kroon (2000). "Carbon isotope fractionation by a marine diatom: Dependence on the growth-rate-limiting resource." Marine Ecology Progress Series **193**: 295-303.

Riebesell, U., D. A. Wolf-Gladrow and V. Smetacek (1993). "Carbon dioxide limitation of marine phytoplankton growth rates." Nature **361**(6409): 249-251.

Ritchie, R. J., C. Nadolny and A. W. D. Larkum (1996). "Driving forces for bicarbonate transport in the cyanobacterium *Synechococcus* R-2 (PCC 7942)." Plant Physiology **112**(4): 1573-1584.

Roeske, C. A. and M. H. O'Leary (1984). "Carbon isotope effects on the enzyme-catalyzed carboxylation of ribulose bisphosphate." Biogeochemistry **23**: 6275-6284.

Rogers, J. C. and R. B. Dunbar (1993). "Carbon isotopic composition of particulate organic carbon in Ross Sea surface waters during austral summer." Antarctic Journal of the United States **28**(5): 81-83.

Rosenthal, Y., M. Dahan and A. Shemesh (2000). "Southern Ocean contributions to glacial-interglacial changes of atmospheric pCO_2: An assessment of carbon isotope records in diatoms." Paleoceanography **15**(1): 65-75.

Rotatore, C., B. Colman and M. Kuzma (1995). "The active uptake of carbon dioxide by the marine diatoms *Phaeodactylum ticornutum* and *Cyclotella* sp." Plant, Cell & Environment **18**(8): 913-918.

Roy, R. N., L. N. Roy, M. Lawson, K. M. Vogel, C. Porter-Moore, W. Davis and F. J. Millero (1993). "Thermodynamics of the dissociation of boric acid in seawater at S = 35 from 0 to 55 degree C." Marine Chemistry **44**(2-4): 243-248.

Roy, R. N., L. N. Roy, K. M. Vogel, C. Porter-Moore, T. Pearson, C. E. Good, F. J. Millero and D. M. Campbell (1993). "The dissociation constants of carbonic acid in seawater at salinities 5 to 45 and temperatures 0 to 45 degree C." Marine Chemistry **44**(2-4): 249-267.

Rye, R., P. H. Kuo and H. D. Holland (1995). "Atmospheric carbon dioxide concentrations before 2.2 billion years ago." Nature **378**: 603-605.

Sakshaug, E. and O. Holm-Hansen (1977). "Chemical composition of *Skeletonema costatum* (Grev.) *Cleve* and *Paplova* (Monochrysis) *lutheri* (Droop) Green as a function of nitrate-, phosphate-, and iron-limited growth." Journal of Experimental Marine Biology and Ecology **29**(1): 1-34.

Salon, C. and D. T. Canvin (1997). "Simulation of C_i fluxes in cyanobacteria: Comparison between the carboxysome hypothesis and the equilibrium proposal." Canadian Journal of Botany/Revue Canadienne de botanique **75**(12): 2117-2130.

Salon, C., N. A. Mir and D. T. Canvin (1996). "Influx and efflux of inorganic carbon in *Synechococcus* UTEX 625." Plant, Cell & Environment **19**(3): 247-259.

Santrock, J., S. A. Studley and J. M. Hayes (1985). "Isotopic analyses based on the mass spectrum of carbon dioxide." Analytical Chemistry **57**: 1444-1448.

Sarmiento, J. L. and C. Le Quere (1996). "Oceanic carbon dioxide uptake in a model of century-scale global warming." Science **274**(5291): 1346-1350.

Sarmiento, J. L. and J. R. Toggweiler (1984). "A new model for the role of the oceans in determining atmospheric P_{CO2}." Nature **308**(5960): 621-624.

Satoh, D., Y. Hiraoka, B. Colman and Y. Matsuda (2001). "Physiological and Molecular Biological Characterization of Intracellular Carbonic Anhydrase from the Marine Diatom *Phaeodactylum tricornutum*." Plant Physiology **126**(4): 1459-1470.

Schimel, D. S., J. I. House, K. A. Hibbard, P. Bousquet, P. Ciais, P. Peylin, B. H. Braswell, M. J. Apps, D. Baker, A. Bondeau, J. Canadell, G. Churkina, W. Cramer, A. S. Denning, C. B. Field, P. Friedlingstein, C. Goodale, M. Heimann, R. A. Houghton, J. M. Melillo, B. Moore, III, D. Murdiyarso, I. Noble, S. W. Pacala, I. C. Prentice, M. R. Raupach, P. J. Rayner, R. J. Scholes, W. L. Steffen and C. Wirth (2001). "Recent patterns and mechanisms of carbon exchange by terrestrial ecosystems." Nature **414**(6860): 169-172.

Sciandra, A., J. Gostan, Y. Collos, C. Descolas-Gros, C. Leboulanger, V. Martin-Jezequel, M. Denis, D. Lefevre, C. Copin-Montegut and B. Avril (1997). "Growth-compensating phenomena in continuous cultures of *Dunaliella tertiolecta* limited simultaneously by light and nitrate." Limnology and Oceanography **42**(6): 1325-1339.

Selinioti, E., D. Nikolopoulos and Y. Manetas (1987). "Organic cosolutes as stabilisers of phosphoenolpyruvate carboxylase in storage: an interpretation of their action." Australian Journal of Plant Physiology **14**: 203-210.

Shuter, B. (1979). "A Model of Physiological Adaptation in Unicellular Algae." Journal of Theoretical Biology **78**: 519-552.

Siegenthaler, U. and T. Wenk (1984). "Rapid atmospheric CO_2 variations and ocean circulation." Nature **308**(5960): 624-626.

Six, K. D. and E. Maier-Reimer (1994). "Effects of plankton dynamics on seasonal carbon fluxes in an ocean general circulation model." Global Biogeochemical Cycles **10**(4): 559-583.

Skirrow, G. and M. Whitfield (1975). "The effect of increases in the atmospheric carbon dioxide content on the carbonate ion concentration of surface ocean water at 25 degrees C." Limnology and Oceanography **20**(1): 103-108.

Smith, L. H., C. Lillo, H. G. Nimmo and M. B. Wilkins (1996). "Light regulation of phosphoenolpyruvate carboxylase in barley mesophyll protoplasts is modulated by protein synthesis and calcium and not necessarily correlated with phosphoenolpyruvate carboxylase kinase activity." Planta **200**: 174-180.

Smith, R. G. and R. G. S. Bidwell (1989). "Inorganic carbon uptake by photosynthetically active protoplasts of the red macroalga *Chondrus crispus*." Marine Biology **102**(1): 1-4.

Sonnerup, R. E., P. D. Quay and A. P. McNichol (2000). "The Indian Ocean ^{13}C Suess effect." Global Biogeochemical Cycles **14**(3): 903-916.

Stamatakis, K., N. A. Gavalas and Y. Manetas (1988). "Organic cosolutes increase the catalytic efficiency of phosphoenolpyruvate carboxylase, from *Cynodon dactylon* (L.) Pers., apparently through self-association of the enzymic protein." Australian Journal of Plant Physiology **15**: 621-631.

Stemler, A. (1985). Carbonic anhydrase: molecular insights applied to photosystem II research in thylakoid membranes. Inorganic carbon uptake by aquatic photosynthetic organisms. W. J. L. a. J. A. Berry. Rockville, Md., American Society of plant physiologists**:** pp.377-387.

Stevens, S. E. and C. Van Baalen (1973). "Characteristics of nitrate reduction in a mutant of the blue-green alga *Agmenellum quadruplicatum*." Plant Physiology **51**: 350-356.

Sueltemeyer, D., B. Klughammer, M. R. Badger and G. D. Price (1998). "Fast Induction of High-Affinity HCO_3^- Transport in Cyanobacteria." Plant Physiology [Plant Physiol.], **116**(1): 183-192.

Sueltemeyer, D., B. Klughammer, M. R. Badger and G. D. Price (1998). "Fast induction of high-affinity HCO_3^- transport in cyanobacteria." Plant Physiology **116**: 183-192.

Sukenik, A., J. Bennett and P. Falkowski (1987). "Light-saturated photosynthesis -- limitation by electron transport or carbon fixation?" Biochimica et Biophysica Acta **891**(3): 205-215.

Sukenik, A., D. Tchernov, A. Kaplan, E. Huertas, L. M. Lubian and A. Livne (1997). "Uptake, efflux, and photosynthetic utilization of inorganic carbon by the marine eustigmatophyte *Nannochloropsis sp.*" Journal of Phycology **33**(6): 969-974.

Syrett, P. J. (1988). Uptake and utilization of nitrogen compounds. Biochemistry of the algae and cyanobacteria. L. J. R. a. J. R. Gallon. Oxford, Clarendon Press**:** 23-40.

Taraldsvik, M. and S. Myklestad (2000). "The effect of pH on growth rate, biochemical composition and extracellular carbohydrate production of the marine diatom *Skeletonema costatum*." European Journal of Phycology **35**: 189-194.

Tchernov, D., M. Hassidim, B. Luz, A. Sukenik, L. Reinhold and A. Kaplan (1997). "Sustained net CO_2 evolution during photosynthesis by marine microorganisms." Current Biology **7**(10): 723-728.

Tchernov, D., M. Hassidim, A. Vardi, B. Luz, A. Sukenik, L. Reinhold and A. Kaplan (1998). "Photosynthesizing marine microorganisms can constitute a source of CO_2 rather than a sink." Canadian Journal of Botany/Revue Canadienne de botanique **76**(6): 949-953.

Thomas, W. H. and A. N. Dodson (1972). "On nitrogen deficiency in tropical Pacific oceanic phytoplankton. II. Photosynthetic and cellular characteristics of a chemostat-grown diatom." Limnology and Oceanography **17**(4): 515-523.

Tortell, P. D. (2000). "Evolutionary and ecological perspectives on carbon acquisition in phytoplankton." Limnology and Oceanography **45**(3): 744-750.

Tortell, P. D. and F. M. M. Morel (2002). "Sources of inorganic carbon the phytoplankton in the eastern Subtropical and Equatorial Pacific Ocean." Limnology and Oceanography **47**(4): 1012-1022.

Tortell, P. D., G. H. Rau and F. M. M. Morel (2000). "Inorganic carbon acquisition in coastal Pacific phytoplankton communities." Limnology and Oceanography **45**(7): 1485-1500.

Tortell, P. D., J. R. Reinfelder and F. M. M. Morel (1997). "Active uptake of bicarbonate by diatoms." Nature **390**(6657): 243-244.

Turpin, D. H. and G. C. Vanlerberghe (1991). "The inorganic carbon requirements for nitrogen assimilation." Canadian Journal of Botany/Revue Canadienne de botanique **69**(5): 1139-1145.

Vanlerberghe, G. C., K. A. Schuller, R. G. Smith, R. Feil, W. C. Plaxton and D. H. Turpin (1990). "Relationship between NH_4^+ assimilation rate and in vivo phosphoenolpyruvate carboxylase activity. Regulation of anaplerotic carbon flow in the green alga *Selenastrum minutum*." Plant Physiology **94**(1): 284-290.

Verardo, D. J., P. N. Froelich and A. McIntyre (1990). "Determination of organic carbon and nitrogen in marine sediments using the Carlo Erba NA-1500 Analyzer." Deep-Sea Research **37**(1A): 157-165.

Vidal, J. and R. Chollet (1997). "Regulatory phosphorylation of C_4 PEP carboxylase." Trends in Plant Sciences **2**: 230-237.

Volokita, M., D. Zenvirth, A. Kaplan and L. Reinhold (1984). "Nature of the inorganic carbon species actively taken up by the cyanobacterium *Anabaena variabilis*." Plant Physiology **76**: 599-602.

Wilbur, K. M. and N. G. Anderson (1948). "Electrometric and colorimetric determination of carbonic anhydrase." Journal of Biological Chemistry **176**: 147-154.

Williams, T. G. and D. H. Turpin (1987). "Photosynthetic kinetics determine the outcome of competition for dissolved inorganic carbon by freshwater microalgae: Implications for acidified lakes." Oecologia **73**(2): 307-311.

Wolf-Gladrow, D. and U. Riebesell (1997). "Diffusion and reactions in the vicinity of plankton: A refined model for inorganic carbon transport." Marine Chemistry **59**(1-2): 17-34.

Zeebe, R. E. and D. Wolf-Gladrow (2001). CO_2 in Seawater: Equilibrium, Kinetics, Isotopes, Elsevier Science.

Zimba, P. V., M. J. Sullivan and H. E. Glover (1990). "Carbon fixation in cultured marine benthic diatoms." Journal of Phycology **26**(2): 306-311.